URANIUM-LEAD ISOTOPIC INVESTIGATION OF THE ARCHEAN IMATACA COMPLEX, GUAYANA SHIELD, VENEZUELA

by

CARLA PAIGE WESTLUND MONTGOMERY

A.B. Wellesley College
(1972)

A.M. Dartmouth College
(1974)

SUBMITTED TO THE DEPARTMENT OF EARTH AND PLANETARY SCIENCES

IN PARTIAL FULFILLMENT OF THE REQUIREMENTS

FOR THE DEGREE OF

DOCTOR OF PHILOSOPHY

at the

MASSACHUSETTS INSTITUTE OF TECHNOLOGY

May, 1977

Signature of Author.....Carla Paige Westlund Montgomery.....
Department of Earth and Planetary Sciences

Certified by.....Patrick M. Hurley.....
Thesis Supervisor

Accepted by.....Theodore R. Madden.....
Chairman, Departmental Committee on Graduate Studies

URANIUM-LEAD ISOTOPIC INVESTIGATION OF THE ARCHEAN IMATACA COMPLEX, GUAYANA SHIELD, VENEZUELA

by

CARLA PAIGE WESTLUND MONTGOMERY

Submitted to the Department of Earth and Planetary Sciences, May, 1977, in partial fulfillment of the requirements for the Degree of Doctor of Philosophy

ABSTRACT

Uranium-lead isotopic analyses of total-rock samples and feldspars from the Imataca Complex in the northern Guayana Shield have been carried out in an attempt to clarify the primary age of the region. On the basis of the new uranium-lead work and combination of uranium-lead data with previous rubidium-strontium results, that age now appears to be in the 3.5-3.8 b.y. range.

Lead isotopic evolution in most samples may formally be described by a two-stage model, or a special three-stage model with a resticted range of second-stage μ values. The start of the third stage, where indicated, is generally marked by metamorphism up to pyroxene-granulite grade. Some

of the resulting metasediments are charnockitic. The metamorphism is frequently characterized by severe depletion of uranium relative to lead. Other investigators have reported no comparable rubidium depletion, perhaps due to the abundance of K-bearing phases. Although this granulite metamorphism was accompanied by strontium isotopic homogenization over distances of the order of 10 cm, equilibration of lead isotopes was less complete at this scale. The granulite event is dated at 2-2.3 b.y. ago. It appears to have been more intense in the eastern part of the Complex, and may be correlated with thermotectonic activity in the adjacent Pastora-Supamo region at that time.

Some of the U-Pb data may indicate a disturbance at 2.9 b.y. ago, at the time of emplacement of the La Ceiba migmatite, but the evidence is limited and equivocal. The lead isotopic composition of the feldspars does not appear to have been affected by a minor thermal event at 1.2 b.y. which is recorded by a rubidium-strontium mineral isochron.

Confirmation of the presence of ancient Archean crust in the Imataca Complex supports its previous tentative correlation with the basement complex in Liberia - Sierra Leone.

Thesis supervisor: Patrick M. Hurley

Title: Professor of Geology

Acknowledgments

A great many individuals have contributed to the success of this project.

My advisor, Prof. Patrick Hurley, inspired the present study. His scientific advice and insight, his enthusiasm, encouragement, and unflagging interest in the work have all been enormously helpful, and are most gratefully acknowledged.

Prof. Stanley Hart generously allowed me to dirty up his new mass spectrometer running some of my samples. Through our discussions of the preliminary draft of the thesis, he has also helped me to evaluate my data more critically and imaginatively.

My introduction to the practical side of uranium-lead dating in the laboratory came from Prof. Henri Gaudette of the University of New Hampshire, whose careful reading of the thesis in its early stages is also very much appreciated.

I would further like to thank Dr. Abdalla Abdel-Monem for many lively discussions, and Profs. Harold Fairbairn and John Dickey, Jr. for assistance with the petrographic and petrologic portions of the thesis.

Several other graduate students have aided this study in various ways; I would particularly like to mention Marc Loiselle, Masaaki Obata, Maggie Riggs, and Dr. Don Skibo. A special vote of thanks goes to my fellow geochronologist and office-mate, Bill Olszewski, whose calculator I have quite thoroughly broken in, and who has provided a thoughtful audience for many of the ideas presented here while they were being developed.

The thesis has been typed through the courtesy of Danielle Chouet, who permitted me to monopolize her typewriter and generally clutter up her office for several weeks.

Without the constant support of all my family, this work would have been much more difficult. The unlimited confidence and encouragement of my mother have been a very special help. While writing this thesis I have come to appreciate particularly her many past efforts to improve my English!

Perhaps the greatest contribution to the success of this effort has come from my husband Warren. Despite the demands of his own graduate program, he has always found

the time and patience to listen, to share my excitements and sympathize with my frustrations. In the course of my thesis research he has certainly learned far more about geochronology than he ever wanted to know, and has somehow put up with me through it all.

Financial support for the author and the research has been provided by many sources: teaching assistantships in the Department of Earth and Planetary Sciences; research assistantships funded by National Science Foundation grants A40242, 76-03726-EAR, and 76-22487-EAR to Prof. Hurley, National Science Foundation grant 76-03766-EAR to Prof. Hart, and Army Research Office grant DAHC04-73-C-0017 to Prof. William F. Brace; funding for microprobe analyses from the Department of Earth and Planetary Sciences; and a one-year M.I.T. endowed tuition fellowship. Additional support for the research was provided by special funds from the Department of Earth and Planetary Sciences authorized by Dr. Frank Press, whom I would especially like to thank for his consideration.

Table of Contents

Index of Figures

Index of Tables

1. Introduction

The history of the oldest Precambrian is still imperfectly known. Aside from the restricted exposure of very ancient rocks, one of the principal reasons for this is the difficulty of obtaining reliable radiometric dates on rocks which may have been subjected to multiple thermotectonic episodes.

Recent work in highgrade metamorphic terranes (e.g. Moorbath et al., 1969; Black et al., 1971; Gray and Oversby, 1972; and Moorbath et al., 1973) has suggested that whole-rock lead isotopes may provide an especially valuable geochronometer in such cases. The particular usefulness of the uranium-lead system lies in the fact that it comprises two independently-decaying radioactive parent isotopes each decaying to a different daughter isotope ($U^{238} \longrightarrow Pb^{206}$, $U^{235} \longrightarrow Pb^{207}$). In natural systems there is no significant relative fractionation of the two uranium or various lead isotopes (Doe, 1970), although fractionation of uranium and lead relative to each other frequently occurs. The two decay schemes thus provide an internal check on each other. Moreover, it has appeared to some investigators (Gray and Oversby, 1972) that under highgrade metamorphic conditions, lead isotopes may be somewhat less mobile than strontium isotopes, and thus less susceptible to resetting of the radiometric age.

Reconnaissance geochronology in the Guayana Shield region of South America (Figure 1) led to the identification of a region of crust yielding apparently Archean ages (3.0 - 3.6 b.y.; see Chapter 2). The age data were, however, scattered and ambiguous. It was hoped that investigation of the behavior of uranium and lead isotopes in these rocks would permit much-needed refinement of the previous geochronologic work. In particular, we wanted to learn, if possible, just how old the primitive crust in this region really is.

Figure 1. Sketch-map of the principal shield regions of South America. The Guayana Shield is the northernmost of these three. Map after Benavides (1968), p. 251.

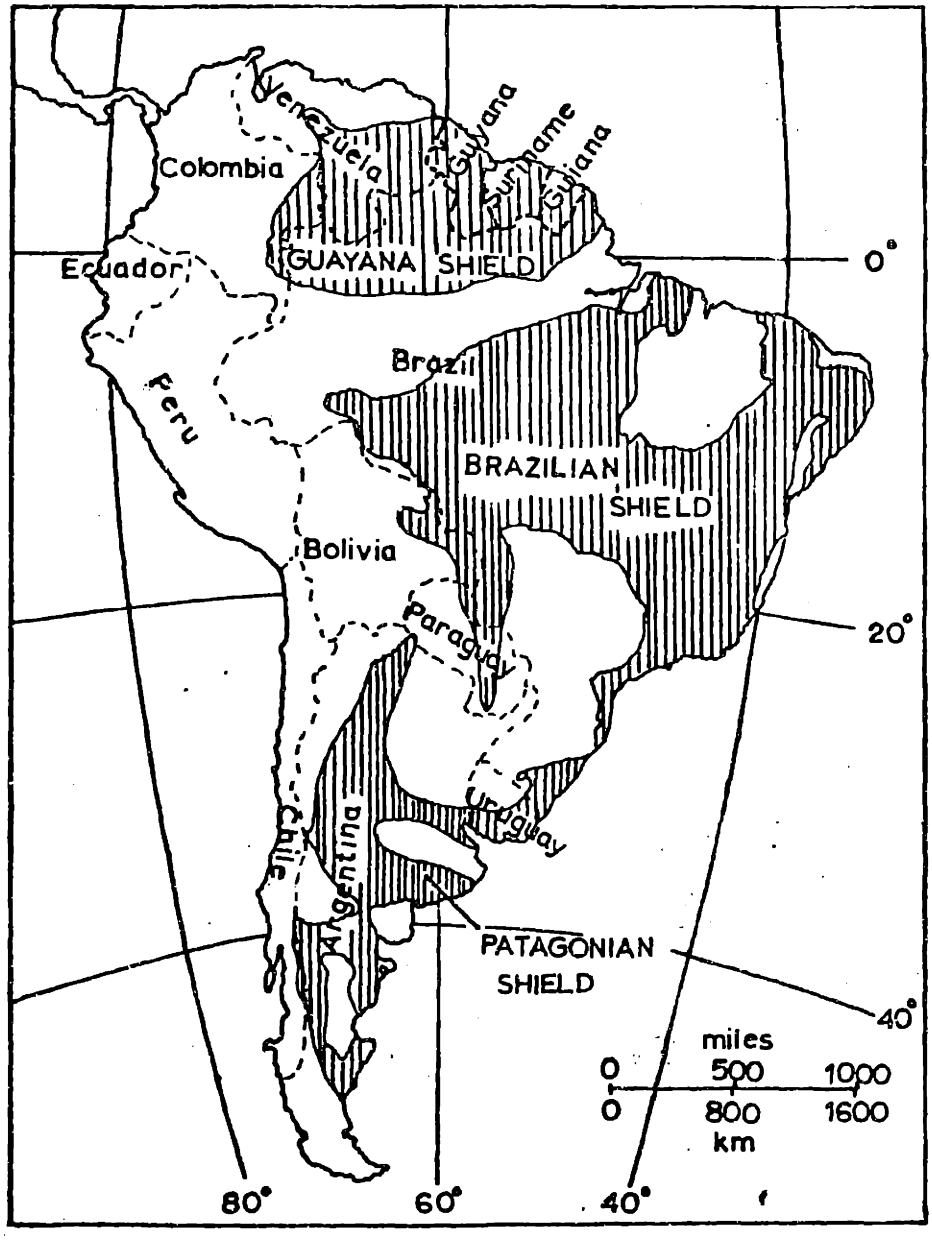
Venezuela
Guyana
Surname
Guiana
Colombia
GUAYANA SHIELD
Ecuador
0°
Brazil
Peru
BRAZILIAN SHIELD
Bolivia
20°
Paraguay
Uruguay
Chile
Argentina
PATAGONIAN SHIELD
40°
miles
0 500 1000
0 800 1600
km
80°
60°
40°

2. Geologic and Geochronologic Setting

I. Geology

The Guayana Shield is the northernmost of the three large shield regions of South America (see Figure 1). It extends over approximately half of Venezuela and most of British Guyana, French Guiana, and Suriname (Jenks, 1956; López et al., 1956). Early researchers (Liddle, 1946; López et al., 1956) distinguished two units within the oldest rocks of the Venezuelan portion of the shield: the "Guayana System", consisting of granite and hornblende gneisses and mica schist, and an overlying "Imataca Series" of ferruginous quartzites. Subsequent practice has been to consider all the ancient, highly-metamorphosed basement rocks together as the Imataca Complex or Imataca Series. The Imataca Series as described by Kalliokoski (1965a) occurs as an east-northeast-striking belt approximately 510 km long, varying between 65 and 130 km wide, partially bounded and transected by a series of faults of similar trend. Figure 2 is a geologic sketch-map of the Imataca and surrounding regions; Figure 3 shows in greater detail the area studied in the present project.

Principal rock types in the Imataca Complex include quartzofeldspathic gneisses, pyroxene-amphibole gneisses, and metamorphosed iron formation (Kalliokoski, 1965a, 1965b; Dorr, 1973; Ríos, 1972; Hurley et al., 1972). The rocks have been extensively deformed and subjected to metamorphism

Figure 2. Geologic sketch-map of major rock units in the vicinity of the Imataca Complex; after Kalliokoski (1965a), Bellizzia (1972), and Mendoza (1972).

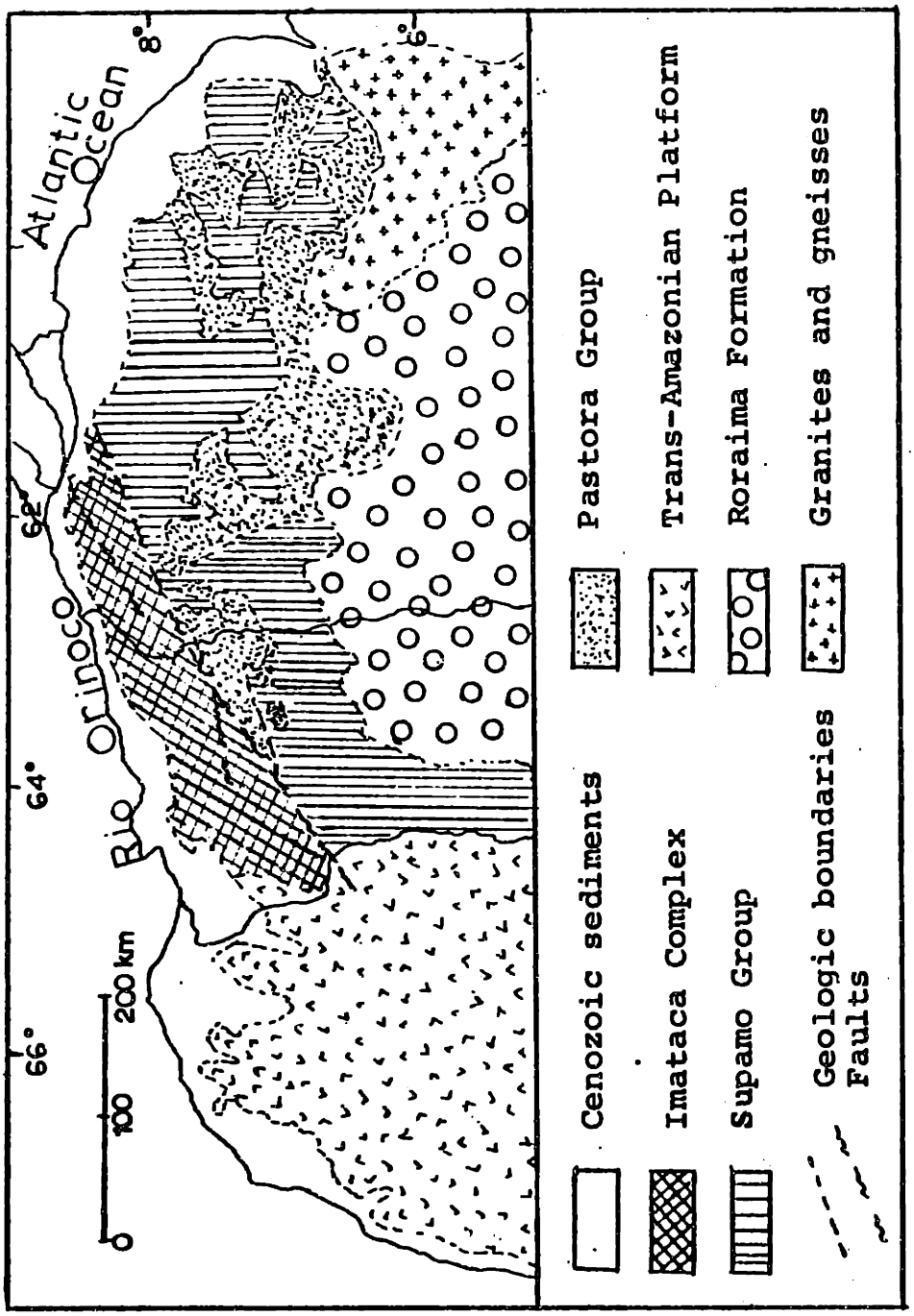
Atlantic Ocean
Rio Orinoco
8°
6°
64°
66°
0
100
200 km
Cenozoic sediments
Imataca Complex
Supamo Group
Geologic boundaries
Faults
Pastora Group
Trans-Amazonian Platform
Roraima Formation
Granites and gneisses

Figure 3. Simplified geologic sketch-map of the area investigated; after Kalliokoski (1965a). The following points should be noted:

(1) Geologic contacts are frequently approximated on the basis of aeromagnetic interpretation.

(2) The contact south of and approximately parallel to the Orinoco River represents the farthest extent of sedimentary cover. However, the Imataca is inferred on the basis of scattered outcrops to extend north at least to the Orinoco under this cover.

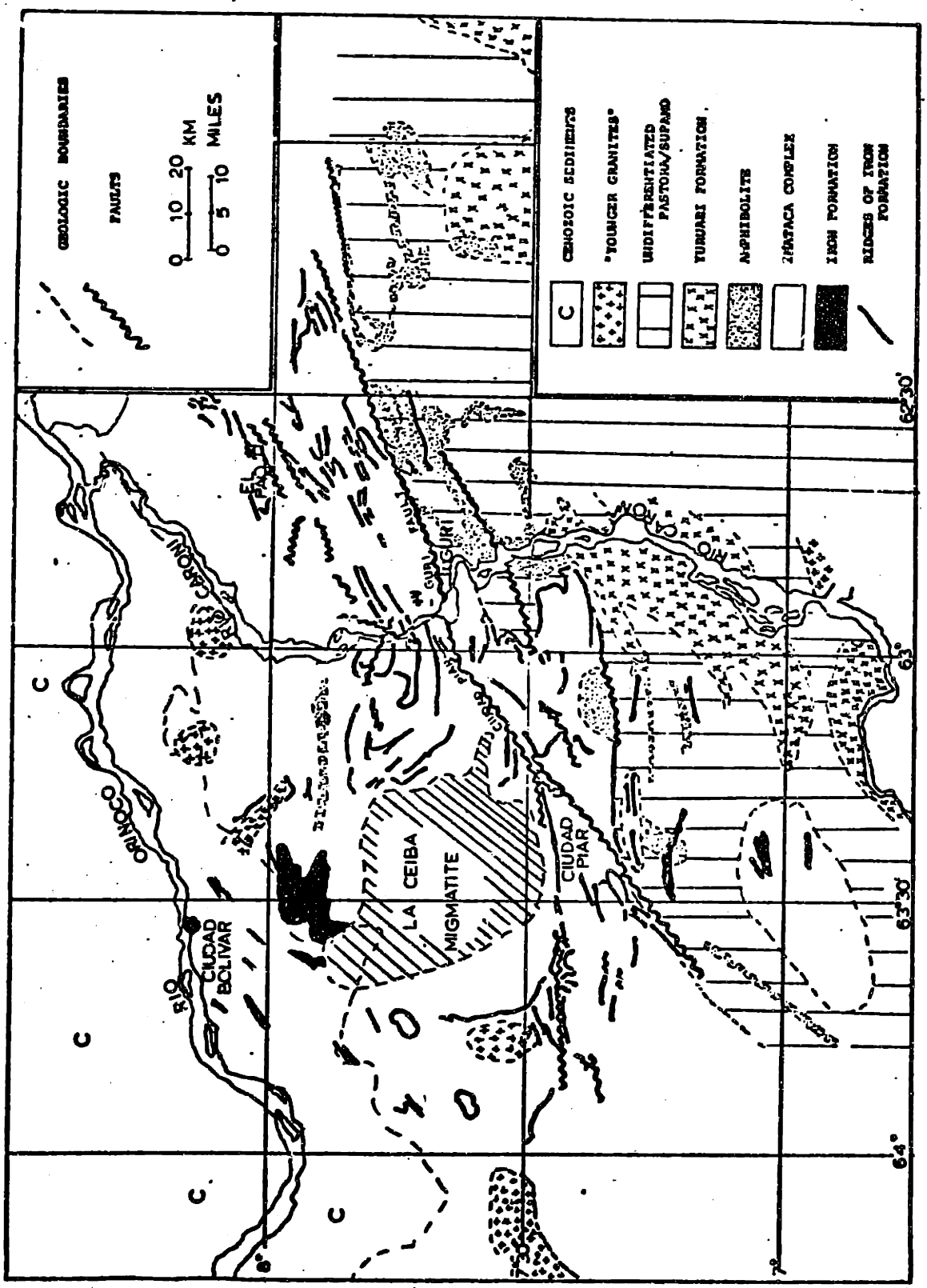
GEOLOGIC BOUNDARIES
FAULTS
0 10 20 KM
0 5 10 MILES
CENOZOIC SEDIMENTS
"YOUNGER GRANITES"
UNDIFFERENTIATED PASTORA/SUPAMO
YURUARI FORMATION
AMPHIBOLITE
ZÁRAZACA COMPLEX
IRON FORMATION
RIDGES OF IRON FORMATION
ORINOCO
RIO CARONI
RIO CARONI
RIO
CIUDAD BOLIVAR
LA CEIBA
MIGMATITE
CIUDAD PIAR
62°30'
63°
63°30'
64°
C

of almandine-amphibolite to granulite grade, with the metamorphic grade increasing to the east (Dorr, 1973). They are extensively intruded by the La Ceiba Migmatite (see Figure 3) and are bounded or intruded also by various younger Precambrian metamorphics and granites (Posadas and Kalliokoski, 1967; Kalliokoski, 1965a; Hurley, 1972; Hurley et al., 1968, 1972, 1973).

The original nature of these Imataca rocks is unclear. There is general agreement that the iron formations were initially sediments (Ruckmick, 1963; Kalliokoski, 1965b; Dorr, 1973). Certain of the other units also are probably metasediments, considering such evidence as concordant stratification, the occurrence of rounded zircons, and the existence of quartz-rich horizons and rocks whose mineralogical makeup is over 90% quartz plus perthite (Chase, 1965; Kalliokoski, 1965a; Dougan, 1976; Ríos, 1972; Quesada et al., 1968). On the other hand, some of the lithologic types, for example the amphibolites, suggest a volcanic contribution as well (Dougan, 1974; Hurley et al., 1972; deRatmiroff, 1965). The long-accepted solution has been to interpret the Imataca as a typically eugeosynclinal sequence (Kalliokoski, 1965a). Recently, an intensive petrologic and geochemical study of the Imataca Complex in the vicinity of Ciudad Piar and Guri south of the major fault zone (Dougan, 1974, 1976) has indicated that at least in that area, the bulk of the rocks may be metaigneous

rather than metasedimentary. In that case, much of the protolith might be approximated by a suite of calc-alkaline continental-margin-type volcanics, and/or an anatectic melt derived from greywackes (Dougan, 1976). This interpretation represents a significant departure from previous investigators' conclusions, and demonstrates the extent of confusion and disagreement about both the significance of the Imataca and the nature of the protolith.

Any ancient rocks immediately to the north of the Imataca are overlain by Cenozoic sediments and alluvium from the Orinoco River, but other Precambrian units are exposed to the south and west (see Figure 2). South and southeast of the Imataca, largely separated from it by the Ciudad Piar - Guri fault zone, are rocks of the Supamo Complex, which consists of quartz-feldspar-biotite paragneiss, migmatite, and K-feldspar-poor acid igneous rocks, and the Pastora Province, which is composed of a lower unit (the Carichapo Formation) of amphibolites (including metamorphosed pillow lavas), finely foliated granites, andesitic tuff, greywacke, and some iron formation, and an upper unit (the Yuruari Formation) which includes feldspathic sandstones and siltstones, phyllites, and dacitic lavas, tuffs, and volcanic breccias (Menéndez et al., 1972; Menéndez, 1968, 1972). The Supamo has the same east-northeast structural trend as the Imataca (Ríos, 1972), and has been tentatively correlated with it (Menéndez et al., 1972).

Apparently the Supamo originally formed the basement on which the Carichapo and Yuruari Formations were laid down, but the Supamo was remobilized during the Transamazonian episode about 2 b.y. ago and subsequently partially intruded into the overlying strata, so that it exhibits both concordant and intrusive contacts with the Pastora rocks (Menéndez, 1968, 1972). Dougan (1976) has even suggested that the Carichapo could underlie the Imataca, but this is not supported by direct field evidence.

Beyond the Caura River to the west, the Imataca-Supamo-Pastora association is bounded by a portion of the Amazonian Platform which Mendoza (1972) has described as the Cedeño Supergroup. This Cedeño Supergroup, which consists of the Transamazonian Cuchivero Group and the younger Suapure Group, includes primarily assorted granites, and is interpreted as an acid plutonic-volcanic platform bounding the "Pastora geosyncline" to the east. The granites of the Suapure Group may perhaps be correlated with the many small bodies of sodium-poor granite known simply as "younger granites" in the Imataca and other units to the east (Mendoza, 1972; Menéndez et al., 1972).

II. Regional History

In summary, the geologic history of the northeastern Guayana Shield has tentatively been reconstructed as follows (Kalliokoski, 1965a; deRatmiroff, 1965; Menéndez et al., 1972; Mendoza, 1972; Ríos, 1972):

1. Deposition of the protolith of the Imataca Complex (and the Supamo Complex?) - a mixture of submarine sediments and volcanics.

2. Considerable folding, migmatization, and metamorphism to amphibolite to (?) granulite grade. Intrusion of granites and migmatites.

3. Erosion, followed by deposition of the Pastora sequence of lavas and sediments.

4. A second period of folding, with the formation of broad domes and synclinal troughs of east-northeast trend, involving both the Imataca and Pastora rocks. A second period of metamorphism, also highgrade. Faulting along the east-northeast structural trend, resulting in several broad mylonitized zones (up to 3.5 km wide along the El Pao fault zone). Remobilization of the old Supamo basement; further igneous intrusions in the Imataca-Pastora-Supamo area. Extensive granite intrusions in the Cuchivero province and in the platform to the west, where a more north-south structural trend developed. Approximately Trans-amazonian in age.

5. Uplift and considerable erosion of the whole north-eastern Guayana Shield.

6. Minor deformation and intrusion equivalent to, but far less intense than, the Kibaran episode in Africa. Following this small disturbance, the Imataca region was essentially stable to the present.

III. Previous geochronology

The above chronology has largely been confirmed by recent reconnaissance radiometric dating. Early whole-rock rubidium-strontium analyses of some of the Imataca granulites suggested that the complex might be in excess of 3 b.y. old (Hurley et al., 1972). The first period of thermal metamorphism with migmatization has also been dated, also by whole-rock Rb-Sr, by analysis of granitoid or migmatoid rocks in the vicinity of Cerro La Ceiba (see Figure 3); their age is around 2700 m.y. (Hurley et al., 1973). A similar age is preserved by zircons in some Supamo basement rocks (Gaudette et al., 1974). Further rubidium-strontium dating, of the Encrucijada Granite which intrudes the Imataca, yielded a 2100-2200 m.y. age for the younger period of thermotectonic activity (Posadas and Kalliokoski, 1967), and this is supported by Rb-Sr and K-Ar dating of rocks from the rejuvenated Supamo, which give ages of about 2200 and 1800 m.y. respectively by these two methods (Hurley et al., 1973; Espejo and Santamaria, 1972). Excellent zircon ages of about 2100 m.y. have recently been obtained both from the rejuvenated Supamo and from the "younger granites" (P. Klar, personal communication), which further confirms an intense thermal episode at this time. Some whole-rock potassium-argon ages on several of the "younger granites" are closer to 1500 m.y. (Espejo and Santamaria, 1972); K-Ar mineral ages of samples from the Pastora show a small thermal disturbance

at 1300 m.y. (Kalliokoski, 1965a); and a rubidium-strontium mineral isochron for one of the Imataca granulites gives an age of 1190 m.y. (Hurley et al., 1973); all this probably indicates the time of the last minor thermotectonic activity in the Imataca. Such activity within the Imataca could be related to whatever event produced the Parguaza granite in the Cuchivero Province, which is dated at 1550 m.y. by whole-rock Rb-Sr and zircon U-Pb (Gaudette et al., 1977).

The geologic and geochronologic evidence taken together in fact produce a pattern in the northern Guayana Shield which resembles results from West Africa (Bellizzia, 1972), and the matching of lithologies, structures, and radiometric ages between the two areas has both helped to confirm the existence of continental drift and aided in the pre-drift reassembly of the two continents (Hurley, 1972).

It is unfortunately the oldest, and therefore perhaps the most interesting, part of this history about which the most uncertainty has existed. The Imataca Complex appeared to be somewhat older than 3 b.y., but how much older? Whole-rock rubidium-strontium studies in the complex yielded only "errorchrons" or "scatterchrons" of points which generally fell between bounding isochrons representing 3.0 and 3.6 b.y. ages (Figure 4). Uranium-lead analyses of Imataca zircons (Gaudette et al., 1973) provided no additional information about the primary age of the rocks. The data points were nearly concordant

Figure 4. Total-rock rubidium-strontium analyses of samples from the Imataca Complex.

(a) Gneisses from the Guri Dam area and elsewhere; after Hurley et al. (1972).

(b) Granulites from El Pao; after Montgomery et al. (1977).

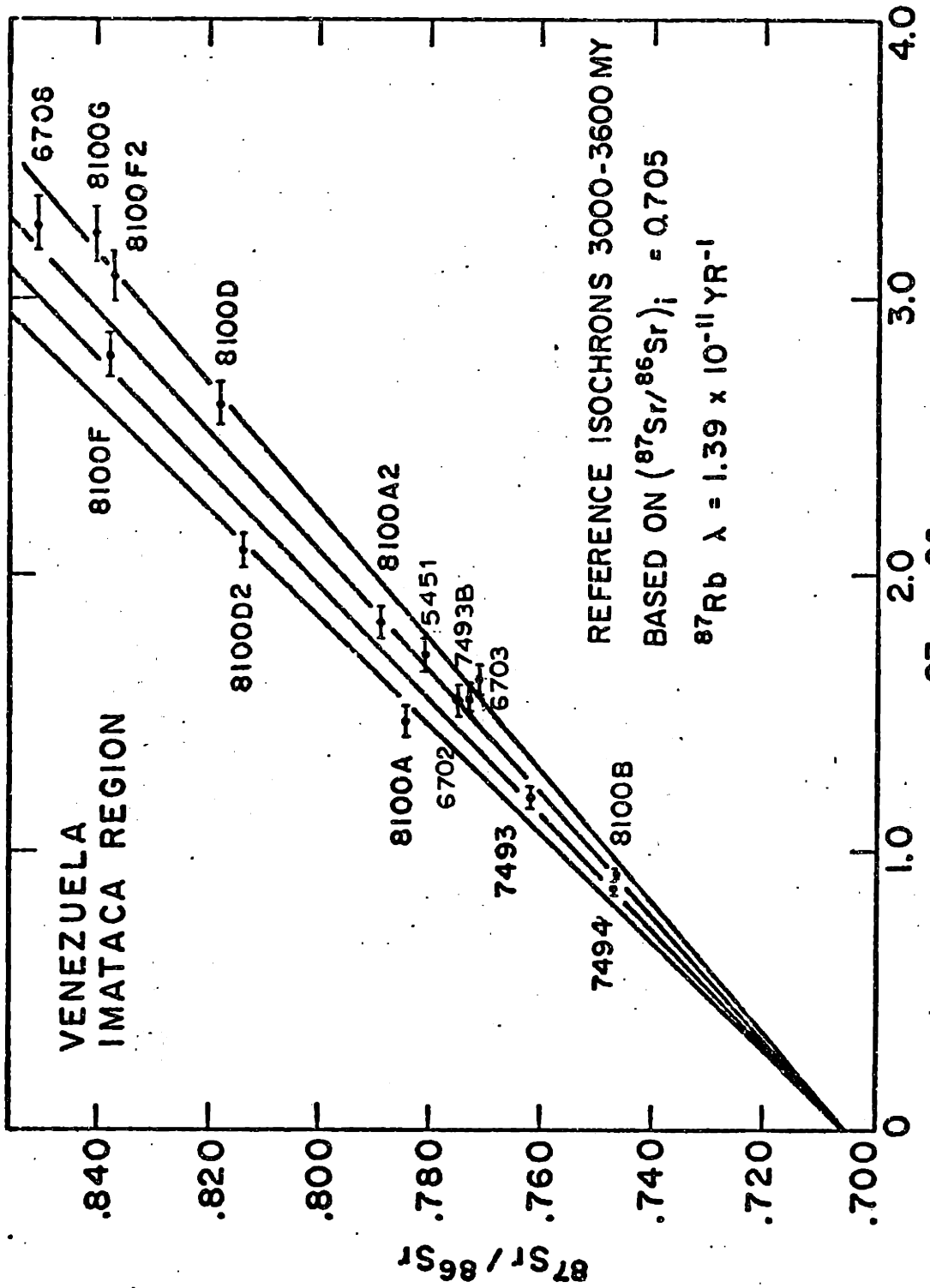
VENEZUELA
IMATACA REGION
REFERENCE ISOCHRONS 3000-3600 MY
BASED ON $(^{87}Sr/^{86}Sr)_i$ = 0.705
^{87}Rb λ = 1.39 x 10^{-11} YR^{-1}
$^{87}Sr/^{86}Sr$
$^{87}Rb/^{86}Sr$
6706
8100G
8100F2
8100D
8100F
8100A2
8100D2
5451
7493B
6703
8100A
6702
7493
8100B
7494
.840
.820
.800
.780
.760
.740
.720
.700
0
1.0
2.0
3.0
4.0

(a)

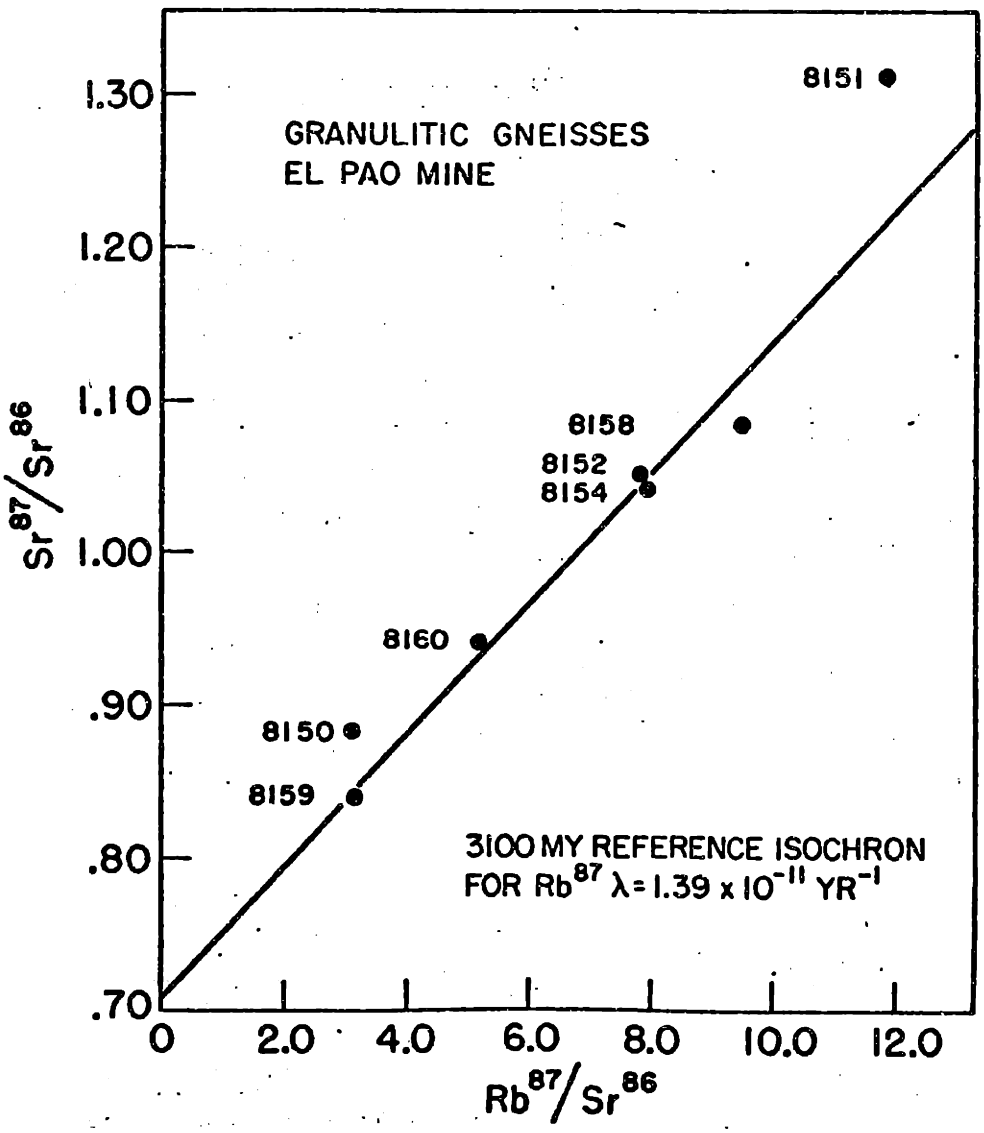
GRANULITIC GNEISSES
EL PAO MINE
8151
8158
8152
8154
8160
8150
8159
3100 MY REFERENCE ISOCHRON
FOR Rb87 λ = 1.39 x 10-11 YR-1
1.30
1.20
1.10
1.00
.90
.80
.70
Sr87/Sr86
0
2.0
4.0
6.0
8.0
10.0
12.0
Rb87/Sr86

(b)

Figure 5. Detail of Concordia plot of zircon U-Pb data; samples from the Guri Dam (after Gaudette et al., 1973).

1. Sample 8100E -80+170 mesh nonmagnetic
2. Sample 8100E -80+170 mesh magnetic
3. Sample 8100G -80+170 mesh nonmagnetic
4. Composite -80+170 mesh
5. Composite -170+200 mesh
6. Composite -200+250 mesh
7. Composite -250+325 mesh

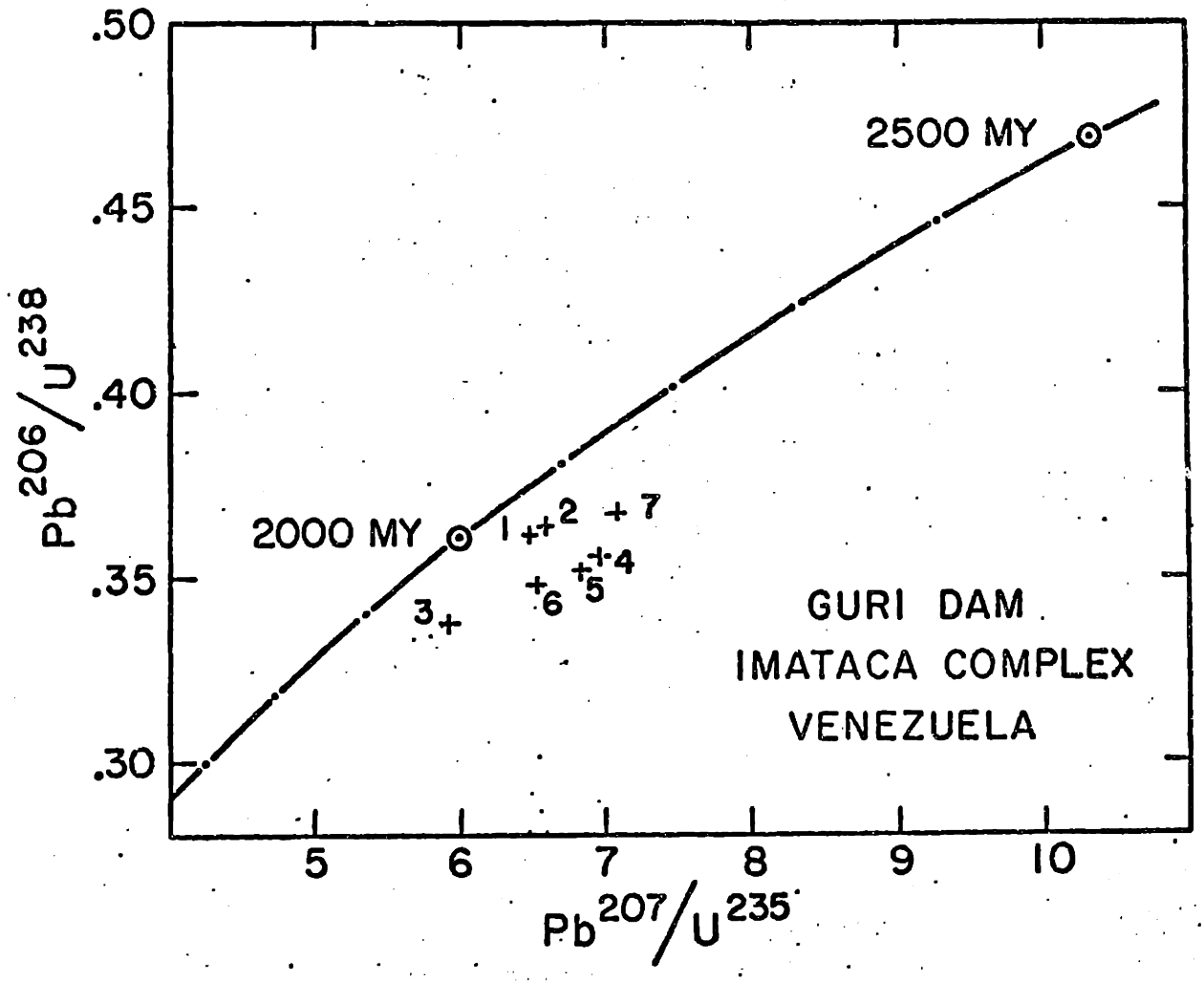
.50
.45
.40
.35
.30
5
6
7
8
9
10
Pb^{206}/U^{238}
Pb^{207}/U^{235}
2500 MY
2000 MY
1
2
3
4
5
6
7
GURI DAM
IMATACA COMPLEX
VENEZUELA

(Figure 5). It appeared that at some time, probably around 2200 m.y. ago, the zircon ages were almost completely reset. Apparently the metamorphic episode which caused this resetting was an intense one: large as well as small zircons showed nearly complete loss of radiogenic lead. Presumably this event was the Transamazonian thermotectonic episode reflected in the ages of the Encrucijada Granite, "younger granites", and other units as discussed above.

Further clarification (if possible) of the Imataca's true age was clearly desirable. Whole-rock lead techniques had recently been applied with considerable success to Archean granulites by Moorbath et al.(1969) and Black et al. (1971), so it was decided to try whole-rock uranium-lead analyses of Imataca samples in an effort to define more clearly the primary age of the Complex.

3. Uranium-Lead Analytical Techniques

I. Chemistry and Mass Spectrometry

A variety of methods for the extraction of uranium and lead from geological materials exist. Doe (1970) summarizes techniques used up to 1970. The methods he lists were rejected for use in the present study, for different reasons: some were inappropriate to whole rocks; some required larger quantities of material than were available for some of our samples; some had unacceptably high lead blanks.

The Oxford group have had good results using a two-stage electrodeposition technique on whole rocks (see Black et al., 1971, 1973; Moorbath et al., 1973). However, while the method works well once the equipment is set up and functioning, Moorbath (personal communication) advised that the equipment could be extremely tricky to set up initially, and that it might be many months before it worked properly. Since there was no intention to establish a permanent facility for whole-rock lead work, the potentially great investment in apparatus and in time required before any analytical results could be obtained were not considered to be worthwhile.

The ion-exchange technique developed by Krogh (1973) to extract uranium and lead from zircons offered considerable promise of adaptability to whole-rock work. The basic method is uncomplicated, has a low inherent blank, and requires relatively inexpensive equipment. Moreover, other

workers in the M.I.T. geochronology laboratory had used the technique previously (for zircons), and the necessary hydrothermal dissolution bombs were already available.

The modified technique as used in the present study may be briefly summarized as follows:

Approximately 0.1 g of powdered sample (whole rock or feldspar) is placed in the clean Teflon capsule of the hydrothermal bomb with about 3 ml of concentrated (ultrapure) hydrofluoric acid plus 1 ml concentrated (ultrapure) nitric acid, and spiked with a solution of high-purity U^{235} spike. The bomb is then placed in a 205°C oven for one week to dissolve the sample. Thereafter the dissolved sample is evaporated to dryness under a heat lamp. Approximately 3-4 ml of 3.1 N hydrochloric acid are added to the residue and the bomb returned to the oven overnight to ensure complete redissolution of this residue. The resulting solution is split into two aliquots, one of which is spiked with a high-purity Pb^{208} spike solution; the spiked aliquot is warmed under a heat lamp for several minutes to equilibrate.

Two resin columns are next prepared. The columns themselves are made from 15-cm lengths of heat-shrinkable Teflon FEP tubing; one end of the tube is shrunk to hold in place a 1/16-inch-thick disk of hydrophilic polyethylene which supports the resin. A resin bed of approximately 2 cm^3 of Dowex 1-X8 anion exchange resin, 200-400 mesh,

Cl^- form, is placed in each column. The resin is successively washed with 8 ml each of 6.2 N HCl and pure water, and conditioned with 4 ml of 3.1 N HCl. One aliquot of sample is then loaded onto each column. The columns are rinsed with 4 ml of 3.1 N HCl to remove interstitial solution which contains elements not held on the columns, and the effluent to this point is discarded. The lead from each column is eluted with 4 ml of 6.2 N HCl; uranium is then eluted with 4 ml of water, and the uranium extracted from the two columns combined. Lead and uranium fractions are evaporated to dryness under a heat lamp.

Resin is discarded after each use to avoid possible contamination. Empty columns are cleaned with concentrated pure HCl and clean water. The Teflon capsules of the bombs are cleaned by placing 3 ml HF and 1 ml HNO_3 in them and putting the bombs in the oven overnight; this procedure is carried out twice between successive samples so there is no possibility of cross-contamination. All water used in the above procedure is ultraclean water prepared by distilling demineralized water twice in quartz. All acids used are likewise ultrapure, and are prepared in concentrated form by sub-boiling distillation in Teflon bottles (Mattinson, 1971). Acids for the column separation are then diluted to the required normality with the quartz-distilled water. Aliquots are kept in Teflon beakers which are cleaned after each use by heating in a bath of 50%

HNO_3 for several hours at temperatures just below boiling, and rinsing in the pure water.

To this point the procedure outlined differs in only minor respects from that of Krogh (1973). The uranium spike is added before rather than after dissolution in order to minimize the potential problem of poor equilibration of the uranium spike with the sample, which he discusses. Volumes of resin and reagents used in the column separation have been increased by a factor of four. This was done to allow for the fact that some iron may be held on the resin with lead, uranium, and other trace elements (Zweig and Sherma, 1972, p. 281). The exchange capacity thus allowed is far greater than needed for most common rocks, but it seemed desirable to allow this safety margin. Note that for feldspars the precaution is unnecessary, as none of the major elements in feldspar are at all adsorbed onto the column.

Some iron is eluted from the column with the lead; most of it comes off with the uranium. Therefore when this procedure is used for whole rocks, a second separation is required to purify the uranium fraction. (Otherwise the iron interferes drastically with the stability of the mass spectrometer run.) This second separation, based on the data of Diamond et al. (1954) and Nelson et al. (1964), is accomplished using a second resin column, of the same dimensions as the anion column, this time containing Dowex

50-X8 cation exchange resin (200-400 mesh, H^+ form). Two ml of cation exchange resin are washed and conditioned simultaneously by the addition of 8 ml of ultrapure concentrated HCl. The dried uranium-plus-iron fraction from the anion column extraction is taken up in 2 ml of the same acid, and the solution loaded onto the column. Over 99% of the iron is held on the column, while most of the uranium passes through. Further uranium is washed through by the addition of more of the concentrated HCl. The limiting factor on the efficiency of this separation is the amount of iron in the sample, which determines how soon significant iron appears in the effluent (identified by the greenish-yellow color of its solution). At least 6 ml of concentrated HCl may be added to the column before iron appears even in the "limiting case" of iron formations. After this volume of acid has passed through the column, a little over 80% of the uranium has been recovered.

Iron formations likewise present a difficulty with the lead fraction. The same procedure as outlined above for separation of iron and uranium may be used to separate iron and lead; in this case 100% of the lead is recovered after washing the cation column with only an additional 4 ml of concentrated HCl.

The dried lead and uranium fractions are taken up in a few drops of 0.75 N H_3PO_4 for loading. The phosphoric acid solution is added to a thin film of dried silica-gel

suspension on a single rhenium ribbon filament, and dried down. At operating temperatures the load forms a glassy matrix which ideally produces a stable beam with no significant relative fractionation of isotopes (Cameron et al., 1969). Samples were analyzed in 9-inch and 12-inch solid-source Nier(1947)-type mass spectrometers, at filament temperatures of approximately 900-1200°C for lead, 1200-1400 °C for uranium (depending on the sample). Analyses of CIT lead standard PN-2 and NBS standard 983 (see Table 1) confirm that no consistent relative fractionation of lead isotopes can be observed at the level of precision of the analyses; therefore no instrument corrections were made to the analytical data.

Recent practice among other investigators (e.g. Krogh, 1973) has been to run uranium samples with a matrix of tantalum oxide and phosphoric acid. This procedure was initially tried in the present study, but proved unsatisfactory. The very small quantities of uranium analyzed made very high operating temperatures necessary, and at those temperatures, the load burned off the filament far too rapidly to permit data collection. In fact, not only did the uranium burn off, but several large, stable, extraneous peaks appeared in the uranium mass range to swamp out the fast-fading uranium peaks. (The nature of these spurious peaks is unknown. They were presumably some sort of minor contaminant or peculiar tantalum compound.)

TABLE 1. STANDARD LEAD TEST RUNS

Run #	Pb^{208}/Pb^{204}	Pb^{207}/Pb^{204}	Pb^{206}/Pb^{204}
PN-2/1	36.326 ± 0.056	15.490 ± 0.018	16.689 ± 0.117
PN-2/2	36.286 ± 0.134	15.459 ± 0.230	16.649 ± 0.090
PN-2/3	36.326 ± 0.146	15.411 ± 0.077	16.651 ± 0.048
PN-2/4	36.269 ± 0.232	15.470 ± 0.023	16.568 ± 0.060
PN-2/5	36.232 ± 0.092	15.446 ± 0.039	16.591 ± 0.036
MEAN 1-5	36.288	15.455	16.630
PN-2 ACCEPTED VALUE*	36.30	15.475	16.625

	Pb^{208}/Pb^{206}	Pb^{207}/Pb^{206}
NBS 983	0.013597 ± 0.000068	0.071394 ± 0.000500
NBS 983 ACCEPTED VALUE*	0.013619	0.071201

*(Doe, 1970).

Errors quoted on measured values are ± 2σ (95% confidence level) standard error of the mean. In every case the accepted value coincides with the measured one within the error of the measurement; in fact, agreement is usually within 1σ error of the measurement. Deviations of measured values are not consistent with appreciable isotopic fractionation.

Accordingly the silica-gel method was tried for uranium also, and proved highly successful. The resulting matrix is not as refractory as the Ta_2O_5 - H_3PO_4 matrix, but detectable uranium emission begins at lower temperatures and is quite stable at these temperatures. Also, no spurious peaks were observed with the silica-gel loads.

The total procedure blank for the standard lead procedure is 13 $\pm$ 3 ng, or less then 1% of sample lead, so the blank correction is quite small. Composition of the laboratory blank was measured as Pb^{206}/Pb^{204} = 19.49 $\pm$ 0.09, Pb^{207}/Pb^{204} = 16.30 $\pm$ 0.10, Pb^{208}/Pb^{204} = 40.32 $\pm$ 0.21 (errors quoted at 1σ error of the mean). These ratios were used for all blank corrections. The blank for the iron-formation lead procedure (including the cation-column step) is somewhat higher; it is 18 $\pm$ 5 ng. The lead blank is composed of an estimated 2-3 ng loading blank and the rest an "ambient blank" arising from handling of samples, periods of exposure during evaporation, and the like. It is unlikely that any of the reagents are at fault: none showed an appreciable blank above the loading blank when tested, and other workers in the laboratory, using the usual Krogh procedure (with essentially 1/4 the reagents used in the modified method) have still obtained a blank of approximately 10 ng (Gaudette, personal communication). Carrying out as much of the work as possible in a laminar-flow hood did not appreciably reduce the measured

blank, perhaps because the hood cannot exclude tetraethyl lead vapors which undoubtedly are abundant in the air in this area. The uranium blank for the complete procedure in approximately 0.15 ng, and is negligible with respect to all but the most uranium-poor samples.

II. Reproducibility of Analytical Results

Due to some initial difficulties with the experimental procedure, during which the uranium fraction of many samples was lost (before the second stage of uranium purification was perfected and the silica-gel matrix adopted for uranium runs), the lead from the gneiss samples was run twice, on separate 0.1-gram portions of the rock powder. This provided very interesting insight into the question of reproducibility of analyses of Pb^{206}/Pb^{204} and Pb^{207}/Pb^{204}.

First, it should be noted that the second round of analyses are generally of higher quality (show higher analytical precision) than the first set. This is very likely due to increased experience on the part of the analyst. Second, the later analyses form more coherent groupings - in general, in fact, sets of related samples much more closely define straight lines on a Pb^{207}/Pb^{204} - Pb^{206}/Pb^{204} plot according to the later analyses. This improved coherence further increases confidence in the second analyses, and is probably also due to greater analyst expertise.

Approximately 40% of the samples have replicate analyses which agree within the 95% confidence limits of the two

analyses. Nearly all of the remaining samples have Pb^{206}/Pb^{204} and Pb^{207}/Pb^{204} ratios which vary by less than 5% at the 95% confidence limits, most of these by less than 3%; three samples differ by up to 10% in these ratios. The Pb^{208}/Pb^{204} analyses frequently show more variability: while 2/3 of these pairs of analyses agree to within 2-3%, about 15% differ by 5-10%; several more differ by as much as 15-20%; and for one sample, the two Pb^{208}/Pb^{204} analyses differ by a factor of 2.5! Moreover, the concentrations of lead and uranium measured vary by up to 30%. Clearly some sample inhomogeneity is indicated by these results.

This is not entirely surprising. The radioactive elements such as uranium and thorium are probably concentrated in the very fine grains of trace minerals such as zircon, not dispersed evenly throughout the rock or any of its major phases. Therefore although the samples are ground to powder, which should guarantee that they will be well mixed, a 0.1-gram portion may not be large enough to ensure that, for example, a stray grain of zircon more or less will not appreciably affect the composition of lead and the amounts of uranium and lead measured. (The sample size used in this procedure is constrained empirically by the maximum which will readily dissolve in the hydrothermal bombs, which in turn were used because this was likely to be by far the cleanest possible dissolution method.) The problem is not confined to the present study, either.

Oversby (1976), discussing reproducibility of lead isotope measurements on Archean acid igneous rocks from Australia, states that "...Separate dissolutions of the same total rock powder do not generally give results that agree with the [analytical] precision quoted above...due to heterogeneous distribution of Pb, U, Th... not overcome by our sampling technique."

Variability in Pb^{208}/Pb^{204} is distressing only insofar as it indicates incompletely representative sampling. But variability in Pb^{207}/Pb^{204} and Pb^{206}/Pb^{204} ratios reflects on the reliability of lead-lead plots and other diagrams used in lead-isotope geochronology. Fortunately, there is a pattern to the variability which is reassuring. Within any set of related samples, individual data points which show sigificant shifts in position on a lead-lead plot from the first analysis to the second in fact shift approximately along the line defined by all the points, within the precision of the data (see Figure 6). It is suggested that the effect observed is directly analogous to that found by researchers using the multistage volatilization method for lead extraction (Cumming et al., 1970). With the latter technique, it is found that analysis of leads extracted from a single whole-rock sample in several steps, at successively higher temperatures, produces a linear array of points on a lead-lead plot - in effect, an isochron from a single rock. It is consequently proposed that lead is

Figure 6. Patterns of variation of replicate lead isotope analyses; groups shown are those which include the samples with the most extreme variations between the two analyses. All error bars shown are 95% confidence limits on the mean. Pairs of replicate analyses are connected by solid lines; the later analysis of each pair is circled. Note how coherence of groupings improves with second analyses; this effect is attributed to improved quality of second analyses. Major shifts, however, are along isochron trend of the appropriate group. Anomalous shifts in (d) show Pb^{204} error-line trend; first runs on these two samples were especially poor, as shown by large error bars.

(a) large gneiss samples, Guri Dam (8100 series)

(b) reconnaissance samples, western Imataca (5451, 6702, 6703)

(c) gneisses from El Pao (8150-8160)

(d) Kalliokoski Guri Dam samples (7491-7494, 6708)

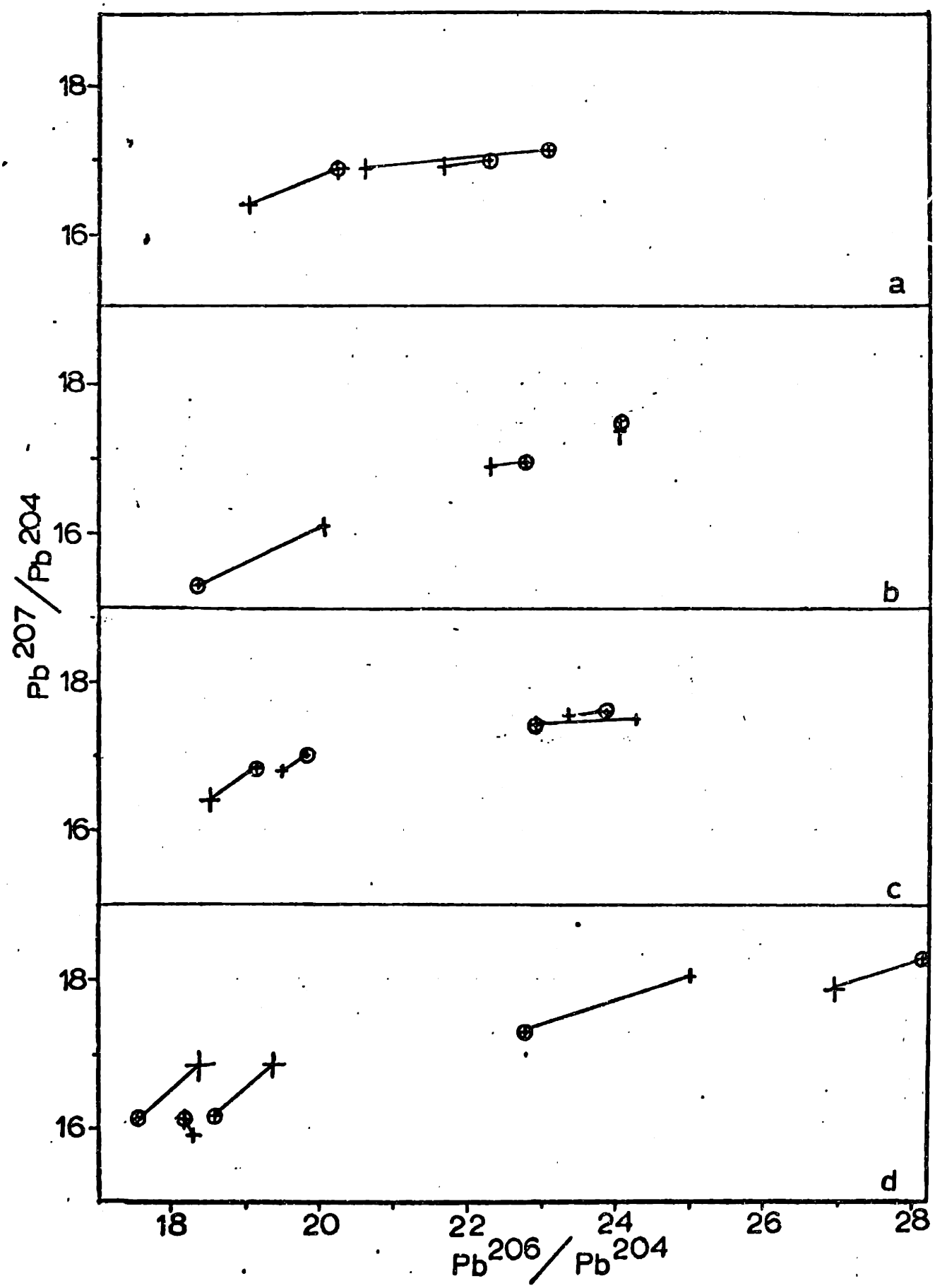
18
16
a
18
16
b
18
16
c
18
16
d
Pb207/Pb204
18
20
22
24
26
28
Pb206/Pb204

extracted from different minerals, of different U/Pb ratios, at different temperatures. The leads extracted at various temperatures then consist of different proportions of the common lead in the rock at the time of the last isotopic homogenization, and radiogenic lead produced since then. Likewise in the current instance: if the powdered rock is slightly inhomogeneous, then different portions of it may have different lead isotopic compositions (arising out of the uneven distribution of uranium among mineral phases). However, provided that a suite of rocks all equilibrated with respect to lead isotopic composition at the same past time (and the U-rich phases last equilibrated with the rocks at the same time), then all analyses, whether of different rocks (of variable U/Pb) in the suite or of slightly different portions of the same rock (also of variable U/Pb), <u>should</u> fall along the same line on the Pb^{207}/Pb^{204} - Pb^{206}/Pb^{204} plot. Precisely such an effect is seen in Figure 6. Certainly it would be most desirable to have perfectly homogeneous powdered samples so that each 0.1-gram split would be truly representative. The replicate analyses made and above discussion suggest, however, that this may well not be essential for valid isochron diagrams using the uranium-lead system. It is noted in passing that a pattern such as is observed in Figure 6 is frequently not seen in a Pb^{208}/Pb^{204} - Pb^{206}/Pb^{204} plot; but such a pattern would

not in fact be expected unless the distribution and behavior of thorium and of uranium in the system were identical.

III. Statistical Treatment of Data

Before proceeding to discussion of the analytical results, a brief mention of the statistical treatment of the data is indicated.

Errors quoted in the following chapters will be $\pm$ 1σ limits. The errors cited will reflect the analytical errors (measurement uncertainties) for the individual runs only, and not take into account the reproducibility considerations outlined in this chapter, as the latter uncertainties are impossible to quantify. Since every run of the standards has produced ratios which agree within this single-run analytical error with the accepted values, it is assumed that each run of a sample gives, to the limits of its individual analytical imprecision, a true measure of that sample composition. This is not, of course, the same thing as saying that the given split of sample powder is representative of the whole.

Fitting of isochrons was carried out using a York (1969) Model II treatment, which provides for correlation of errors of data points and considers analytical errors in computing the uncertainties of the isochron parameters. Correlation of errors is an important consideration with both lead-lead and Concordia diagrams. One may derive, strictly from the known analytical errors, single-sample

correlation coefficients (r values) by the following method:

Consider a lead-lead diagram, which is a plot of Pb^{207}/Pb^{204} against Pb^{206}/Pb^{204}. Usually the value of Pb^{207}/Pb^{204} is calculated from measurements of Pb^{206}/Pb^{204} and Pb^{207}/Pb^{206}. Let $x = Pb^{206}/Pb^{204}$, $y = Pb^{207}/Pb^{206}$. Then the variance of the product xy (= Pb^{207}/Pb^{204}) is given by (Friedlander et al., 1967):

$$\frac{\sigma_{xy}^2}{x^2y^2} = \frac{\sigma_x^2}{x^2} + \frac{\sigma_y^2}{y^2} + \frac{\sigma_x^2\,\sigma_y^2}{x^2y^2} \quad .$$

The last term is sufficiently small in the present work that it may be discarded, so effectively

$$\sigma_{xy}^2 = \sigma_x^2\, y^2 + \sigma_y^2\, x^2 \quad ; \text{ or, if } \sigma_z = f_z z,$$

$$f_{xy}^2\, x^2y^2 = f_x^2\, x^2y^2 + f_y^2\, y^2x^2 \quad , \text{ so that}$$

$$f_{xy}^2 = f_x^2 + f_y^2 \quad .$$

The analytical-error correlation coefficient r for the sample is then $\partial f_{xy} / \partial f_x$, which means that

$$r = \frac{\partial f_{xy}}{\partial f_x} = \frac{1}{2}\left(f_x^2 + f_y^2 \right)^{-\frac{1}{2}} \left(2f_x \right) = \frac{f_x}{\sqrt{f_x^2 + f_y^2}}$$

Logically enough, the correlation coefficient r for the errors is then dependent on the relative magnitudes of the analytical errors of x and y only. For the case of a lead-

lead diagram, it is usually, but not invariably, true that $f_y < f_x$, and as f_y approaches zero, r approaches +1.

On a Concordia diagram, the quantities plotted are Pb^{206}/U^{238} and Pb^{207}/U^{235}. They are related as follows:

$$\frac{Pb^{207}}{U^{235}} = 137.88\left(\frac{Pb^{207}}{Pb^{206}}\right)\left(\frac{Pb^{206}}{U^{238}}\right)$$

When the relationship is written in this way, it is clear that a perfectly analogous derivation is possible for r in the case of a Concordia diagram. In this case, the uncertainty in the determination of Pb^{207}/Pb^{206} is much less than the uncertainty in Pb^{206}/U^{238}, which depends on determining the absolute amounts of uranium and lead in the sample, so r is almost always equal to +1.

The strong positive correlation of errors on these two types of diagrams should be borne in mind when looking at plotted error bars in subsequent chapters. Only in the case of simple isochron plots (Pb^{207}/Pb^{204} vs. U^{235}/Pb^{204} and Pb^{206}/Pb^{204} vs. U^{238}/Pb^{204}) does such correlation not exist. For the isochron plots, values of Pb^{206}/Pb^{204} and Pb^{207}/Pb^{204} are measured directly in the unspiked aliquot of lead, while U^{238}/Pb^{204} and U^{235}/Pb^{204} depend on the measured concentrations of lead and uranium determined from the uranium and spiked lead aliquots; clearly the errors of the former and latter quantities are uncorrelated (r=0).

The quality of the fit of points to a line is measured

by a mean square of weighted deviates (MSWD). For an infinitely large number of regressed points with precisely-determined experimental errors, where all points fit the line within these experimental errors, the value of MSWD should equal 1 or less. In the real world, the nature of small-sample regression is such that actual values of MSWD greater than one may not be inconsistent with the existence of an isochron, where an isochron is defined as a regression line along which all points fit within their experimental errors (Brooks et al., 1972). The practice of assigning experimental errors to the data points which are equal simply to the measured analytical uncertainty (the "noise" in the run) could lead to underestimation of the true experimental error. However, an increase in the experimental error assignment will lead to a decrease in MSWD (coupled with an increase in the error of the regression parameters, for the York Model II program), so in fact MSWD values quoted for the regression analyses in the present work will err on the high side, if at all. If a regression line appears to be a true isochron on the basis of assigned errors which may be unrealistically low, it is at least that good (Hart, personal communication). That is, increasing the assigned errors could only improve the apparent quality of fit (judging from the MSWD value). Therefore if the regression lines in the present study seem to be isochrons, rather than errorchrons, they probably are.

The following chapters contain detailed discussions of results from several different sets of samples from the Imataca Complex. Lead isotopic compositions of total-rock samples of gneisses are based on the second series of analyses as described above. Petrographic descriptions are listed in Appendix A. A brief outline of uranium-lead systematics and discussion of the various types of graphical representations used in presenting uranium-lead data are given in Appendix B.

4. Equilibrated Domains in a Banded Gneiss

I. Rubidium-Strontium Study

In view of the scattered results of the rubidium-strontium whole-rock analyses, other workers in the M.I.T. geochronology group decided to try a different approach to the problem of dating the Imataca, using a method pioneered by Krogh and Davis (1968,1969). A study was made of fine-scale variations in rubidium and strontium isotopes in a single rock specimen (Hurley et al., 1976b; Montgomery et al., 1977). A 30-kg block of fresh banded granulite gneiss was obtained from the excavation for the Guri Dam on the Caroni River (Figures 3, 16). The rock (sample number 8100A2) is charnockitic, composed primarily of quartz, K-feldspar (much of it perthitic), plagioclase, and hypersthene, with some biotite and actinolite, and minor zircon, apatite, opaques, garnet, calcite, chlorite, and (?)augite. Intensive deformation is indicated by considerable granulation along the boundaries of the large quartz and feldspar grains, and undulatory extinction in quartz.

Part of the block was cut, along planes parallel to the compositional layering, into a suite of 1-cm-thick slices, each of which was then treated as a separate total-rock sample. (For petrographic descriptions of individual samples, see listings for #8519 in Appendix A.) The rubidium-strontium results are plotted in Figure 7. Samples 5-10 form an isochron which is perfect within experimental

Figure 7. Whole-rock rubidium-strontium analyses of 1-cm slices from gneiss samples 8519. Note that sample #4 deviates from lower isochron outside of analytical error. After Montgomery et al. (1977).

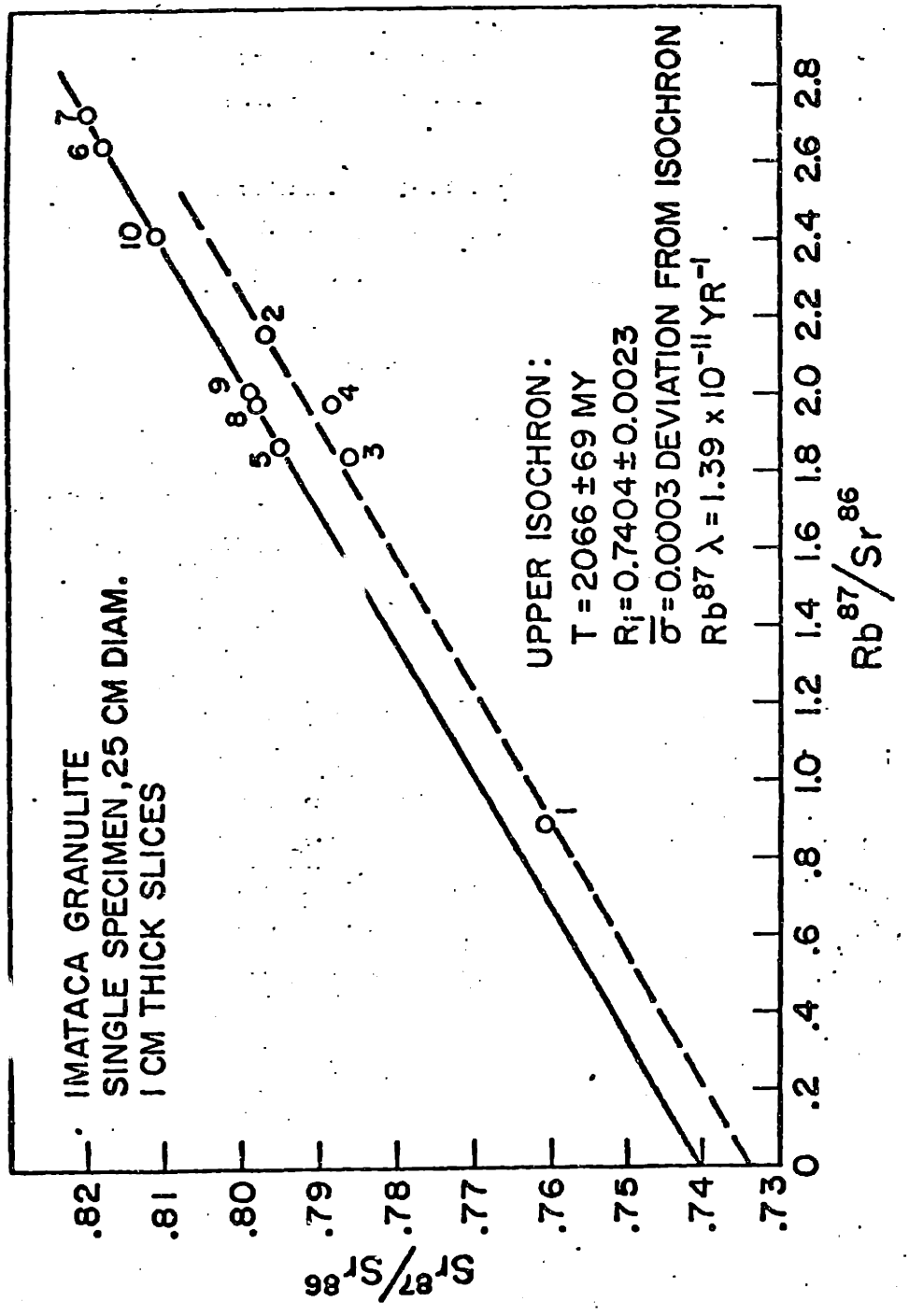
IMATACA GRANULITE
SINGLE SPECIMEN, 25 CM DIAM.
1 CM THICK SLICES
UPPER ISOCHRON:
T = 2066 ± 69 MY
R_i = 0.7404 ± 0.0023
$\overline{\sigma}$ = 0.0003 DEVIATION FROM ISOCHRON
Rb^{87} λ = 1.39 x 10^{-11} YR^{-1}
Sr^{87}/Sr^{86}
Rb^{87}/Sr^{86}
.82
.81
.80
.79
.78
.77
.76
.75
.74
.73
0 .2 .4 .6 .8 1.0 1.2 1.4 1.6 1.8 2.0 2.2 2.4 2.6 2.8
1
2
3
4
5
6
7
8
9
10

error, yielding an age of 2066 ± 69 m.y. The quality of this isochron, defined as it is by six adjacent 1-cm slices of the gneiss, indicates that at 2066 m.y. ago there was complete strontium isotopic equilibration over distances of at least six centimeters in this rock unit. These slices together then constitute what will be termed an "equilibrated domain". In fact, since no edge effects are observed over this distance, the actual equilibration distance, or size of the equilibrated domain, must be some centimeters greater. Six centimeters is a minimum, based on the Rb-Sr data. Bands 1-3 define nearly as good an isochron, parallel to the first, but with a different initial ratio of Sr^{87}/Sr^{86}; they constitute a second equilibrated domain. Band #4 falls off both isochrons. In hand specimen, this sample appears to consist of somewhat more coarsely crystalline material which could be interpreted as a micropegmetite or other injected material. (There is evidence for minor injections of granitic material throughout gneisses in the Guri Dam area - see Montgomery et al., 1977.)

It thus appears that at 2066 m.y. ago, some intense thermal metamorphic event resulted in the total equilibration of strontium isotopes through rock volumes centimeters across. Thereafter, a shearing deformation brought about the juxtaposition of blocks of rock from distinct equilibrated domains without disrupting the isotopic integrity

within each domain. Isotopic equilibration across the shear plane is not observed. Some minor addition of injected material may have occurred along the shear planes, but at sufficiently low temperatures that Sr isotopic equilibration between the injection and adjacent equilibrated domains is not seen at the 1-cm scale.

Of course, the 2066 m.y. age is a metamorphic age, reflecting the Transamazonian disturbance in the region; no additional light has been shed on the primary age of the Imataca granulites by the study outlined above. The rubidium-strontium data are, however, extremely helpful in the interpretation of the uranium-lead results obtained in the present study.

II. Uranium-Lead Results

The identification of equilibrated domains in the rubidium-strontium system raised the question of whether similar behavior might characterize the uranium-lead system as well. Accordingly, whole-rock lead and uranium analyses were carried out on the same suite of 1-cm gneiss slices, by the methods described in the previous chapter. Analytical results are listed in Table 2.

Since whole-rock lead isotope geochronologic data are most frequently plotted on a lead-lead diagram, this type of diagram was used initially to examine the data (Figure 8). The results were not precisely useful for geochronologic purposes, although some limited information can be obtained

TABLE 2. U-Pb analytical data from 1-cm gneiss slices, sample 8519

Sample	Pb^{208}/Pb^{204}	Pb^{207}/Pb^{204}	Pb^{206}/Pb^{204}	Pb, ppm	U, ppm	μ
1	43.67 ± 0.32	16.86 ± 0.07	18.86 ± 0.08	8.67	0.537	4.31
2	41.69 ± 0.14	16.46 ± 0.05	18.33 ± 0.04	22.4	0.786	2.36
3	40.17 ± 0.19	16.45 ± 0.08	17.75 ± 0.08	16.6	0.488	1.91
4	53.15 ± 0.23	16.78 ± 0.05	20.66 ± 0.06	35.1	2.90	6.55
5	44.66 ± 0.15	17.00 ± 0.03	18.93 ± 0.03	25.1	0.879	2.47
6	40.94 ± 0.16	16.23 ± 0.05	17.82 ± 0.05	24.4	0.754	2.03
7	39.50 ± 0.20	16.66 ± 0.06	17.96 ± 0.06	23.8	0.600	1.64
8	44.21 ± 0.16	16.56 ± 0.04	18.66 ± 0.04	19.0	1.26	4.61
9	46.84 ± 0.20	16.40 ± 0.04	18.77 ± 0.03	21.4	1.60	5.35
10	44.89 ± 0.15	16.38 ± 0.02	18.44 ± 0.01	25.8	1.42	3.84
11	41.12 ± 0.06	16.19 ± 0.01	17.67 ± 0.01	27.9	0.931	2.19
12	45.55 ± 0.15	16.32 ± 0.03	18.14 ± 0.03	28.2	1.33	3.30
K-feldspar composite	37.78 ± 0.10	16.28 ± 0.05	16.94 ± 0.04	29.7	0.075	0.16

All samples corrected for 13 ng Pb blank of composition Pb^{208}/Pb^{204} = 40.32, Pb^{207}/Pb^{204} = 16.30, Pb^{206}/Pb^{204} = 19.49; and 0.15 ng U blank where significant.

Errors quoted are 1σ standard error of the mean, analytical errors only.

Figure 8. Lead-lead plot of individual 1-cm slices, charnockitic samples 8519, Guri Dam. (Numbering scheme same as in Figure 7.) Error bars represent 1σ error of the mean. Reference growth curve is the mantle lead curve of Doe and Zartman (1977).

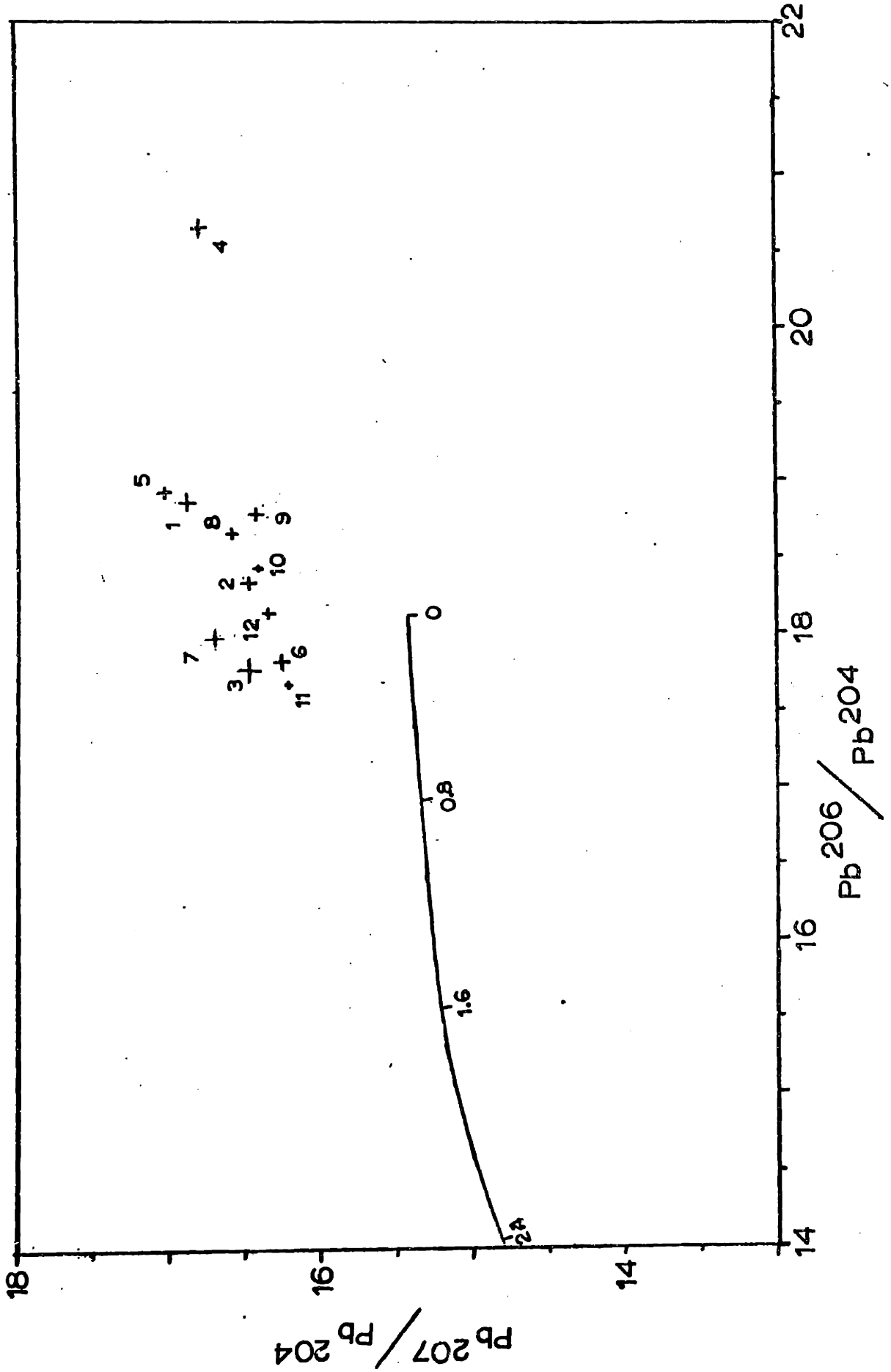
Pb207/Pb204
Pb206/Pb204
18
16
14
22
20
18
16
14
0
0.8
1.6
2.4
1
2
3
4
5
6
7
8
9
10
11
12

from the plot.

The lead data confirm the anomalous character of band #4, which contains appreciably more radiogenic lead than the rest of the samples. This is consistent with the observation that its μ value (Table 2) is higher than that of any other sample in the group.

The remaining data points form a loose cluster approximately centered above the zero point of the mantle growth curve of Doe and Zartman (1977). The position of the cluster relative to that curve suggests a period of evolution in a crustal environment (an environment of higher μ than the mantle), followed by depletion of uranium with respect to lead, so that evolution has most recently proceeded in a comparatively low-μ environment. This too is borne out by the measured μ values as shown in Table 2.

It is obvious from inspection of Figure 8 that the data do not define a linear array which could be interpreted as a secondary or tertiary isochron. Even if attention is focused only on slices from the larger equilibrated domain (as defined by the Rb-Sr data) by eliminating points 1-4, this situation is not greatly improved. The scatter cannot on the whole be attributed to sample-inhomogeneity problems. If lead isotopes were truly in equilibrium at the time of the 2.1-b.y. metamorphism, such that their current compositions defined an isochron, then analysis of nonrepresentative splits should simply produce points that

vary along the same trend, as discussed in the previous chapter. Moreover, for many of these samples, the two replicate analyses agree within experimental error, so the scatter is still more likely to be true geologic scatter. Alternative graphical means of presenting the data were then considered.

Whole-rock modified Concordia plots have only recently become popular (e.g. Ulrych, 1967; Russell et al., 1968). This is probably due to the often-unreliable behavior of uranium in exposed crustal rocks. In igneous rocks especially, much of the uranium may be located along grain boundaries, not locked into a crystal structure, since it is an "incompatible" element (Heier and Adams, 1965; Ahrens, 1965). Leaching and redistribution of the uranium by circulating modern groundwater may then be observed (Richardson and Adams, 1964; Rosholt et al., 1973). Such recent redistribution of uranium would of course distort the Concordia plot, although the usefulness of the lead-lead plot might be unimpaired.

The overall low uranium levels noted in Table 2, coupled with the present lead isotopic ratios, suggested that any intergranular uranium might have been lost earlier in the geologic history of the samples, during the dehydration which would have accompanied granulite-grade metamorphism. This would not preclude distortion of results by recent uranium addition, but at least leaching by

modern groundwater would be far less a potential problem. It was thought, therefore, that a Concordia plot might be useful here.

Figure 9 shows that this is so. The data points do approximate a linear array. There is no reason to expect *a priori* that samples from both equilibrated domains should define exactly the same line, so attention was concentrated only on the points of the larger equilibrated domain in order to make use of the maximum number of related samples. The quality of fit of these latter points to a single line is so good that even though the points all fall well above the Concordia curve proper, the errors in the intercepts with that curve are quite small (Figure 9(b)). These intercepts occur at 2.22 $\pm$ 0.04 and approximately 4.2 b.y.

Several things are shown by the Concordia plot:

1. The samples have been subjected to severe depletion of uranium relative to lead at some time in their history. (This is indicated by their position relative to the standard Concordia curve.) Depletion factors may be graphically estimated at from two to seven, depending on the sample. Such uranium depletion is known to be characteristic of granulite facies metamorphism (Fahrig *et al.*, 1967; Sighinolfi, 1971; Gray and Oversby, 1972). The event represented might be that responsible for the extensive homogenization of strontium isotopes also, which implies that the 2.1-b.y. event was the granulite metamor-

Figure 9. Whole-rock modified Concordia plot, banded gneiss 1-cm slices. Present measured values corrected for primordial lead composition of Tatsumoto et al. (1973).

(a) Dashed line represents best fit to points 5-12. Regression parameters for this line: slope = 0.0091336 $\pm$ 0.0000076, intercept = 0.34020 $\pm$ 0.00320, MSWD = 16.1 .

(b) Detail of (a) showing intersection of line (solid) with Concordia curve. Dashed error limits are, as usual, $\pm 1\sigma$. Younger intercept with Concordia is at 2.22 $\pm$ 0.04 b.y. Single dotted-dashed line is fit without points 5 and 7 (see text). Its regression parameters are slope = 0.0094934 $\pm$ 0.0000113, intercept = 0.24864 $\pm$ 0.00324, MSWD = 12.6. Its younger intercept with Concordia is at 1.62 $\pm$ 0.04 b.y.

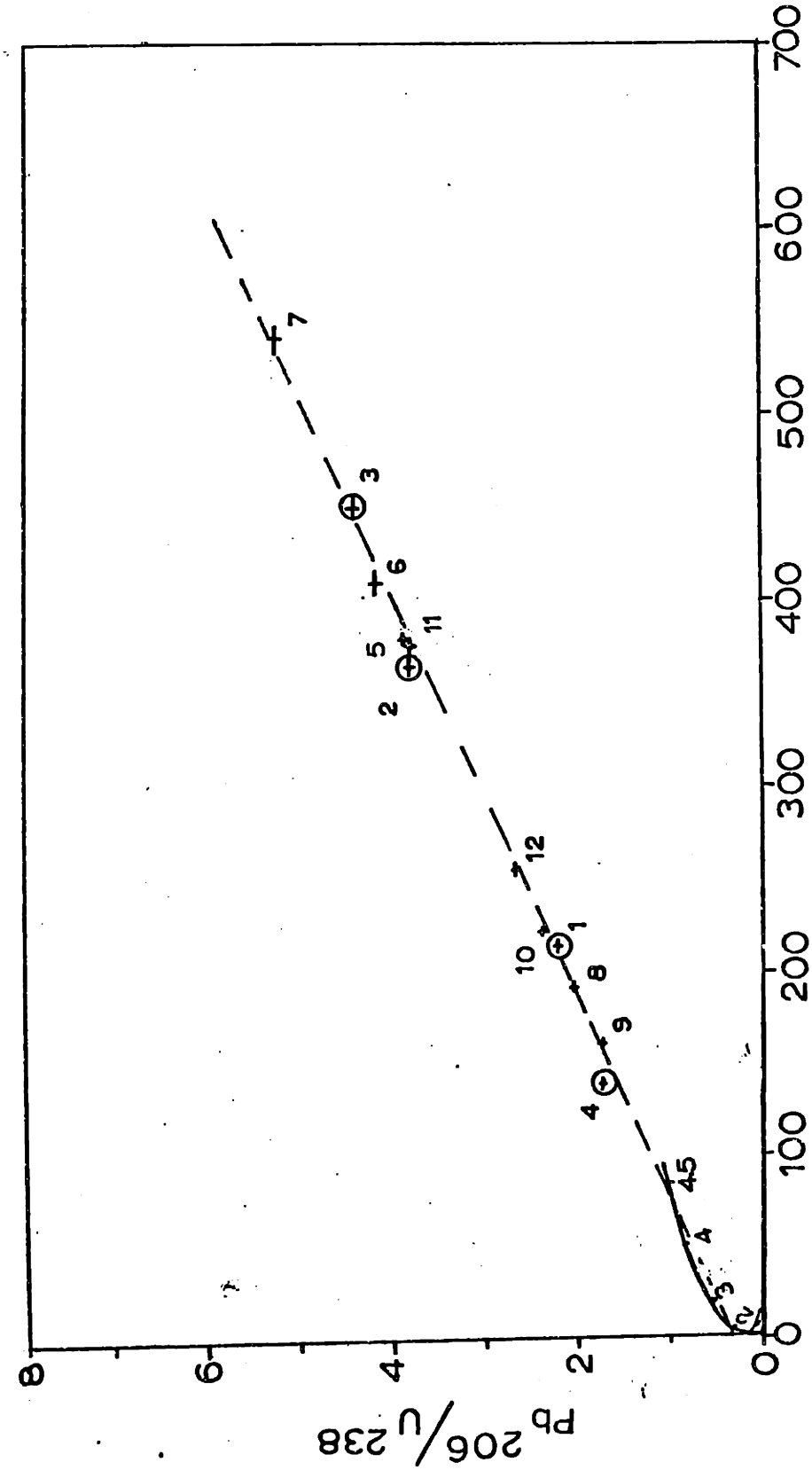
Pb^{206}/U^{238}
Pb^{207}/U^{235}
0
2
4
6
8
100
200
300
400
500
600
700
1
2
3
4
5
6
7
8
9
10
11
12
45

(a)

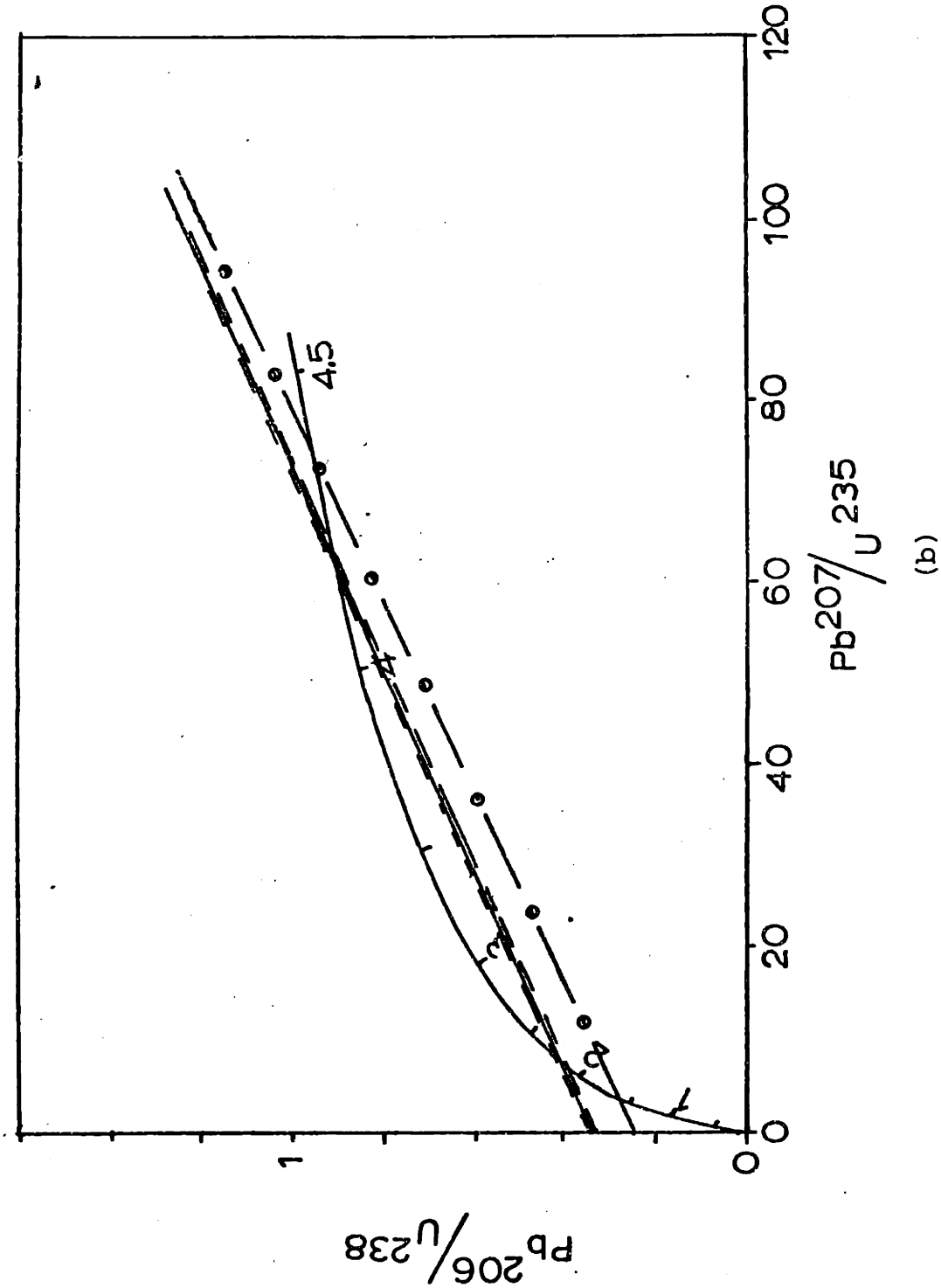
0
20
40
60
80
100
120
Pb207/U235
(b)
0
1
Pb206/U238
4.5
4
3
2
1

phism. Any subsequent retrograde thermal disturbance resulted at most in small perturbations of the data, which is also consistent with other investigators' findings (Heier and Thoresen, 1971).

2. Modern weathering has not greatly altered the uranium-lead isotopic composition of the system, so measured quantities fairly accurately reflect the last-stage evolution of the system. Scatter about the line on the Concordia plot may be attributed partially to the small scatter in the lead data and partially to some relatively minor modern redistribution of uranium. It would be difficult to preserve such a coherent arrangement of points in spite of large recent weathering effects. (We will return to the question of recent disturbance of uranium later in this chapter.)

3. The history of these samples may be approximated by a comparatively simple evolutionary model. To see why this is so, it is necessary to consider the significance of this linear array and the possible significance of the intercepts in Figure 9(b).

The nature of lead isotope evolution is such that only a two-stage or special case of three-stage model, or the equivalent, will result in a straight line on a lead-lead or modified Concordia diagram (Gale and Mussett, 1973). Higher-order models will yield straight-line plots only if they can be reduced to one of these simpler models. For example, if the duration of the last stage of a four-stage

history is known, the lead produced during that stage can be subtracted from the present measured lead, and the "age-corrrected" lead-lead diagram treated as for a three-stage case. The conditions under which linear plots are obtained in the three-stage case are for either $f_{1i} = \mu_1/\mu_{2i}$ = constant or $f_{2j} = \mu_{2i}/\mu_{3j}$ = constant (see Appendix B for discussion and illustration of these cases).

Evolution of the Imataca has obviously not been two-stage. An ititial stage during which lead isotope evolution proceeded in the mantle must be assumed. Thereafter at least two further stages must be postulated: a premetamorphic and a postmetamorphic crustal stage, where the metamorphism is the Transamazonian granulite event. Even in the absence of other geologic and lead isotopic evidence of the antiquity of the protolith, the elevated Sr^{87}/Sr^{86} initial ratios of 0.734 - 0.740 in Figure 7 suggest a considerable prehistory in the crust before the 2066 m.y. event.

The f_2 = constant case is, on consideration, geologically unlikely. The probability that a uranium-depletion event as severe as that indicated would cause the loss of a constant fraction of the uranium from each sample is quite slim. It is easier to imagine that during the formation of the protolith, the material separated from the mantle with essentially a homogeneous μ_2 value throughout, to keep $f_1 \cong$ constant. Slight deviation from constant f_1 would explain the small scatter of the points on the lead-lead

plot while not disturbing appreciably the linearity of the Concordia array.

But if the history is approximately equivalent to a three-stage f_1 = constant model, then at least one of the Concordia intercepts, the younger one, is meaningful (Gale and Mussett, 1973). The fact that it coincides in this case with the Rb-Sr age adds support to the supposition made earlier, that the uranium depletion event and the strontium isotopic homogenization episode were one and the same, namely the granulite metamorphism.

With a history of more than two stages, the older intercept with Concordia is <u>not</u> meaningful. Still, it may be possible to arrive at t_1, the end of the first stage, by extrapolation from known data.

It should be realized first that on a lead-lead diagram, a three-stage or higher-order model of variable f's with a lead isotopic homogenization episode at the end of the penultimate stage is formally identical with the three-stage f_1 = constant case, insofar as one may derive the time of the start of the last stage from the slope of the present array. In the former instance, however, incomplete homogenization of lead isotopes would result in a scatter in the present lead isotopic compositions, such as we see in Figure 8. Again, some scatter in the Concordia diagram would also result if a three-stage f_1 = constant model is not quite appropriate, but provided that it is approxi-

mately correct, the scatter will be minimal. If the uranium depletion were the last major event before the present, the younger Concordia intercept will still be significant.

We shall return later to the question of whether a special three-stage or restricted higher-order model is most appropriate to the present case. For the moment, a three-stage $f_1 \cong$ constant model will be provisionally assumed correct.

III. Three-Stage Lead Isotope Evolution Model

Consider next a hypothetical evolution of lead isotopes for this gneiss, shown on a generalized lead-lead diagram in Figure 10. The system develops in the mantle from t_i to t_1 and thus follows the mantle growth curve during that interval. At t_1, the lead isotope composition corresponds to point A. At this point the system is differentiated from the mantle and emplaced into the crust. Suppose that the subsystems share a common μ_2 value (varying within a restricted range only) or that they are homogenized at t_2. The lead-lead plot (Figure 8) indicated that, as would be expected from fundamental geochemical principles, the mean μ_2 value is somewhat higher than that of the mantle. During the period t_1 to t_2 the system evolves without major disturbance. Since the subsystems began with the same lead isotopic composition at t_1, any minor mixing or homogenization episodes between t_1 and t_2

Figure 10. Hypothetical model of lead isotope evolution according to a three-stage $f_1 \cong$ constant model. (For explanation, see text.)

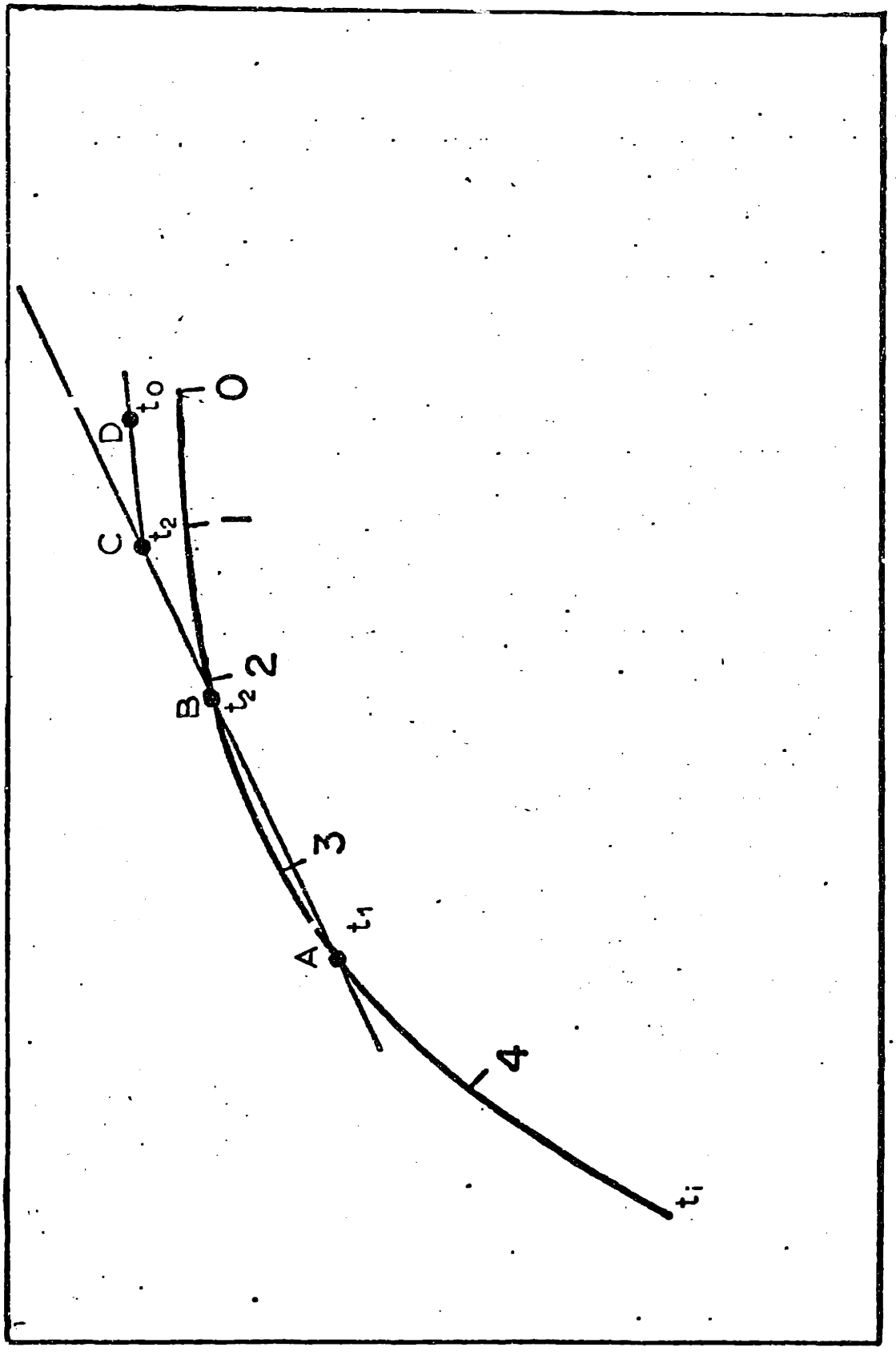
Pb^{207}/Pb^{204}
Pb^{206}/Pb^{204}
0
1
2
3
4
A
B
C
D
t_0
t_1
t_2
t_2
t_i

can only serve to bring the subsystems closer to a single common apparent μ_2 value and a single second-stage evolution curve. Provided only, then, that no additional material from some other system is introduced, at time t_2 the subsystems will have lead isotopic compositions that cluster about point C along line ABC, where B is the composition of mantle lead at time t_2, whether they shared a common pre-metamorphic μ_2 value or were homogenized with respect to lead isotopic composition during the metamorphism. At t_2 the uranium depletion occurs also, resulting in an assortment of μ_3 values all less than the μ_2 value. So from t_2 to the present, evolution continues in a series of low-μ subsystems. At the present time, the lead isotope compositions measured should all fall along line C-D, the tertiary isochron, whose slope corresponds to age t_2.

As has already been noted, the points in Figure 8 do not fall along a well-defined line C-D. The vertical scatter is likely to reflect variability in f_1, coupled with incomplete lead isotopic homogenization at t_2. However, the tertiary isochron would be of only limited usefulness anyway, for already we essentially know t_2, from the Rb-Sr data and Concordia plot. The time t_1, the "primary age" of the protolith, is of far more interest. If we could find point C, then given t_2 we could extrapolate back to A (and t_1).

IV. Extrapolation to the Apparent Protolith Age

Isochron diagrams (Figures 11 and 12) make this extrapolation possible. Again the samples from the larger equilibrated domain only are used for the extrapolation, to avoid the confusion of data from two possibly dissimilar systems. The age t_2 is provisionally chosen as 2.066 b.y., based on the Rb-Sr results. A line with slope corresponding to this age is passed through the average of all points from the larger equilibrated domain except 5 and 7, which fall away from the coherent grouping of the rest on both isochron diagrams. The y-intercept values of Pb^{206}/Pb^{204} and Pb^{207}/Pb^{204} represent the lead isotope initial ratios, the average lead isotopic compositions which characterize the subsystems at time t_2. These then define the coordinates of point C. The initial ratios so determined are $Pb^{206}/Pb^{204} = 16.91$, $Pb^{207}/Pb^{204} = 16.18$. Maximum probable errors estimated from vertical freedom in positioning the 2.066 b.y. reference isochrons are $\pm$ 0.1 for each ratio. If lines are fitted to the same points without regard to slope constraints, the results are: Pb^{206}-U^{238} diagram, slope = 0.33783 $\pm$ 0.01338, for a slope age of 1.88 $\pm$ 0.07 b.y., with an initial ratio of 17.05 $\pm$ 0.05; Pb^{207}- U^{235} diagram, slope = 11.657 $\pm$ 1.561, for a slope age of 2.58 $\pm$ 0.14 b.y., with an initial ratio of 16.04 $\pm$ 0.04. The intercepts thus obtained are within the errors assigned to the intercepts derived

Figure 11. Pb^{206}/Pb^{204} - U^{238}/Pb^{204} isochron diagram, banded gneiss slices. Circled points omitted from isochron fitting; points also boxed are from the smaller equilibrated domain, samples 1-3. Line shown has a slope age of 2066 m.y. and is forced through the average of the points used. The initial ratio thus obtained is Pb^{206}/Pb^{204} = 16.91 .

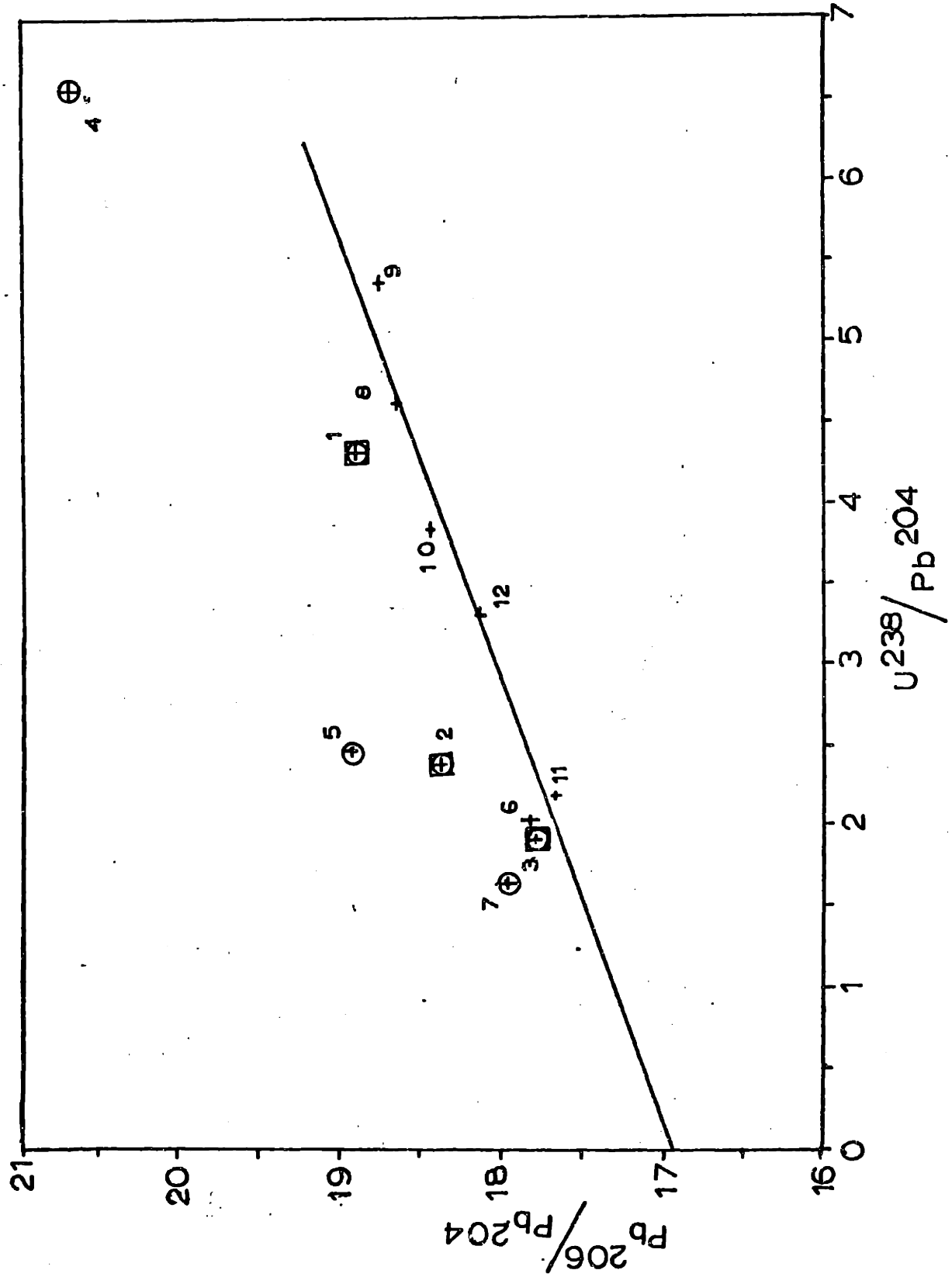
Pb206/Pb204
U238/Pb204
21
20
19
18
17
16
0
1
2
3
4
5
6
7

Figure 12. Pb^{207}/Pb^{204} - U^{235}/Pb^{204} isochron diagram, banded gneiss slices. Points and procedure used for line fitting identical to those of Figure 11. The initial ratio in this case is Pb^{207}/Pb^{204} = 16.18 .

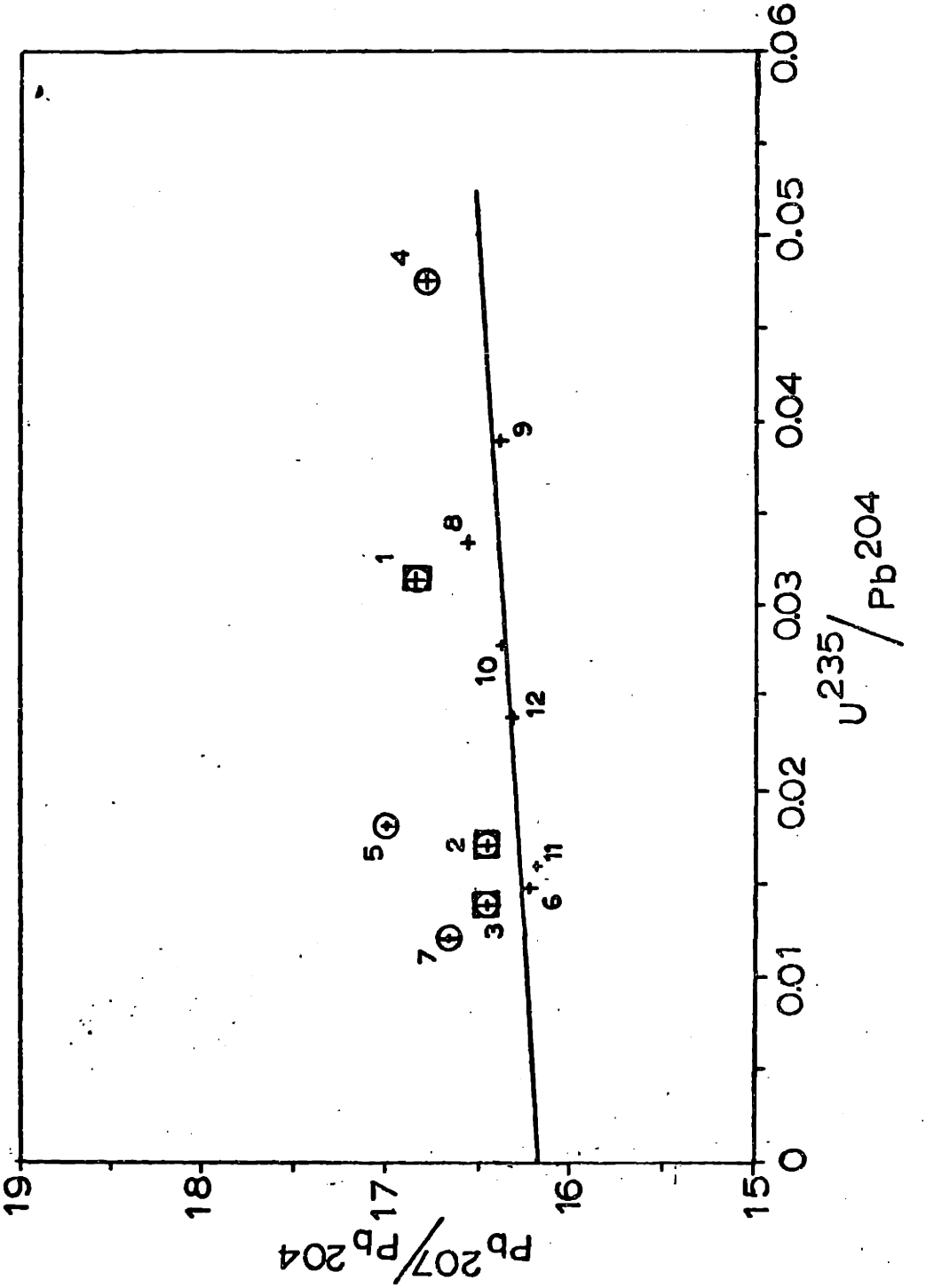
19
18
17
16
15
0
0.01
0.02
0.03
0.04
0.05
0.06
Pb^{207}/Pb^{204}
U^{235}/Pb^{204}
1
2
3
4
5
6
7
8
9
10
11
12

by the constrained-slope approach. The constrained-slope intercepts, with their errors, are then acceptable estimates for point C.

The point C thus defined is projected back through the 2.066 b.y. point on the primary growth curve to an older intercept (Figures 13 and 14). Depending on the model chosen, the intercept age t_1 is in the 3.5-3.6 b.y. range, and is fairly model-independent. (Even considering the maximum probable errors on C only increases the range to 3.4 - 3.7 b.y.) This, then should be an estimate of the primary age of the system, subject to uncertainties in the initial ratios and precise projection point.

The reader might suggest that the practice of applying geochronologic data from one isotopic system to another is of questionable validity. The following arguments are advanced as justification in this instance:

1. The same type of sample (i.e. total rock) and the same scale of sampling are used in both cases; in fact the actual samples chosen are the same.

2. The scale of sampling is small. On a scale of meters, the Rb-Sr and U-Pb systems might well behave significantly differently, but on the 1-cm scale, differences are likely to be minimal.

3. Equilibration of strontium was quite complete, within each domain, at 2.066 b.y.; it seems highly improbable that nearly-complete equilibration of lead isotopes

Figure 13. Back-extrapolation from whole-rock initial lead isotopic composition through 2066-m.y. point on growth curve I. Error circle around initial ratio point estimated from vertical freedom of the isochron plots in Figures 11 and 12 (see text). Reference growth curve is mantle lead evolution curve of Doe and Zartman (1977).

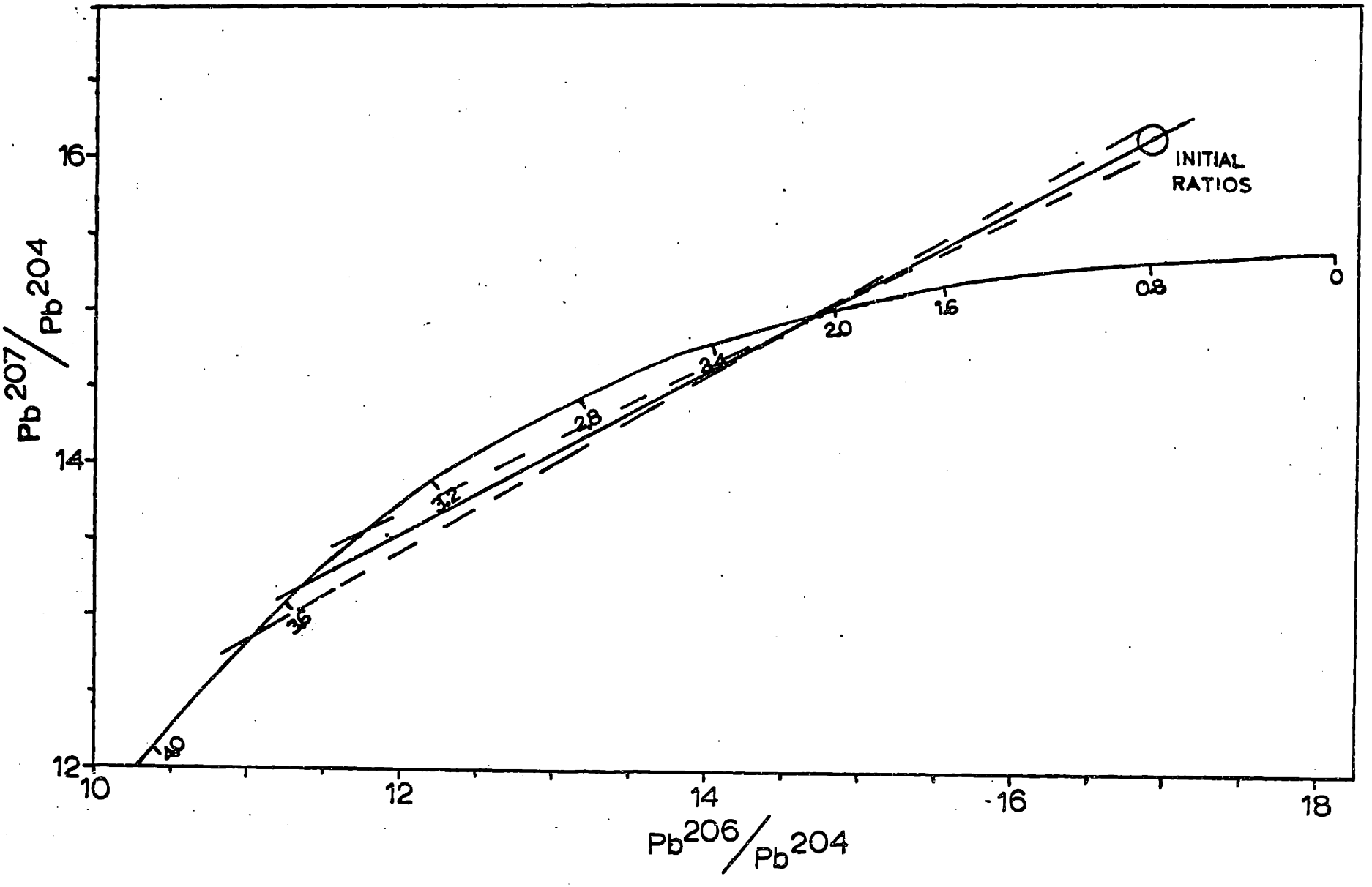
INITIAL RATIOS
0
0.8
1.6
2.0
2.4
2.8
3.2
3.6
4.0
16
14
12
10
12
14
16
18
Pb207/Pb204
Pb206/Pb204

Figure 14. Back-extrapolation from whole-rock initial lead isotopic composition through 2066-m.y. point on growth curve II. Error circle same as that in Figure 13. Reference growth curve is that of Stacey and Kramers (1975).

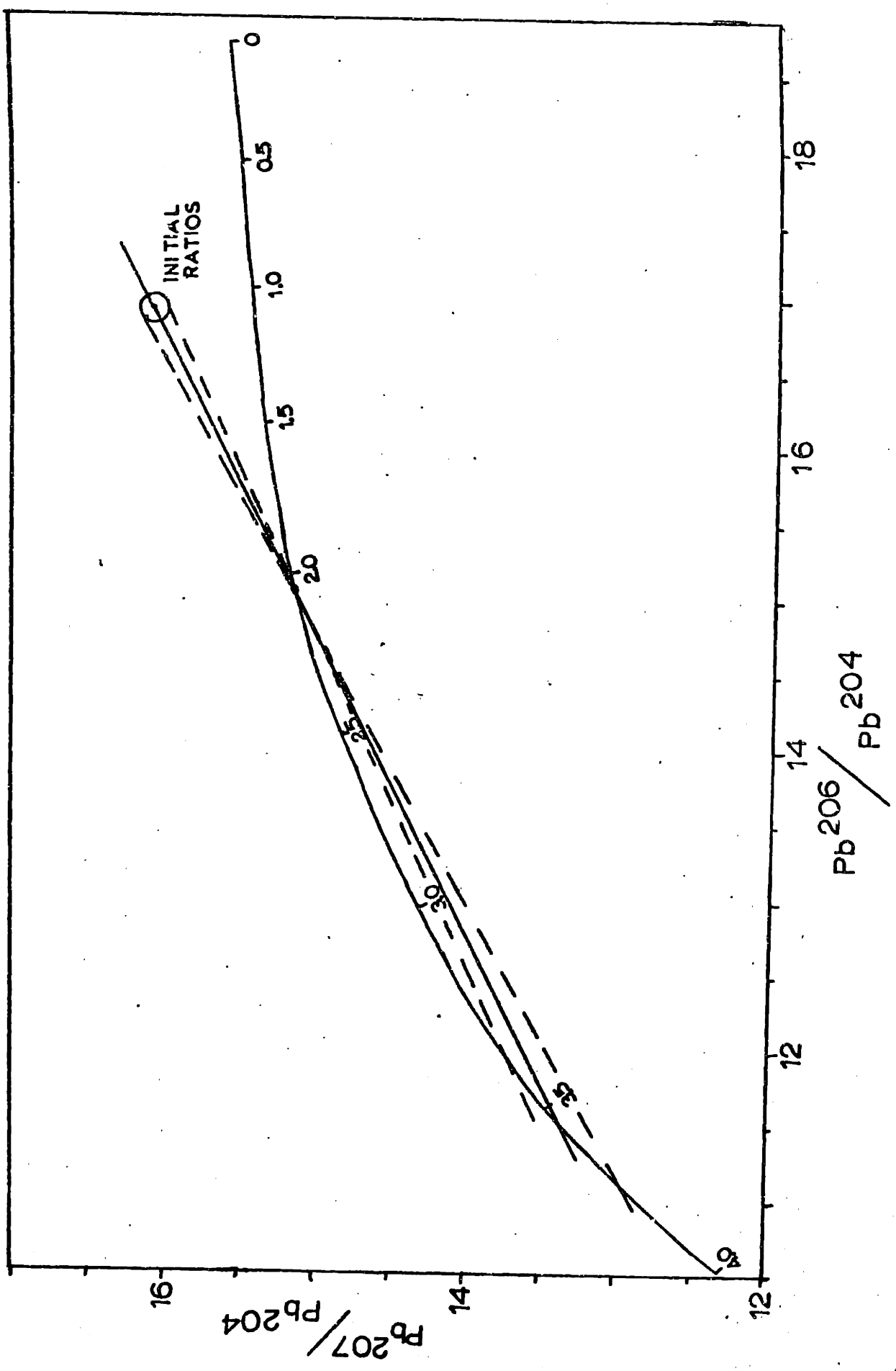
INITIAL RATIOS
0
0.5
1.0
1.5
2.0
25
30
35
40
12
14
16
18
Pb^{207}/Pb^{204}
Pb^{206}/Pb^{204}

should not have occurred then also as a result of the same event.

4. The 2.066 b.y. isochrons constructed in Figures 11 and 12 fit the U-Pb data quite well, further supporting the inference drawn from the Concordia plot that this date, or something very close to it, is significant in the U-Pb system also.

Item 4 above has additional implications. In particular, it suggests that the earlier conclusion that recent perturbation of μ values in the system was minimal is basically sound. Any modern redistribution of uranium would account for the scatter in both the isochron and Concordia diagrams.

The validity of the three-stage model approximation may also be crudely tested. Using present measured μ values, which should in most cases be essentially correct, we can age-correct the lead isotopic compositions of the samples back to about 2.1 b.y. (Figure 15). We find that these age-corrected points lie along or very close to a reference line through 2.1 b.y. and the inferred primary age on the mantle growth curve, which is perfectly consistent with a three-stage model with some variation in f_1. Scatter along the line reflects this variability in μ_2 values, incompletely masked by lead isotopic homogenization at t_2. Scatter about the line would simply mean that measured μ values are not perfectly representative of

Figure 15. Age-corrected compositions of banded gneiss slices. Anomalous band #4 omitted from diagram. Crosses represent present measured lead isotopic compositions; circles, compositions corrected to 2.1 b.y. ago on the basis of measured μ values. Age-corrected points fall approximately along a reference line through 2.1 b.y. and the inferred primary age t_1 on the growth curve. Reference growth curve, mantle growth curve of Doe and Zartman (1977).

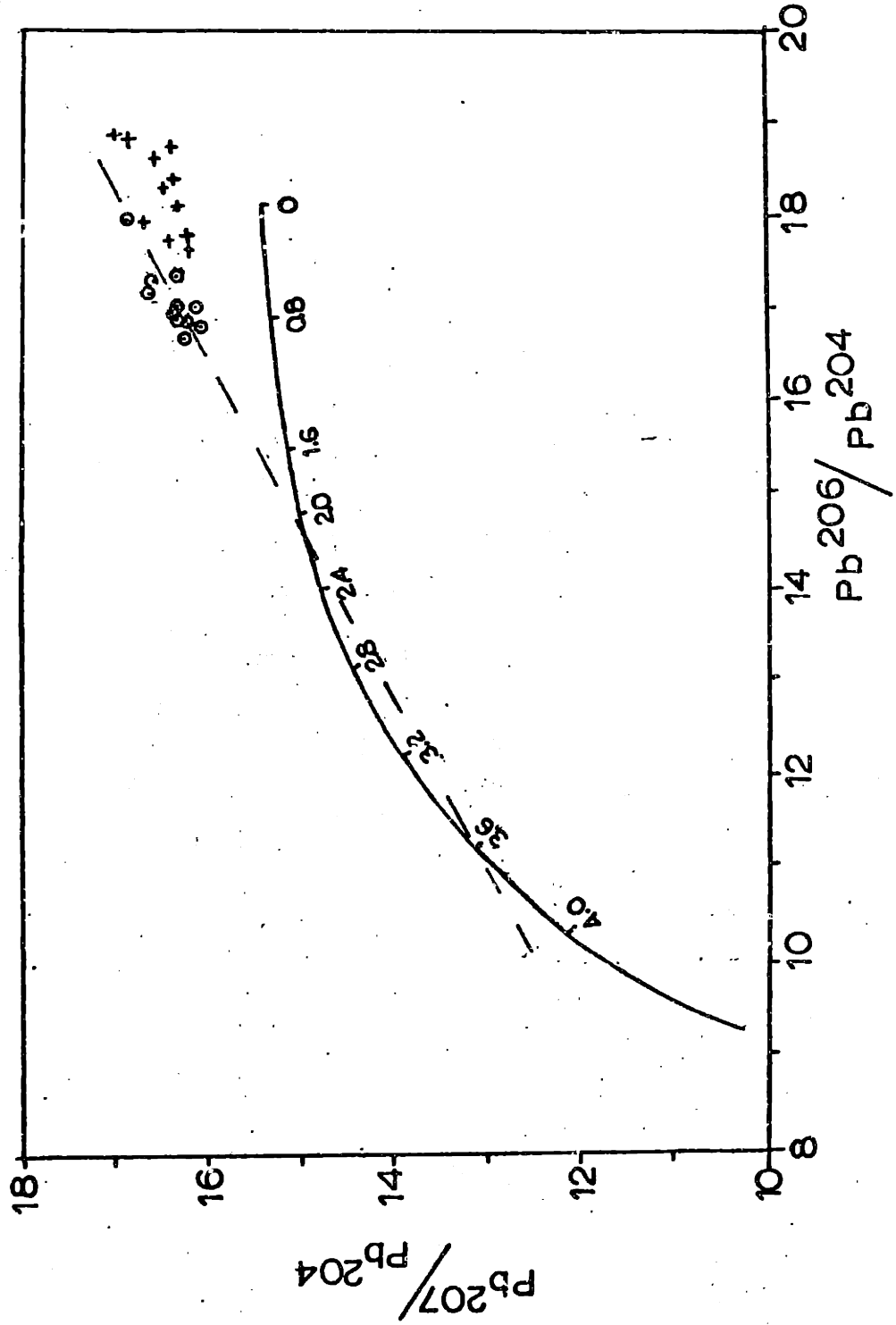
Pb207/Pb204
Pb206/Pb204
18
16
14
12
10
8
10
12
14
16
18
20
0
0.8
1.6
2.0
2.4
2.8
3.2
3.6
4.0

true third-stage μ values, a problem which was anticipated from the scatter in the isochron diagrams.

It may be asked why the 2.1-b.y. Rb-Sr age, rather than the 2.2-b.y. Concordia age, was chosen for the age-correction in Figure 15. Actually, the 0.1-b.y. difference would really have a negligible effect on corrected compositions, and the two ages do in fact agree within their error limits at the 95% confidence level. However, the Rb-Sr age was considered to be the more reliable, despite the apparently-high precision of the Concordia age. When points 5 and 7, which appeared on the basis of the isochron diagrams to be unusual, are omitted from the line fitting in Figure 9, the regression parameters change drastically, to a slope of 0.0094934 $\pm$ 0.0000113, intercept 0.24864 $\pm$ 0.00324, with a new younger Concordia intercept of 1.62 $\pm$ 0.04 b.y. This result casts doubt on the significance (accuracy) of the exact intercept value of any one line constructed, although the general similarity of Rb-Sr and Concordia ages is probably still worth noting. Since there exists uncertainty as to the precise time of uranium depletion as deduced from the U-Pb data, the well-established Rb-Sr date for the granulite event was used.

Suppose next that the actual end of the U-Pb equilibration/ U depletion was somewhat later than this Rb-Sr metamorphic age - for example, nearer to 1.6 b.y. The initial ratio point C shifts very slightly to the right, but the

projection point B shifts considerably further to the right, to the 1.6-b.y. point on the mantle growth curve. The net result is that the apparent t_1 is then older: 4 b.y. or more. This is not particularly reasonable geologically. Recent models of the earth's early thermal history (Oversby and Ringwood, 1971; Murthy and Hall, 1970; Boulos and Manuel, 1971) do suggest that core infall and its attendant heating of the earth should have been essentially complete within 10^8 years or so of accretion, so the upper limit for the age of the first stable crust is not constrained to such low values as formerly thought probable (e.g. Hanks and Anderson, 1969). Still, there is no reliable radiometric date on any terrestrial rock greater than about 3.8 b.y., so this is more likely to represent the earliest time from which any quantity of crustal material is preserved. The derived t_1 value thus rather closely approaches the (resonable) maximum possible. Conversely, there is no convincing evidence from the U-Pb data for a $t_2 \gg$ 2.1 b.y., so our graphically-derived t_1 value is probably a minimum realistic value for this three-stage model.

V. The Use of Feldspar Lead Isotopic Composition

In some instances it may not be necessary to go to all the effort of constructing the isochron diagrams, which are after all potentially subject to error if uranium has been

recently disturbed, in order to generate point C. Analysis of a low-μ phase such as potassium feldspar may provide the necessary data. The composition of the composite K-feldspar separate from the gneiss samples, listed in Table 2, is $Pb^{206}/Pb^{204} = 16.94 \pm 0.04$, $Pb^{207}/Pb^{204} = 16.28 \pm 0.07$. Correcting for the minor feldspar uranium ($\mu = 0.16$) back to 2.066 b.y. changes these ratios only slightly, to $Pb^{206}/Pb^{204} = 16.88 \pm 0.04$, $Pb^{207}/Pb^{204} = 16.27 \pm 0.07$. This age-corrected feldspar composition coincides with the whole-rock initial ratio values within the estimated uncertainty in the initial ratio determination. The feldspar composition thus projects back into the same age-range as did the whole-rock initial ratio point with its errors.

Such behavior will, of course, only be observed where any subsequent thermal disturbance of the system has not caused appreciable re-equilibration between the feldspar and whole-rock lead isotopes. This condition seems to be satisfied in the present instance, despite the 1200-m.y. Rb-Sr mineral isochron mentioned previously, further suggesting that the "Kibaran" thermotectonic episode was of low intensity in this region of the Imataca. In general, however, it can be difficult to say confidently that the feldspar composition can be used for point C in the absence of the whole-rock work, unless other data indicate unequivocally that no significant metamorphism has occurred after the time of interest.

VI. General Discussion

The 3.5-3.6 b.y. lead age indicates indirectly that the apparent Rb-Sr ages are not artificially old as a result of rubidium loss during the granulite event. Rubidium loss had been considered a possibility when the extensive uranium loss was discovered; Rb loss also is frequently characteristic of highgrade metamorphic terranes (Heier and Thoresen, 1971; Sighinolfi, 1971). But the projected lead age is at the upper end of the range of the scattered rubidium-strontium apparent ages, so it seems that actually no great loss of Rb relative to Sr occurred during the Transamazonian granulite metamorphism. It is tentatively suggested that the abundance of K-bearing phases is responsible for the conservation of rubidium. Uranium acceptor phases (e.g. zircon) are, by contrast, present in extremely small amounts, which could explain the widespread U loss. Scatter in the large-sample whole-rock Rb-Sr results is attributed to incomplete equilibration between adjacent equilibrated domains, and the trend toward younger (3 b.y.) values simply to the minor injections previously deduced from other Rb-Sr data (see Montgomery et al., 1977).

The chronology of injection and shearing can be re-examined with reference to the anomalous point 4 and Figure 9(a). Note that this sample has apparently also suffered some depletion of uranium relative to lead. Its

position on the Concordia diagram is unfortunately ambiguous: it does not precisely fall along the uranium-depletion trend of the other slices. It could therefore have been depleted in uranium at 2 b.y. starting from a slightly different composition point from the rest of the samples', or it may only have suffered modern uranium depletion. Without knowing the lead isotopic composition of this sample at 2 b.y. ago, there is no way to distinguish between these possibilities from the U-Pb data. Lack of strontium isotopic equilibration with adjacent equilibrated domains indicates emplacement at or near the end of the Transamazonian event, but is conceivable that injection took place early enough that some uranium depletion of the injected material occurred before the system had cooled down entirely. The shearing which juxtaposed the two equilibrated domains, presumably prior to the injection, could have occurred late in the metamorphic period, rather than long afterward.

The tentative regional history outlined in Chapter 2 on the basis of earlier geologists' work can be amended using the U-Pb data. Previously, a period of amphibolite to granulite grade metamorphism had been postulated around the time of the emplacement of the La Ceiba migmatite (about 2.7 b.y., as dated by Hurley et al., 1973). The Concordia plot (Figure 9) indicates instead that a regional event of such intensity did not take place at that time. Either amphibolite or granulite metamorphism

would be expected to result in uranium depletion (Fahrig et al., 1967). The rubidium-strontium data identify one intense thermal event at about 2.1 b.y. It is difficult to superimpose two events of episodic U loss without destroying the linearity of the Concordia plot. At each time of episodic loss, each point will move an unspecified distance along a straight line directly away from that time on the Concordia curve (Wasserburg, 1963). Clearly two such episodes, at 2.7 and 2.1 b.y., should result in a scatter of points in a region bounded by the episodic uranium-loss lines corresponding to each of these two times. Such a distribution is not observed in Figure 9. The present arrangement of points could possibly be produced by episodic loss of uranium at 2.7 b.y. followed by a 2.1-b.y. loss which for each sample was proportional to the 2.7-b.y. depletion, but such behavior seems highly improbable. Therefore only one highgrade metamorphic event is likely to have affected these samples.

VII. Significance of the Protolith Age

There still remains a question about the significance of the derived "primary age" or "protolith age" t_1. Clearly it indicates the time of the first major change of μ in the system; this is presumably the time of separation from the initial (mantle) system, if the history is three-stage. However, t_1 bears no simple interpretation unless the protolith is igneous. (The term "protolith"

is here restricted to mean the crustal rock which was the immediate precursor of the metamorphic rocks as we now see them.) In the case of the samples discussed in this chapter, an igneous protolith is unlikely.

The rocks contain almost no mafic phases, being composed predominantly of quartz and feldspar. Such mineralogy would certainly be appropriate to a granite. But the zircon in these samples occurs principally as extremely well-rounded, sometimes even slightly pitted grains - grains, in other words, with a characteristically detrital appearance. Many of the grains do show some facets, but these could be either relict facets not entirely obliterated by mechanical rounding, or the first hint of metamorphic refaceting, rather than an indication that these are primary igneous zircons which crystallized in a spheroidal habit. While metamorphic recrystallization of zircon well below granulite facies conditions is possible, cases in which detrital zircons have survived high-grade metamorphic conditions are documented (see, for example, Eckelmann and Kulp, 1956; Stern et al., 1965; Gastil et al., 1967). Somewhat rounded zircons may be produced by metamorphic overgrowths on older cores (e.g. Grauert and Hall, 1973), but obvious cores are not observed in the rounded zircons in the present instance. On the whole, then, the well-rounded (as distinguished from merely equidimensional) zircons are taken as indicating a sedi-

mentary protolith for this gneiss.

Consequently a three-stage model for lead isotope evolution cannot necessarily be justified. The premetamorphic crustal stage must, strictly, have consisted of two stages: a period of evolution in the igneous source region of the eventual sediments, and a premetamorphic evolution in those sediments. The exact interpretation of the 3.5-3.6 b.y. "age" then depends on the nature of the events marking the ends of the first two stages in this four-stage history, for both of these events could potentially alter the μ of the system.

If the differentiation of the igneous source region occurred with no change in μ, the result is graphically identical to the three-stage case, and the "primary age" is really the time of sedimentation. Conversely, if the igneous differentiation caused the major change in μ, and the average μ of the sediments as represented by our initial ratio point was the same as that of the igneous source region, a three-stage model applies, but the "primary age" is then the time at which the source region was formed, and provides no information on the time of sedimentation.

The most probable case involves a change in μ during igneous differentiation and a change in average μ during sedimentation. Still, Figure 15 suggests that a three-stage model is approximately correct. It is therefore suggested

that the period between source region differentiation and sedimentation was comparatively short; the derived "primary age" of 3.5-3.6 b.y. is then likely to be a hybrid age bounded by the times of these two events. Such an interpretation is consistent with what limited geologic constraints we have, namely the maximum resonable age for the source region, as discussed earlier, and the minimum date for the sedimentation, which is just prior to the event represented by the emplacement of the La Ceiba migmatite and related granitoid rocks. These are broad limits only; actually the source region differentiation and weathering/sedimentation were probably much closer in time, if a three-stage model is approximately correct.

VIII. Summary

The important conclusions of this chapter, based on the combined U-Pb and Rb-Sr results, may be summarized as follows:

1. The banded gneiss block investigated has been subjected to metamorphism of granulite grade. This granulite event is dated at 2066 $\pm$ 69 m.y. by a "perfect" Rb-Sr isochron defined by a suite of 1-cm-thick slices of that block.

2. The granulite-grade metamorphism had several significant chemical effects. Strontium isotopes were homogenized over distances of the order of 10 cm at least; less-complete equilibration of lead isotopes took place on a

similar scale at the same time. Severe depletion of uranium relative to lead also occurred then. However, there is no evidence for corresponding depletion of rubidium.

3. Late in or following the metamorphic pulse, shearing deformation took place throughout the system. It may be that this shearing is associated with the large-scale deformation which produced the regional trend.

4. Any material injected along the shear planes was added at sufficiently low temperatures that isotopic equilibration with adjacent "equilibrated domains" is not observed at the 1-cm scale.

5. U-Pb isochrons corresponding in slope to the Rb-Sr age were constructed to obtain "initial ratios" of lead isotopes at the time of the granulite metamorphism. These initial ratios define a point on the lead-lead diagram which may be projected back through the mantle growth curve to an apparent "primary age" of 3.5-3.6 b.y.

6. While this primary age confirms the antiquity of the protolith, its precise significance is unclear. The U-Pb data do suggest that the history of this gneiss may be approximated by a three-stage evolutionary model. The "primary age" is therefore interpreted as a hybrid age: some time between the differentiation of the igneous source region and the weathering and deposition of the protolith sediments, which two events are inferred to have occurred fairly close together in time.

5. Other Whole-Rock Uranium-Lead Results

The next step in the investigation was to carry out uranium and lead analyses on a number of larger-sized whole rock samples, as is more commonly done, to see whether the results would corroborate or conflict with the thin-slice data.

Sample locations are given in Figure 16; individual samples' petrographic descriptions are listed in Appendix A; analytical results are found in Table 3.

I. Guri Dam Samples - 8100 Series

The first group of large (tens of kilograms) samples analyzed, numbers 8100A2, 8100B2, 8100D2, 8100F2, and 8100G2, were from the same location as the gneiss discussed in the previous chapter; in fact, the block from which the thin slices were cut was a piece of 8100A2. All these rocks are quartzofeldspathic charnockites. They are composed primarily of perthitic alkali feldspar and quartz, with lesser amounts of hypersthene, microcline, and biotite, and traces of opaque minerals, zircon, and chlorite. Individual samples may in addition contain garnet, actinolite, plagioclase, apatite, calcite, or (?)augite. Gneissic texture is seen in handsamples. Thin sections characteristically show strongly cataclastic textures, accompanied by strain shadows in quartz and occasional kink banding in biotite. These rocks are judged to be metasedimentary,

Figure 16. Sample locations, large whole-rock samples. Dashed outline encircling Cerro La Ceiba represents approximate extent of La Ceiba migmatite, which is included for geologic reference.

(a) Locations from which gneiss samples were collected.

(b) Locations from which iron formation samples were collected.

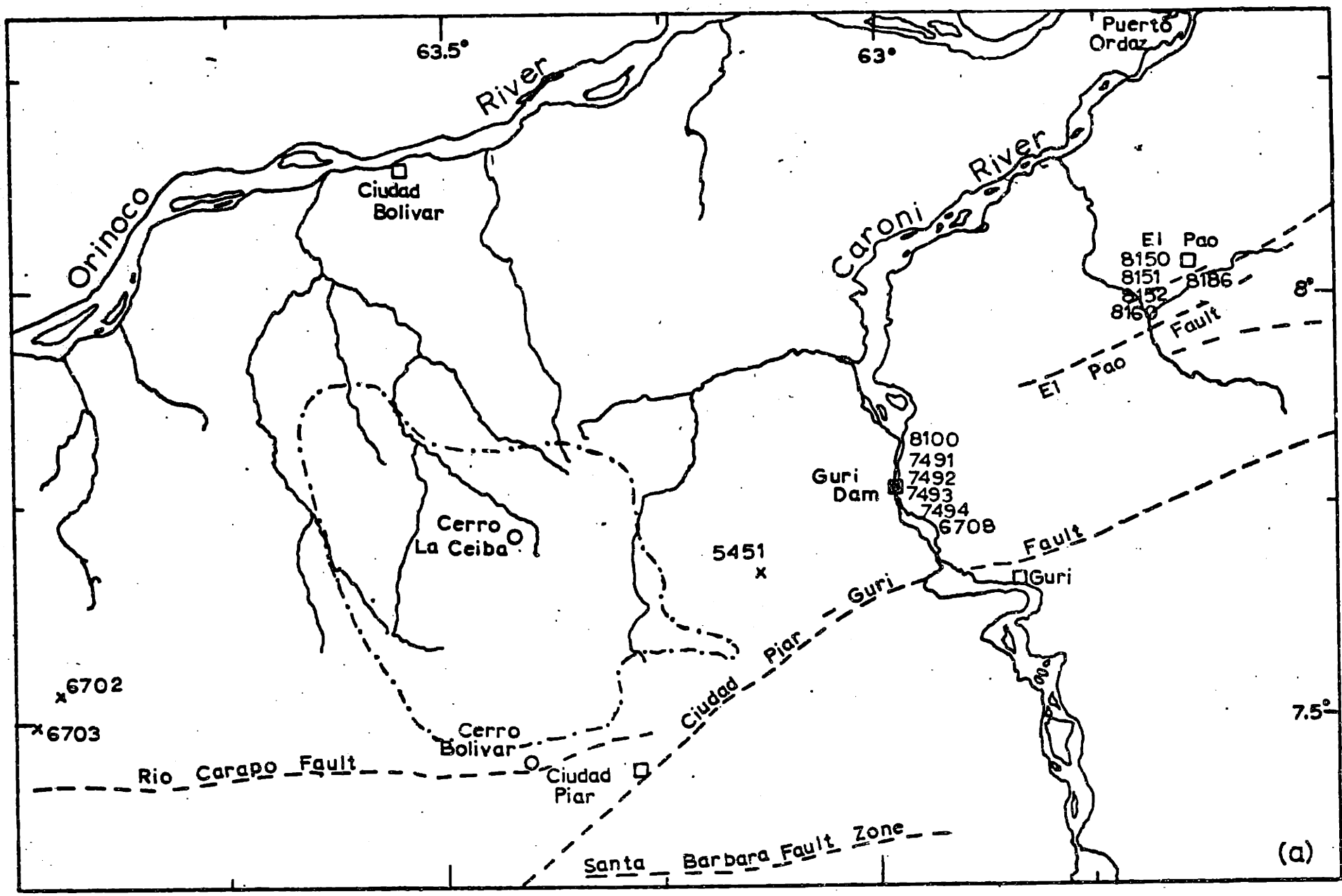
63.5°
63°
Puerto Ordaz
Orinoco River
Ciudad Bolivar
Caroni River
El Pao
8150
8151
8186
8152
8160
8°
Fault
El Pao
8100
7491
7492
Guri Dam
7493
7494
6708
Fault
Guri
Cerro La Ceiba
5451
Guri
Ciudad Piar
6702
6703
7.5°
Cerro Bolivar
Rio Carapo Fault
Ciudad Piar
Santa Barbara Fault Zone
(a)

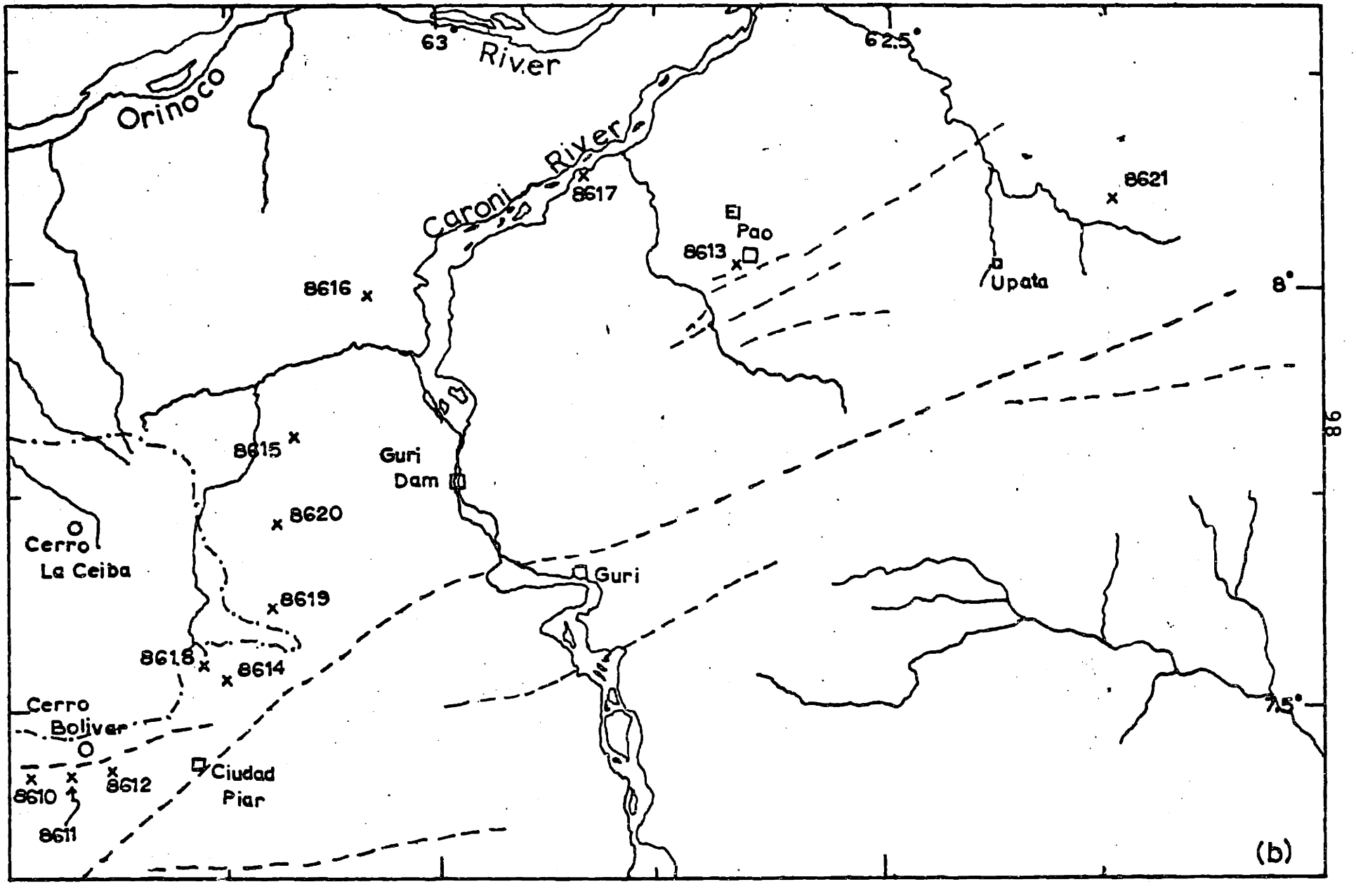
63
River
Orinoco
62.5°
Caroni River
8617
El
Pao
8613
8621
Upata
8616
8°
8615
Guri
Dam
8620
Cerro
La Ceiba
Guri
8619
8618
8614
Cerro
Bolivar
Ciudad
Piar
8610
8612
8611
7.5°
(b)

TABLE 3. U-Pb analytical results, whole rocks

Sample	Pb^{208}/Pb^{204}	Pb^{207}/Pb^{204}	Pb^{206}/Pb^{204}	Pb, ppm	U, ppm	μ
5451	41.30 ± 0.07	15.36 ± 0.02	18.35 ± 0.02	18.8	3.10	10.9
6702	39.12 ± 0.04	17.48 ± 0.02	24.03 ± 0.02	29.6	3.32	7.91
6703	43.70 ± 0.07	16.90 ± 0.03	22.74 ± 0.03	34.8	3.72	7.79
6708	44.04 ± 0.10	17.29 ± 0.04	22.80 ± 0.05	30.5	5.03	12.2
7491	73.29 ± 0.07	18.24 ± 0.02	28.14 ± 0.02	25.8	6.49	26.3
7492	43.42 ± 0.26	16.13 ± 0.09	18.18 ± 0.10	21.8	1.39	4.33
7493	41.65 ± 0.11	16.09 ± 0.04	17.54 ± 0.04	23.1	1.20	3.61
7494	44.80 ± 0.14	16.16 ± 0.05	18.59 ± 0.06	20.9	0.933	2.94
8100A2	43.64 ± 0.22	16.54 ± 0.08	18.72 ± 0.08	20.1	1.09	3.76
8100B2	46.18 ± 0.21	16.88 ± 0.07	20.20 ± 0.08	26.0	2.89	8.08
8100D2	46.64 ± 0.16	16.79 ± 0.05	20.22 ± 0.06	23.4	1.64	5.15
8100F2	44.78 ± 0.09	16.98 ± 0.03	22.24 ± 0.04	27.1	2.28	6.16
8100G2	68.98 ± 0.22	17.14 ± 0.05	23.03 ± 0.07	105	4.42	4.00

TABLE 3. (continued)

Sample	Pb^{208}/Pb^{204}	Pb^{207}/Pb^{204}	Pb^{206}/Pb^{204}	Pb, ppm	U, ppm	μ
8150	35.54 ± 0.11	17.43 ± 0.06	22.92 ± 0.07	15.9	2.15	8.96
8151	34.92 ± 0.03	16.82 ± 0.01	19.13 ± 0.01	25.5	0.298	0.726
8152	35.70 ± 0.03	17.01 ± 0.01	19.80 ± 0.01	25.4	0.664	1.66
8160	35.43 ± 0.06	17.56 ± 0.02	23.84 ± 0.02	23.1	3.86	11.2
8186	35.62 ± 0.12	17.22 ± 0.03	23.22 ± 0.04	26.9	3.95	9.78
8610	36.77 ± 0.85	14.86 ± 0.28	18.04 ± 0.30	1.44	0.0975	4.14
8611	46.53 ± 0.46	15.94 ± 0.10	19.04 ± 0.08	1.84	0.127	5.04
8612	38.48 ± 0.29	15.62 ± 0.08	18.70 ± 0.08	1.13	0.0410	2.32
8613	39.71 ± 0.23	15.72 ± 0.07	19.44 ± 0.06	2.25	0.114	3.31
8614	42.40 ± 0.38	15.92 ± 0.08	18.52 ± 0.10	1.76	0.170	6.49
8615	58.25 ± 1.48	15.87 ± 0.07	20.52 ± 0.12	1.32	0.193	12.1
8616	39.61 ± 0.13	16.30 ± 0.05	21.78 ± 0.11	3.09	0.280	6.16
8617	46.77 ± 0.63	19.18 ± 0.13	24.58 ± 0.46	1.10	0.173	12.4
8618	41.51 ± 0.41	16.06 ± 0.13	21.06 ± 0.26	0.896	0.0953	7.32

TABLE 3. (continued)

Sample	Pb^{208}/Pb^{204}	Pb^{207}/Pb^{204}	Pb^{206}/Pb^{204}	Pb, ppm	U, ppm	μ
8619	42.31 ± 0.19	16.59 ± 0.03	23.29 ± 0.16	2.97	0.344	8.32
8620	42.92 ± 0.18	15.99 ± 0.04	18.08 ± 0.07	3.25	0.115	2.39
8621	40.18 ± 0.05	23.63 ± 0.82	78.17 ± 6.43	0.881	0.829	116

Errors quoted are 1σ standard error of the mean: analytical errors only, except in the case of iron formations, where blank correction error is significant and is included in the total error quoted.

Banded iron formation analyses (#8610-8621) corrected for 18 (± 5) ng lead blank with composition $Pb^{208}/Pb^{204} = 40.32$, $Pb^{207}/Pb^{204} = 16.30$, $Pb^{206}/Pb^{204} = 19.49$; other results corrected for 13 ng blank of same composition.

Uranium analyses corrected for 0.15 ng U blank where significant.

principally on the evidence of the exceptionally well-rounded zircons present.

A lead-lead plot for 8100A2-G2 is shown in Figure 17. The points define an isochron with a slope of 0.12239 ± 0.01670, intercept 14.311 ± 0.349, MSWD = 1.26. This MSWD value indicates that the points essentially all fit this isochron within their analytical precision. As discussed at some length in the previous chapter and Appendix B, a two-stage or special three-stage model may formally describe this linear array. A two-stage model may be rejected not only on the available geologic evidence but also because the line lies wholly above the mantle growth curve (i.e. does not intercept it). If the data are interpreted on the basis of the geologically-reasonable $f_1 \cong$ constant case, the slope then gives the time of the beginning of the third stage of the history. In this case the slope age is 2.0 ± 0.3 b.y., in good agreement with the Rb-Sr thin-slice results. The isochron thus reflects the granulite metamorphic age.

A whole-rock Concordia diagram for these samples (Figure 18) provides less specific information. Uranium depletion is again indicated, presumably to some extent resulting from the 2-b.y. event, but the data points form a scatter, not a line. The presumption of a three-stage history is not necessarily invalidated by this Concordia plot. It is quite possible that the evolution was three-

Figure 17. Lead-lead plot, 8100 series samples, Guri Dam. Points in this and subsequent figures plotted with 1σ error bars as usual. Isochron is defined by a slope of 0.12239 $\pm$ 0.01670, intercept = 14.311 $\pm$ 0.349, MSWD = 1.26. This corresponds to a slope age of 2.0 $\pm$ 0.3 b.y.

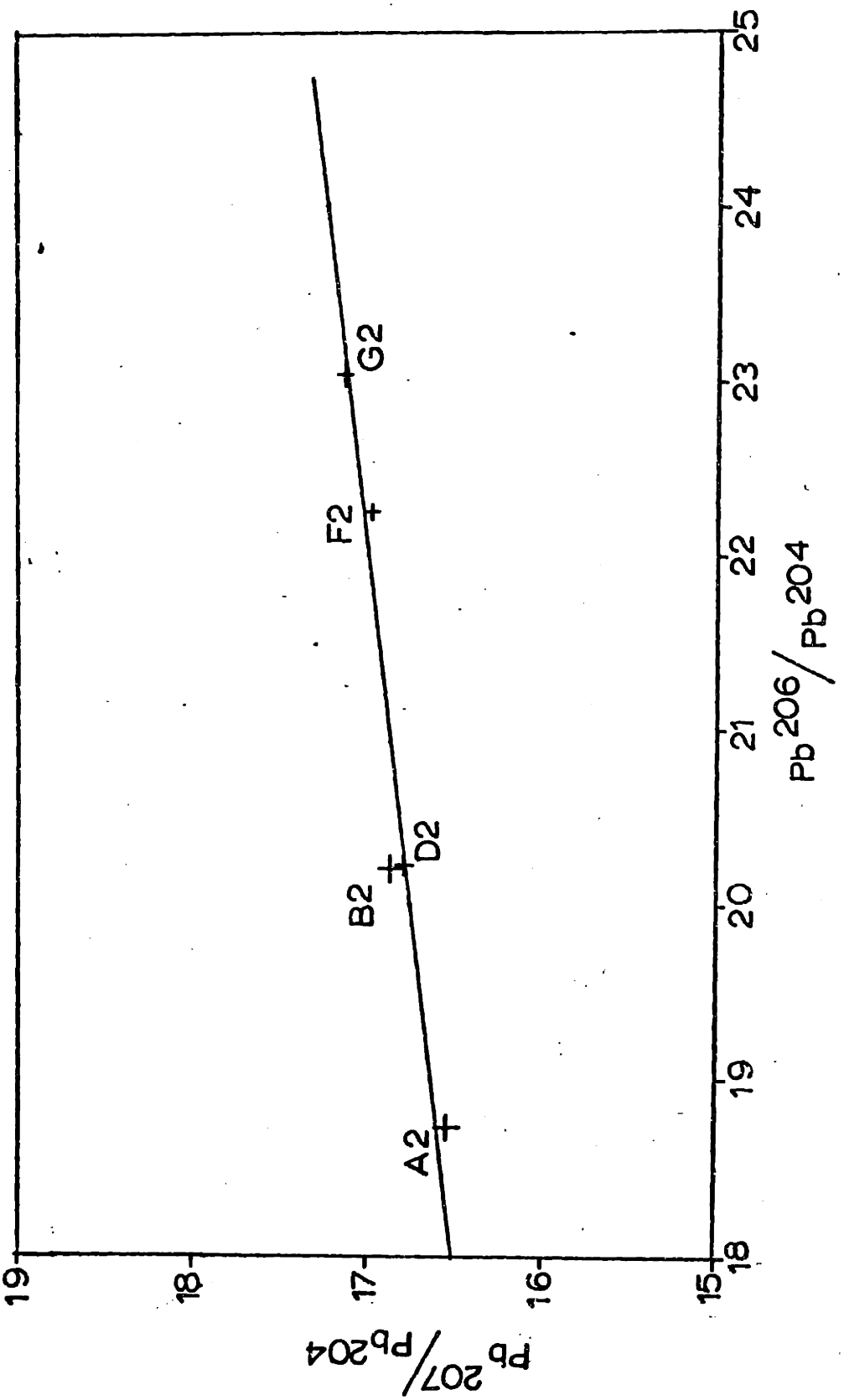
A2
B2
D2
F2
G2
15
16
17
18
19
18
19
20
21
22
23
24
25
Pb^{207}/Pb^{204}
Pb^{206}/Pb^{204}

Figure 18. Concordia diagram, 8100 series samples, Guri Dam.

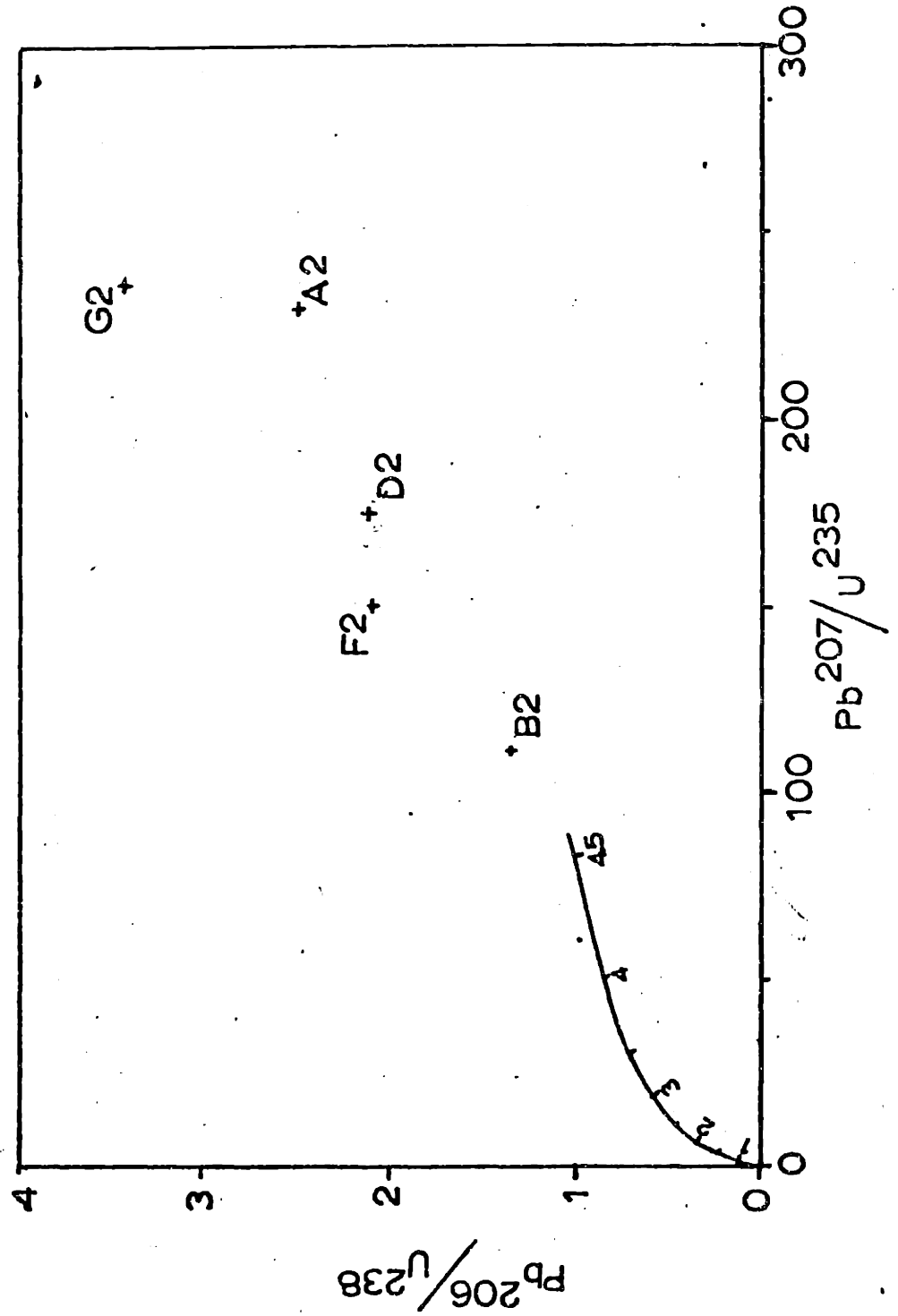
G2
A2
D2
F2
B2
45
0
100
200
300
Pb^{207}/U^{235}
0
1
2
3
4
Pb^{206}/U^{238}

stage except for a "geological instant" at the end, a brief very recent period during which the uranium in the system was disturbed. Given the very long half-lives of both the uranium isotopes, the effect of recent uranium loss on present lead isotopic ratios would be negligible, as noted earlier. What is difficult to explain is why recent uranium loss should be significant; it would be more reasonable had the samples lost most of the uranium that was to be lost during the granulite event. (A similar scatter of points could be produced by recent lead gain, through groundwater action or spurious laboratory contamination - but then the isotopic composition of the lead should be affected, and likewise the lead-lead plot. Lead gain is considered a much less likely possibility than uranium loss.) The samples were collected at the freshly-excavated Guri Dam site precisely so that unweathered material could be obtained, and they did appear fresh in hand sample. However, in thinsection some of the feldspars look sericitized, which indicates some post-recrystallization alteration, and whatever process caused the sericitization might likewise be responsible for disturbance of the uranium in the system. It is worth noting here too that such disturbance need not necessarily have been <u>extremely</u> recent. The slope of the 2-b.y. isochron is quite shallow; perturbations of uranium due to the alteration might simply be reflected in slightly increased scatter about the line. (Recall that there is

after all considerable uncertainty in the slope age: ± 600 m.y. at the 95% confidence level!)

The isochron diagrams for these samples (Figure 19) demonstrate, still more dramatically than the Concordia plot, that the system has not remained closed and developed straightforwardly from the last time of lead isotopic homogeneity. Nevertheless, the slope age obtained from the lead-lead plot may be regarded as supporting the previous conclusion that some intense metamorphic event occurred in that part of the Imataca near the Guri Dam somewhere around 2 b.y. ago.

It is interesting to compare the apparent behavior of uranium and lead isotopes in the large gneiss samples with their behavior in thin slices of a single gneiss block as described in the previous chapter. Obvious differences between the two cases exist. The fine-slice samples show a scatter in the lead-lead plot but define a good line on the Concordia diagram, while just the reverse is true of the large samples.

The scale of sampling in the latter case (at least meters or tens of meters) indicates that lead isotopic composition was essentially homogeneous on that scale at (after) the time of the granulite metamorphism. It does <u>not</u>, however, imply that active homogenization of lead isotopes on that scale resulted from the metamorphism. Indeed, since the fine-slice study indicated that some

Figure 19. Isochron diagrams, 8100 series samples, Guri Dam.

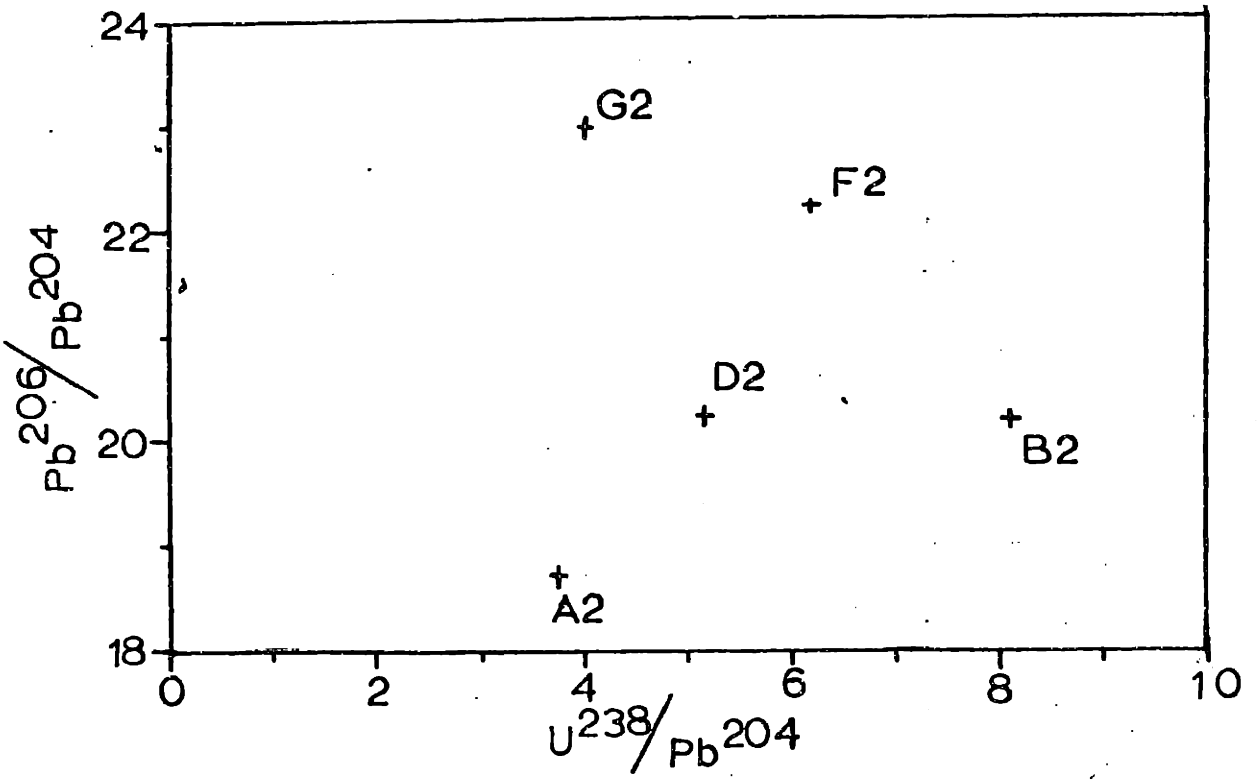
24
22
20
18
0
2
4
6
8
10
G2
F2
D2
B2
A2
Pb^{206}/Pb^{204}
U^{238}/Pb^{204}

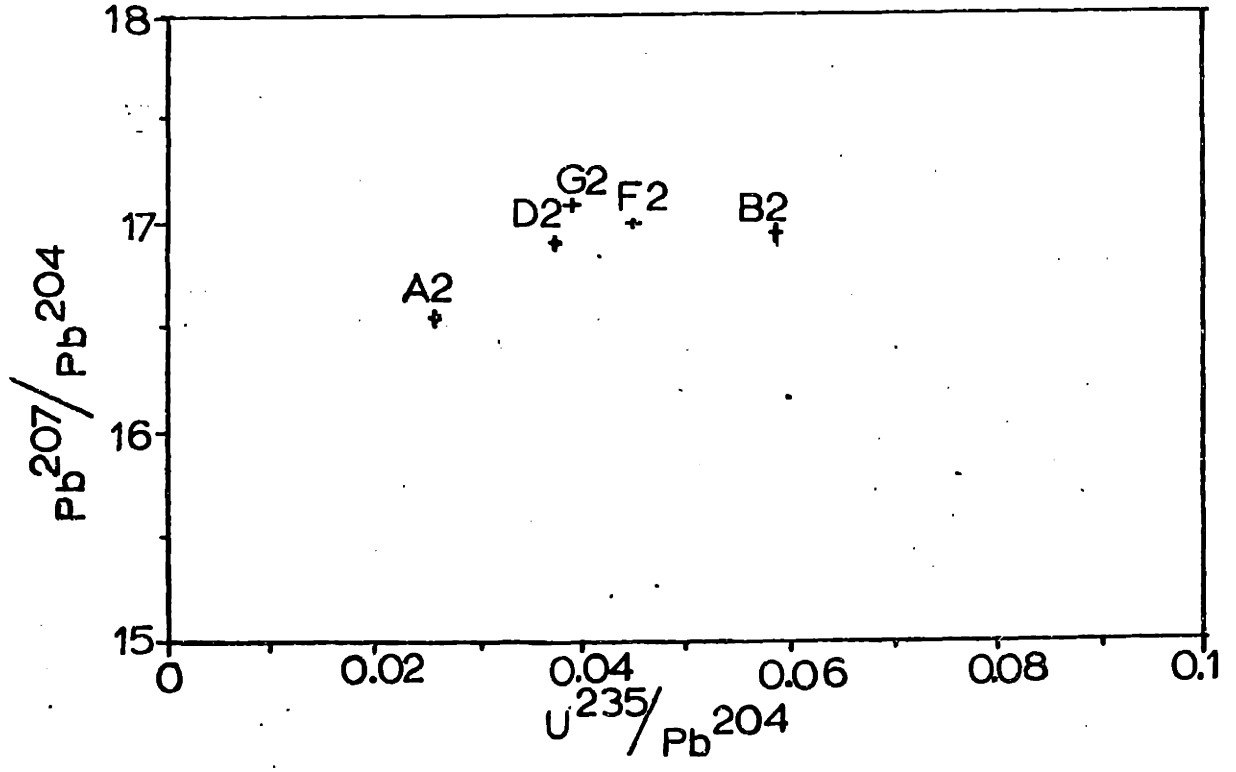
18
17
16
15
0
0.02
0.04
0.06
0.08
0.1
G2
D2
F2
B2
A2
Pb^{207}/Pb^{204}
U^{235}/Pb^{204}

variations in lead isotopic composition existed on a scale of centimeters despite the metamorphism, homogenization on a scale of meters would be unexpected. Instead, suppose that on a large scale the 3-stage $f_1 \cong$ constant model approximation is appropriate. Then the large samples would (more or less) share a single lead isotopic composition prior to the granulite event. The metamorphism would simply cause uranium depletion in varying degrees in the large samples, creating the variable μ to account for the tertiary isochron. On a fine scale, such as the scale of the sedimentary bedding, local variations in second-stage μ could still have existed. If the metamorphism failed to eliminate completely the resulting local variations in premetamorphic lead isotope composition, scatter in the present lead-lead diagram would result, as we have seen. It should be noted also that perfectly uniform premetamorphic lead isotopic composition among the large samples is not necessary. The uncertainty which still exists in the isochron they define, which arises from some small scatter of the points about the line, could be due to very limited variation in premetamorphic μ at the large-sample scale.

The difference in the behavior of uranium is more puzzling. The thin-slice samples all have apparently suffered minimal modern uranium depletion. The position on the Concordia diagram of the large sample 8100A2 from which

the fine slices were cut is consistent with uranium depletion at 2 b.y. only, but several of the large samples plot in such a way as to suggest considerable recent loss of uranium in addition. There is no obvious explanation for this seemingly inconsistent behavior, unless it is perhaps illusory and arises from extreme sample-inhomogeneity problems, which seems quite unlikely.

II. Guri Dam Samples - 6708, 7491-7494

A second set of gneiss samples, also from the vicinity of the Guri Dam, was collected by Kalliokoski (#6708, 7491, 7492, 7493, 7494); these were treated as a separate suite. In thinsection they appear rather similar to the 8100 group (thinsections of 6708 and 7492 were not, however, available). Quartz and feldspar are the dominant minerals; the major feldspar is alkali perthite in all three samples examined. Minor phases present in all cases include plagioclase, biotite, opaques, and zircon. Samples 7491 and 7494 at least may be called charnockites, for they include some hypersthene. In addition, 7491 contains garnet. All samples in this group show deformation such as was observed in the 8100 series samples: undulatory extinction in quartz, granulation of grain boundaries, ribbonlike boundaries between quartz grains. Some sericitization of the perthite is also apparent, especially in 7491 and 7494.

A lead-lead plot for these samples (Figure 20) reveals an interesting distribution of points. Samples 7492-7494

Figure 20. Lead-lead plot, samples 6708, 7491-7494, Guri Dam. The isochron is defined by a slope of 0.21396 ± 0.00469, intercept 12.277 ± 0.098, MSWD = 2.77, The corresponding slope age is 2.94 ± 0.04 b.y. Reference growth curve, mantle growth curve of Doe and Zartman (1977).

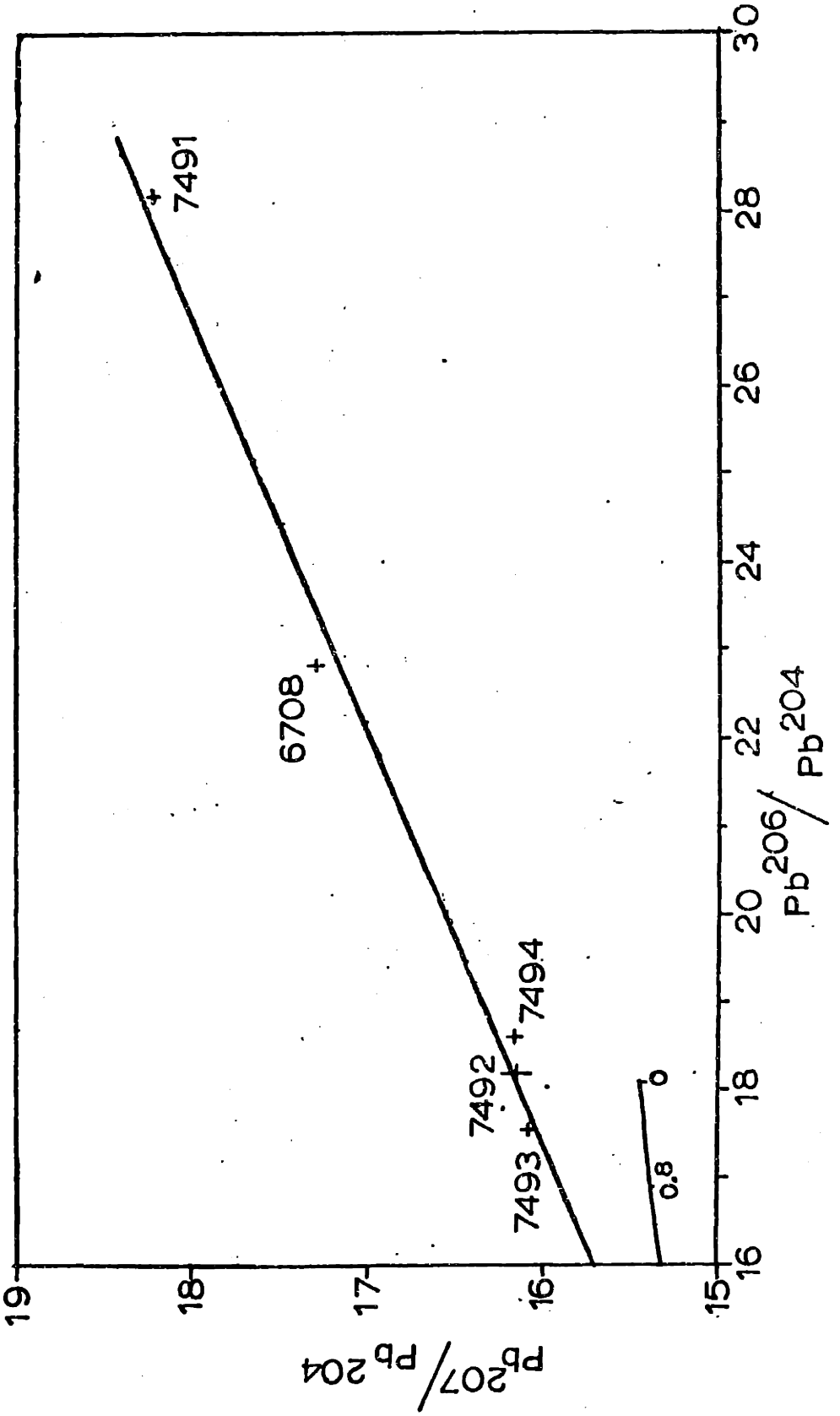
7491
6708
7492
7494
7493
0.8
0
Pb^{206}/Pb^{204}
Pb^{207}/Pb^{204}
16
18
20
22
24
26
28
30
15
16
17
18
19

are clumped fairly closely above the zero point of the mantle growth curve, while 6708 and especially 7491 show significantly more radiogenic lead (Pb^{206}/Pb^{204} = 28.14 for 7491), consistent with their relatively high μ values (12.2 and 26.3 respectively). The resultant isochron is defined by these regression parameters: slope = 0.21396 $\pm$ 0.00469, intercept = 12.277 $\pm$ 0.098, MSWD = 2.77. This slope corresponds to an age of 2.94 $\pm$ 0.04 b.y. At first impulse it might be tempting to interpret this as a reflection of the thermal event which produced the La Ceiba migmatite. However, one must then explain why the samples do not reflect the 2-b.y. metamorphic age as did the 8100 series also from the Guri Dam.

Actually, it should be realized that samples 7492-7494 show a trend vaguely parallel to the 2-b.y. isochron of the 8100 series samples, although they have relatively slightly lower Pb^{207}/Pb^{204} values for given values of Pb^{206}/Pb^{204}. It is only the positions of points 6708 and 7491 relative to them which are "unusual" and to a great extent determine the anomalous slope of the line fit to this set of points. Either the slope is geologically "real", or meaningful, or it is not. Arguments can be advanced in favor of either interpretation; for the moment, we shall proceed on the former assumption.

First, note that both 7491 and 7494 contain hypersthene, so they must both have been subjected to the granulite meta-

morphism. This may seem a rather obvious conjecture, since they both come from the same site as the 8100 series charnockites. But it is a very important point, which must be considered in attempting to interpret the 2.9-b.y. age. Note further that, despite this metamorphism, 7491, and, less so, 6708 still have relatively high μ's, which are uncharacteristic of the other granulites so far discussed. The case of 7491 is especially striking.

One explanation for this unexpected response to the granulite event (or lack of it) could be a difference in premetamorphic rock type. For instance, uranium in an igneous rock might be localized or held in quite a different way from uranium in a sediment, and might be more resistant to later depletion during the granulite event. Uranium in sediments occurs not only in "resistant" phases such as zircon, apatite, and sphene, but also as uranyl carbonate complexes, uranyl ion adsorbed onto the surfaces of clays and other minerals, etc. (Adams et al., 1965), and the latter types of materials would not be found in igneous rocks.

The zircons in 7491 are markedly different from those of the 8100 series samples. They are far more frequently euhedral to subhedral; some are corroded or embayed; some show overgrowths. Their appearance, in short, is not so plainly detrital, and could be consistent with crystallization of 7491 from a melt which incorporated an older popu-

lation of zircons.

Consider a 3^{+}-b.y. sedimentary sequence such as we have previously discussed. Now suppose that a thermal event, perhaps the same event which produced the granitoid rocks around Cerro La Ceiba, caused local heating and melting elsewhere at about the same time. If sample 7491, for example, is a product of such a process, then its unusual behavior might be explained. Moreover, if, as we have already hypothesized, the whole sedimentary sequence is characterized by a roughly uniform lead isotopic composition up to the time of the granulite event, then an igneous rock formed by melting some of these sediments prior to that event would share the common lead isotopic composition at the time of the melting, without any need for active homogenization at that time. Subsequent differences in between igneous and sedimentary rocks would then result in the preservation of the date of the thermal event which caused the melting.

Whether or not this theory is valid to this point, it remains to be explained why the 2.9-b.y. age, if real, has not been masked by the 2.1-b.y. granulite event.

Mathematically, one possibility is that of constant f for the granulite event, or constant proportional change in μ as a result of that thermal episode. This interpretation is not geologically reasonable, for it would require a premetamorphic μ on the order of 100 for 7491. Alter-

natively, suppose that 7491 lost virtually none of its uranium during the granulite event, for whatever reason. Obviously 7492-7494 lost a large part of their uranium. Evolution of these three samples in a moderate-μ system between 2.9 and 2.1 b.y. ago, followed by evolution in a low-μ system to the present, is graphically almost equivalent to single-stage evolution from 2.9 b.y. to the present in a system with μ just a little higher than the post-metamorphic μ . To a first approximation, then, the system as viewed at present would not reflect the granulite disturbance, and the slope of a line defined by 7491-7494 would approximately correspond to the time of the melting. (An analogous explanation could presumably be constructed to fit point 6708 into the same scheme, but as neither thinsection nor mineral separates of this sample are available, it is not considered specifically in any great detail.)

Not only do the two sets of samples from the Guri Dam record different ages, but even points 7492-7494 do not fall quite on the isochron of the 8100 series samples. A tentative explanation for the discrepancies may be advanced. The two sets of samples were collected several years apart at the dam site; during the intervening years excavation was presumably continuing. It is conceivable that the two suites of samples represent different stratigraphic levels which show correspondingly different

behavior. Faults also crisscross the site, as can be seen from Figures 3 and 16. The two groups of samples might once have been more widely separated in space than they now are.

It is emphasized that all the above discussion is aimed at reconciling two apparently-contradictory sets of data, and cannot be regarded in any way as a unique or definitive explanation for the observations. It is quite possible, on the basis of the evidence presented, to argue simply that an anomalous sample such as 7491 is genetically unrelated to the rest - that the 2.9-b.y. age is a graphical "accident", and its similarity to the La Ceiba age purely fortuitous.

The Concordia diagram (Figure 21) and isochron plots (Figure 22) provide further indications that 7491 and 6708 are unusual. They have not obviously suffered great uranium depletion; 7491 even falls below the Concordia curve. Again, there may be some feature of uranium distribution in these samples which prevented appreciable uranium loss at 2.1 b.y. (Their compositions could be described also in terms of selective loss of radiogenic lead, but this is geologically far less likely.) The scatter among the remaining three points on all diagrams is such that lines cannot be constructed through these points alone. Their position on the Concordia plot, however, is not inconsistent with uranium depletion at about 2 b.y.,

Figure 21. Concordia diagram, samples 6708, 7491-7494, Guri Dam. Note especially the unusual position of point 7491.

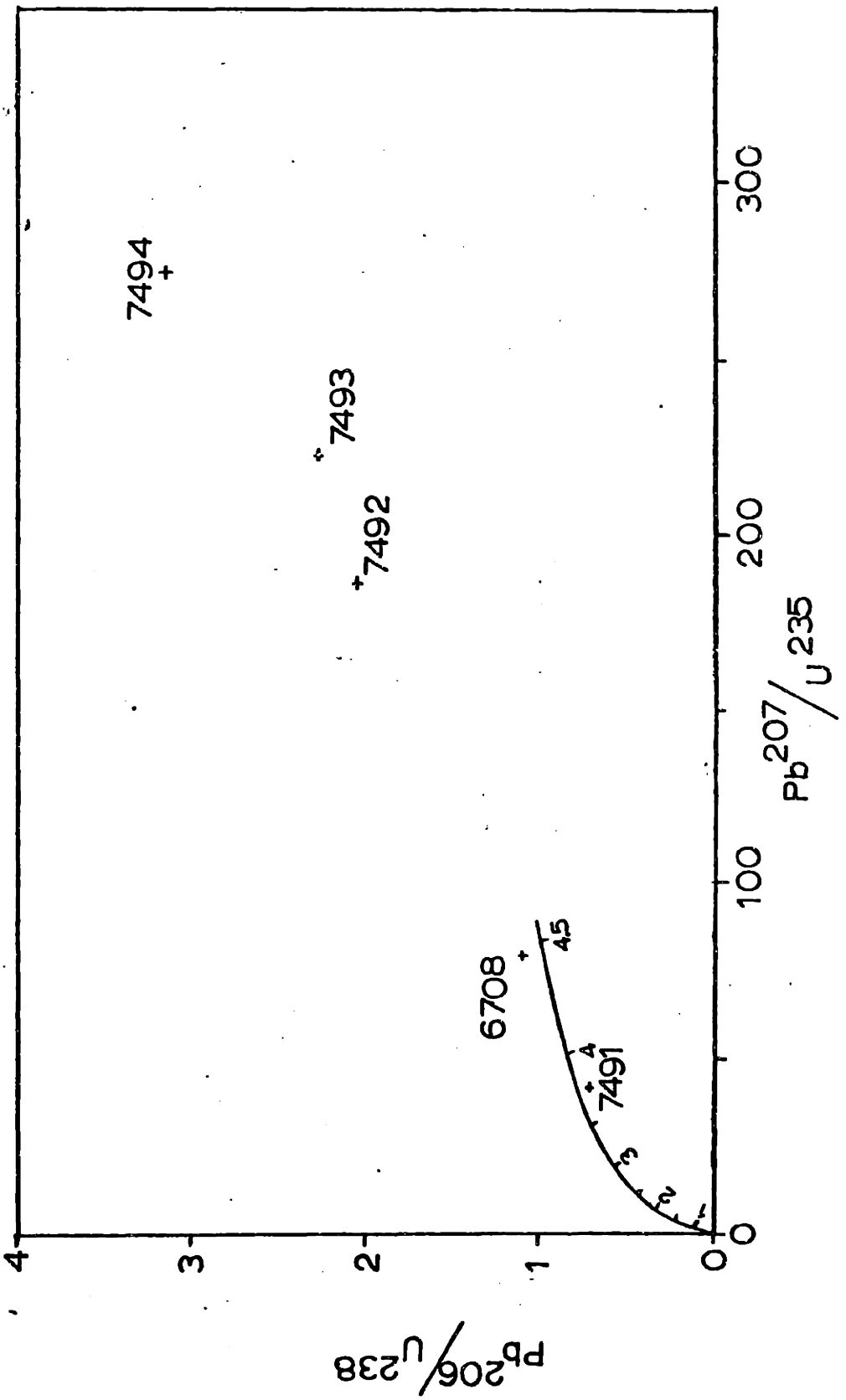
7494
7493
7492
6708
7491
45
4
3
2
1
0
100
200
300
Pb^{207}/U^{235}
Pb^{206}/U^{238}

Figure 22. Isochron diagrams, samples 6708, 7491-7494, Guri Dam. If regression lines are fit to each, the results are:

Pb^{206}-U^{238} diagram: slope= 0.47004 ± 0.00557, intercept = 16.444 ± 0.044, MSWD = 8.28, for a slope age of 2.48 ± 0.03 b.y.

Pb^{207}-U^{235} diagram: slope = 13.335 ± 0.392, intercept = 15.827 ± 0.034, MSWD = 3.69; slope age 2.70 ± 0.03 b.y.

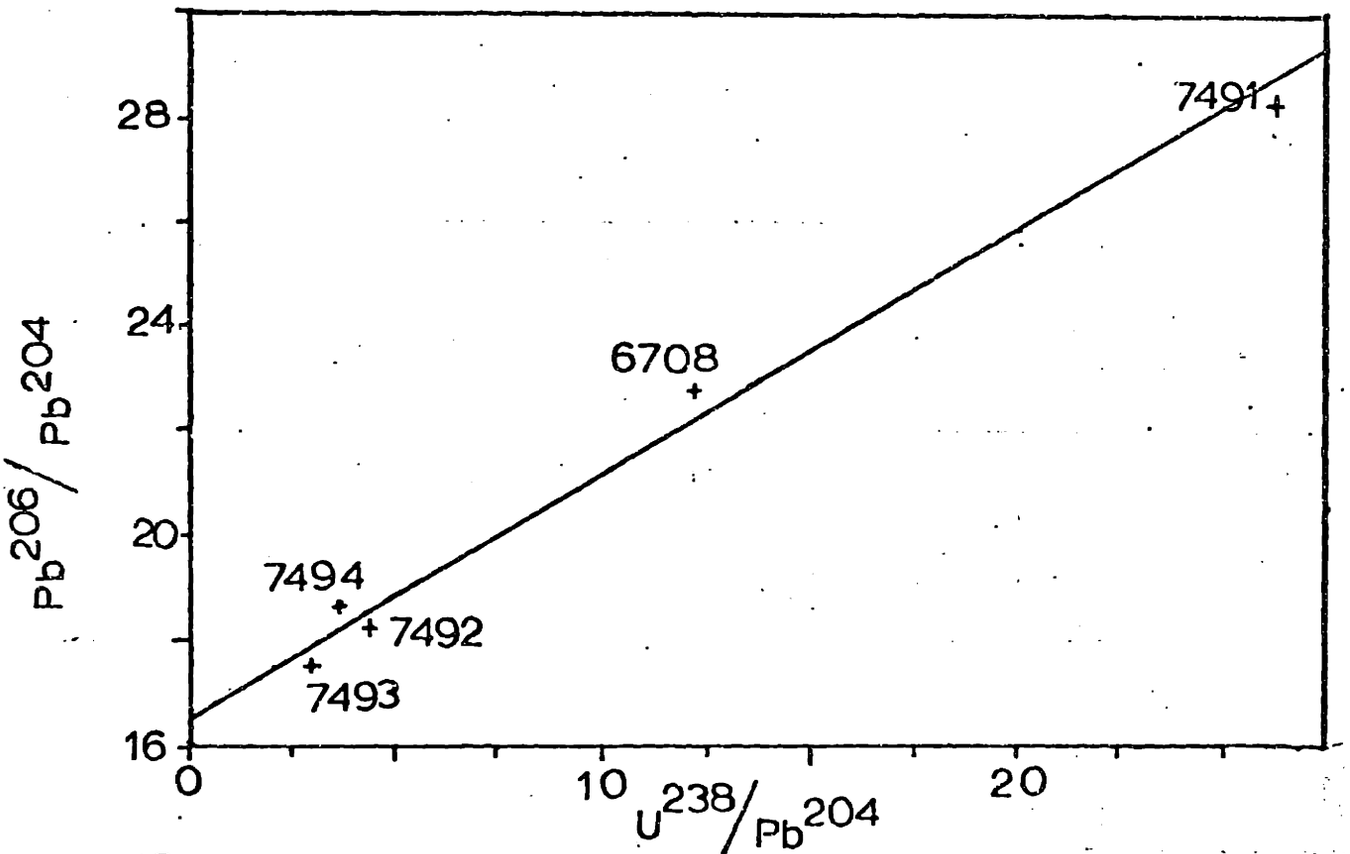
28
24
20
16
0
10
20
Pb^{206}/Pb^{204}
U^{238}/Pb^{204}
7491
6708
7494
7492
7493

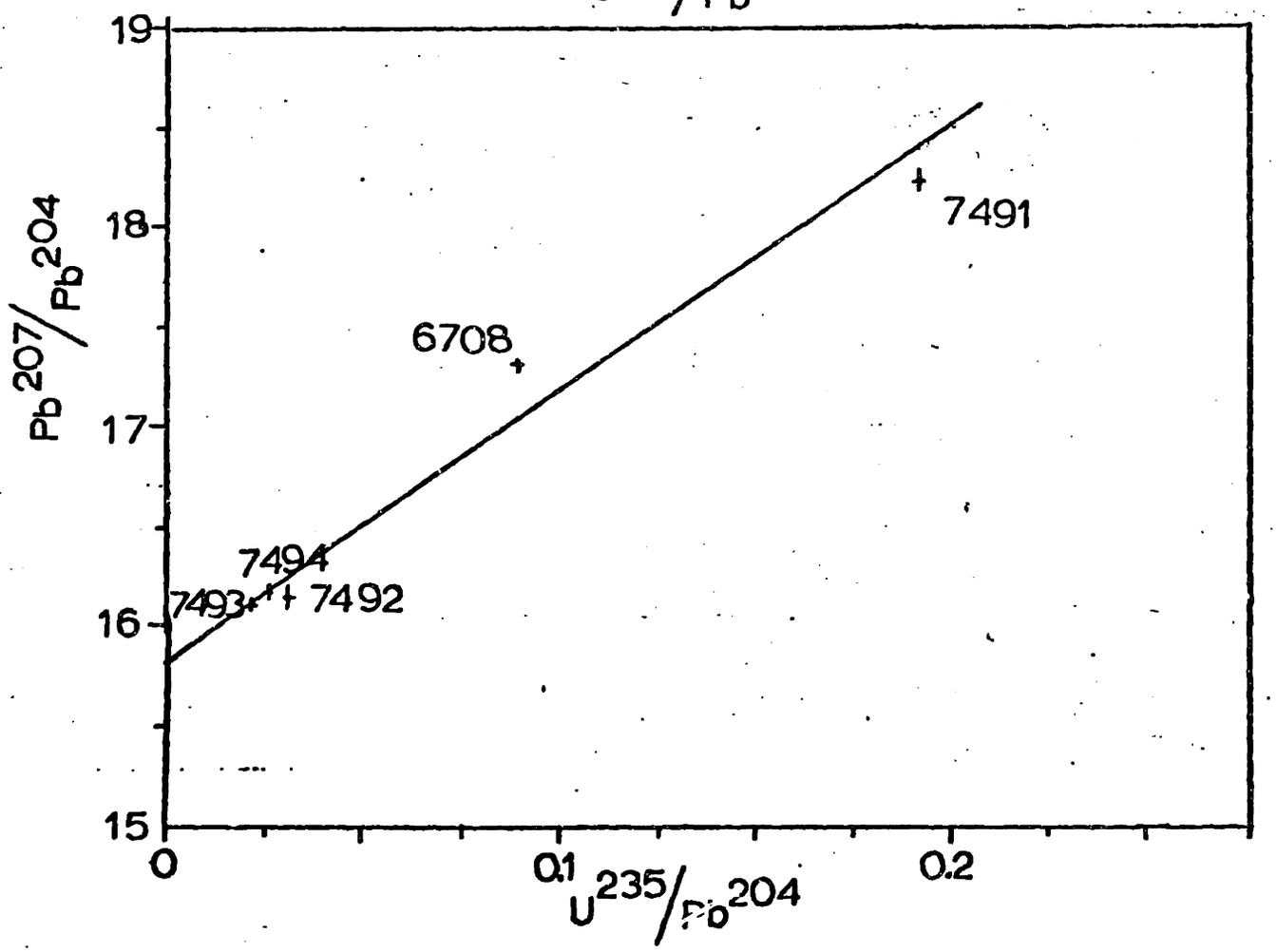
19
18
17
16
15
0
0.1
0.2
Pb^{207}/Pb^{204}
U^{235}/Pb^{204}
7491
6708
7494
7493
7492

with minor additional uranium loss more recently. (If regression lines are constructed for all points in Figure 22, the resulting slope ages are approximately 2.5 and 2.7 b.y., but the fit of the points to these lines is rather poor.)

In short, the indications from the second set of Guri Dam samples are rather different from those of the 8100 series previously discussed. This second suite may reflect local disturbance at the time of the La Ceiba migmatization, but the evidence is equivocal.

III. Gneisses from El Pao (8150-8160, 8186)

Five samples from El Pao (#8150, 8151, 8152, 8160, and 8186) were next analyzed, in an effort to determine the extent, if any, to which results would vary from place to place within the Imataca. Sample 8150, a mafic granulite, is composed of plagioclase, hypersthene, and hornblende, with minor biotite and opaques, and traces of apatite and zircon. Samples 8151 and 8152 are more typical charnockites, consisting principally of quartz plus perthite, with lesser microcline, garnet, hypersthene, and biotite, and traces of chlorite and rutile. Also present in 8152 are minor plagioclase and traces of zircon and (?)calcite. Sample 8160 is similar to 8152, but contains no definite hypersthene, and has some additional accessory minerals: opaques, apatite, and finegrained dispersed hematite. Sample 8186 is somewhat unusual. It is composed mainly of quartz and perthite

with minor microcline, opaques, chlorite, and rounded zircon, but contains in addition a significant amount of fine hematite. Some of this hematite is dispersed throughout the sample, but occasional parallel bands of it do occur which transsect the grain boundaries of major phases. In addition, some of the quartz is present as lenses which are elongated at an angle to the orientation of the hematite bands. All of the El Pao samples in thinsection show the typical indications of stress - strained quartz, granulation of grain boundaries, sutured grain boundaries between quartz grains. Sometimes the biotite grains appear to have been forced apart along the cleavage planes.

A lead-lead plot for these samples (Figure 23) shows an approximately linear array, especially if 8186 is excluded. Since 8186 falls significantly off the line defined by the other samples, and was not collected at the same time, it may be that it represents a distinct unit; it is omitted from line fitting for the rest of the samples. The regression line in Figure 23 for 8150-8160 is described by the regression parameters slope = 0.14965 $\pm$ 0.00741, intercept 14.000 $\pm$ 0.160, MSWD = 1.47; the corresponding slope age is 2.34 $\pm$ 0.09 b.y. The slope age obtained for these El Pao samples thus agreees with that from the 8100 series Guri Dam samples and with the fine-slice Rb-Sr date within the uncertainties of the various determinations. As was expected from their min-

Figure 23. Lead-lead plot for El Pao gneisses. Isochron, excluding point 8186 (see text) has a slope of 0.14965 ± 0.00741, intercept 14.000 ± 0.160, MSWD = 1.47. The corresponding slope age is 2.34 ± 0.09 b.y.

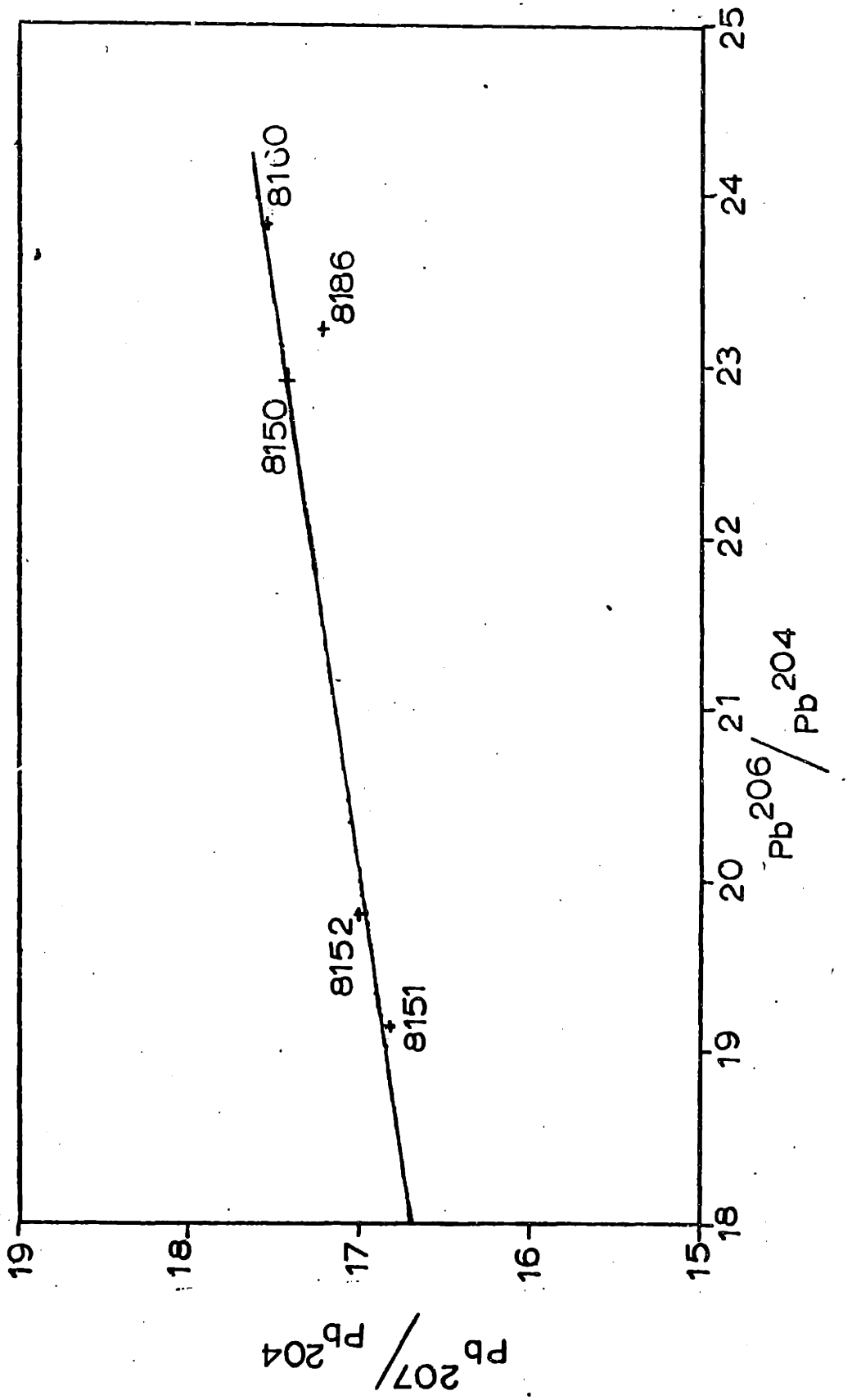
8150
8186
8152
8151
Pb^{207}/Pb^{204}
Pb^{206}/Pb^{204}
19
18
17
16
15
25
24
23
22
21
20
19
18

eralogy and pattern of deformation, then, it seems that the El Pao samples too reflect the granulite metamorphic event. It is interesting that this group includes one sample (8150) which is not likely to be metasedimentary; its behavior is nevertheless consistent with that of the other samples. Since it was taken from the same large block of gneiss as 8151 and 8152, perhaps we are seeing evidence for lead isotopic equilibration at the handsample scale at El Pao as a result of the granulite metamorphism. If this has occurred, however, it is surprising that strontium isotopes should not have equilibrated also, and they do not appear to have done so (Figure 4(b)).

A whole-rock Concordia diagram (Figure 24) presents additional data to support the granulite-metamorphic age and further evidence of uranium depletion during that event. While several of the samples show only limited uranium depletion, 8152 and especially 8151 show extreme depletion (note Concordia curve for scale). Again excluding sample 8186, the regression line for the Concordia plot is defined by the parameters: slope = 0. 010624 $\pm$ 0.000025, intercept = 0.35556 $\pm$ 0.00273, MSWD = 9.78. The younger intercept of this regression line with the Concordia curve occurs at 2.46 $\pm$ 0.03 b.y. The large MSWD value suggests that the fit of the points to the line is far from perfect, despite the small uncertainty in the intercept value. The slope of the line is to a great extent deter-

Figure 24. Concordia diagram, El Pao gneisses.

(a) Line shown excludes point 2186. It is defined by a slope of 0.010624 ± 0.000025, intercept 0.35556 ± 0.00273, MSWD = 9.78.

(b) Detail of (a) showing intersection with Concordia curve. Younger intercept is at 2.46 ± 0.03. Dashed lines approximately indicate ± 1σ limits on the line.

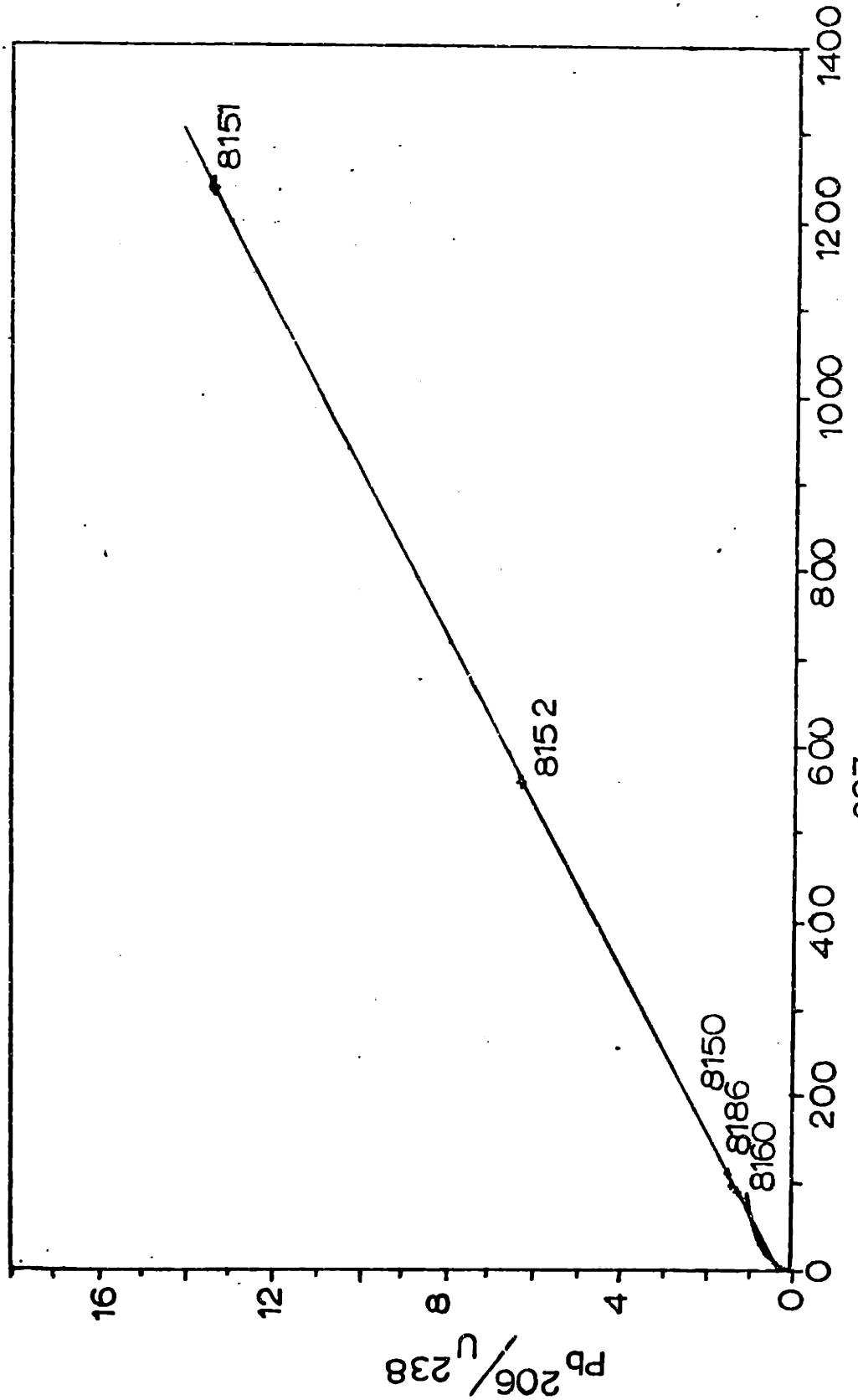
8151
8152
8150
8186
8160
0
200
400
600
800
1000
1200
1400
Pb^{207}/U^{235}
0
4
8
12
16
Pb^{206}/U^{238}

(a)

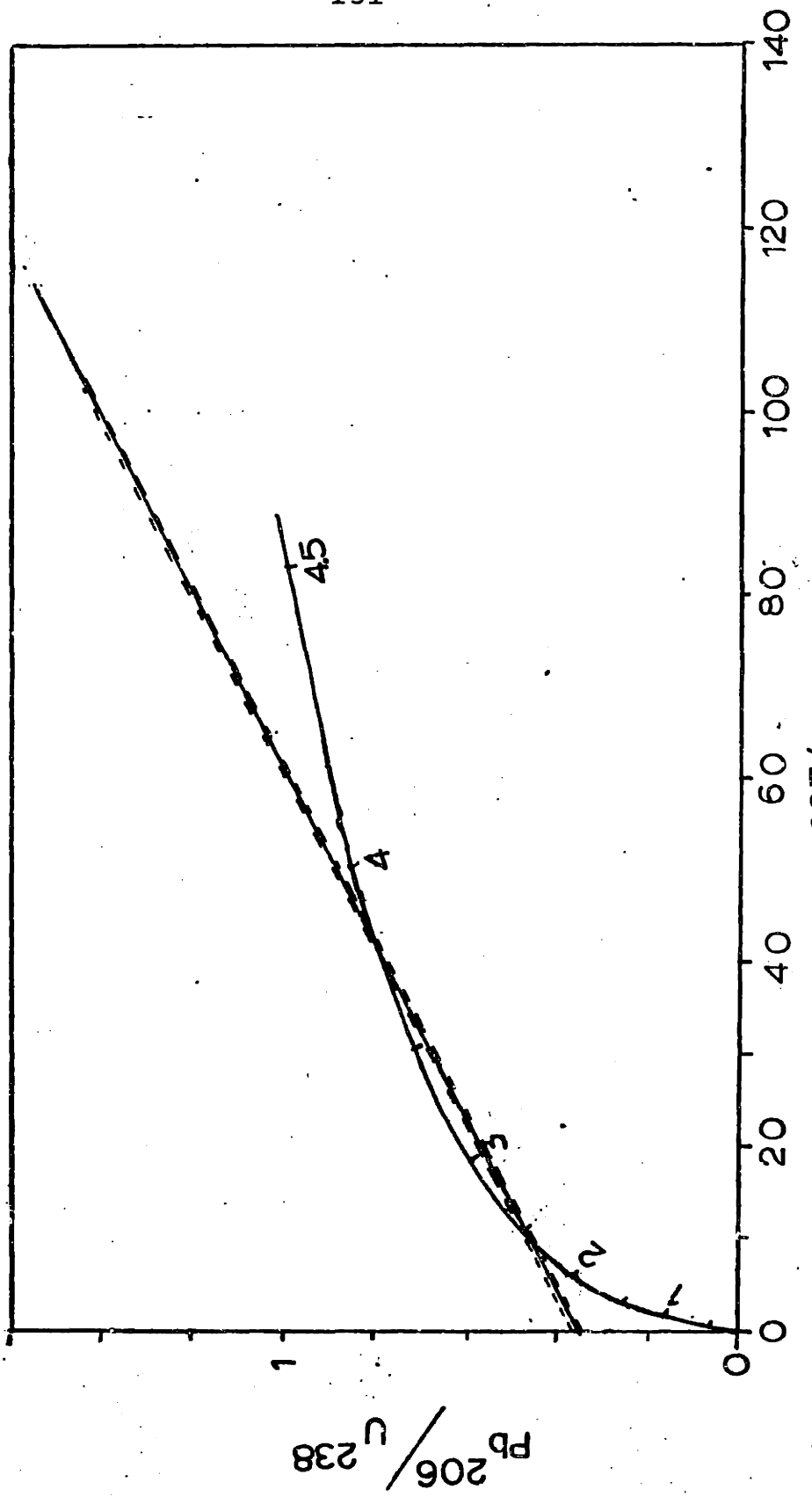

(b)

mined by the extreme point 8151; a small error in determining the U/Pb for that sample could have a disproportionately large influence on the intercept value. Therefore not too much importance is attached to the exact value of this intercept. Rather, the results are taken as supporting in a general way the previously-determined age of the granulite event.

The isochron diagrams (Figure 25) do not show perfectly linear arrays, but the slope ages for points 8150-8160 show a remarkable correspondence with the lead-lead age. The individual isochron ages are: Pb^{206}-U^{238}, 2.37 $\pm$ 0.02 b.y.; Pb^{207}-U^{235}, 2.34 $\pm$ 0.03 b.y. Not only does this correspondence increase confidence in the lead-lead age, but it strongly indicates that modern disturbance of uranium in the system has been minimal.

The distinctive mineralogy of 8150 might suggest a somewhat different protolith from the rest of the samples'. It is, however, only a small mafic band from a larger chunk of what is basically charnockite gneiss, so it is difficult to be certain. This sample may represent a mafic metamorphic segregation within the gneiss, or it could very possibly have been a small mafic volcanic contribution to an otherwise sedimentary sequence. The rare zircons in this sample may be somewhat more angular than those in the charnockites, but this evidence is inconclusive.

Figure 25. Isochron diagrams, El Pao gneisses. Regression lines fit to points 8150-8160 are characterized by the following parameters:

Pb^{206}-U^{238} diagram: slope = 0.44449 ± 0.00366, intercept = 18.921 ± 0.016, MSWD = 6.54. The resultant slope age is 2.37 ± 0.02 b.y.

Pb^{207}-U^{235} diagram: slope = 9.0779 ± 0.2689, intercept = 16. 834 ± 0.014, MSWD = 3.85, for a slope age of 2.34 ± 0.03 b.y.

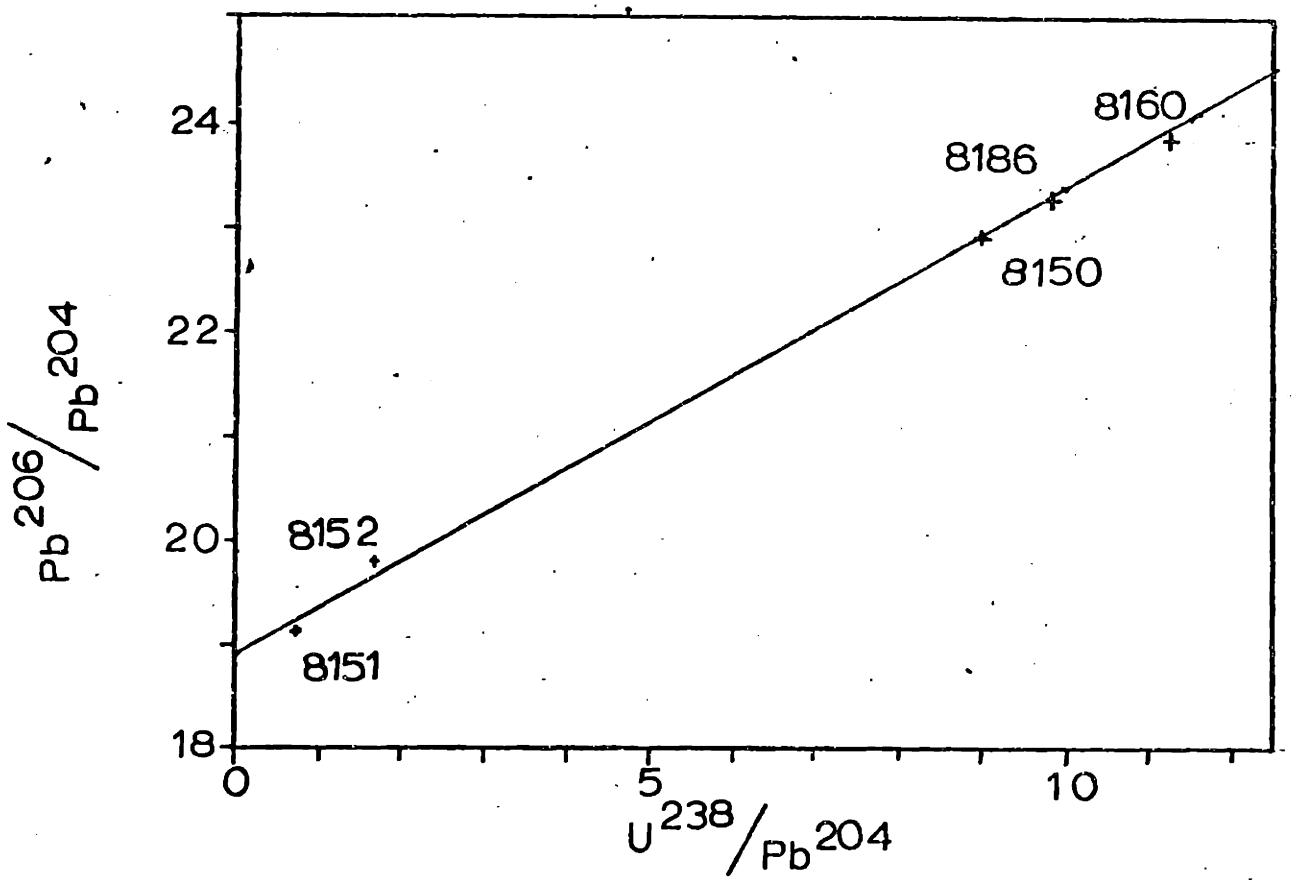
24
22
20
18
0
5
10
Pb^{206}/Pb^{204}
U^{238}/Pb^{204}
8160
8186
8150
8152
8151

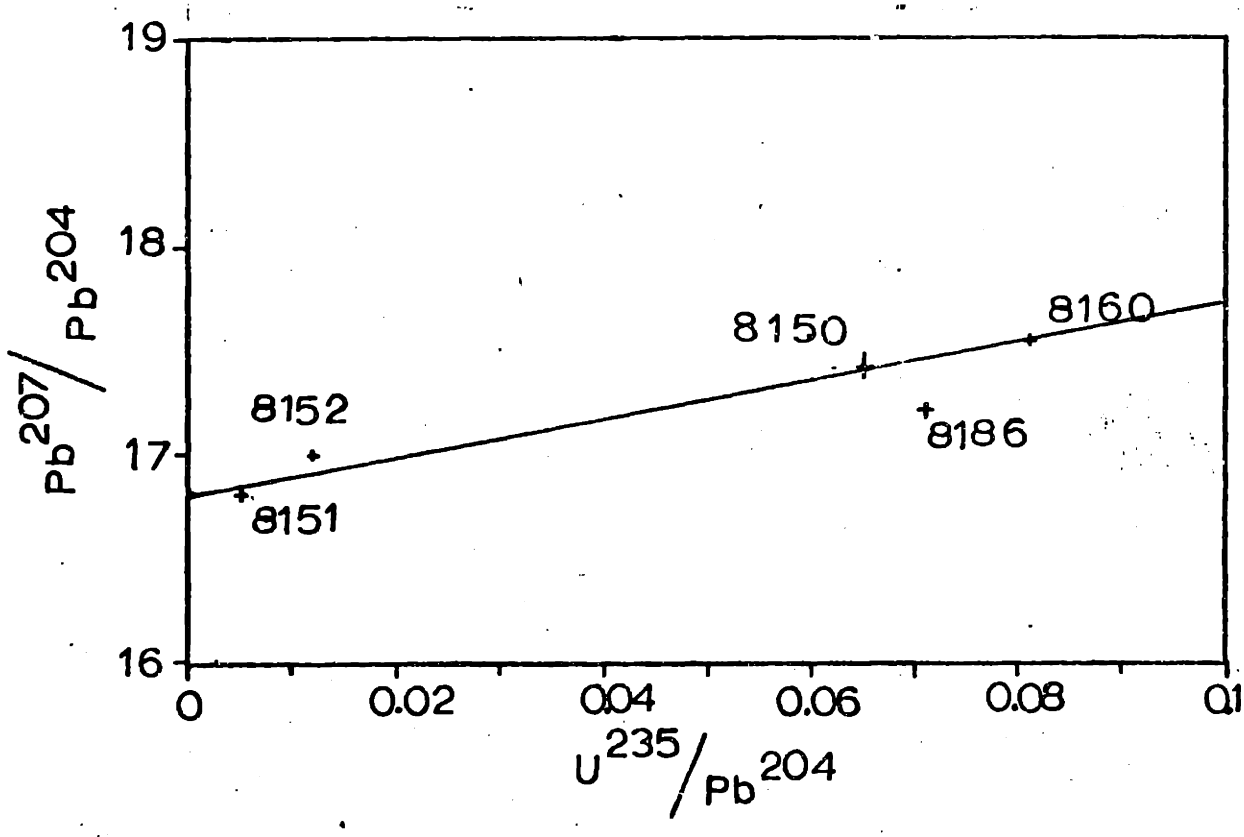
19
18
17
16
0
0.02
0.04
0.06
0.08
0.1
Pb^{207}/Pb^{204}
U^{235}/Pb^{204}
8150
8160
8152
8186
8151

IV. Reconnaissance Samples (5451, 6702, 6703)

Three samples from various locations west of the Guri Dam (5451, 6702, 6703) were also analyzed. No thinsection of 6702 is available. Sample 5451 consists primarily of quartz, microcline, plagioclase, and biotite, with minor garnet and traces of zircon. Sample 6703 is mainly composed of quartz, microcline/perthite, plagioclase, and biotite, with traces of apatite, actinolite, opaques, and zircon. Both samples, but especially 6703, show sericitization of feldspar, and both have a cataclastic texture.

Lead-lead diagrams for these samples (Figures 26 and 27) produced an entirely unexpected result: evidence of apparently two-stage evolution. The regression line is characterized by the parameters: slope = 0.36528 $\pm$ 0.00375, intercept = 8.6462 $\pm$ 0.0814, MSWD = 4.78. The slope age of this line is 3.77 $\pm$ 0.02 b.y., quite different from the (expected) metamorphic age. Moreover, the regression line intercepts the mantle growth curve at approximately 3.9 b.y. for the Stacey and Kramers (1975) model and 3.8 b.y. for the model of Doe and Zartman (1977), and runs close by the zero point on both. It is the coincidence of slope and intercept ages and the general orientation of the line which supports the idea of a two-stage history. What is especially intriguing about such an interpretation is that the 3.8-b.y. slope age is not greatly different from the extrapolated "primary age" for the Guri Dam banded gneiss

Figure 26. Lead-lead plot, reconnaissance Imataca samples I. Slope of best-fit line is 0.36528 ± 0.00375, intercept 8.6462 ± 0.0814, MSWD = 4.78. This corresponds to a slope age of 3.77 ± 0.02 b.y. Reference growth curve, mantle growth curve of Doe and Zartman (1977); approximate intercept with this curve, 3.8 b.y.

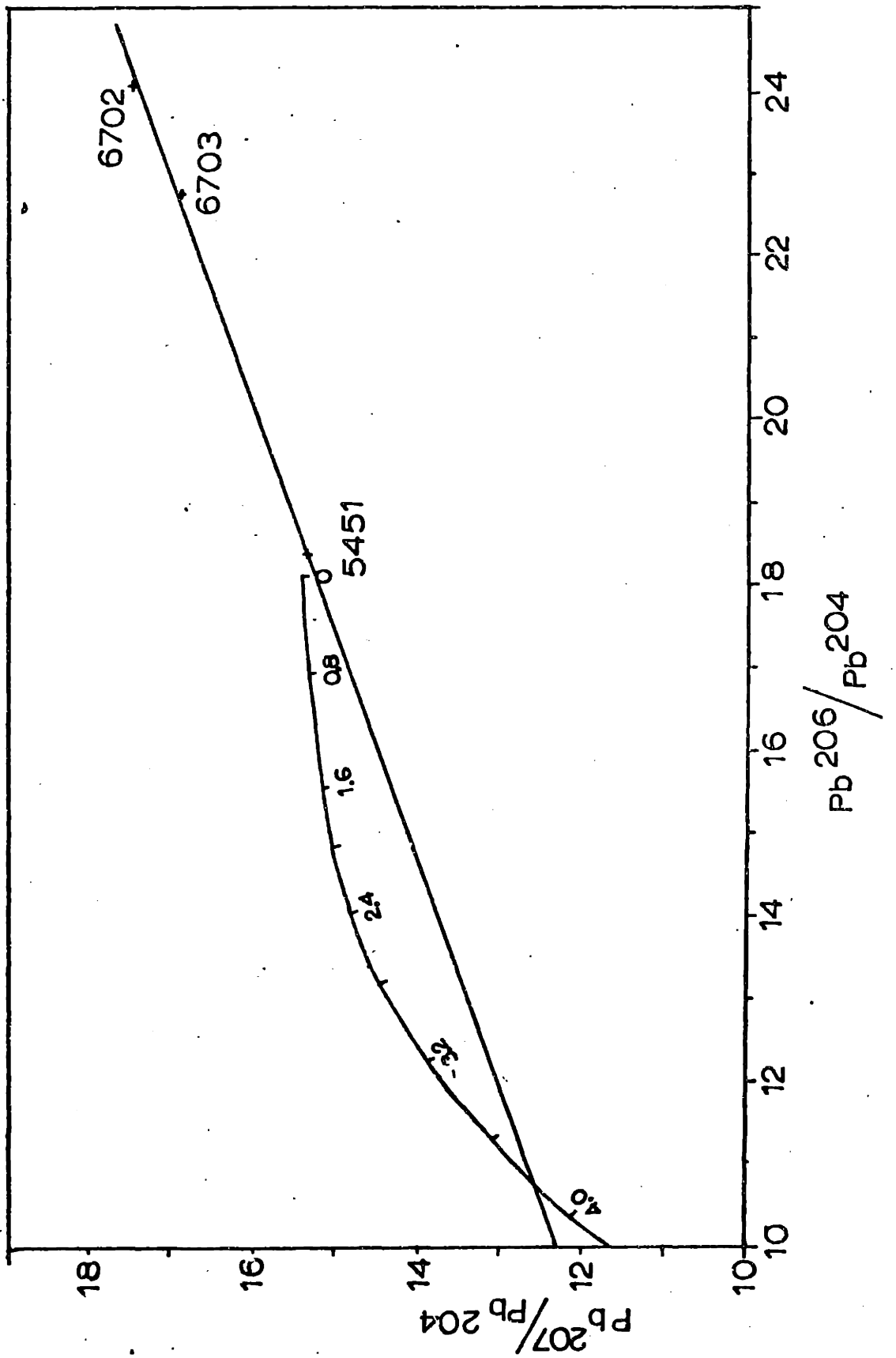
6702
6703
5451
0
0.8
1.6
2.4
3.2
4.0
10
12
14
16
18
20
22
24
Pb^{206}/Pb^{204}
Pb^{207}/Pb^{204}

Figure 27. Lead-lead plot, reconnaissance Imataca samples II. Best fit line is the same as that in Figure 26, with slope age of 3.77 ± 0.02 b.y. Reference growth curve, mantle growth curve of Stacey and Kramers (1975); the approximate intersection with this curve is at 3.9 b.y.

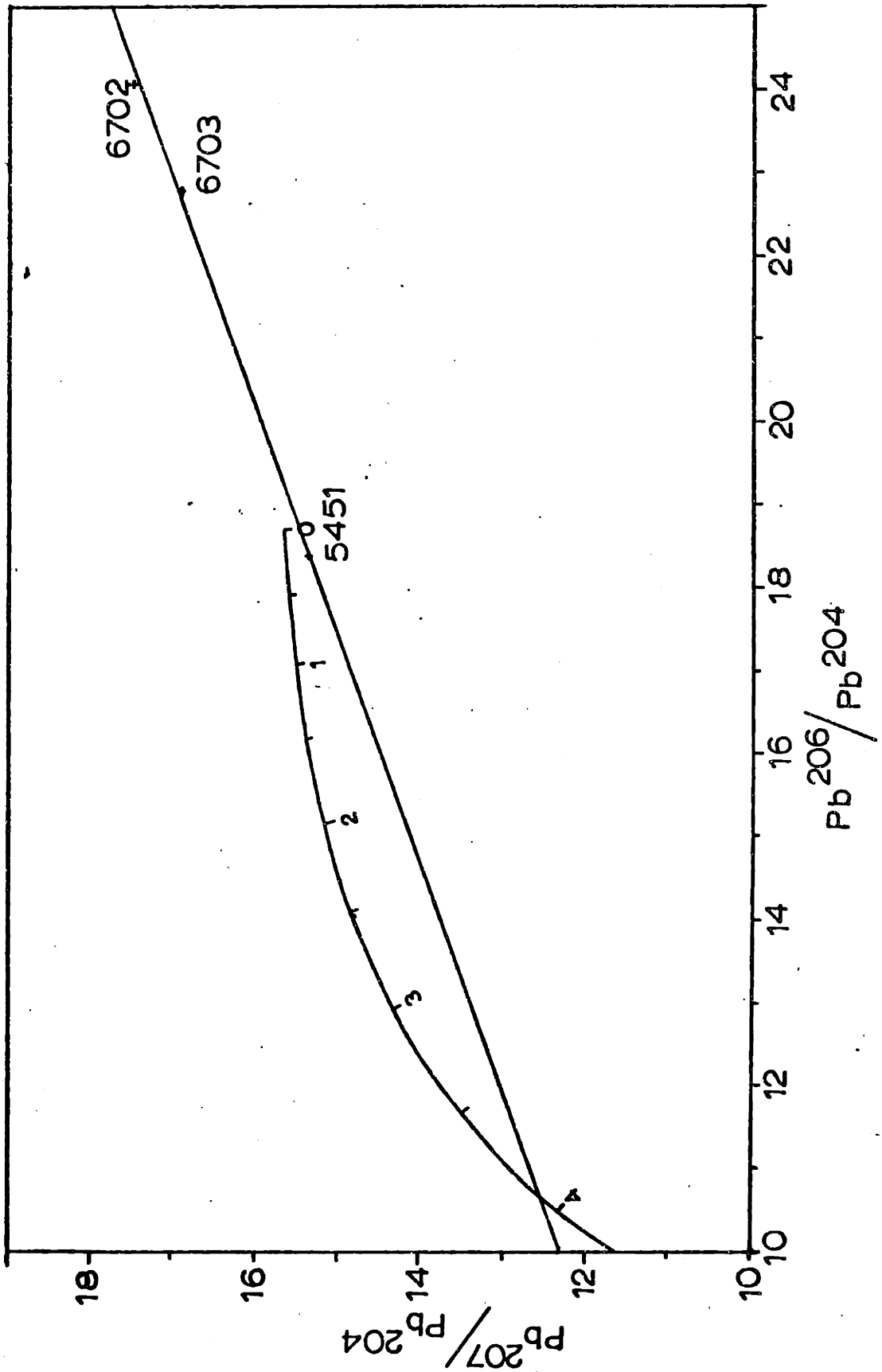
6702
6703
5451
0
1
2
3
4
10
12
14
16
18
20
22
24
Pb^{206}/Pb^{204}
Pb^{207}/Pb^{204}

samples discussed in Chapter 4.

The immediate objection to the two-stage model is, of course: why should these rocks have survived granulite-grade conditions without suffering disturbance of the U-Pb system, which would then be reflected in the lead-lead plot? It is tentatively proposed that the answer is that these rocks were never metamorphosed to granulite grade. Nothing in the mineralogy of these samples suggests granulite grade metamorphism. Certainly dynamic metamorphism has affected these rocks, but that does not mean that temperatures must have been correspondingly high throughout the region. Perhaps, as has been suggested by Dorr (1973), the metamorphism was most intense to the east, near the Pastora province which we know to have been active around 2 b.y. It is also possible that samples 5451 and 6703 are orthogneisses,and, as previously suggested for 7491, did not respond to the metamorphic event with uranium depletion as the obvious metasediments did. (The zircons in these samples do not appear particularly well rounded.) Either or both of these alternatives could explain why the apparently primary age of 3.8 b.y. is preserved by this set of samples.

A whole-rock Concordia diagram (Figure 28) is unhelpful in clarifying the situation. The points approximate a line, but with a negative intercept. Modern disturbance of uranium is probably responsible for the observed plot. Likewise, the isochron diagrams (Figure 29) are consistent

Figure 28. Concordia diagram, reconnaissance Imataca samples. Note negative younger intercept. Line is defined by regression parameters: slope = 0.016902 ± 0.000032, intercept = -0.27478 ± 0.00312, MSWD = 45.05 (indicating poor fit of points to the line).

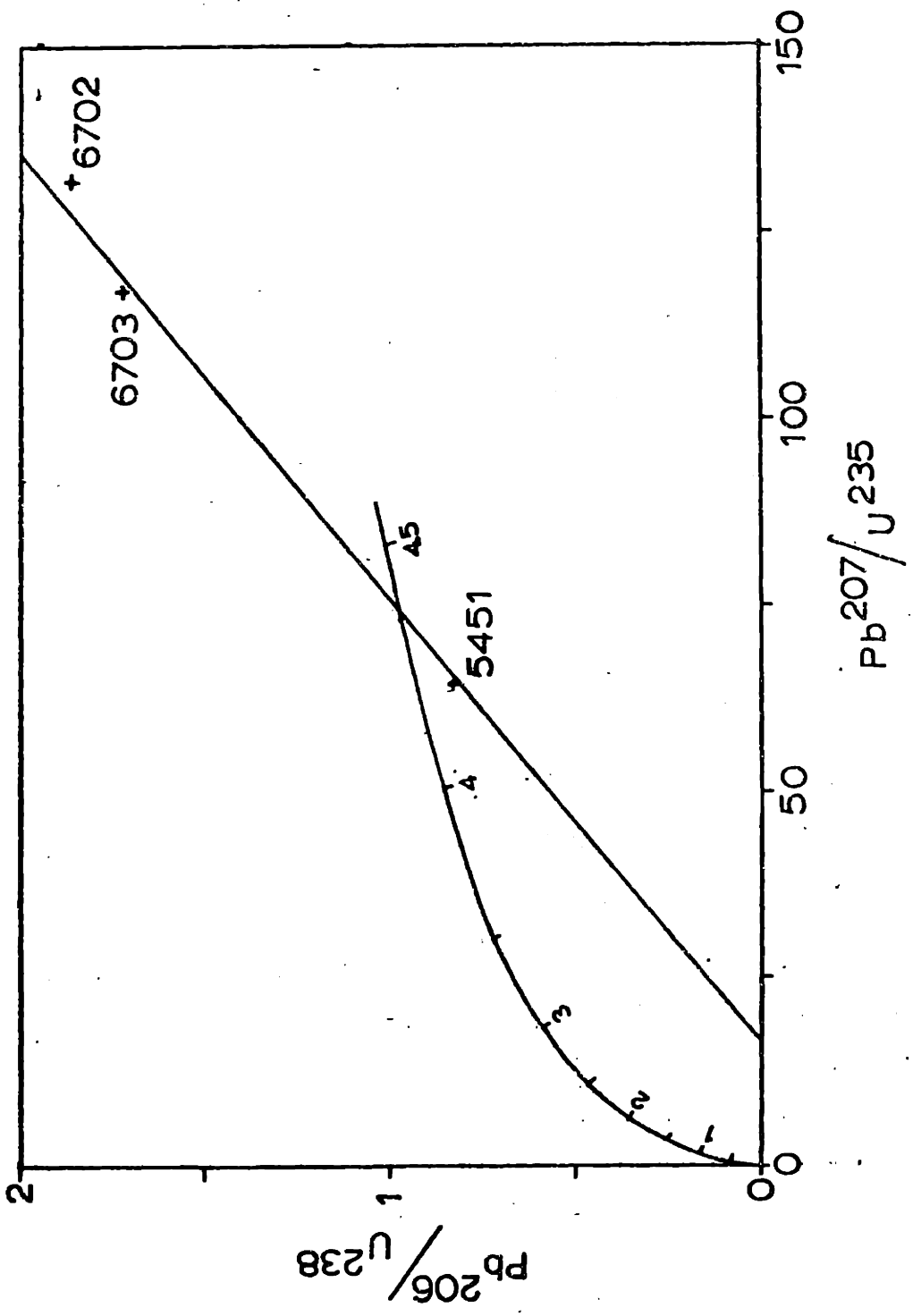
6702
6703
5451
45
4
3
2
1
0
50
100
150
Pb^{207}/U^{235}
2
1
0
Pb^{206}/U^{238}

Figure 29. Isochron plots for reconnaissance Imataca samples.

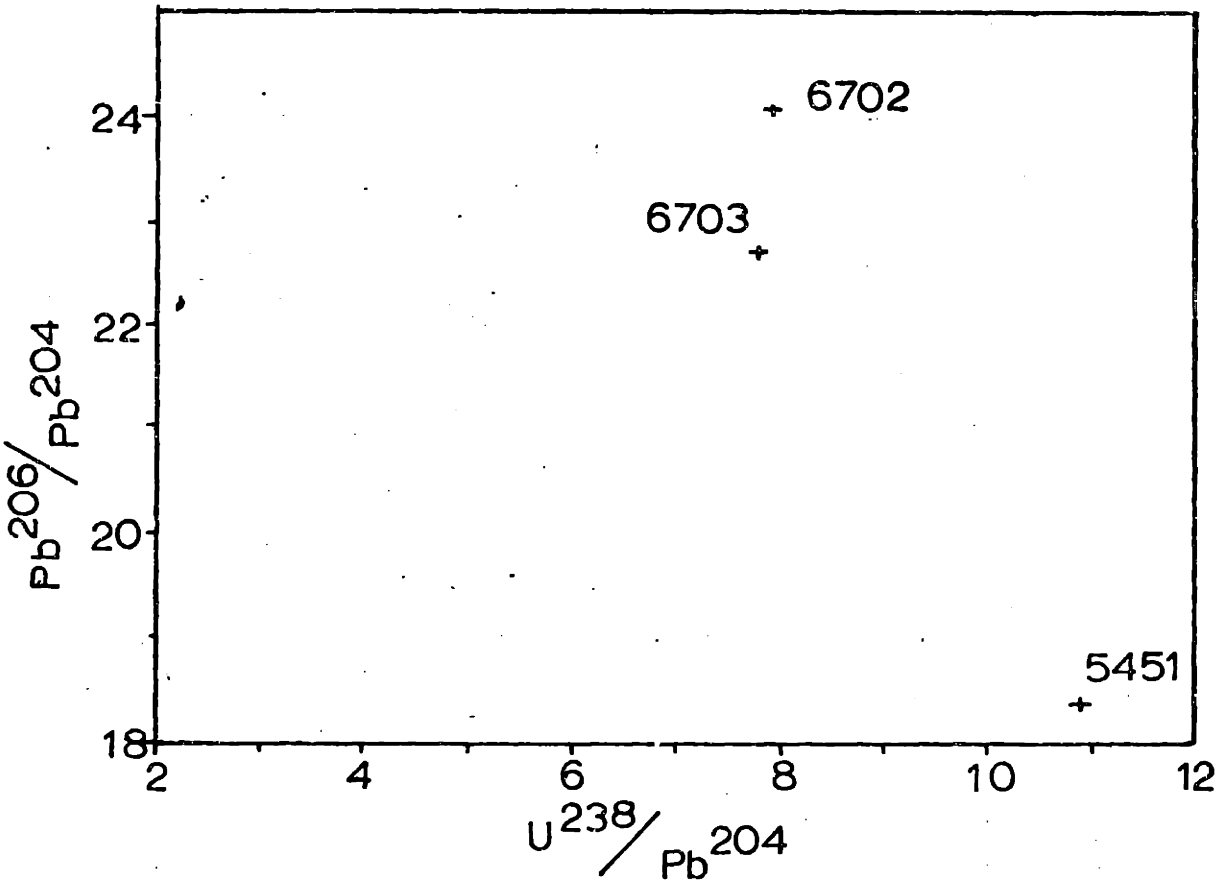
6702
6703
5451
24
22
20
18
2
4
6
8
10
12
Pb^{206}/Pb^{204}
U^{238}/Pb^{204}

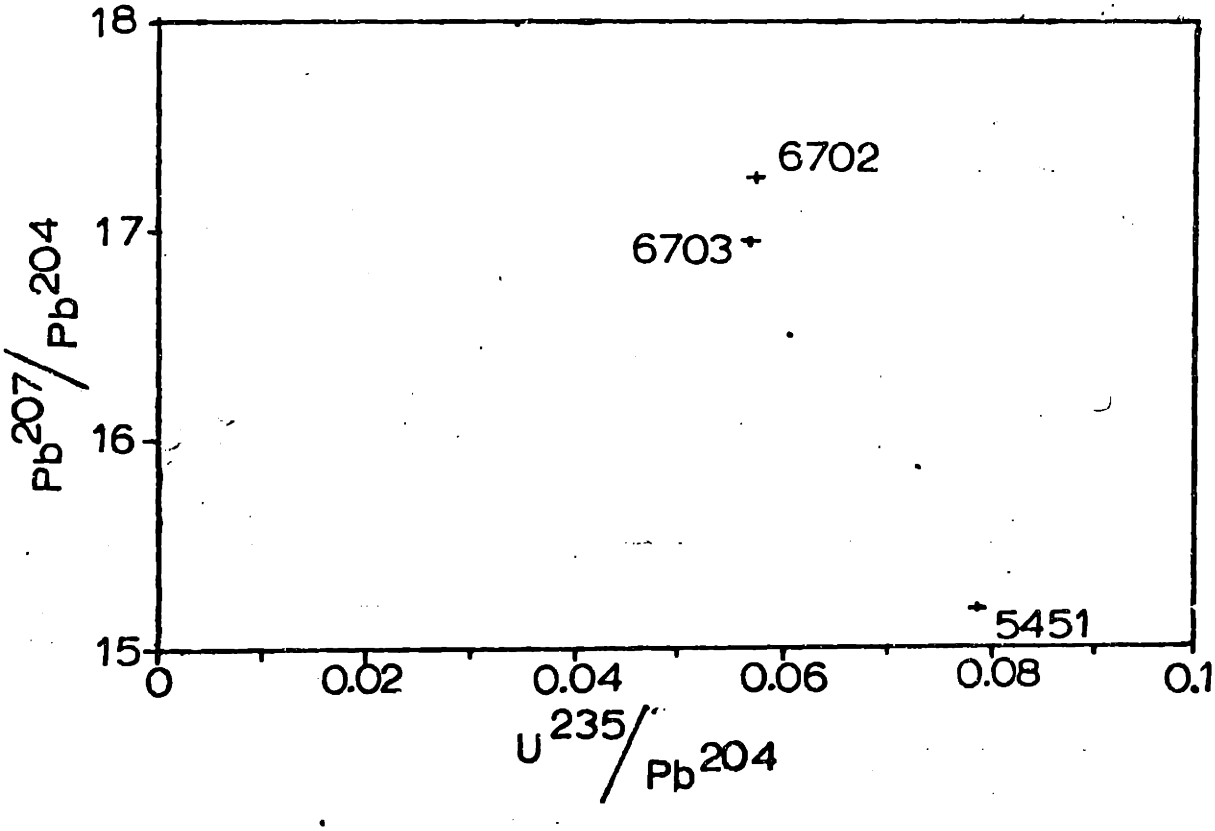
6702
6703
5451
18
17
16
15
0
0.02
0.04
0.06
0.08
0.1
Pb^{207}/Pb^{204}
U^{235}/Pb^{204}

with recent uranium loss or gain for these samples.

It is obviously theoretically possible that the linearity of the lead-lead plot is purely accidental. However, the correspondence of slope and intercept ages is reassuring support for a two-stage interpretation. If these three samples are orthogneisses, then the 3.8-b.y. age would just be the time this igneous material was separated from the mantle. The same age is a perfectly reasonable one for the source region of the metasediments, according to our earlier models. If 5451, 6702, and 6703 are also metasediments, the constraint of a two-stage model appears to require a very short period between source-region formation and sedimentation, unless one or the other of these processes was accomplished without change in μ, or with constant f, and an exact interpretation of the 3.8-b.y. age is not possible.

V. Iron Formations (8610-8621)

A dozen samples of iron formations were collected from various localities throughout the Imataca (see Figure 16(b)). In thinsection, most appear to be composed of nearly equal proportions of quartz and opaque minerals. Four samples (#8615-8618) also contain some mafic silicates, in varying proportions: ortho- and clinopyroxene, actinolite, and grunerite. Typical trace minerals include apatite, rutile, and zircon. Patches and strings of hematite/limonite, which on the whole appear to be secondary, occur in most samples, especially infilling cracks and grain boundaries. Most

specimens show banding in some degree; several (#8610-8612, 8618, and 8621) preserve the characteristic finely-laminated structure of banded iron formations, with alternating quartz-rich and opaque-rich layers, and 8611 even includes a distinct apatite-rich layer with prismatic crystals oriented parallel to the layering. Quartz in all sections is obviously strained. A few of the samples (especially 8613, 8620) show extreme granulation. Other evidence of deformation which may be observed in thin section includes "microboudinage" (sample 8612) and fine-scale faults (8612, 8621).

Originally it had been hoped that the iron formations would be especially low-μ samples which, ideally, would then provide "anchor points" - points with comparatively unradiogenic lead - to aid in the definition of the whole-rock lead-lead lines. This expectation was based particularly on work in the Archean of Greenland (Moorbath, 1973). The Isua iron formation from that area indeed contains exceptionally unradiogenic lead, with measured Pb^{206}/Pb^{204} values as low as 12.073. Isua leads are the least-radiogenic total-rock crustal leads yet analyzed.

However, as is immediately apparent from the lead-lead diagram for the Imataca iron formations (Figure 30), similar results are not found here. All twelve samples contain lead as radiogenic as the gneisses', and in one, 8621, the lead isotopic composition is vastly more radiogenic than that

Figure 30. Lead-lead plot, Imataca iron formations. Most samples show compositions in the same range as the gneiss samples, but note the exceptionally radiogenic lead of 8621 (see inset). Magnitude of error bars is partially due to uncertainty in the blank correction, since these iron formations have uniformly extremely low lead levels.

Reference regression line parameters for 8611-8620, excluding 8617: slope = 0.12597 $\pm$ 0.01487, intercept = 13.471 $\pm$ 0.299, MSWD = 2.65. Slope age is 2.04 $\pm$ 0.20 b.y.

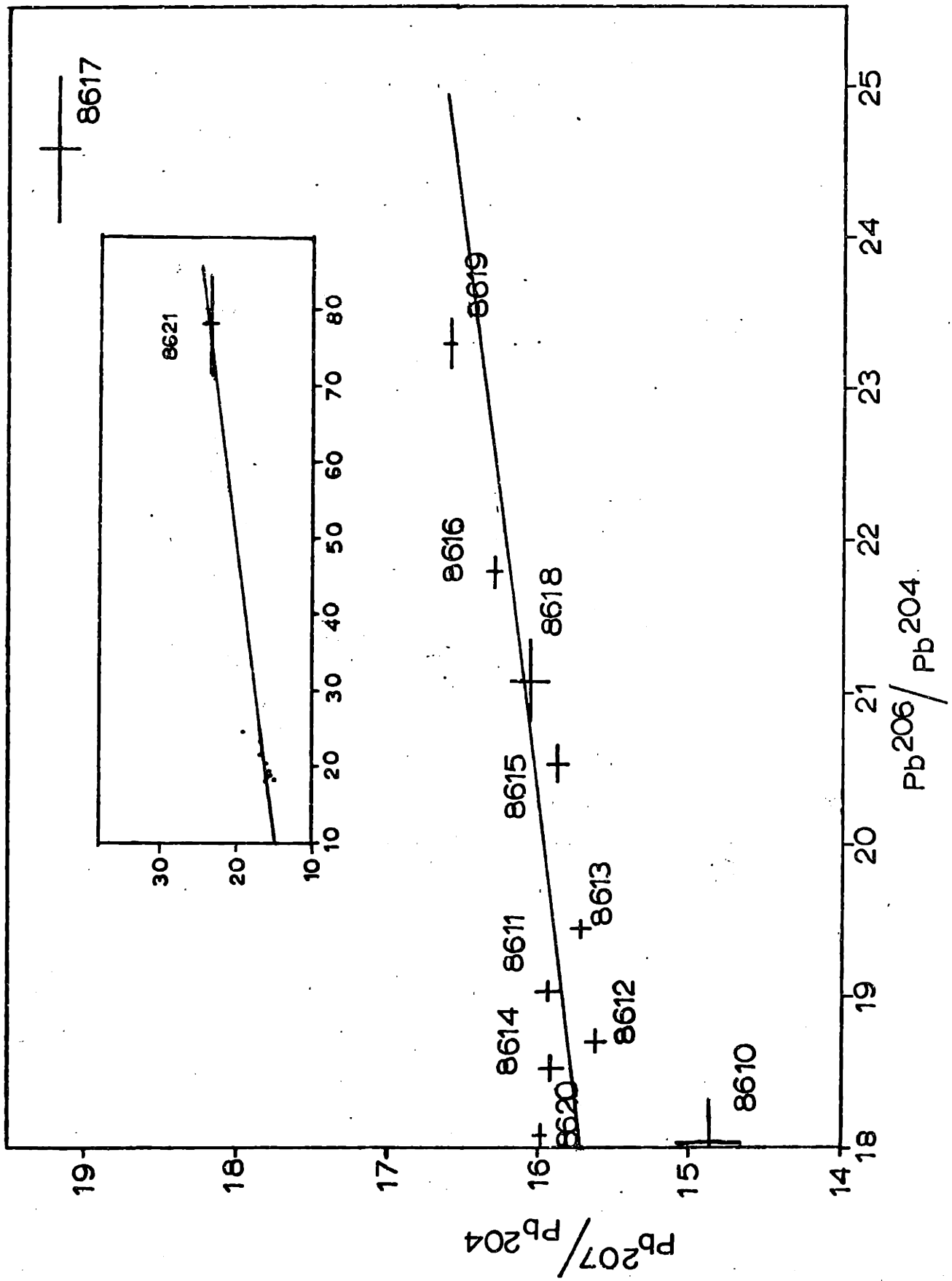
8617
8621
8619
8616
8618
8615
8611
8613
8614
8612
8620
8610
Pb207/Pb204
Pb206/Pb204

of any other rock analyzed in this study.

There are two main difficulties with attempting to derive a slope age from these points, one geologic and one analytical. The geologic problem is that there is no obvious way to decide a priori which of a number of geographically scattered samples may be stratigraphically equivalent, or genetically related, especially in a region as deformed as the Imataca. Samples which do not share a common history cannot be expected to define a meaningful line. The analytical problem arises from the unusually low levels of lead and uranium in these iron formations, and is twofold. First, uranium concentrations of the order of 0.1 pp. are difficult to determine very precisely. Second, the low sample lead levels (generally 1-2 ppm) mean that not only can the blank correction become relatively large, but the uncertainty in the total blank correction can contribute significantly to the uncertainty in the corrected lead isotopic composition. This latter effect explains the large error bars in Figure 30.

In spite of the uncertainties involved, the points on the lead-lead plot show a remarkably coherent distribution. Omitting 8617 and 8610 as being anomalous, for whatever reason, and 8621 because of the enormous error bars associated with it and its unusual composition, we obtain a line with a slope of 0.12597 $\pm$ 0.01487, intercept of 13.471 $\pm$ 0.299, MSWD = 2.65 - for a slope age of 2.04

± 0.20 b.y.! So it would appear that despite any differences in the details of their histories, the iron formations as a group also approximately record the metamorphic age of the Complex. What is equally remarkable is that 8621 lies along this reference isochron.

One important point to be made from the iron formation data is that the three-stage f_1 = constant model approximation made on the basis of samples from individual localities seems to hold true in a general way for the whole Complex, or at least for the iron formations. They record the metamorphic age with relatively little scatter about the reference isochron, which implies that at the time of that event they shared a similar lead isotopic composition. This fact suggests a fairly uniform evolution for all such samples up to the time of the metamorphism.

The scatter on the whole-rock Concordia plot (Figure 31) and isochron diagrams (Figure 32) is such that no attempt was made to fit a regression line to these data. The isochron diagrams could indicate recent, as well as ancient, disturbance of uranium, which would account for the scatter in the Concordia plot as well. It is interesting that the general trend of points on the latter diagram is still consistent with principal uranium depletion at the time of the granulite event. Consequently, the difference between the Isua and Imataca iron formations in the character of the lead they contain (radiogenic vs. nonradiogenic)

Figure 31. Concordia diagram, Imataca iron formations. Large error bars are a function of generally low levels of lead and especially uranium, leading to analytical difficulties (with U) and relatively large uncertainty in lead blank correction.

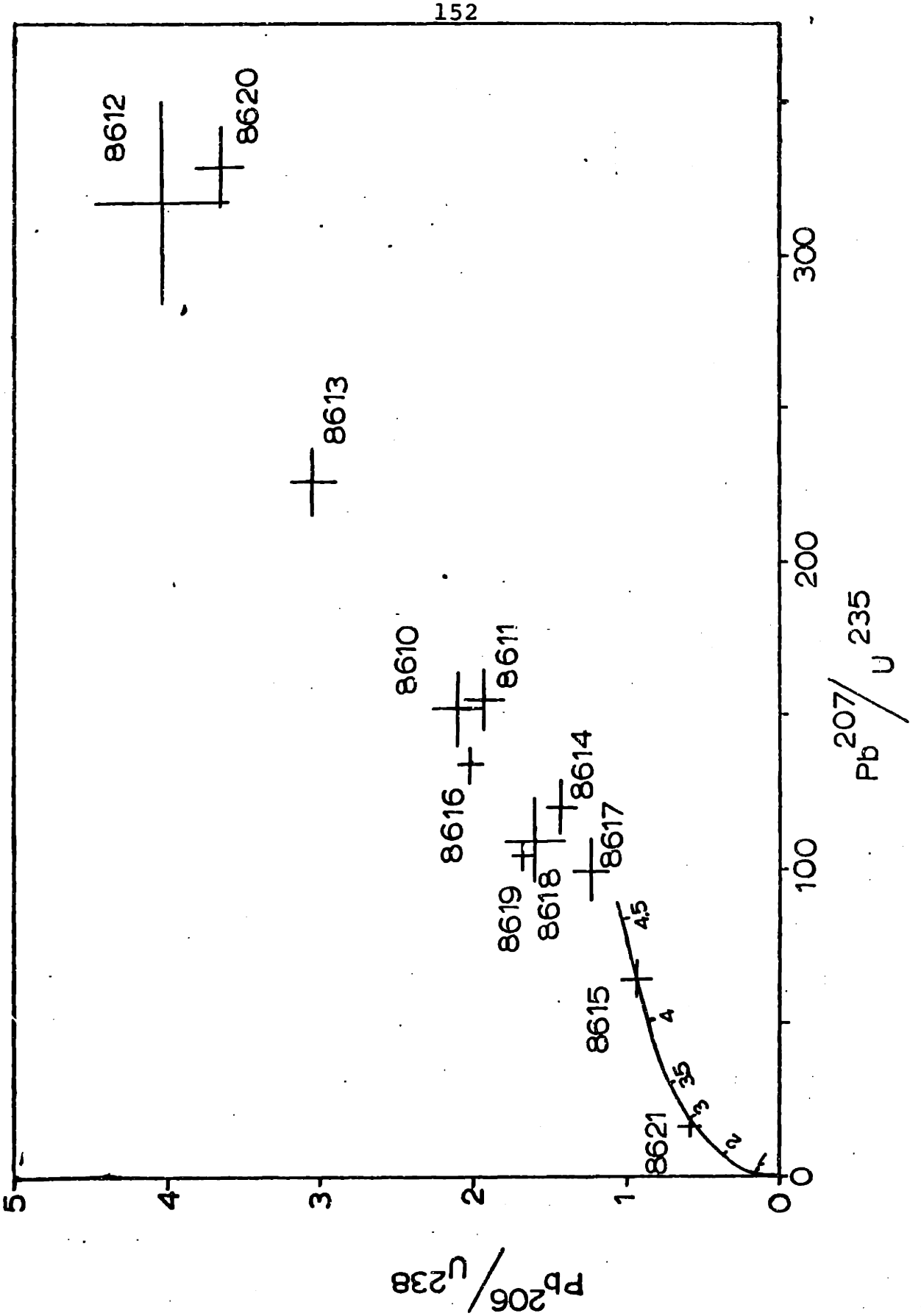
8612
8620
8613
8610
8611
8616
8614
8617
8619
8618
8615
8621
4.5
4
3.5
3
2
1
0
100
200
300
5
4
3
2
1
0
Pb^{207}/U^{235}
Pb^{206}/U^{238}

Figure 32. Isochron diagrams, Imataca iron formations. Sample 8621 has been omitted since it falls so far from the main grouping of points.

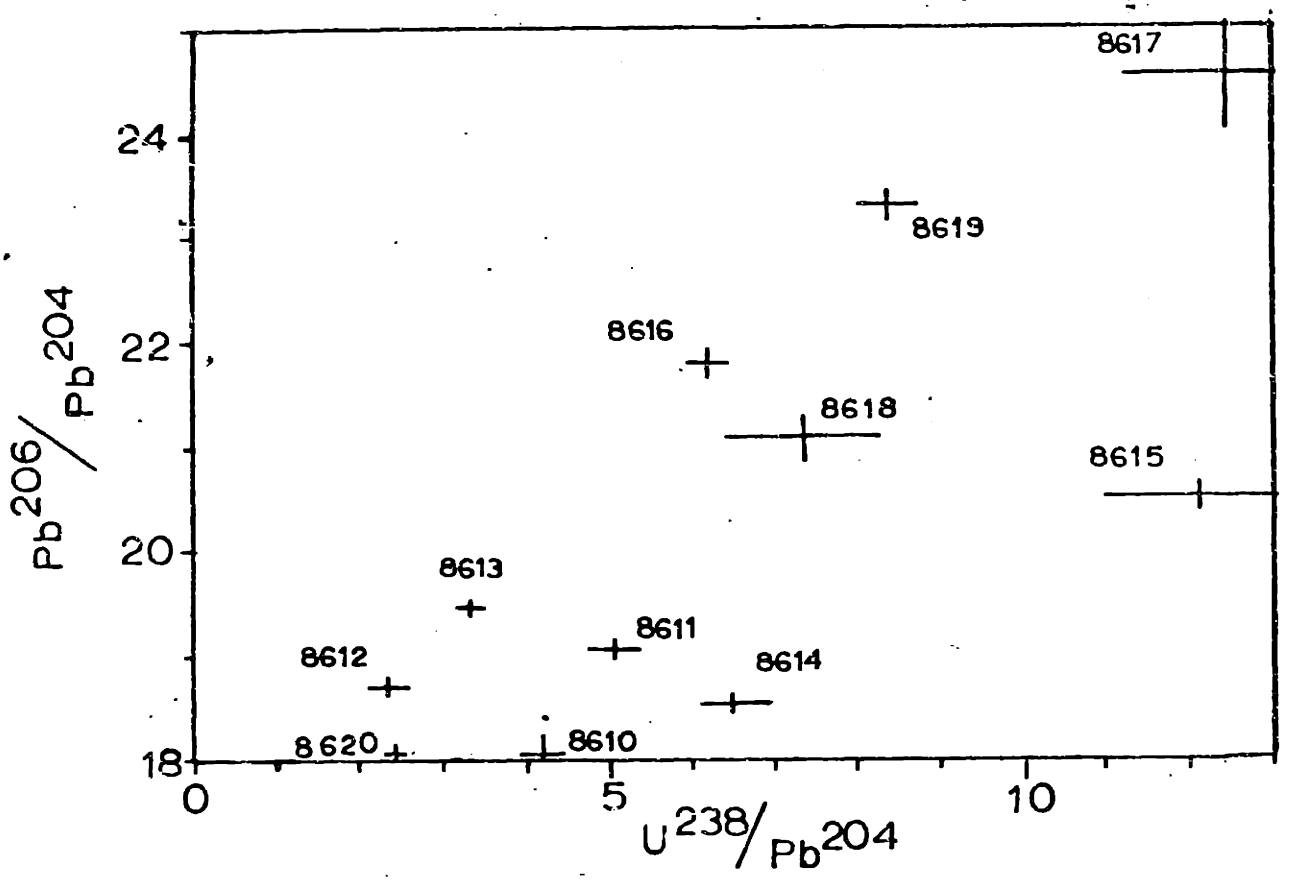
8617
8619
8616
8618
8615
8613
8611
8612
8614
8620
8610
24
22
20
18
0
5
10
Pb^{206}/Pb^{204}
U^{238}/Pb^{204}

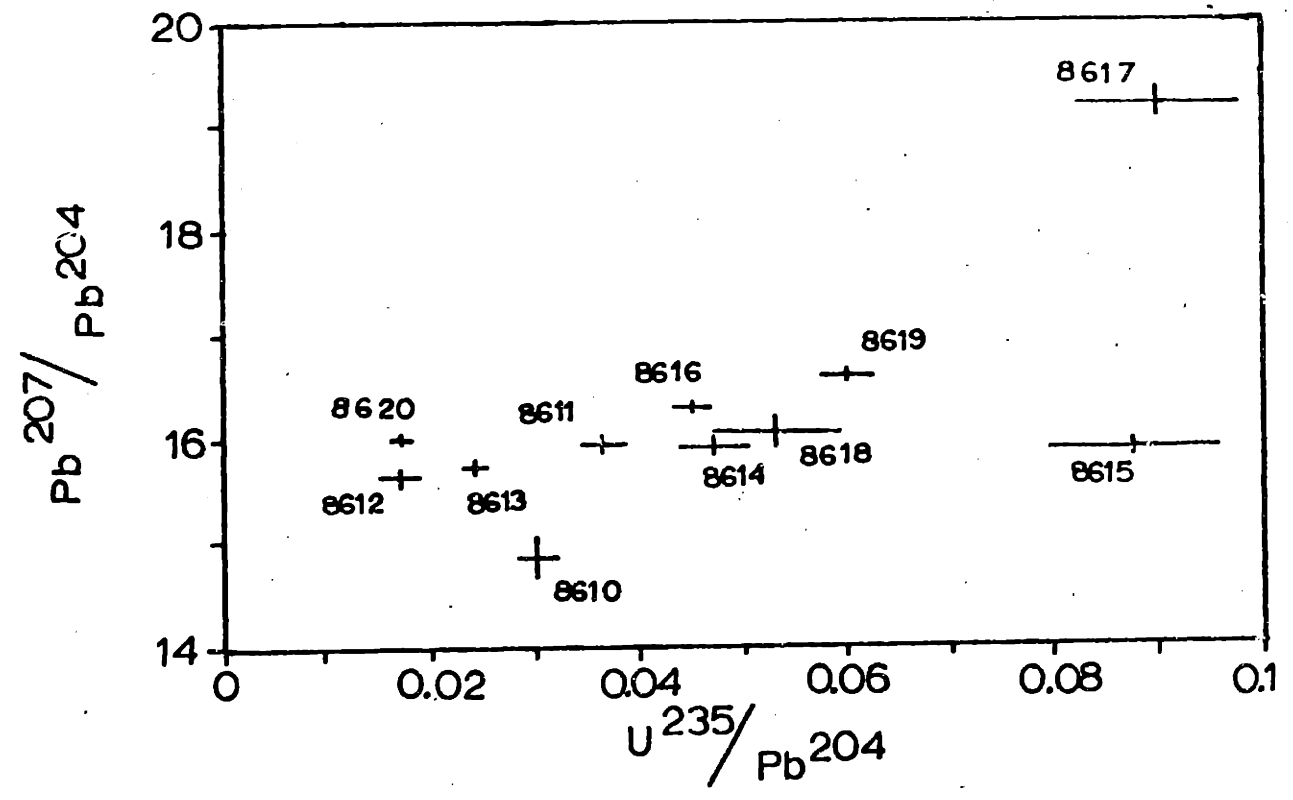
8617
8619
8616
8620
8611
8618
8614
8615
8612
8613
8610
20
18
16
14
0
0.02
0.04
0.06
0.08
0.1
Pb^{207}/Pb^{204}
U^{235}/Pb^{204}

may simply be attributed to different times of uranium depletion (i.e. highgrade metamorphism) in the two regions: in Greenland, intense metamorphism closely followed deposition, at 3.7-3.8 b.y. (Moorbath et al., 1973).

VI. Summary

The main points made in this chapter are summarized briefly below.

1. Whole-rock uranium-lead analyses on a variety of large total-rock samples confirm an age for the granulite metamorphism in the 2-2.3 b.y. range, as indicated by the previous Rb-Sr and fine-scale U-Pb results.

2. As expected, the granulite metamorphism was generally, though not invariably, accompanied by considerable uranium loss. In some samples it appears that a further more recent minor redistribution of uranium has taken place. The cause of this later disruption may or may not have been the same as that which resulted in sericitization of the feldspars of many samples.

3. A few samples from the western part of the Imataca Complex may reflect only a two-stage history. On a lead-lead plot they yield a slope and mantle growth curve intercept age of approximately 3.8 b.y. The preservation of this age could mean that the 2^{+}-b.y. metamorphism was of lower intensity in the western part of the Complex.

4. Measured lead isotopic composition of most other samples is consistent with a restricted higher-order

evolutionary history, which involved only limited variability in μ values prior to the time of the granulite metamorphism.

5. There may be some evidence from the total-rock lead data for a disturbance in the Guri Dam area at about the time of the La Ceiba migmatization.

6. It is theoretically possible to account for some of the observed scatter in Concordia and isochron diagrams in terms of sample-inhomogeneity problems. The assumption made throughout is that if a given split of sample powder is not perfectly representative of the total rock, at least it is internally consistent - that is, if it has a high μ value, it contains also the more radiogenic lead produced by that uranium. To the extent that this assumption is violated, scatter in Concordia or isochron diagrams may result. It seems improbable that the assumption should consistently hold for some suites of samples (the fine slices (Chapter 4), the El Pao gneisses) yet be violated for several samples at once from other groups. Therefore this effect is probably not generally significant, although it may occasionally occur.

6. Feldspar Lead Analyses

I. General

The use of lead isotopic compositions in potassium feldspars as a means of determining total-rock lead isotope composition at some past date has been practiced for some time (e.g. Catanzaro and Gast, 1960; Doe and Hart, 1963; Doe et al., 1965; Zartman, 1965). The principle involved is quite simple. Potassium feldspars can readily accommodate significant amounts of lead but not of uranium in the crystal lattice (Ahrens, 1965). Consequently, once a feldspar has become a closed system with respect to lead (and uranium) migration, it should essentially preserve that lead isotopic composition regardless of the continued evolution of radiogenic lead in the total rock. When the method was first used, measurement of the extremely small amounts of uranium present in the feldspar was difficult, so the assumption was frequently made that the change in feldspar lead isotopic composition from the time of closure to the present was negligible. It is now possible to measure this minor uranium, so feldspar lead ratios are customarily corrected for this last-stage radiogenic lead. Thus one can in theory "see through" the last stage of the evolution of the total-rock lead by this means, which may be very useful in reducing multistage systems to soluble cases. It is especially useful where post-equilibration behavior of uranium in the total rock is uncertain, so that correction

of whole-rock lead isotopic composition back to the equilibration time on the basis of present measured μ value is an unreliable approach.

Sixteen feldspars from various of the Imataca samples were analyzed in the hope of gaining additional information about the possible primary age of the region. Feldspar was separated from crushed rock of -80+170 mesh size using acetylene tetrabromide (to separate light minerals from those with a density greater than 2.96) and then a mixture of acetylene tetrabromide and acetone (to separate K-feldspar from quartz, plagioclase, and denser phases). In samples containing pure K-feldspar, this phase was separated for analysis; more commonly, alkali perthite (which either floats or hangs suspended in the second separation fluid) was used. Separates were washed briefly in warm 6N ultrapure HCl and rinsed twice in warm ultrapure water to remove surface contamination from the heavy-liquid separation. Separates appeared to be about 99% pure.

There exists some question as to the advisability of acid washing of feldspars. They lose a little relatively radiogenic lead and may lose a considerable fraction of their uranium during the washing (Oversby, 1975; Zartman, 1965). The net result may be an incorrectly low measured μ value for the feldspar. In the present study, it was felt that the desirability of removing surface lead contamination outweighed the danger of distorted μ values. In

general, the corrected lead isotopic compositions differed little from the measured values anyway, so increasing somewhat the μ on which the correction is based would make little difference. In no case did the analytical uncertainty in the quantitative determination of uranium introduce any significant uncertainty into the correction. Lead and uranium extraction and analysis were carried out as described in Chapter 3. Analytical data are summarized in Table 4.

The immediate question, which must be answered before the data may be discussed, is: at what time did the feldspars last equilibrate with their host rocks? This will have a profound effect on the interpretation of the results, unless the data fall along the primary growth curve and can be assigned model ages directly. If they form any sort of linear array, the slope m may be used to determine a prehistory age t_1 for the start of the stage recorded by that slope, according to the equation

$$m = \frac{1}{137.88} \left(\frac{e^{\lambda' t_1} - e^{\lambda' t_2}}{e^{\lambda t_1} - e^{\lambda t_2}} \right)$$

where t_2 is the reference time at which we are viewing the system (the age to which the feldspar compositions have been corrected, which should be the last equilibration between feldspars and host rocks), and t_1 the start of the stage t_1 to t_2, at which time the feldspars (rocks) shared a common

TABLE 4. Feldspar analyses

Sample	Pb^{208}/Pb^{204}	Pb^{207}/Pb^{204}	Pb^{206}/Pb^{204}	Pb, ppm	U, ppm	μ
5451	37.10 ± 0.03	15.63 ± 0.01	16.00 ± 0.01	52.44	0.290	0.334
6702	35.81 ± 0.03	16.84 ± 0.01	19.67 ± 0.01	43.39	0.754	1.10
6703	36.32 ± 0.03	16.23 ± 0.01	18.19 ± 0.01	41.00	0.541	0.818
7491	40.05 ± 0.04	17.20 ± 0.02	20.21 ± 0.02	28.72	0.0842	0.199
7492	35.89 ± 0.04	15.96 ± 0.02	16.67 ± 0.02	51.43	0.0951	0.111
7493	36.29 ± 0.07	15.85 ± 0.02	16.51 ± 0.02	37.66	0.0498	0.0796
7494	36.52 ± 0.04	16.21 ± 0.01	17.70 ± 0.01	37.16	0.244	0.405
8100A2	37.32 ± 0.04	16.37 ± 0.02	18.01 ± 0.02	45.00	0.109	0.152
8100B2	37.88 ± 0.06	16.25 ± 0.02	17.70 ± 0.02	38.60	0.179	0.292
8100D2	39.05 ± 0.06	16.69 ± 0.02	18.46 ± 0.02	34.96	0.182	0.338
8100F2	38.51 ± 0.07	16.48 ± 0.02	18.17 ± 0.02	40.78	0.151	0.238
8100G2	39.46 ± 0.04	16.44 ± 0.02	18.09 ± 0.02	38.96	0.122	0.203
8150	34.65 ± 0.04	16.86 ± 0.02	19.60 ± 0.02	46.20	0.256	0.345
8151	34.57 ± 0.04	16.65 ± 0.02	18.75 ± 0.01	39.59	0.0861	0.133
8152	34.90 ± 0.05	16.78 ± 0.02	19.02 ± 0.02	33.86	0.0895	0.164
8160	34.66 ± 0.04	17.02 ± 0.02	20.18 ± 0.02	30.99	0.251	0.511

lead isotopic composition. (Decay constants λ and λ' are the usual decay constants for U^{238} and U^{235} respectively.) While the choice of t_2 does not greatly affect the corrected lead isotope compositions of the feldspars, or, therefore, m, its occurrence in exponential terms of the above equation will definitely affect the derived prehistory age t_1.

The simplest assumption to make for the Imataca is that $t_2 \cong 2$ b.y. - that is, that the time of last equilibration of feldspars and host rocks was the time of the granulite event. It is not likely to have been earlier than this, at least where the total rocks reflect the granulite metamorphic age. Could it have been later? Perhaps. Recall that a rubidium-strontium mineral isochron including plagioclase and biotite from one of the Guri Dam samples (8100F2) yields an age of about 1.2 b.y. This may indicate lowgrade (retrograde) metamorphism. But it is unclear whether or not we can expect re-equilibration of lead isotopes also between feldspar and host rocks at that time. Doe and Hart (1963) conclude that under contact-metamorphic conditions, lead in K-feldspar re-equilibrates more readily than rubidium and strontium in feldspars, but less easily than Rb-Sr in biotite. On the other hand, in a regional-metamorphic setting, Doe et al. (1965) observe that metamorphism below the kyanite zone of amphibolite grade does not significantly affect the composition of feld-

spar lead. Metamorphism up to amphibolite grade would very likely have resulted in widespread retrograding of the hypersthene, and probably caused partial re-equilibration of strontium isotopes among the fine-slice samples of Chapter 4 as well. So it is assumed, as a first approximation, that indeed $t_2 \cong 2$ b.y.

A crude test of this assumption is possible. One can construct, for each sample, 2-point "isochrons", given the total-rock and feldspar lead isotopic compositions and μ values, and the isochron slopes ought to yield the time at which the feldspar and total-rock lead isotope compositions were the same. Of course, this will only be exactly true if the measured lead ratios and μ are "correct" for both points. (That is, the lead isotopic composition of a given sample must reflect evolution according to the measured μ for that sample since the time of last lead isotopic equilibration.) More recent alteration of uranium distribution, for instance, would mar the accuracy of the determination; recent uranium loss from the total rocks would steepen the "isochrons" and give anomalously old equilibration ages. Still, some samples were noted in Chapter 5 which appeared to have retained the uranium from their post-granulite history: 8150-8160, possibly 8100A2-D2 or 7491-7493. For such samples the two-point "isochron" ages generally cluster in the range 1.4-2.5 b.y., with an average of 2.17 $\pm$ 0.14 b.y. Omitting 8151 and 8152, which have such

low total-rock μ's that the feldspar is an important determinant of the slopes, the average is 1.91 $\pm$ 0.09 b.y. So it appears that $t_2 \cong 2$ b.y. is not a bad supposition after all.

It should be pointed out that if the isotopic composition of lead in the total rocks was absolutely homogeneous throughout a given suite of rocks at $t=t_2$, the feldspars should have identical lead compositions also when reduced to that time. This result is not observed for any of the groups of feldspars analyzed. Therefore, as we suspected from the scatter in the total-rock lead-lead plots, the three (or four) stage constant-f models are only approximately correct; premetamorphic μ's varied somewhat among subsystems in a given system, producing a corresponding variability in premetamorphic lead isotopic composition among the total-rock samples.

It should further be noted that at least for most granulites, for which the last stage of lead isotopic evolution on the total-rock scale began at the time of the metamorphism to which we are correcting the feldspar compositions, the feldspars should in turn reflect a history of one fewer stages. That is, if a special three-stage model is appropriate to describe total-rock lead evolution, the feldspar compositions seen at the time of the granulite event should reflect a two-stage history, and so on.

TABLE 5. Feldspar analyses, corrected to 2 b.y.

Sample	Present measured Pb^{207}/Pb^{204}	Present measured Pb^{206}/Pb^{204}	Values 2 b.y. ago Pb^{207}/Pb^{204}	Values 2 b.y. ago Pb^{206}/Pb^{204}
5451	15.63	16.00	15.62	15.88
6702	16.84	19.67	16.79	19.23
6703	16.23	18.19	16.19	17.89
7491	17.20	20.21	17.19	20.14
7492	15.96	16.67	15.96	16.63
7493	15.85	16.51	15.85	16.48
7494	16.21	17.70	16.19	17.55
8100A2	16.37	18.01	16.36	17.95
8100B2	16.25	17.70	16.24	17.59
8100D2	16.69	18.46	16.67	18.34
8100F2	16.48	18.17	16.47	18.08
8100G2	16.44	18.09	16.43	18.02
8150	16.86	19.60	16.84	19.47
8151	16.65	18.75	16.64	18.70
8152	16.78	19.02	16.77	18.96
8160	17.02	20.18	17.00	19.99

Feldspar lead isotopic compositions corrected to 2 b.y. ago on the basis of measured μ values are listed in Table 5, together with the corresponding present ratios.

II. Guri Dam Samples - 8100 Series

Lead isotopic compositions of the feldspars from the 8100 series of Guri Dam samples, corrected to 2 b.y. ago, are plotted in Figures 33 and 34. The corrected compositions define a small linear spread. Regression parameters for this line are: slope = 0.53946 $\pm$ 0.03034, intercept = 6.7199 $\pm$ 0.5473, MSWD = 3.03. For a t_2 of 2 b.y., the corresponding calculated t_1 age is 3.67 $\pm$ 0.10 b.y. If t_2 is varied by $\pm$ 0.1 b.y., the t_1 age only changes by about $\pm$ 0.5 b.y., so even if t_2 is not exactly 2.0 b.y., the calculated t_1 age should be fairly accurate.

It appears from Figures 33 and 34 that the older intercept of the regression line with a typical mantle growth curve is closer to 3.8-3.9 b.y. and the upper intercept correspondingly a little younger than 2 b.y. But considering the uncertainties in the regression parameters increases the range of the intercept ages, to include 3.7 and 2 b.y. In any case, the calculated t_1 age is, of course, determined solely from the slope of the regression line, independently of the growth curve used for reference. Still, the near-coincidence of slope and intercept t_1 ages is interesting.

The feldspar compositions are plainly consistent with

Figure 33. Feldspar analyses, 8100 series samples, Guri Dam I. Age-corrected and uncorrected compositions are nearly identical. Points shown are corrected to 2.0 b.y. ago on the basis of present measured values. Regression line has a slope of 0.53946 ± 0.03034, intercept of 6.7199 ± 0.5473, MSWD = 3.03. For a t_2 age of 2.0 b.y., the corresponding t_1 is calculated to be 3.67 ± 0.10 b.y. Reference growth curve, mantle growth curve of Doe and Zartman (1977).

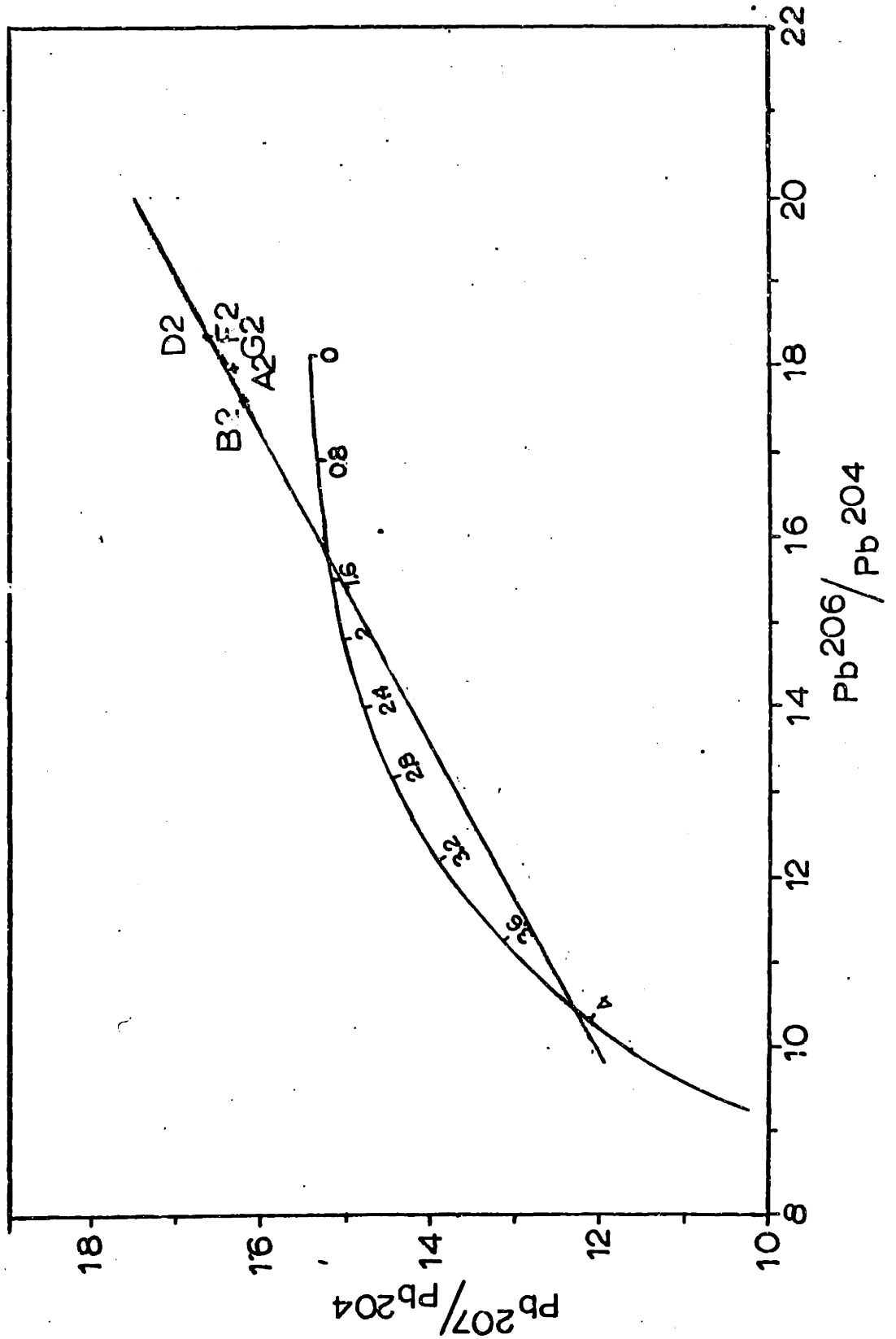
D2
F2
A2G2
B2
0
0.8
1.6
2
2.4
2.8
3.2
3.6
4
Pb^{207}/Pb^{204}
Pb^{206}/Pb^{204}
18
16
14
12
10
8
12
14
16
18
20
22

Figure 34. Feldspar analyses, 8100 series samples, Guri Dam II. Data points shown and regression line plotted are identical to those in Figure 33. Reference growth curve, mantle growth curve of Stacey and Kramers (1975).

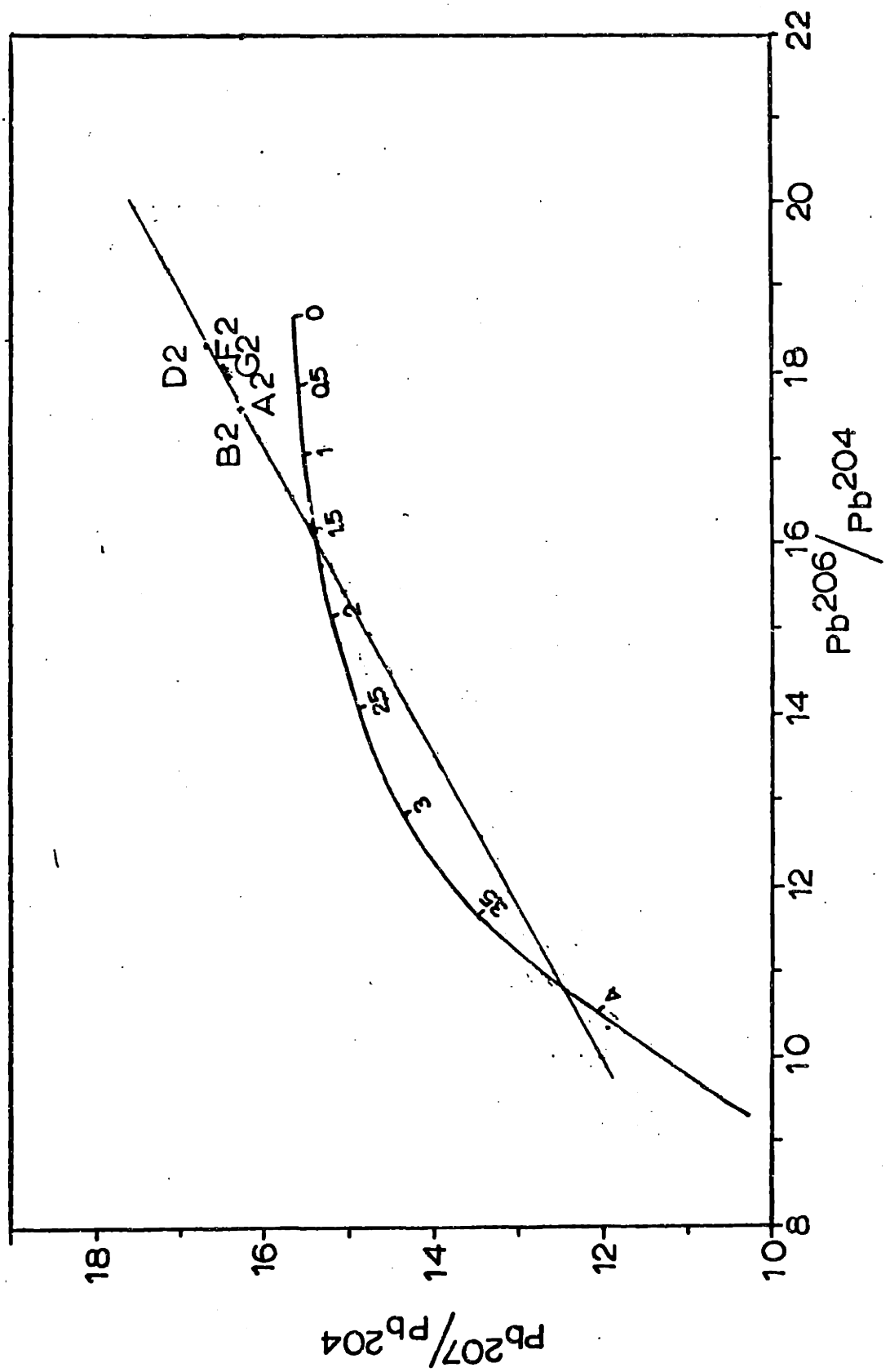
Pb207/Pb204
Pb206/Pb204
D2
F2
G2
A2
B2
0
.5
1
1.5
2
2.5
3
3.5
4
8
10
12
14
16
18
20
22

an approximately two-stage history (prior to 2 b.y.) with $t_1 \cong 3.7$ b.y. Therefore the approximately three-stage history by which we had formally described the lead isotopic evolution in the fine-slice samples (Chapter 4) and the 8100 series total-rock samples (Chapter 5) looks to have been a reasonable model. (It is re-emphasized here that the model does not distinguish between the case in which f_1 is truly nearly constant and that in which homogenization of lead isotopes has occurred at t_2, just as a three-stage model cannot be distinguished from a strictly four-stage model with very short second stage.) More importantly, this rather well-defined slope age (t_1) of 3.7 b.y. for the start of the pre-2-b.y. stage strongly supports the "primary age" of 3.5^+ b.y. previously inferred both from the fine-slice data (Chapter 4) and the reconnaissance total-rock samples (5451, 6702-03 - Chapter 5).

III. Guri Dam Samples - 7491-7494

The other suite of Guri Dam samples (7491-7494) once again create a different picture. The compositions of these feldspars, corrected to 2 b.y. ago, are plotted in Figure 35. The most stiking point about this diagram is that the feldspars seem to reflect a three-stage history prior to 2 b.y., for the regression line does not intercept the primary growth curve. Regression parameters for the line defined are: slope = 0.35913 $\pm$ 0.00544, intercept = 9.9436 $\pm$ 0.0965, MSWD = 3.15. For t_2 = 2.0 b.y., the calculated t_1 age is 2.88 $\pm$

Figure 35. Feldspar analyses, samples 7491-7494, Guri Dam. Present (uncorrected) and age-corrected values are virtually the same; points shown are corrected to 2.0 b.y. ago. Reference growth curve, mantle growth curve of Doe and Zartman (1976). Regression line drawn has a slope of 0.35913 $\pm$ 0.00544, intercept of 9.9436 $\pm$ 0.0965, MSWD = 3.15. For a t_2 age of 2 b.y., the calculated t_1 age is 2.88 $\pm$ 0.04 b.y.

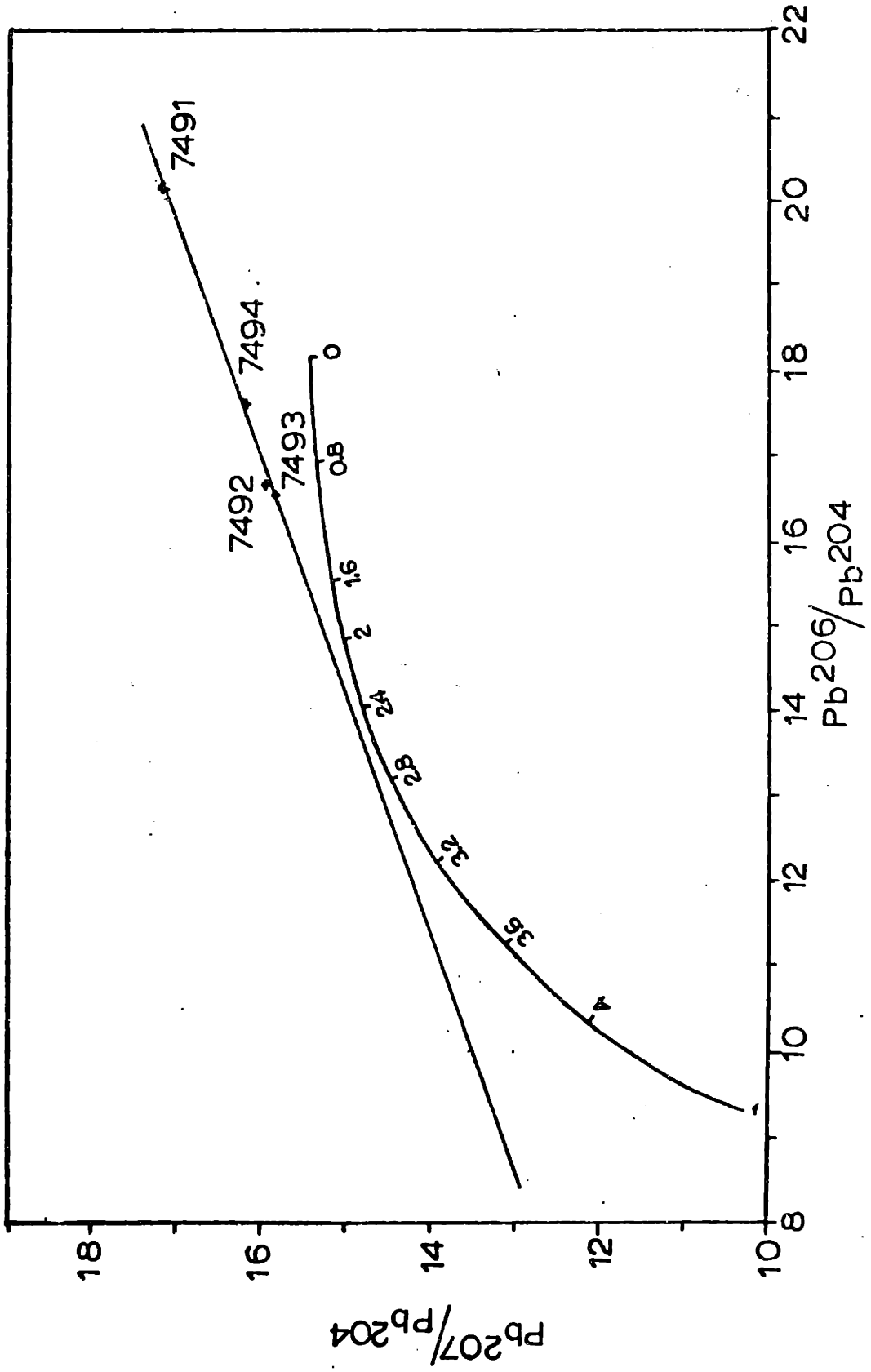
7491
7494
7493
7492
0
0.8
1.6
2
2.4
2.8
3.2
3.6
4
Pb^{207}/Pb^{204}
Pb^{206}/Pb^{204}
8
10
12
14
16
18
20
22

0.03 b.y.

What is intriguing is that this age closely coincides with the total-rock lead-lead age for these same samples of 2.94 ± 0.04 b.y. Perhaps the 2.9-b.y. age is meaningful after all.

It should, incidentally, be observed that the apparently three-stage pre-2-b.y. history for the feldspars does not mean that a three-stage history cannot also describe the total-rock system. There is after all no evidence that the rocks shared a common lead isotopic composition at 2 b.y.; we are only supposing that the feldspars equilibrated with the total rocks with respect to lead isotopic composition at that time. Both total rocks and feldspars suggest a homogeneous lead isotopic composition at 2.9 b.y.; this may be t_2 for the total-rock system.

It is still quite possible that the 2.9-b.y. age is not geologically significant. If t_2 for the feldspars is taken as 1.2 b.y., t_1 is close to 3.3 b.y., rather nearer to our expected primary age. In such a case the total-rock results must be attributed to graphical accident. Still, the 8100 series feldspars do seem to have equilibrated last with their host rocks around 2 b.y., as do also most other samples, according to the crude test described earlier. The more ways in which the two series of Guri Dam samples must be supposed to have behaved differently, the less plausible the resulting interpretation of the isotopic data. Therefore,

for lack of evidence to the contrary, we take 2 b.y. to be the time of last equilibration between feldspars and whole rocks for the 7491-7494 series samples as well. In that case, the feldspar and total-rock lead isotopic data seem to reinforce each other in indicating a 2.9-b.y. age. If that date is meaningful, it could be explained by the theory outlined in the previous chapter.

IV. Reconnaissance Samples (5451, 6702, 6703)

Feldspars from the reconnaissance gneiss samples (5451, 6702, 6703) are likewise interesting (Figure 36). The points are corrected back to 2 b.y. on the assumption that these feldspars are most likely to have equilibrated with their host rocks at the time of the granulite event elsewhere, if at all; and they have obviously equilibrated with the more radiogenic rock lead at some time after their separation from the mantle. This is shown by where they presently plot. A two-stage history was suggested for the total rocks, as discussed in the previous chapter. If the feldspars had remained closed since the apparent primary age of 3.8 b.y., they would all cluster along the primary growth curve at that age, which they obviously do not do. Regardless of the time at which they all equilibrated with the host rocks, they should, when corrected to that time, define a line through the age of the equilibration and the primary age. This they do not do either, whatever reasonable t_2 age is chosen. If t_2 = 2 b.y. is chosen, the regression line has a slope of 0.33930 $\pm$

Figure 36. Feldspar analyses, reconnaissance Imataca samples (5451, 6702, 6703). Circled points are measured isotopic compositions; corresponding uncircled points are corrected back to 2 b.y. ago on the basis of present measured μ's. Slope of regression line for corrected points is 0.33930 $\pm$ 0.00499, intercept 10.202 $\pm$ 0.0881, MSWD = 9.06. This slope corresponds to a t_1 age of 2.76 $\pm$ 0.04 b.y. for t_2 = 2 b.y. Reference growth curve, mantle growth curve of Doe and Zartman (1977).

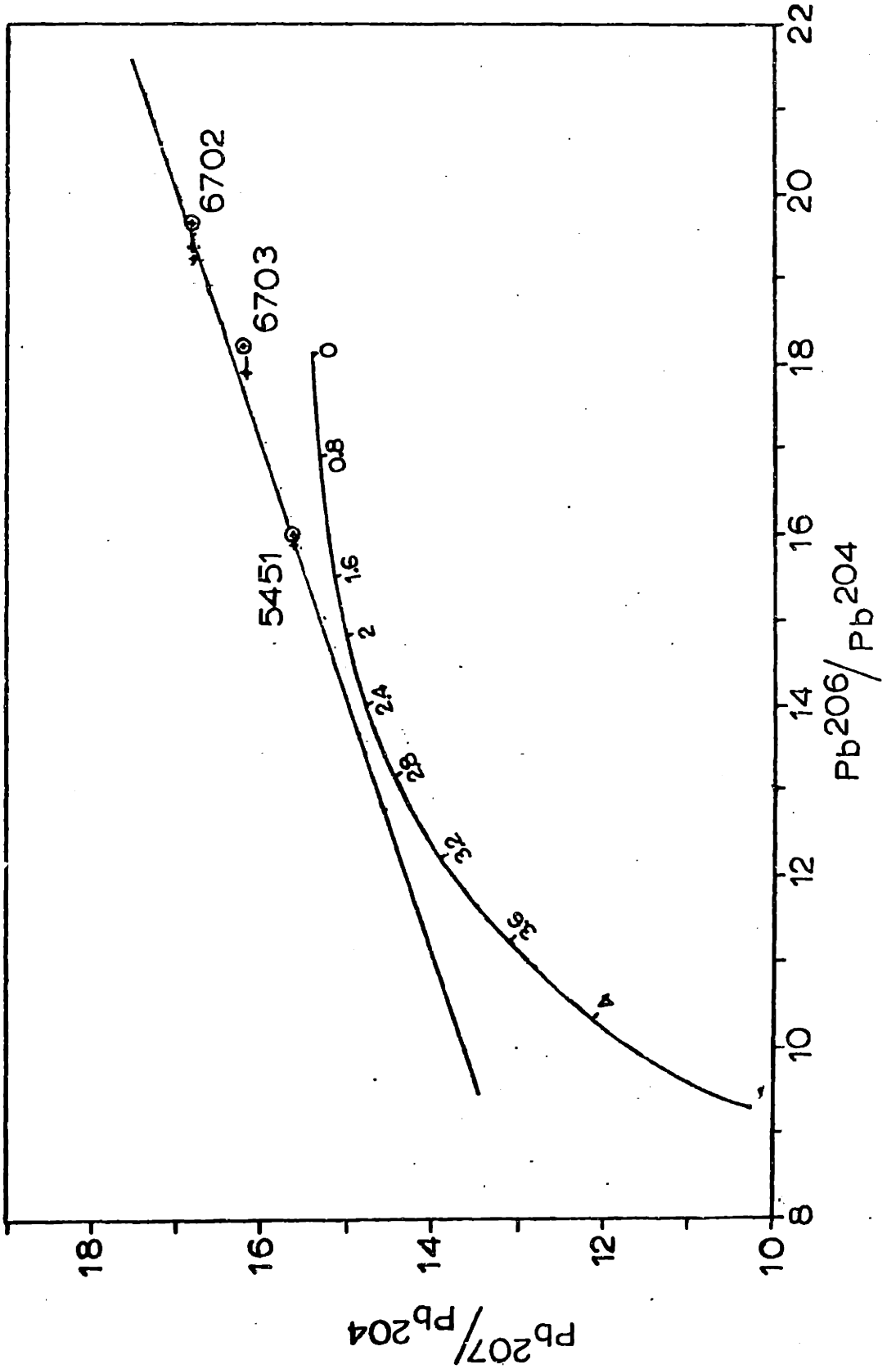
6702
6703
5451
0
.8
1.6
2
2.4
2.8
3.2
3.6
4
Pb^{207}/Pb^{204}
Pb^{206}/Pb^{204}

0.00499, intercept of 10.202 ± 0.0881, MSWD = 9.06. For t_2 = 2 b.y., the calculated t_1 age is 2.76 ± 0.04 b.y. While there is some temptation to seize on this age as indicating that the 7491-7494 results are meaningful, several objections may immediately be raised: 1. The relatively large MSWD value, a factor of 2-5 greater than those for other lead-lead lines reported in this research, shows a poorer fit of the data to the line than we have previously found, so the interpretation may be proportionately less reliable. 2. No simple geologic explanation for the data exists. The total-rock data suggest that lead isotopic composition of the three samples diverged with time after 3.8 b.y. or so. No mechanism which would produce the same feldspar composition in all samples at 2.8 b.y. without disturbing the total-rock uranium-lead systems is readily apparent. 3. There is no evidence after all that the three feldspars last equililbrated with their host rocks at the same time, let alone at 2 b.y.

This last objection underscores the fact that one should not be too quick to conclude that a date is meaningful just because it resembles another date from somewhere else. In this case, it is proposed that the 2.8 b.y. t_1 age is in fact only accidental, arising from unsubstantiated assumptions about equilibration times. If in fact we suppose that 5451 (collected between the Guri Dam and the migmatite) may have equilibrated with its host rocks at one time (say 2

b.y.), and 6702 and 6703 (located close to each other, but far west of the migmatite) at another, then it is impossible to draw a meaningful line through all three feldspar compositions for any t_2. Considering the two areas separately leads to much simpler (though not unique) interpretations which are at least consistent with the total-rock data.

Since lead in feldspars from other rocks east of the migmatite seems to have equilibrated last at about 2 b.y. ago, suppose first that the feldspar in 5451 did likewise. Projected back through the 2 b.y. point on a mantle growth curve (Figures 37,38), this feldspar lead indicates a primary age of about 3.8-3.9 b.y., depending somewhat on the model used - in excellent agreement with the total-rock data. (This is obviously not to be construed as proof of the primary age. It is simply a demonstration that a straightforward model, involving two-stage evolution at the total-rock scale ($t_1 \cong 3.8$ b.y.) with feldspar equilibration at independently-inferred $t_2 = 2$ b.y. is internally consistent, and consistent also with other conclusions.)

The compositions of 6702 and 6703 fall to the right of this projection line (are more radiogenic), so suppose that these feldspars equilibrated with their host rocks a little later, perhaps at 1.2 b.y. It is certainly possible that the 1.2 b.y. event was more significant to the west. Forcing a line through these data (corrected to 1.2 b.y.) and the corresponding point on the mantle growth curve (Figures 37,

Figure 37. Back-projection of reconnaissance Imataca feldspar compositions I. Reference growth curve, mantle growth curve of Doe and Zartman (1977).

Solid line: 5451 corrected to 2 b.y. ago, projected through 2 b.y. point on growth curve.

Dashed line: best fit of 6702 and 6703, corrected to 1.2 b.y. ago, with 1.2 b.y. point on growth curve (slope = 0.4736 $\pm$ 0.0068, intercept = 7.642 $\pm$ 0.123, MSWD = 5.15).

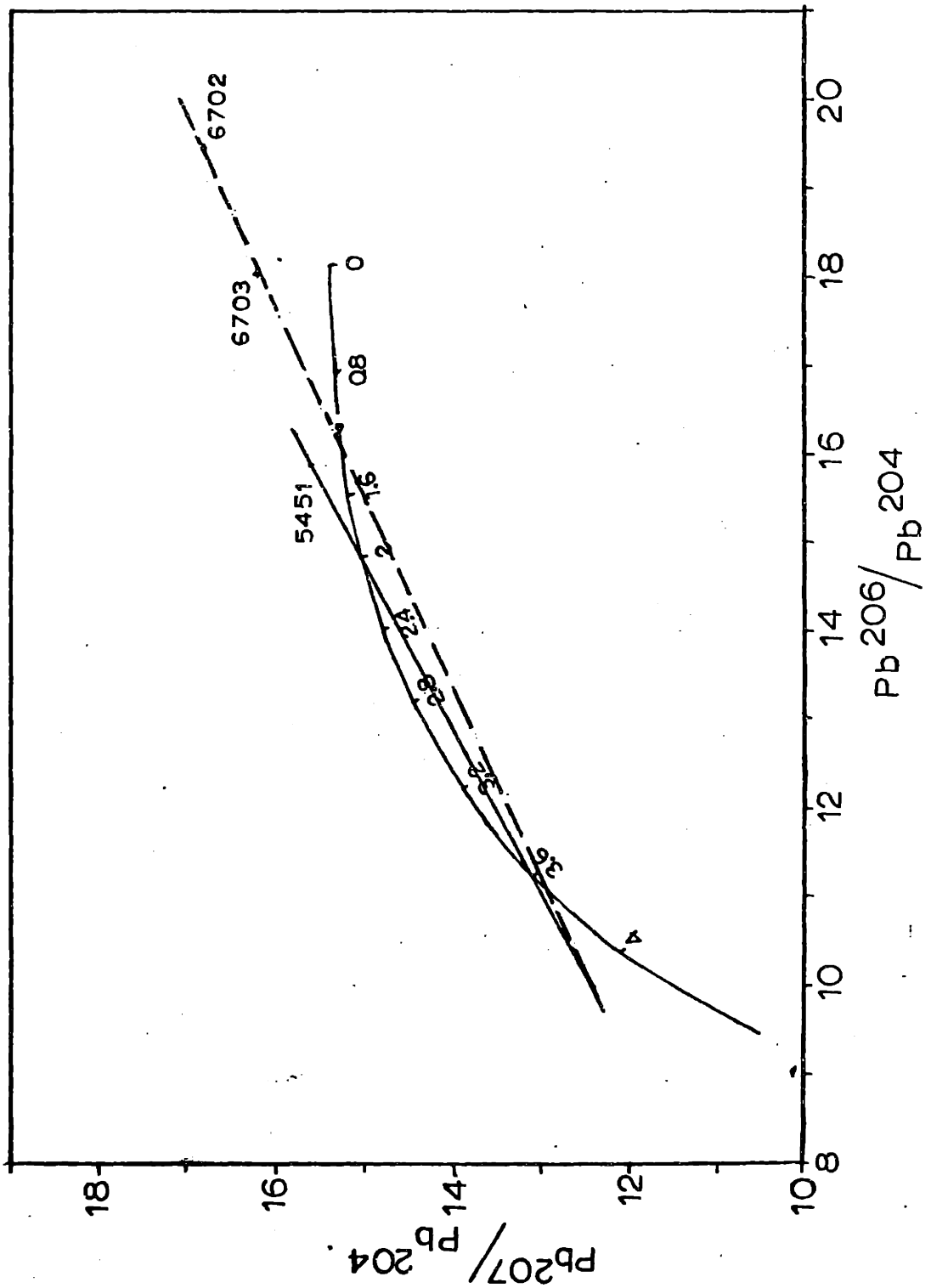
6702
6703
5451
0
08
1.6
2
2.4
2.8
3.2
3.6
4
Pb^{207}/Pb^{204}
Pb^{206}/Pb^{204}
18
16
14
12
10
8
20
18
16
14
12
10

Figure 38. Back-projection of reconnaissance Imataca feldspar compositions II. Reference growth curve, mantle growth curve of Stacey and Kramers (1975).

Solid line: composition of 5451, corrected to 2 b.y. ago, projected back through 2-b.y. point on growth curve.

Dashed line: best fit of 6702 and 6703, corrected to 1.2 b.y. ago, and 1.2 b.y. point on growth curve (slope = 0.4825 $\pm$ 0.0075, intercept = 7.472 $\pm$ 0.137, MSWD = 6.48).

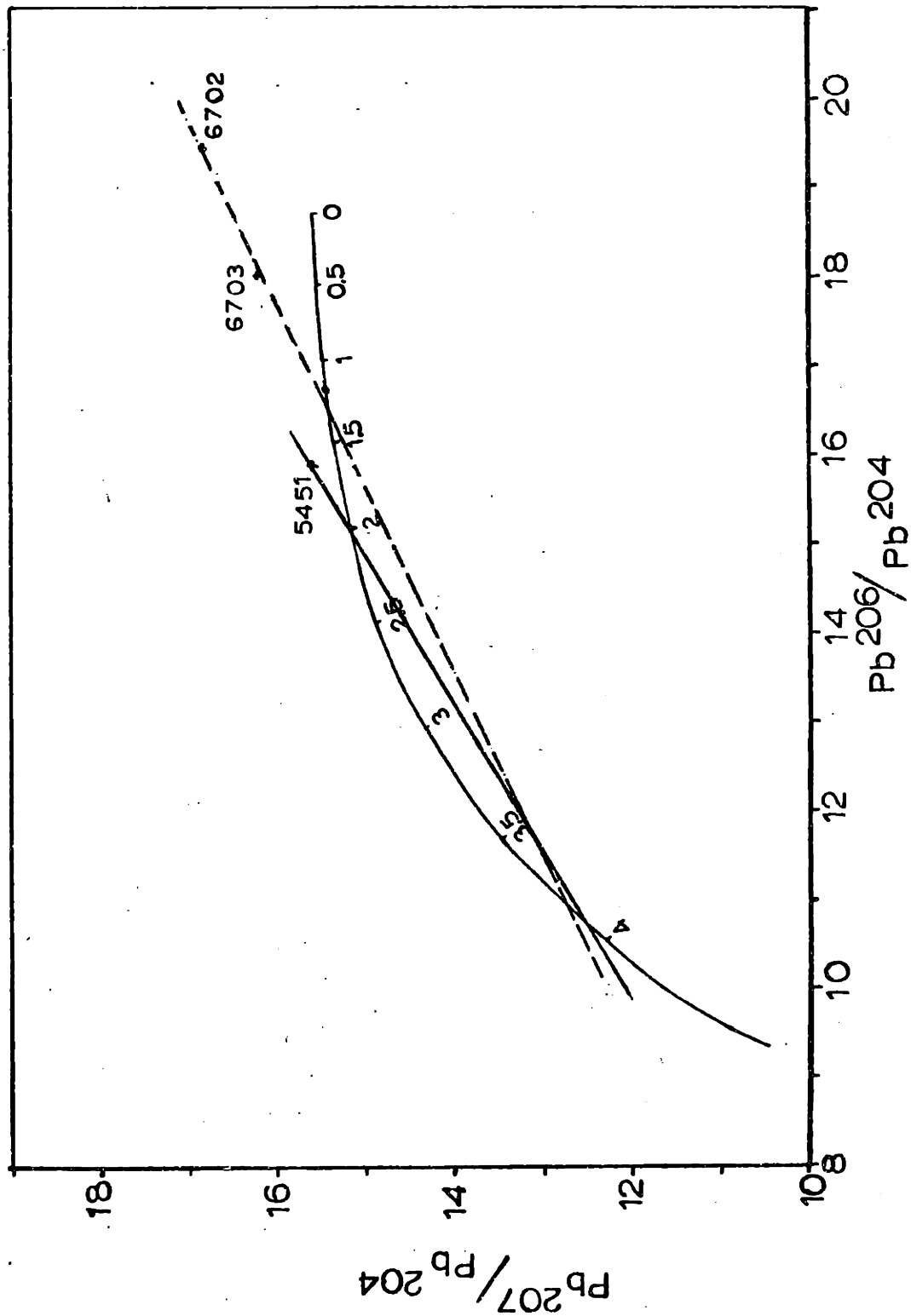
6702
6703
5451
0
0.5
1
1.5
2
2.5
3
3.5
4
Pb^{207}/Pb^{204}
Pb^{206}/Pb^{204}
18
16
14
12
10
8
20
18
16
14
12
10

38) likewise leads to a good approximation of the inferred primary age. Again a very simple evolutionary model for the feldspar leads suffices. Note that whether or not the feldspars in 6702 and 6703 equilibrated with the host rocks at 2 b.y., re-equilibration at 1.2 b.y. would wipe out the earlier equilibration date, and projections based on a 1.2-b.y. age-corrected feldspar compositions would be unaffected, provided that no change in total-rock μ occurred at 2 b.y. It should be clearly stated that there is no evidence for a 1.2-b.y. equilibration time for these samples; only, again, that such an assumption leads to an internally-consistent model.

In short, the feldspar data from this group of samples show nothing conclusive, except that the feldspar leads have equilibrated with the total-rock leads subsequent to the separation of the rocks from the mantle.

V. El Pao Samples (8150-8160)

Finally, the results from the El Pao gneisses (8150-8160) give most unusual results which, unfortunately, do not lend themselves to simple mathematical analysis. The 2-b.y. age-corrected compositions (Figure 39) form a linear array defined by slope = 0.25467 $\pm$ 0.0203, intercept = 11.902 $\pm$ 0.392, MSWD = 1.80. Using a t_2 age of 2.0 b.y., the t_1 age computed from this slope is 2.12 $\pm$ 0.17 b.y. - in other words, indistinguishable from the chosen t_2 age! Since these

Figure 39. Feldspar analyses, El Pao samples. Reference growth curve, mantle growth curve of Doe and Zartman (1977). Corrected and uncorrected points are nearly identical; plotted points are age-corrected to 2.0 b.y. ago. The regression line drawn has a slope of 0.25467 $\pm$ 0.0203, intercept 11.902 $\pm$ 0.392, MSWD = 1.80. For t_2 = 2.0 b.y., the calculated t_1 age is 2.12 $\pm$ 0.18 b.y. - which is indistinguishable from the chosen t_2 age.

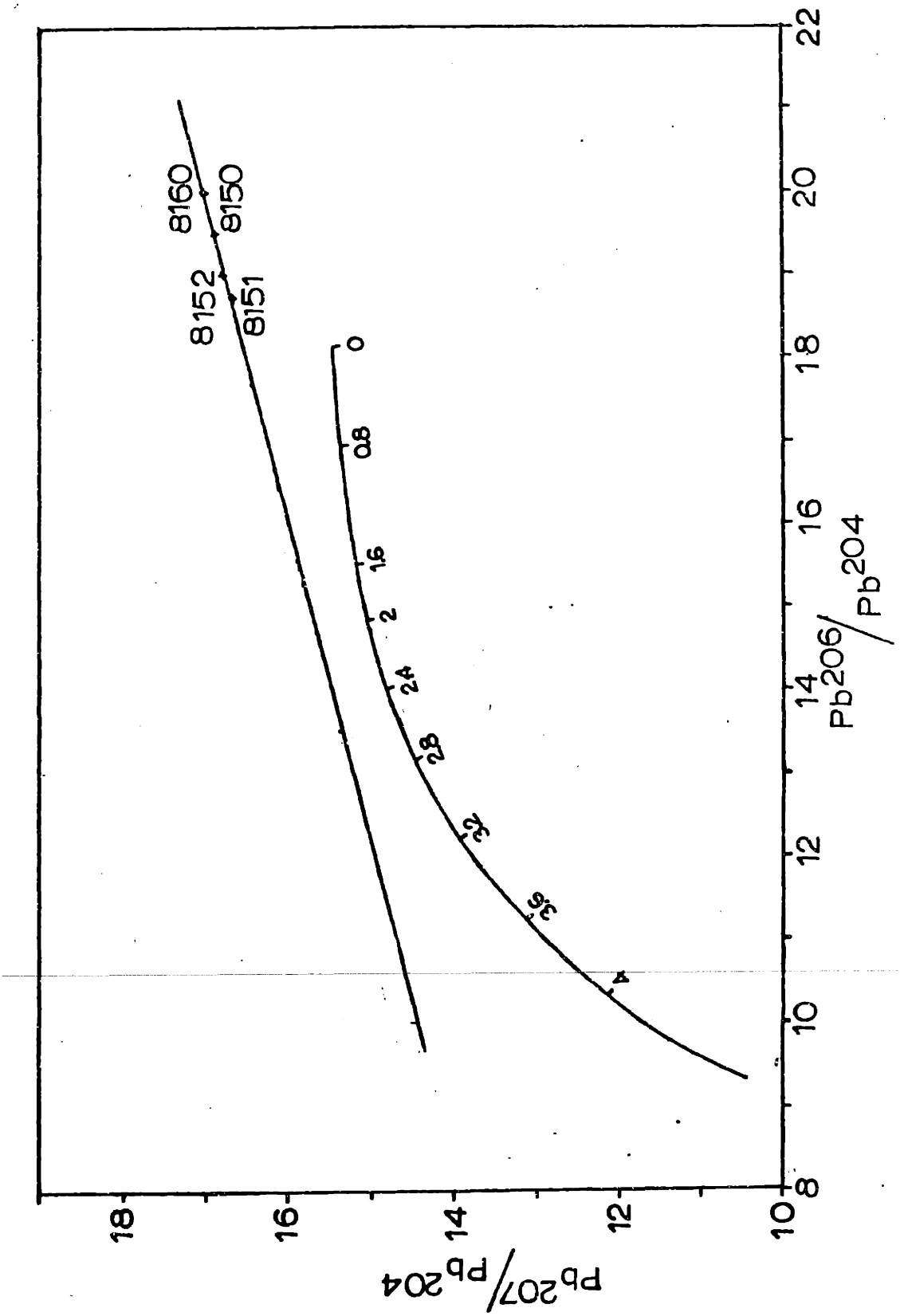
8160
8150
8152
8151
0
08
16
2
24
28
32
36
4
Pb^{207}/Pb^{204}
Pb^{206}/Pb^{204}
8
10
12
14
16
18
20
22

are samples for which the total rock lead isotopes, and therefore those of the feldspars, seem to have equilibrated no later than 2 b.y., assuming $t_2 < 2$ b.y. is not useful. If a younger t_2 is correct, t_1 should simply work out to 2 b.y. again, the time at which the feldspar compositions were last the same. If a younger t_2 is not correct, the calculated t_1 will be meaningless. In this case, for example, assuming $t_2 = 1.2$ b.y. leads to $t_1 = 2.6$ b.y., which is obviously wrong. While this incidentally supports our assumption of $t_2 = 2$ b.y., it brings us no closer to the primary age. (That the primary age of the El Pao samples is significantly greater than 2 b.y. is of course shown by the orientation of the array relative to the mantle growth curve.) If, conversely, we assume that the true t_2 is a little older than 2 b.y., on the basis of the total-rock date of approximately 2.35 b.y., the calculted t_1 age works out to be <u>younger</u> than t_2.

One way to account for these rather peculiar results is to suppose that for these particular samples, the feldspar lead-lead plot reflects not an isochron, but a mixing line. The unusual mineralogy of 8150 has already been noted. If 8150 is genetically unrelated to the rest of the samples - if, for example, it is a band of metabasalt - then its pre-granulite-metamorphic composition need not have been similar to the rest. At the time of the granulite event, a tendency toward homogenization of lead isotopes on the scale

of sampling would result in movement of isotopic compositions along one or more mixing lines. It may be that the line in Figure 39 in part reflects such a mixing process. The unsatisfactory aspect of this interpretation is that it is rather difficult to reconcile with the total-rock results. Recall that the whole-rock lead suggested quite complete homogenization at the time of the granulite event. Homogenization of total-rock lead in turn implies homogenization of the lead isotopic compositions of the constituent feldspars. Perhaps the homogenization at the total-rock scale was not quite complete during the granulite event after all; such a finding would agree better with the behavior expected on the basis of the fine-slice study. Again, the residual inhomogeneity does not appear to have been so great as to cause the metamorphic age from the El Pao samples to differ significantly from the age for this event obtained from other suites of samples.

VI. Summary

The information deduced from analysis of feldspar leads from four groups of Imataca gneisses generally contributes little to confirmation of the primary age of the Complex. The 8100 series of Guri Dam samples does record a t_1 age of 3.71 $\pm$ 0.10 b.y., which (a) suggests that the simple lead isotopic evolution model previously developed for total-rock samples in this group is reasonable, and (b) reinforces other

indications that at least some of the crust in this region predates 3.5 b.y. ago. The other suite of Guri Dam samples (7491-7494) give a t_1 age of about 2.9 b.y., consistent with their total-rock results, which may mean that the indications of a local disturbance of La Ceiba age here are genuine. The El Palo samples (8150-8160) in an odd way seem to record as t_1 the same age as the assigned t_2: the granulite-metamorphic age. This result might be attributed to incomplete isotopic homogenization during that event between genetically unrelated protolith materials. Finally, the only self-consistent interpretation for the data from the reconnaissance samples (5451, 6702, 6703), taking into account the total-rock lead data, seems to require different feldspar - host rock equilibration times for 5451 and for 6702 and 6703. Assuming geologically-reasonable values of t_2, the feldspar leads then do appear simply to reflect total-rock compositions which evolved uninterrupted from the primary protolith age (about 3.8 b.y. ago).

7. Conditions of Metamorphism

In view of what has been learned concerning the behavior of uranium during the granulite metamorphic event, a brief closer look at the probable prevailing metamorphic conditions is of interest.

I. General Mineralogical Considerations

First, in this thesis the term "granulite" is used to describe mineralogical, rather than purely textural, characteristics, as is currently usually the case, although many of the samples do show the classic granulite fabric. Mineralogically, any quartzofeldspathic rock containing orthopyroxene may now be classed as of granulite metamorphic grade (Winkler, 1967; Turner, 1968; Miyashiro, 1973). The pressure range for this regional-metamorphic facies is wide, from one or two kilobars (the limit of the contact-metamorphic hornfelses) through lower-crustal pressures (10^+ kb). The temperature range is more resticted, extending from an estimated 600-700°C minimum up to first melting in the system. A precise measure of this lower limit is unavailable, however. The key index mineral which distinguishes granulites from amphibolites is the orthopyroxene, and the temperature at which this forms will vary depending on the reaction by which it is formed. If the pyroxene were to be formed by the direct breakdown of amphibole, unreasonably high temperatures are required. Yoder and Tilley

(1962), for example, estimate that dehydration of a multi-component amphibole occurs at approximately 1000°C for $P_{H_2O} = P_{total}$ = 6 kb, nearer to 900°C if P_{H_2O} = 1 kb at the same P_{total}, and at lower temperatures for proportionately lower P_{H_2O}. But Brown and Fyfe (1970) feel that the first melting even in a dry rock of granitic composition would occur within 100-300°C of the water-saturated minimum melt temperature of approximately 650°C (Tuttle and Bowen, 1958). Since hornblende and other amphiboles do not occur in the highest-grade granulites, they must decompose before melting temperatures are reached, but by their very breakdown they add water to the system, further lowering melting temperatures and restricting the range of possible granulite conditions. Either the breakdown of amphibole in an otherwise dry system occurs at much lower temperatures than those indicated above, or an alternative paragenesis is necessary for the pyroxene.

DeWaard (1965) has suggested a whole series of possible prograde metamorphic reactions marking the transition from amphibolite to granulite facies in acid rocks in the Adirondacks. Some examples of these are:

hornblende + quartz $\longrightarrow$ opx + cpx + plagioclase + H_2O

biotite + quartz $\longrightarrow$ opx + almandine + orthoclase + H_2O

hornblende + biotite + quartz $\longrightarrow$

opx + plagioclase + orthoclase + H_2O

Such reactions would account both for the presence of garnet in some of the granulites, and for the consumption of the hornblende in the hornblende-granulite subfacies (which is transitional between the uppermost amphibolite grade and the pyroxene-granulite subfacies). They apparently occur at much lower temperatures than does the spontaneous dehydration of amphibole in the absence of other phases. DeWaard specifically notes also that the assemblage quartz-perthite-biotite-hornblende of the amphibolite facies changes to the chemically-equivalent pyroxene-granulite association of quartz-perthite-biotite-orthopyroxene with increasing metamorphism. Precisely this latter assemblage is typical of many of the Imataca granulites examined in the present research, where the complete assemblage is usually quartz + perthite + hypersthene + biotite $\pm$ plagioclase $\pm$ garnet $\pm$ microcline $\pm$ opaques. Unfortunately, experimental data on the position in the P-T plane of the univariant curves for such complex reactions are lacking. Aside from concluding that we are looking at an assemblage characteristic of the highest grade of regional metamorphism, we are no closer to accurate estimates of pressure and temperature for granulite conditions in the Imataca.

The presence of biotite as part of an otherwise anhydrous mineral assemblage at such high temperatures may at first seem surprising. Yet much of the biotite in the Imataca samples shows no particular petrographic evidence

that it is either a relict or a retrograde phase; it frequently seems to be in equilibrium with the other major minerals, including hypersthene. As previously noted, stable biotite is present in granulites elsewhere also. In fact, biotite is probably stable throughout the granulite facies (Wones and Eugster, 1965; Wones, 1972). With f_{O_2} between that of the hematite-magnetite and magnetite-wüstite buffers, the assemblage biotite-magnetite-sanidine is stable at least from 400-900°C (Wones and Eugster, 1965). Nor is high P_{H_2O} required for its stability. In the Adirondack gneisses, P_{H_2O} estimates based on coexisting biotite, magnetite, and K-feldspar range from 1-10 bars for a 500°C assemblage to 10-50 bars for a 600°C assemblage (Wones, 1972), so clearly $P_{H_2O} << P_{total}$. Presumably the latter condition would obtain at higher temperatures as well. The stable coexistence of biotite, magnetite, and K-feldspar actually suggests quite low P_{H_2O} for the given temperature, considering the reaction

$$\text{biotite} \longleftrightarrow \text{K-feldspar} + \text{magnetite} + H_2O \quad .$$

Addition of quartz and pyroxene to the association only increases the equilibrium temperature for a given P_{gas} (Wones and Eugster, 1965). The above association is often seen in Imataca granulites, suggesting that, as expected, most must have been relatively dry by the end of the granulite event.

The exact timing of the dehydration is uncertain. Pre-

sumably any sediments from which the gneisses were derived would have contained appreciable pore fluid. Either this fluid was lost in an earlier metamorphic event (of which we have no record), in which instance uranium depletion from non-resistant phases could be expected; or the pore spaces were sufficiently well interconnected that water was gradually lost with burial, which process might not leach uranium, if the bulk of the water was lost at rather low temperatures; or the granulite pulse was a prolonged one, during the early stages of which the water was driven off, so that the presently-observed assemblages indicate prevailing conditions at the end of the episode only. The last alternative is considered by this author to be the most likely. The presence of narrow rims of actinolite around hypersthene grains in a few of the thin-slice samples would then reflect later retrograding, just as the more common occurrence of minor chlorite does.

Other minerals present are generally still less helpful in restricting metamorphic conditions. The presence of microcline rather than orthoclase is not indicative of maximum temperatures, for the microcline structure is probably not stable above 400-460°C (Steiger and Hart, 1967). Since such a temperature is too low by any reasonable minimum estimates for the granulite facies, the microcline must be a post-granulite-metamorphic feature. The absence of cordierite likewise is not diagnostic of high pressure,

for cordierite stability is to a great extent governed by rock composition (Wynne-Edwards and Hay, 1963), and these rocks are neither highly aluminous nor magnesian, judging by the mineralogy.

Microprobe analyses of various mineral phases were made in an attempt to define better the metamorphic conditions. Microprobe analyses quoted in this chapter were carried out on the MAC-5 automated electron microprobe of the Earth and Planetary Sciences Department at M.I.T. Normal operating conditions were: count length, 30 seconds or 30,000 counts; accelerating voltage, 15 kv; sample current, 15-30 na. Standards used were Geophysical Laboratory standard orthoclase, manganese-bearing ilmenite, and jadeitic diopside ($Di_{65}Jd_{35}$). Data were reduced on line using the GeoLab program of Finger and Hadidiacos (1972), which employs the correction procedures of Albee and Ray (1970).

II. Temperature from Coexisting Pyroxenes

Attempts to determine temperatures on the basis of Fe-Mg partitioning in coexisting ortho- and clinopyroxenes (Wood and Banno, 1973) have thus far failed with the acid gneisses, due to the extremely minor amounts of clinopyroxene present. It occurs in very few samples at all, which is not surprising among acid granulites (Subramanian, 1962). Where present, it is as small, cracked, difficult-to-analyze grains which are of questionable identity to begin with. One sample of banded iron formation (#8616) does

contain some coexisting ortho- and clinopyroxene, although the grains are badly cracked and altered. The quality of their microprobe analyses was correspondingly reduced.

Table 6 lists the analyses of pyroxenes in 8616. These compositions may be used to derive an equilibrium temperature according to the equation (Wood and Banno, 1973):

$$T\ (°K) = \frac{-10202}{\ln\left(\frac{a^{cpx}_{Mg_2Si_2O_6}}{a^{opx}_{Mg_2Si_2O_6}}\right) - 7.65\left(X^{opx}_{Fe}\right) + 3.88\left(X^{opx}_{Fe}\right)^2 - 4.6}$$

where $X^{opx}_{Fe} = \left(\frac{Fe}{Fe + Mg}\right)_{opx}$, $a^{px}_{Mg_2Si_2O_6} = (X^{M1,\ px}_{Mg}) \cdot (X^{M2,\ px}_{Mg})$ = the product of the fractions of the M1 and M2 sites of the pyroxene in question which are occupied by magnesium. For the analyses in Table 6, the calculated equilibrium temperature is about 860°C. This temperature, which is on the high side of reasonable granulite temperatures, does agree with results for the Madras charnockites (Wood and Banno, 1973). It should, however, be considered a crude estimate only. Several possible sources of error may immmediately be cited. Equilibrium, or lack of it, between these phases cannot be demonstrated adequately in their altered condition. No correction for Fe^{+3} was made; such a correction should, however, be negligible if 10% or so of the iron is present as ferric iron (Wood and Banno, 1973). The orthopyroxene analysis is puzzling in that despite the 99.9% total, the

TABLE 6. Pyroxene analyses, sample 8616

	Clinopyroxene		Orthopyroxene	
	Oxide %	Cations*	Oxide %	Cations*
MnO	0.23	0.006	0.55	0.017
FeO	11.41	0.360	28.75	0.926
Na_2O	0.26	0.018	0	0
MgO	13.43	0.756	18.74	1.077
Al_2O_3	0.03	0.001	0.02	0.001
SiO_2	52.95	1.999	51.30	1.977
K_2O	0.01	0	0	0
CaO	21.38	0.864	0.55	0.022
TiO_2	0	0	0	0
Total	99.69	4.004	99.91	4.020

$a_{Mg}^{M1,\ cpx} = 0.677$ $\qquad$ $a_{Mg}^{M1,\ opx} = 0.538$

$a_{Mg}^{M2,\ cpx} = 0.0759$ $\qquad$ $a_{Mg}^{M2,\ opx} = 0.517$

$a_{Mg_2Si_2O_6}^{cpx} = 0.0514$ $\qquad$ $a_{Mg_2Si_2O_6}^{opx} = 0.278$

$X_{Fe}^{opx} = 0.462$

* Cations computed on the basis of six oxygens.

All iron is reported as FeO.

tetrahedral site appears short of cations even if all the aluminum is assigned to it along with the silicon. Assigning Fe^{+3} to bring the tetrahedral cations up to 2 and recalculating accordingly does not significantly alter the calculated equilibrium temperature. It is not clear whether the alteration now observed affecting the phases might have altered the major element content of the remaining material; and for that matter it is difficult to be sure that none of the altered material is included in the analysis. Basically, results from a single rock within a large region are always suspect; additional samples of suitable mineralogy would be most useful.

III. Coexisting Oxide Phases

The distribution of iron and titanium in coexisting oxide mineral phases (ilmenite and magnetite solid solutions) was also considered as a possible measure of metamorphic temperature and f_{O_2}, according to the scheme of Buddington and Lindsley (1964). Analytical results from these phases in samples 8100A2 and 8100D2 are shown in Table 7.

As is readily apparent from an examination of Table 7 and the f_{O_2} - T diagram of Buddington and Lindsley (Figure 40), the compositions do not neatly define the metamorphic conditions, or at least not any probable granulite conditions. Ilmenite and especially magnetite in both samples have nearly pure endmember compositions. If the compositions

TABLE 7. Ilmenite and magnetite analyses, samples 8100A2 and 8100D2

	8100A2		8100D2	
	Magnetite	Ilmenite	Magnetite	Ilmenite
MnO	0.10	0.41	0.02	1.17
FeO	89.48	48.82	91.54	46.90
Na_2O	0	0	0	0.04
MgO	0	0	0.12	0.04
Al_2O_3	0.16	0.04	0.46	0.12
SiO_2	0.16	0	0.70	0.12
K_2O	0	0	0	0
CaO	0.04	0.02	0.01	0
TiO_2	0.18	51.47	0.05	51.68
Total	90.12	100.76	92.90	100.07

Reduced compositions of solid solutions:

8100A2 Magnetite $Mt_{99.5}Usp_{0.5}$

8100A2 Ilmenite $Ilm_{96.9}Hem_{3.1}$

8100D2 Magnetite $Mt_{99.9}Usp_{0.1}$

8100D2 Ilmenite $Ilm_{98.2}Hem_{1.8}$

All analyses corrected for minor constituents according to the methods of Buddington and Lindsley (1964).
Note that totals on magnetite analyses are low, largely because all iron has been calculated as FeO.

Figure 40. Compositions of coexisting magnetite-ulvöspinel and ilmenite-hematite solid solutions; after Buddington and Lindsley (1964). Curves represent the projection on the f_{O_2} - T plane of surfaces in f_{O_2} - T - X space.

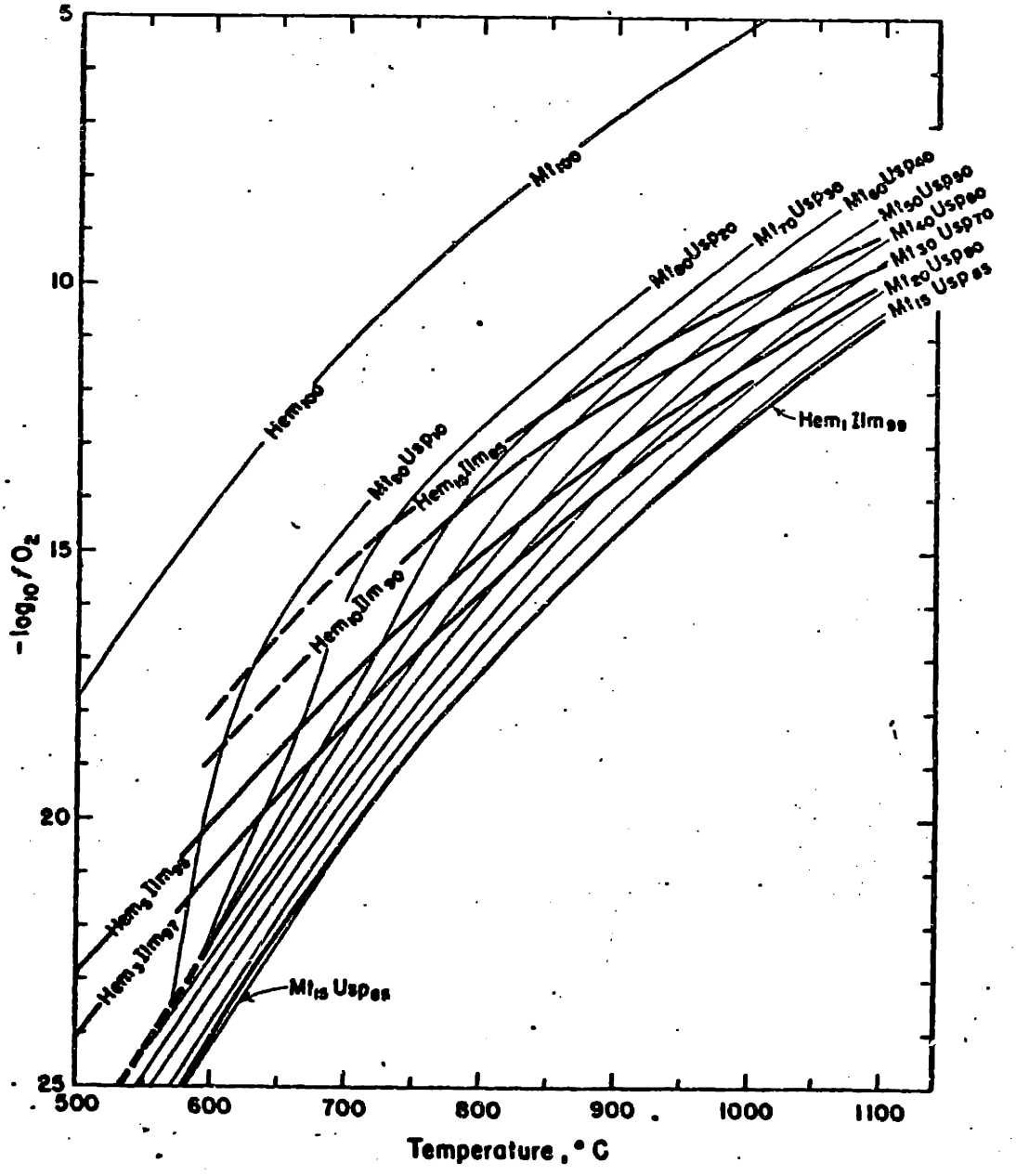
5
10
15
20
25
500
600
700
800
900
1000
1100
Temperature, °C
$-\log_{10} f O_2$
Hem_{100}
Mt_{100}
$Mt_{90}Usp_{10}$
$Mt_{80}Usp_{20}$
$Mt_{70}Usp_{30}$
$Mt_{60}Usp_{40}$
$Mt_{50}Usp_{50}$
$Mt_{40}Usp_{60}$
$Mt_{30}Usp_{70}$
$Mt_{20}Usp_{80}$
$Mt_{15}Usp_{85}$
$Hem_{90}Ilm_{10}$
$Hem_{85}Ilm_{15}$
$Hem_{70}Ilm_{30}$
$Hem_{50}Ilm_{50}$
$Hem_{30}Ilm_{70}$
$Hem_{15}Ilm_{85}$
$Hem_{1}Ilm_{99}$

reflect equilibrium at all, the indicated temperature is below 550-575°C with an oxygen fugacity less than 10^{-22}. This temperature is almost certainly too low for granulite conditions. Equilibrium might have been reached at the height of the metamorphism; migration distance of iron, at least, should have been adequate to permit equilibration (Blackburn, 1968). However, there is no reason to assume that equilibration must have ceased promptly as soon as the system began to cool down from maximum temperatures. Buddington and Lindsley (1964) also suggest that equilibration of iron-titanium oxides under metamorphic conditions might only be achieved when the oxides have undergone complete recrystallization, which is not readily demonstrable in this case. Consider further that since magnetite is only a very small proportion of total oxides in these samples, it may be that all magnetite can be accounted for by very late breakdown of some of the biotite as dehydration of the total rocks became extreme. If sufficiently high temperatures to cause recrystallization and/or re-equilibration were not maintained for an extended period following the formation of this magnetite, the result would be the preservation of a disequilibrium assemblage of oxides.

IV. Pressure Estimation from Orthopyroxene-Garnet

Alumina solubility in orthopyroxene coexisting with garnet was considered as a possible geobarometer (Wood and

Banno, 1973; Wood, 1974), using the equation

$$P = 1 + \frac{RT \ln \left(\frac{(X_{Mg}^{M1})\ (X_{Mg}^{M2})^2\ (X_{Al}^{M1})}{(X_{Mg_1}^{gar})^3} \right) - \Delta G^{\circ}_{1,T}}{\Delta V}$$

where $\Delta G^{\circ}_{1,T}$ is the change in free energy associated with the exchange reaction among pure magnesian endmembers

$$Mg_2Si_2O_{6_{opx\ ss}} + MgAl_2SiO_{6_{opx\ ss}} \longleftrightarrow Mg_3Al_2Si_3O_{12_{gar}}$$

The quantities X_{Mg}^{M1} and X_{Mg}^{M2} are the mole fractions of magnesium in the M1 and M2 sites of the orthopyroxene respectively, X_{Al}^{M1} the mole fraction aluminum in the M1 site, $X_{Mg_1}^{gar}$ the mole fraction of magnesium in the cubic sites in garnet, and ΔV the volume change for the reaction, tabulated by Wood and Banno (1973) for various values of X_{Al}^{M1}. Compositions of coexisting garnet and hypersthene from sample 8100D2 are listed in Table 8. Calculated equilibrium pressures are 4.7-6.4 kb in the temperature range 600°C - 900°C using ΔG° derived by Wood and Banno (1973) from the experimental data of Boyd and England (1964), or 4.4-6.3 kb over the same temperature range if the experimental work of MacGregor (1974) is used to estimate ΔG° (Wood, 1974). The calculated pressure is thus fairly restricted even over this broad temperature range, and is quite reasonable for granulite metamorphism. Confidence in this pressure is limited by two factors in addition to the possible sources

TABLE 8. Coexisting garnet and orthopyroxene, sample 8100D2.

	Orthopyroxene		Garnet	
	Oxide %	Cations*	Oxide %	Cations**
MnO	0.88	0.029	1.56	0.107
FeO	39.36	1.329	35.89	2.443
Na_2O	0	0	0	0
MgO	11.03	0.663	2.36	0.284
Al_2O_3	1.34	0.063	19.13	1.835
SiO_2	47.90	1.934	37.71	3.071
K_2O	0	0	0	0
CaO	0.13	0.004	2.97	0.258
TiO_2	0.10	0.002	0.03	0
Total	100.74	4.025	99.65	7.999

$X_{Mg}^{M1} = 0.333$

$X_{Mg}^{M2} = 0.322$

$X_{Al}^{M1} = 0.0155$***

$X_{Mg_1}^{gar} = 0.097$

*Computed on the basis of 6 oxygen atoms.

**Computed on the basis of 12 oxygen atoms.

***Following the procedure of Wood and Banno (1973) and Wood (1974), this value is computed as the average of the apparent values of X_{Al}^{tet} and X_{Al}^{M1}.

All iron is calculated as FeO.

of error discussed at length by Wood and Banno. First, since no determination of or compensation for Fe^{+3} in the M1 site of orthopyroxene was made, the calculated pressure must be considered a minimum. Secondly, following the practice of Wood and Banno (1973), the value of X_{Al}^{M1} used is actually the average of the apparent values of X_{Al}^{tet} and X_{Al}^{M1}. The rationale behind this practice is that analytical errors, particularly in the determination of SiO_2, may lead to errors in assignment of Al to the tetrahedral sites. In this case, the alumina content of the hypersthene is so low that all the Al was assigned to the tetrahedral position, and therefore half the value of X_{Al}^{tet} was used for X_{Al}^{M1}. The reasonableness of the pressure calculated tends to indicate that the resulting value used for X_{Al}^{tet} is not terribly wrong, but this is admittedly somewhat circular reasoning.

V. From the Literature

Dougan (1974) carried out an in-depth study of geothermometric/geobarometric indicators in a region of the Imataca immediately south of the Ciudad Piar - Guri fault near the Caroni River. The work included studies of Fe-Mg partitioning among coexisting garnet, biotite, and cordierite, the compositions of iron-titanium oxides, and the implications of the presence of sillimanite and the coexistence of K-feldspar, biotite, and magnetite. He concluded that:

1. The probable temperature range for the metamorphism

of the orthopyroxene-bearing rocks is 725-800°C; 2. Total pressure for these same rocks was in the range 5-6 kb, but $P_{H_2O} < 1$ kb was indicated; 3. In general, the oxide minerals do not have compositions consistent with equilibration under the inferred metamorphic conditions. The third conclusion is in accord with the findings of the current research.

This same paper of Dougan's includes analyses of garnet and orthopyroxene from two of his samples. He did not attempt to use these data to estimate metamorphic pressures. If this is done by the method outlined in the previous section, values of 9.5-10.7 kb in one instance, 17.4-19.3 kb in the other are obtained (for temperatures of 700-800°C). Certainly one and probably both of these estimates are too high to be consistent with the stable existence of sillimanite (see, for example, Richardson et al., 1969). They not only disagree with Dougan's own estimate of pressures, but lack internal consistency as well. The problem may be that Dougan's mineral compositions were obtained by bulk chemical analysis of mineral separates, and the possibility of contamination by minor inclusions of other phases must be considered.

VI. Summary

Although the area examined by Dougan (1974) is separated by the major Ciudad Piar - Guri fault from the part of the Imataca Complex studied by this author, and may thus have

been metamorphosed under somewhat different conditions, his conclusions regarding probable temperatures and pressures of metamorphism for his orthopyroxene-bearing samples appear to be reasonable estimates for the granulites of the present study as well. They are consistent with what constraints we have been able to develop on the basis of mineralogical or chemical considerations. Until additional samples with a more "useful" mineralogy are collected from north of the Guri fault zone and investigated with respect probable P and T of metamorphism, we may accordingly estimate the pyroxene-granulite metamorphic conditions throughout the Imataca to have been: temperature, 725-800^{+}°C, pressure, 5-6 kb; with P_{H_2O} much lower than total pressure.

8. Additional Implications of the Research

Information obtained during the present investigation bears directly or indirectly on several major geologic problems. A few of these are briefly discussed below.

I. Banded Iron Formations in the Precambrian

Some of the iron formations in the Imataca Complex are conformably interlayered with the acid granulites and charnockites dated in this and previous research at 3-3.5^{+} b.y. Although the lead data from the iron formations themselves reflect only the granulite-metamorphic age, they may resonably be inferred on the basis of the field evidence to be of the same primary age.

The precipitation of iron oxides requires adequate free oxygen, at least locally, to combine with and/or further oxidize ferrous iron in solution. Cloud (1972, 1973) considers that the development of widespread sedimentary iron formation marks the time of the rise of photosynthetic organisms, which in turn implies a prior period of sufficiently hospitable conditions (low surface temperatures, liquid water) to encourage their evolution. Early Archean iron formations have been recognized elsewhere in the world (e.g. Greenland; Moorbath *et al.*, 1973). If such sediments do have a biologic origin, they put the origins of life on earth very early in its history, well within 700 m.y. of accretion.

Initially this created serious problems with models of the early thermal history of hte earth. According to these, core infall, which would have raised the temperature of the whole earth by 1600-2000°C, might not have occurred before 3-3.5 b.y. ago (see, for example, Hanks and Anderson, 1969; Armstrong, 1968). Obviously this in inconsistent with the existence of advanced microorganisms at 3.5^{+} b.y., and to a lesser extent, with preservation of <u>any</u> crustal material of that age, of whatever origin. But recent evidence, from Xe^{129} (Boulos and Manuel, 1971) and from studies of the partitioning of lead between metal and silicate melt (Oversby and Ringwood, 1971) has suggested that in fact core infall probably occurred much earlier, within 10^{8} years of accretion. The formal "age of the earth" (Patterson, 1956) is now identified with the time of core formation, which is presumed to be virtually simultaneous (in geologic terms) with accretion (Hall and Murthy, 1971).

Dimroth and Kimberley (1976) have recently argued that actually there is no clear evidence in the geologic record for major changes in the level of oxygen in the earth's atmosphere through time, in which case deposition of banded iron formations would be unrelated to the development of early organisms. Still, the continuing possibility of a biologic origin for the oldest Precambrian iron formations leads to interesting speculation about the chronology of

organic evolution on the earth.

II. The Charnockite Problem

The term "charnockite" was introduced by Holland (1893, 1900) to describe a then-unusual dark-looking, quartz-feldspar-hypersthene-"iron ore" rock which occurred, in the type area near Madras, India, as part of an acid-to-basic series, the "charnockite series", which allegedly represented an igneous differentiation series. The term "enderbite" was proposed by Tilley (1936) for a member of the charnockite series in which plagioclase, rather than alkali feldspar, is the dominant feldspar. Although Holland specifically requested that the term charnockite not be used for hypersthene granite not occurring as part of a charnockite series, it is now common usage to apply the term to any rock of charnockitic mineralogy (Howie, 1964).

The "charnockite problem" which subsequently arose was whether charnockites were in fact primary igneous rocks, as they had been interpreted in the type locality, or metamorphic rocks, in some cases even metasediments. Charnockites in Australia (Wilson, 1959), and Uganda (Groves, 1935), and even British Guyana (Singh, 1966), were interpreted as being of igneous origin; others, for example in Ceylon (Cooray, 1962) and Suriname (Dahlberg, 1972) were interpreted as metasediments (as, of course, are the bulk of the Imatacan charnockitic rocks of the present study).

If by definition charnockites *sensu stricto* are part

of an igneous differentiation series, then clearly the problem really reduces to one of semantics: all metasedimentary "charnockites" should simply be called something else. But this approach merely begs the question. Furthermore, Subramanian (1959, 1962) reinterpreted the type area, and concluded that not all the rocks originally attributed to the charnockite series by Holland (1900) could reasonably be genetically related at all to the charnockites proper, although he did retain the igneous-origin hypothesis for the latter. Thereupon he redefined the charnockite sensu stricto as " an orthopyroxene-quartz-feldspar rock with or without garnet, characterized by greenish-blue feldspars and greyish-blue quartz" (Subramanian, 1962) - so the mode of origin is no longer implicit in the term.

Aside from the fact that the feldspars in the Imatacan charnockitic rocks are often whitish or pinkish, not blue-green, these rocks certainly fit the revised definition. To split hairs on the basis of mineral appearance seems pointless, unless the colors have some genetic significance; such significance is yet unproven (Howie, 1964). So the obvious answer to whether charnockites are igneous or metamorphic in origin is: apparently they can be either one.

Cooray (1969) would go still further than this. Noting that even in areas where the authors view the charnockites as igneous rocks, these charnockites are described as "interlayered" or "interbedded" or "conformable" with meta-

sedimentary granulites, that they characteristically are interdigitated with adjacent metasediments, and that they do not show chilled margins, he concludes that virtually all charnockites are of metamorphic origin, if not metasedimentary: "...charnockites as they now occur (emphasis Cooray's) are metamorphic rocks, largely confined to granulite facies areas...". Charnockites whose chemistry is reminiscent of igneous rocks could then represent metavolcanics within a sedimentary succession.

While the present author certainly does not feel competent to judge the affinities of all charnockites sight unseen, the apparently metasedimentary character of the Imataca charnockites demonstrates that at least some charnockites (as these are now defined) are metasediments.

III. Nature and History of the Early Crust

(For a fairly comprehensive survey of recent research on the primitive earth, the reader is referred to the volume edited by Windley (1976).)

For some years argument has continued over whether the highgrade gneissic terranes of the Archean predate or postdate the other typical Archean geologic feature, granite-greenstone belts. While the problem is not definitively resolved - indeed, the answer might vary from shield to shield - it has appeared to some that the gneiss terranes may as a group be a little older (Windley, 1973). The results of the present study provide additional evidence

of very old gneiss terranes, though the protolith age in this case is not known precisely enough to shed any light on the larger question of the relative ages of Archean gneisses and granite-greenstone belts.

The increasing number of 3.5^{+}-b.y. radiometric ages from acid rocks worldwide does argue for a significant quantity of sialic (continental) crust quite early in the earth's history. This must be considered in modeling the development of the primitive crust. Previous models generally invoked a thin basaltic initial crust, with subsequent local differentiation of andesite and eventually more silicic volcanics to create "protocontinents" (e.g. Taylor, 1967; Goodwin, 1968; Glikson and Sheraton, 1972). Exactly what would have happened next to produce the extensive gneisses and granites is unclear. Mobilization and partial melting of sedimentary troughs adjacent to the protocontinents (Glikson, 1970) or the production of juvenile magmas associated with island arcs (Moorbath, 1976) are both possible sources of additional sialic crust. The latter seems likely to be the primary source, based on isotopic evidence of low Sr^{87}/Sr^{86} initial ratios from many sialic terranes and, often, chemical affinity with rocks of the calc-alkaline suite (Moorbath, 1976). If granite-greenstone belts are also to be considered analogues of modern island arcs (Annheuser et al., 1969; Goodwin, 1973), there is growing evidence for plate tectonic activity in the

Precambrian.

It may be noted here that charnockites are apparently largely concentrated in Precambrian, and especially Archean, granulite terranes (Cooray, 1969; Howie, 1964), which may reflect a different thermal regime in the crust-mantle system during the early Precambrian from what we presently observe. The potential for the use of the distinctive character of charnockites to clarify this thermal regime has not been fully exploited to date.

The significant ages in the Imataca Complex are interesting in another connection. Sutton (1963) recognized what he considered long-term cycles in continental evolution - relatively short (200-400 m.y.) periods of intense thermal and/or tectonic activity alternating with longer (750-1250 m.y.) periods of comparative quiescence. Such peaks of activity were identified as occurring at the following times (in m.y.): 3600 $\pm$ 200, 2700 $\pm$ 150, 1900 $\pm$ 100, 1100 $\pm$ 100, 600 $\pm$ 150. He contended that "...with the exception of South America (for which adequate data are not available) the figures cover every continent..." It now seems that the Imataca also fits the pattern remarkably well, aside from the last cycle, so South America need not be excepted. Sutton modeled this periodicity in terms of cyclic coalescence and breakup of convection cells in the mantle. If the pattern he described is real, it bears further investigation.

IV. Pre-drift Continental Reassembly

Continental reassembly may be based on margin morphology, general geology, or the correlation of age provinces across spreading zones. The last method has only recently been used to any great extent (Davies and Windley, 1976; Hurley et al., 1976a; Hurley and Rand, 1969). The present research makes a modest contribution to such efforts by confirming a 3.5^{+}-b.y. age for the Imataca metasediments. This more firmly establishes previous tentative correlation of the Imataca with Archean gneisses in Liberia and Sierra Leone, which also contain some iron formation, have ages in the 3.1-3.7 b.y. range, and, when South America and Africa are suitably juxtaposed, have a similar regional structural trend (Hurley et al., 1976a).

9. Conclusions

Evidence from uranium-lead and combined uranium-lead and rubidium-strontium data indicates that the Imataca Complex in the Venezuelan Guayana Shield has a primary or protolith age in excess of 3.5 b.y. Several samples yield what may be an igneous age of 3.8 b.y. For some obvious metasediments, the apparent primary age is in the 3.5-3.7 b.y. range, and is interpreted as a "mixed" age reflecting a comparatively short period comprising source-region formation and weathering/sedimentation.

Lead isotopic evolution on a total-rock scale may formally be modeled according to a two-stage history or (more commonly) a three-stage history with a restricted range of second-stage μ values. Where a three-stage model seems appropriate, the start of the last stage is usually marked by metamorphism up to pyroxene-granulite grade, with syn- to post-metamorphic shearing and deformation. Among the resulting lithologies are metasedimentary charnockites. Some confirmation was obtained for previous estimates of metamorphic conditions, which place the temperature at 725-800^{+} °C, pressure 5-6 kb with relatively low P_{H_2O}.

The granulite event is characterized by extensive uranium depletion in many samples, even though rubidium may not have been lost to any great extent. While quite com-

plete homogenization of strontium isotopes over distance of the order of 10 cm resulted from this event, homogenization of lead isotopes was less perfect at that scale. The granulite metamorphism, dated at 2-2.3 b.y. ago, may be related to a major upheaval in the Pastora/Supamo region to the southeast of the Imataca. Since 2 b.y. ago, the Imataca has remained essentially stable.

The inferred primary age of the Imataca Complex in turn establishes the antiquity of the Guayana Shield, placing it on a par with other early Archean gneiss terranes. One of the latter is the basement complex of Liberia - Sierra Leone, with which the Imataca might be correlated.

APPENDIX A - PETROGRAPHIC DESCRIPTIONS

Brief thinsection descriptions of the samples dated in the present work are given below. Mineral percentages are estimates; most samples are sufficiently inhomogeneous that exact point-counts of a given thinsection would probably be no more representative of the total rock than are these estimates. Perthite host mineralogy could not in general be determined.

5451 Limited evidence of deformation: strain shadows in quartz, a little fine cataclastic material. Some myrmekite present.

- Microcline, not obviously perthitic - 35-40%
- Quartz - 30-35%
- Plagioclase - 10-15%
- Biotite - 5-10%
- Garnet - 1-2%
- Zircon, generally subhedral - traces

6702 No thinsection available

6703 Sample is strongly deformed with considerable cataclasis. Evidence of alteration seen in feldspar, which is somewhat sericitized; traces of unidentified highly-birefringent material being replaced by quartz and feldspar.

- Microcline, including minor perthite - 50-55%
- Quartz, showing strong strain shadows - 25-30%
- Plagioclase, untwinned - 5-10%
- Biotite - 5-10%
- Opaques - 1-2%
- Actinolite (?) - traces in biotite
- Zircon, generally subhedral - 1%
- Apatite - traces

6708 No thinsection available

7491 Strongly deformed. Quartz shows strain shadows and sutured grain boundaries. Some myrmekite present. K-feldspar has been sericitized.

- Microcline, much of it perthitic - 50-55%
- Quartz - 30-35%
- Plagioclase - 5-10%
- Biotite - 2-3%
- Hypersthene - 2-3%
- Garnet - 2-3%
- Opaques - 1-2%
- Zircon, varying from subhedral to rounded - traces
- Sphene (?) - traces

7492 No thinsection available

7493 Extremely coarse-grained rock, with little of the fine cataclastic material present. Quartz strain shadows are not pronounced, although the grain boundaries are sutured.

Microcline & perthite, greatly sericitized - 45-50%
Quartz - 45-50%
Plagioclase - 2-3%
Biotite, intimately intergrown with (?)actinolite - 2-3%
Opaques - 1-2%
Zircon, subhedral - traces

7494 Severe cataclasis apparent. A large portion of the sample (perhaps as much as 25%) is finegrained fragmented material which appears to consist of quartz and feldspar, though not necessarily in the same proportions as estimated below on the basis of the larger grains.

Perthite, sericitized - 35-40%
Quartz, showing strain shadows and sutured grain boundaries - 30-35%
Plagioclase 10-15%
Hypersthene, some grains broken up and altered, with (?) clinopyroxene exsolution lamellae - 5-10%
Actinolite (?), forming as alteration of hypersthene - 1-2%
Biotite, frequently associated with hypersthene; some grains showing kink banding - 2-3%
Opaques - 1-2%
Zircon, well rounded - 1%

8100 A2 Typically deformed and broken sample.

Quartz, with strain shadows and sutured grain boundaries - 55-60%
Perthite, somewhat sericitized - 20-25%
Microcline - 2-3%
Plagioclase - 5-10%
Hypersthene - 2-3%
Actinolite(?) - traces rimming hypersthene
Augite (?) - traces as very small grains
Biotite - 2-3%
Garnet - 1-2%
Opaques - 1-2%
Chlorite - traces
Zircon, well rounded - traces

8100 B2

Cataclastically deformed, some myrmekitic texture.
Perthite, moderately sericitized - 45-50%
Quartz, with strain shadows and sutured boundaries - 25-30%
Microcline - 2-3%
Garnet - 5-10%
Biotite, often closely associated with garnet and hypersthene - 5%
Actinolite, rimming garnet - traces
Hypersthene, somewhat replaced by biotite - 2-3%
Chlorite - 2-3%
Opaques - 1-2%
Zircon, subhedral - traces

8100 D2

Similar to the preceding sample.
Perthite - 30-35%
Quartz, with strain shadows - 30-35%
Plagioclase, some showing compositional zoning - 5-10%
Microcline - 5-10%
Hypersthene - 5-10%
Biotite, often associated with opaques - 2-3%
Augite (?), very small grains - 1-2%
Opaques - 3-5%
Chlorite, concentrated around pyroxene - 2-3%
Calcite - traces
Zircon - traces

8100 F2

Also similar to the preceding.
Perthite 35-40%
Quartz, with strain shadows - 25-30%
Microcline - 5-10%
Plagioclase - 5-10%
Hypersthene - 2-3%
Biotite, intergrown with opaques, and showing kink banding - 3-5%
Opaques - 3-5%
Garnet - 1-2%
Chlorite - 2-3%
Zircon, subhedral to rounded - 1%
Apatite - traces
Hematite - traces

8100 G2 Extremely sheared and strained sample, with wide variation in grainsize. Prominent myrmekite.
Perthite, sericitized - 55-60%
Quartz, with strain shadows - 25-30%
Plagioclase, untwinned - 5-10%
Microcline, sericitized - 2-3%
Hypersthene, somewhat altered to actinolite - 1-2%
Actinolite, associated with hypersthene and biotite - traces
Biotite, somewhat chloritized - 2-3%
Chlorite - 2-3%
Opaques, associated with other mafic phases - 1-2%
Calcite - 1-2%
Apatite - traces
Zircon - traces

8150 Extremely fresh sample with virtually no evidence of post-recrystallization deformation.
Plagioclase, some grains showing bent twin lamellae - 45-50%
Hypersthene, sometimes rimmed with opaques - 20-25%
Hornblende, green; occasionally contains intergrowths of (?)spinel - 15-20%
Biotite - 5%
Opaques, occurring both as discrete grains and along grain boundaries - 5%
Apatite, subhedral - traces
Zircon, subhedral to euhedral - traces

8151 Strongly cataclastic texture, extremely inhomogeneous grain sizes.
Perthite, somewhat sericitized - 60-65%
Quartz, with strain shadows - 25-30%
Microcline - 3-5%
Hypersthene - 1-2%
Garnet - 2-3%
Biotite - 1-2%
Chlorite - 2-3%
Rutile (?) - traces

8152 Similar to the previous sample; strongly broken up and strained.

Perthite - 55-60%
Quartz, showing strain shadows - 20-25%
Microcline - 3-5%
Plagioclase, some showing compositional zoning - 2-3%
Garnet - 2-3%
Hypersthene (?), closely associated with garnet - 1-2%
Biotite; some grains forced apart along cleavage planes - 3-5%
Chlorite, concentrated in fine broken material - 2-3%
Calcite (?) - traces
Zircon - traces

8160 Also similar to 8151. Notable difference is the presence of finely disseminated hematite throughout the sample. Despite the obvious cataclasis, some streaks of hematite run in parallel bands which transsect grain boundaries, and these might indicate relict bedding planes (?).

Perthite, sericitized - 50-55%
Quartz, with moderate strain shadows - 30-35%
Microcline - 3-5%
Plagioclase, untwinned - 3-5%
Pyroxene (?) (Hypersthene?), mostly altered to chlorite - 1-2%
Garnet, rimmed with finegrained feldspar and opaques - 1-2%
Biotite - 1-2%
Chlorite - 1-2%
Opaques - traces
Apatite - traces
Hematite, dispersed as primarily dusty material - 2-3%

8186 Moderately sheared and strained.

Perthite, sericitized - 55-60%
Quartz, frequently occurring as coarse lenses; showing strain shadows - 30-35%
Microcline - 3-5%
Opaques - 1-2%
Chlorite - 1-2%
Zircon, rounded - traces
Hematite, both disseminated and roughly banded perpendicular to the direction of elongation of the quartz lenses - 3-5%

8519-1 Strongly sheared and strained, with sutured grain boundaries of quartz grains. Some minor retrograding apparent from the actinolite rimming hypersthene.

Orthoclase, some perthitic - 25-30%
Quartz, with strain shadows - 50-55%
Microcline - 3-5%
Plagioclase, untwinned - 3-5%
Hypersthene, with coronas of actinolite - 3-5%
Actinolite - 1-2%
Biotite, frequently associated with hypersthene - 2-3%
Augite (?), very small grains - 1-2%
Calcite - 1-2%
Opaques - traces
Apatite - traces

8519-2 Very similar to the preceding sample.

Orthoclase, somewhat perthitic - 45-50%
Quartz, with strain shadows - 40-45%
Plagicclase - 2-3%
Microcline - 2-3%
Hypersthene (?) - associated with actinolite and biotite - 1-2%
Actinolite, rimming pyroxene - traces
Biotite - 1-2%
Opaques - 1-2%
Chlorite - traces
Calcite (?) - traces
Zircon, rounded - traces

8519-3 Also similar to 1, with strain and granulation evident.

Orthoclase & perthite, sericitized - 55-60%
Quartz, showing strain shadows - 30-35%
Plagioclase - 1-2%
Microcline - 2-3%
Hypersthene - 2-3%
Actinolite, closely associated with the hypersthene - 2-3%
Biotite - 3-5%
Chlorite - traces
Opaques - traces
Zircon, rounded - 1%

8519-4 Somewhat more coarse-grained than 1-3.
Orthoclase & perthite - 40-45%
Quartz, with strain shadows - 35-40%
Plagioclase, some untwinned - 3-5%
Microcline - 2-3%
Hypersthene - 3-5%
Actinolite, rimming some of the hypersthene grains - 2-3%
Biotite, frequently associated with other mafic phases - 3-5%
Opaques - traces
Apatite, subhedral - traces
Zircon, subhedral to rounded - traces

8519-5 Similar to samples 1-3. Granulation of grain boundaries, some myrmekite evident.
Orthoclase and perthite - 40-45%
Quartz, strained - 35-40%
Microcline - 2-3%
Plagioclase, untwinned - 5-10%
Hypersthene, with coronas of actinolite on some grains - 5-10%
Actinolite, rimming hypersthene - traces
Biotite, showing kink banding; usually not closely associated with the hypersthene - 3-5%
Opaques, associated with biotite - traces
Apatite, rounded - traces
Zircon, rounded - 1%

8519-6 Similar to 5, granulated, with myrmekite.
Perthite, sericitized - 25-30%
Quartz, strained, with sutured grain boundaries - 55-60%
Hypersthene, largely replaced by actinolite - 2-3%
Actinolite (?), associated with hypersthene - 2-3%
Biotite, kink banded, often associated with other mafics - 3-5%
Chlorite - traces
Calcite (?) - traces
Zircon, rounded - traces

8519-7 Also similar to the preceding, but with less retrograing of hypersthene.
Orthoclase and perthite, sericitized - 20-25%
Quartz, strained - 45-50%
Plagioclase, some untwinned - 5-10%
Hypersthene - 10-15%
Actinolite, at edges of hypersthene grains - traces
Biotite, often not associated with hypersthene - 3-5%
Opaques - 2-3%
Zircon, rounded - traces

8519-8 Considerable strain evident; also significant amounts of myrmekite.
Orthoclase and perthite, sericitized - 30-35%
Quartz, 25-30%
Plagioclase, some untwinned - 10-15%
Microcline - 2-3%
Hypersthene - 5-10%
Actinolite, rimming hypersthene grains - 3-5%
Biotite, some associated with opaques - 2-3%
Opaques - 1-2%
Apatite, subhedral - traces
Zircon, subhedral to rounded - traces

8519-9 Similar to 8 with significant myrmekite.
Orthoclase and perthite,sericitized - 30-35%
Microcline, some perthitic - 3-5%
Plagioclase - 10-15%
Hypersthene, some grains replaced by actinolite/biotite aggregate - 2-3%
Actinolite (?), replacing hypersthene - 2-3%
Biotite - 2-3%
Zircon, subhedral - 1%

8519-10 Similar to previous samples, with well-developed myrmekite, granulated grain boundaries.
Perthite - 40-45%
Quartz, strained - 30-35%
Plagioclase - 5-10%
Hypersthene, some with undulatory extinction and a texture resembling kink-banding in biotite - 3-5%
Actinolite, rimming hypersthene - 1-2%
Biotite, some kink-banded - 3-5%
Opaques - 1-2%
Zircon, fairly coarse, subhedral to rounded - 1-2%

8519-11 Similar to 10, with sutured boundaries on quartz grains, and some myrmekite.
Perthite - 40-45%
Quartz, with strain shadows - 25-30%
Plagioclase - 2-3%
Microcline - 3-5%
Hypersthene - 5-10%
Actinolite, replacing some of the hypersthene - 3-5%
Biotite, some associated with other mafics - 5-10%
Opaques - 2-3%
Chlorite - traces
Zircon, subhedral to rounded - traces

8519-12 Very similar to 11, with myrmekite.
Orthoclase & perthite - 45-50%
Quartz, with sutured boundaries - 20-25%
Plagioclase, some untwinned - 5-10%
Microcline - 3-5%
Hypersthene, partially replaced by actinolite - 5-10%
Actinolite, as rims on hypersthene - 1-2%
Biotite, frequently associated with opaques - 3-5%
Opaques - 1-2%
Chlorite - traces
Zircon, rounded - traces

8610 Very finely banded, with laminations defined by alternating concentrations of opaques and quartz.
Quartz, showing strain shadows - 45-50%
Opaques - 45-50%
Hematite, apparently secondary; largely concentrated on shear planes - 3-5%
Apatite - traces

8611 Also well-banded like 8610, with some suggestion of rhythmic layering; one "microfault".
Quartz, with strain shadows - 45-50%
Opaques - 45-50%
Apatite, with preferred orientation parallel to the layering, especially concentrated in one "bed" of which it makes up perhaps 10% - 2-3%
Rutile (?) - traces
Hematite, probably secondary, concentrated along cracks - 3-5%

8612 Very finely banded. One of the quartz-rich layers has been pulled into a structure which might be described as a "microboudin".
Quartz, with some strain shadows - 50-55%
Opaques - 40-45%
Hematite, dispersed - 5-10%
Rutile - traces
Apatite - traces

8613 Not very well banded at thinsection scale. Extremely granulated and sheared.
Quartz, showing strain shadows in larger grains; much of the finely pulverized material is quartz - 60-65%
Opaques, concentrated in blotches - 35-40%
Hematite, secondary, concentrated along cracks - traces

8614 Very patchy texture, though not especially broken up or granulated.
Quartz, with strain shadows, much more equigranular than in 8613 - 50-55%
Opaques, concentrated in patches - 40-45%
Hematite, dispersed, patchy - 5-10%

8615 Mostly coarse-grained, blotchy texture; not particularly cataclastic appearance. Amphiboles altered to yellowish material which resembles serpentine or iddingsite.

Quartz, showing strain shadows - 55-60%
Opaques - 25-30%
Actinolite - 5-10%
Grunerite - 3-5%
Apatite - traces
Hematite, secondary, filling cracks - traces

8616 Very crude banding, not especially cataclastic texture. Pyroxenes cracked and altered to yellowish-brown material (serpentine? iddingsite?).

Quartz, with strain shadows - 60-65%
Opaques - 20-25%
Hematite, filling cracks - 2-3%
Orthopyroxene, non-pleochroic - 3-5%
Clinopyroxene - 3-5%
Actinolite, mostly as alteration of pyroxene grains - 3-5%
Zircon, rounded - traces
Apatite - traces

8617 Patchy texture, little cataclasis. In addition to the alteration described for the previous two slides, this one shows an unidentified, colorless, moderately-to-highly-birefringent material surrounding and filling cracks in the mafic silicates.

Quartz, weak strain shadows - 55-60%
Opaques, concentrated in masses - 15-20%
Orthopyroxene - 10-15%
Clinopyroxene (?) - traces
Grunerite - 3-5%
Hematite, apparently secondary, in patches along cracks - 5%

8618 Fairly well-banded texture. Similar alteration to the above sample, with a rather large quantity of the birefringent material present (up to several percent of the rock).

Quartz, with strain shadows - 45-50%
Opaques - 30-35%
Orthopyroxene - 5-10%
Clinopyroxene(?), nonpleochroic - 3-5%
Actinolite, as alteration product of pyroxene - 3-5%
Hematite - traces

8619 Poorly banded, with one large lens of quartz parallel to the faint layering. Much more cataclasis than in the previous few samples.

Quartz, with strain shadows and sutured grain boundaries - 50-55%
Opaques - 45-50%
Hematite, dispersed - traces
Zircon - traces

8620 Extremely cataclastic texture; crude compositional layering approximately parallel to planes of fine granulated material.

Quartz, showing strain shadows in coarse grains; much of the fine material is quartz - 50-55%
Opques, mostly coarser grains only - 35-40%
Hematite, patchy, probably secondary - 5-10%

8621 Very well banded. Sample includes a small fracture infilled with hematite; generally granular texture. Many of the grain boundaries are cracked and partially filled with some sort of alteration product.

Quartz, with strain shadows - 70-75%
Opaques and hematite, intimately associated - 25-30%

APPENDIX B - OUTLINE OF URANIUM-LEAD SYSTEMATICS

The following discussion is based primarily on reviews by Gale and Mussett (1973), Doe (1970), and Kanasewich (1968), with some additional simple derivations.

I. General. There are four stable isotopes of lead: Pb^{208}, produced by the decay of Th^{232}; Pb^{207}, produced by decay of U^{235}; Pb^{206}, produced by U^{238} decay; and Pb^{204}. In this paper we are considering the uranium decay schemes only:

$$U^{238} \longrightarrow Pb^{206} + 8\alpha \qquad \lambda = 0.155125 \times 10^{-9}\ y^{-1}$$

$$U^{235} \longrightarrow Pb^{207} + 7\alpha \qquad \lambda' = 0.98485 \times 10^{-9}\ y^{-1}$$

The constant λ is the decay constant in the standard radioactive decay equation

$$N = N_o\, e^{-\lambda t}\ , \text{ where}$$

N_o = number of radioactive parent atoms initially present in the system;
N = number of parent atoms left after time t.

Values for the decay constants quoted above are taken from Jaffey et al. (1971).

Since in a closed system the number of new daughter atoms produced must be equal to the number of parent atoms decayed, we may readily derive the following relations:

$$(Pb^{206})_o = (Pb^{206})_i + (U^{238})_o(e^{\lambda t} - 1)$$

$$(Pb^{207})_o = (Pb^{207})_i + (U^{235})_o(e^{\lambda' t} - 1)$$

where the subscript o refers to present measured quan-

tities and the subscript $\underline{i}$ refers to quantities in the system at time t ago. (Time is conventionally measured positively into the past, so t=0 is the present.)

Also conventionally, all isotopic quantities are normalized with respect to the amount of Pb^{204} in the system, so (since $(Pb^{204})_o=(Pb^{204})_i$) these relations become

$$\left(\frac{Pb^{206}}{Pb^{204}}\right)_o = \left(\frac{Pb^{206}}{Pb^{204}}\right)_i + \left(\frac{U^{238}}{Pb^{204}}\right)_o (e^{\lambda t} - 1)$$

$$\left(\frac{Pb^{207}}{Pb^{204}}\right)_o = \left(\frac{Pb^{207}}{Pb^{204}}\right)_i + \left(\frac{U^{235}}{Pb^{204}}\right)_o (e^{\lambda' t} - 1)$$

where all ratios are atomic ratios.

The ratio $(U^{238}/Pb^{204})_o$ is a useful parameter by which to describe the relative abundances of uranium and lead in the system, and is denoted simply as μ. Then since the present-day ratio of U^{238}/U^{235} in natural uranium is 137.88 (Stacey and Stern, 1973), our equations become

$$\left(\frac{Pb^{206}}{Pb^{204}}\right)_o = \left(\frac{Pb^{206}}{Pb^{204}}\right)_i + \mu (e^{\lambda t} - 1)$$

$$\left(\frac{Pb^{207}}{Pb^{204}}\right)_o = \left(\frac{Pb^{207}}{Pb^{204}}\right)_i + \frac{\mu}{137.88} (e^{\lambda' t} - 1)$$

Lead evolution in natural systems in characterized

by the number of stages involved, where a stage may be defined as a period of time during which the system remained closed with respect to lead and uranium (and thorium, if that decay scheme is also to be considered). Each stage in turn may be described in terms of the value of μ which prevailed during that stage (no ambiguity arises; note that $\mu = (U^{238}/Pb^{204})_o$, or U^{238}/Pb^{204} normalized to what its present-day value would have been if left undisturbed to the present, when an early stage in a multistage history is being considered).

The equations just derived apply to a single-stage history. For a two-stage history they become

$$\left(\frac{Pb^{206}}{Pb^{204}}\right)_o = \left(\frac{Pb^{206}}{Pb^{204}}\right)_i + \mu_1(e^{\lambda t_i} - e^{\lambda t_1}) + \mu_2(e^{\lambda t_1} - 1)$$

$$\left(\frac{Pb^{207}}{Pb^{204}}\right)_o = \left(\frac{Pb^{207}}{Pb^{204}}\right)_i + \frac{\mu_1}{137.88}(e^{\lambda' t_i} - e^{\lambda' t_1}) + \frac{\mu_2}{137.88}(e^{\lambda' t_1} - 1)$$

where t_i is the "age of the system", and t_1 is some time between t_i and the present at which some change in μ takes place through gain or loss of either component; μ_1 describes the system from t_i to t_1 and μ_2 from t_1 to the present. (Note that if $\mu_1 = \mu_2$, the model collapses to the single-stage case.) For natural (geologic) systems, $(Pb^{206}/Pb^{204})_i$ and $(Pb^{207}/Pb^{204})_i$ are the primordial lead isotope ratios existing at t_i = apparent age of the earth. Values for these primordial lead ratios may be obtained

from analysis of the isotopic composition of lead in troilite from iron meteorites (Patterson, 1956; Oversby, 1970). The primordial lead ratios used in this study are $Pb^{206}/Pb^{204} = 9.307$, $Pb^{207}/Pb^{204} = 10.294$, with t_i taken as 4.57×10^9 years (Tatsumoto et al., 1973).

In principle the equations derived above may be expanded to fit histories of any number of stages. However, the number of unknowns (μ's and t's) rapidly outstrips the number of quantities which may be measured or deduced from laboratory data as the number of stages increases, so the use of lead isotopes in natural systems is usually confined to cases of two- or perhaps three-stage evolution, or systems which may be approximated by two- or three-stage models.

There exist several graphical methods of representing and interpreting lead and uranium data, discussed individually below.

II. Isochron diagrams. These are the simplest means of presenting geochronologic data. On an isochron diagram the present (normalized) daughter-element ratio (vertical axis) is plotted against the radioactive parent (horizontal axis). Only one decay scheme is represented at a time on such a plot. Given a set of analyses which fall along a line, we can obtain a date for the rocks (which may be either a primary or a metamorphic age). For

illustration of the method, see Figure B-1. Suppose that at some past time t a suite of rocks (or minerals) existed with a single common ratio of $Pb^{206}/Pb^{204} = y_t$, but variable proportions of uranium to lead. This situation could arise either by the differentiation of a single source material into subsystems among which uranium and lead were inhomogeneously distributed, or by a complete metamorphic homogenization with respect to lead isotopic composition of a diverse set of older rocks which still preserved a range of U/Pb ratios after the isotopic homogenization. If the system remained undisturbed from time t to the present, the present measured values of Pb^{206}/Pb^{204} and μ will show a positive correlation: samples with higher μ will produce a higher proportion of radiogenic lead in that time. Now consider a single sample in the set which at time t had $Pb^{206}/Pb^{204} = y_t$ (by definition) and $U^{238}/Pb^{204} = x_t$. Call the present isotopic composition point (x,y), and consider a line drawn through (x,y) and the point $(0, y_t)$, which represents not only the initial lead composition in its y-intercept value, but also the limiting case of the present composition of lead in any system which contained no uranium at time t. The slope m of this line is $m = (y - y_t)/(x - 0) = (y - y_t)/x$. But $y = y_t + \mu(e^{\lambda t}-1) = y_t + x(e^{\lambda t}-1)$, so the equation becomes

Figure B-1. Illustration of the use of the isochron diagram to obtain a radiometric age. Circles represent starting points at time t ago; crosses represent present measured values. The lead isotope "initial ratio" at time t is y_t. For details, see text.

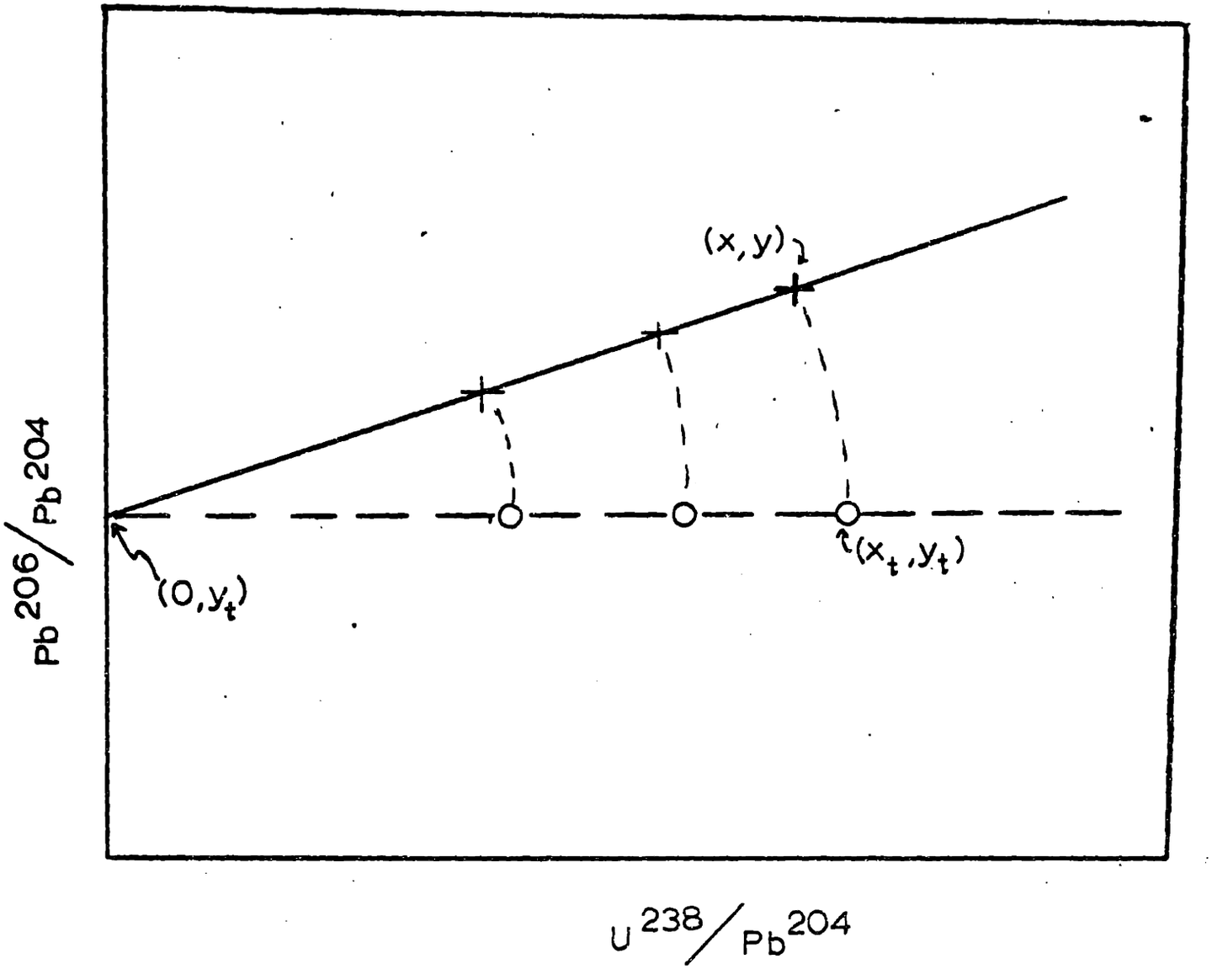
$(x, y)_1$
$(0, y_t)$
(x_t, y_t)
Pb^{206}/Pb^{204}
U^{238}/Pb^{204}

$$m = \frac{(y_t + x(e^{\lambda t}-1)) - y_t}{x} = \frac{x(e^{\lambda t}-1)}{x} = e^{\lambda t}-1 \quad .$$

Straightforward algebraic manipulation reduces this to the relation

$$t = \frac{\ln (m+1)}{\lambda} \quad .$$

Notice that this relation is independent of the μ value of the sample; it involves only the constant λ, the time t since the last isotopic homogenization (which by definition is the same for all samples), and the slope m of the line drawn. From this it is clear that all samples must fall on this line (m must be the same for all). Thus we see that given the stipulated conditions, the present measured values (x,y) must all lie along a line, or isochron, whose slope yields the time t by the above equation, and whose intercept with the y-axis is the initial ratio (at time t) of y.

The derivation is perfectly analogous if a plot of Pb^{207}/Pb^{204} against U^{235}/Pb^{204} is used.

III. The lead-lead plot. In this diagram the present measured values of Pb^{206}/Pb^{204} and Pb^{207}/Pb^{204} are plotted (the former on the horizontal axis, the latter on the vertical), so isotopic information from the two decay schemes is plotted on one diagram. Evolution of a single-stage system is described by means of a growth curve, which is the locus of points described by

the parametric equations

$$\left(\frac{Pb^{206}}{Pb^{204}}\right)_t = \left(\frac{Pb^{206}}{Pb^{204}}\right)_i + \mu\,(e^{\lambda t} - 1)$$

$$\left(\frac{Pb^{207}}{Pb^{204}}\right)_t = \left(\frac{Pb^{207}}{Pb^{204}}\right)_i + \frac{\mu}{137.88}\,(e^{\lambda' t} - 1)\,.$$

The shape of the curve is always the same - that is, the slope of the curve at any point corresponding to lead isotopic composition at time t is a function only of t. But clearly the rate of increase of radiogenic lead, and hence the rate of change of lead isotopic composition with time, is a function of μ, so growth curves are defined by their characteristic μ-value. By convention, the starting point of the single-stage growth curve is taken as the age of the earth, so $(Pb^{206}/Pb^{204})_i$ and $Pb^{207}/Pb^{204})_i$ are the primordial lead isotope ratios. See Figure B-2(a) for illustration.

Consider next a two-stage model (Figure B-2(b)). In this case the geologic system evolves during the first stage (t_i to t_1) with $\mu = \mu_1$, and then at t_1 is divided into j subsystems of varying μ_{2j}, which develop undisturbed to the present day. The present lead compositions of these subsystems will plot along a straight line (isochron) called Houterman's isochron (Houtermans, 1953). This isochron has the property that its slope m is related to the time t of change of μ by the equation

Figure B-2. Illustrations of lead-lead plots. In all cases t_i = age of the earth, with primordial lead isotope ratios (x_i, y_i). After Gale and Mussett, 1973.

(a) Single-stage history.

(b) Two-stage model, with episodic μ change at t_1.

(c) Three-stage model, f_1 = constant, with events at t_1 and t_2.

(d) Three-stage model, f_2 = constant, with events at t_1 and t_2.

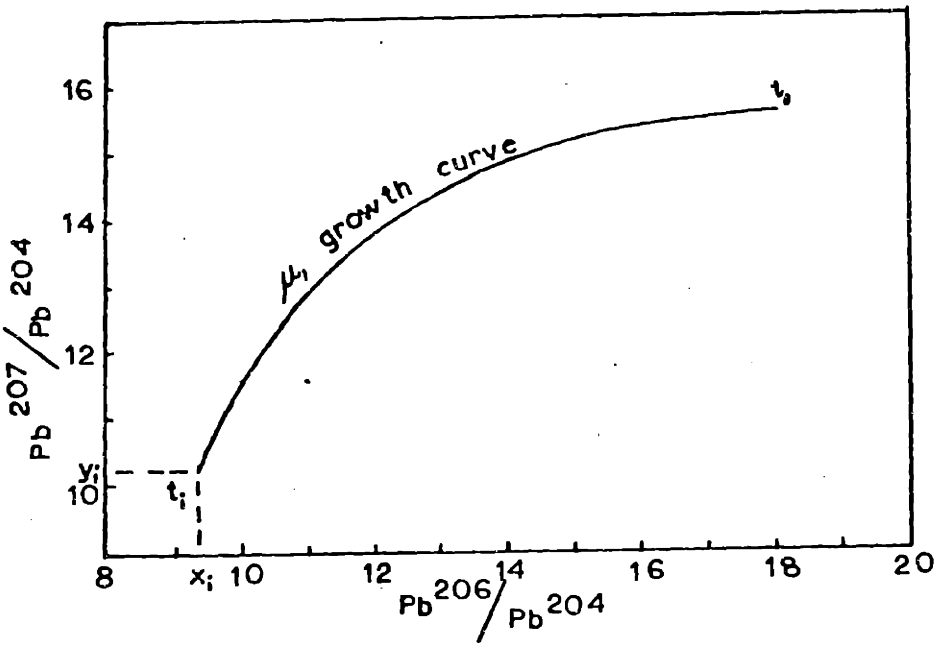
16
14
12
10
8
Pb^{207}/Pb^{204}
μ_1 growth curve
t_0
t_1
y_i
x_i 10
12
14
16
18
20
Pb^{206}/Pb^{204}

(a)

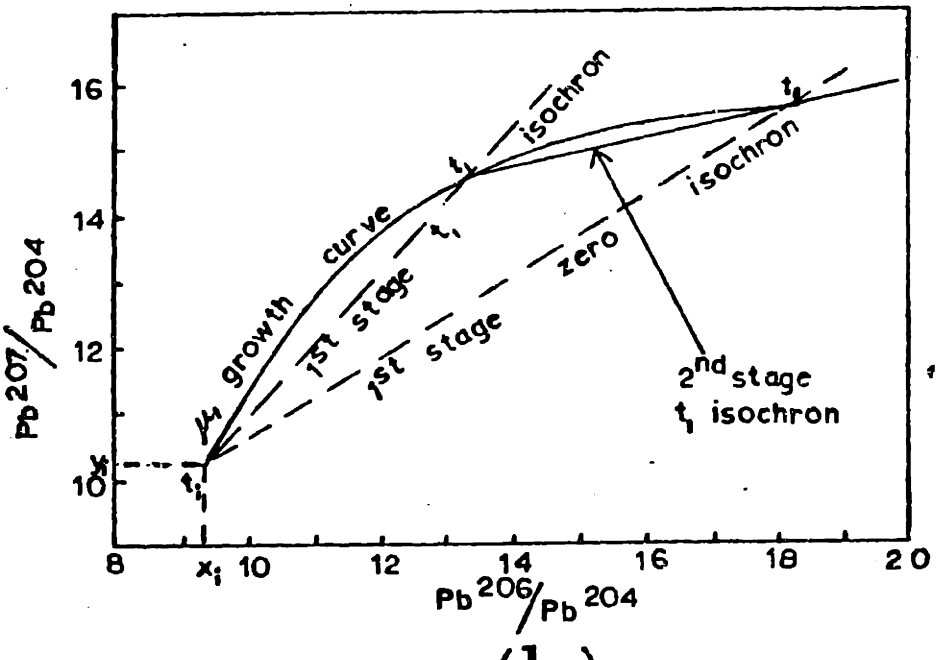
16
14
12
10
8
Pb^{207}/Pb^{204}
μ_1 growth curve
isochron
t_2
t_1
1st stage
zero
1st stage
isochron
2^{nd} stage
t_1 isochron
y_i
x_i 10
12
14
16
18
20
Pb^{206}/Pb^{204}

(b)

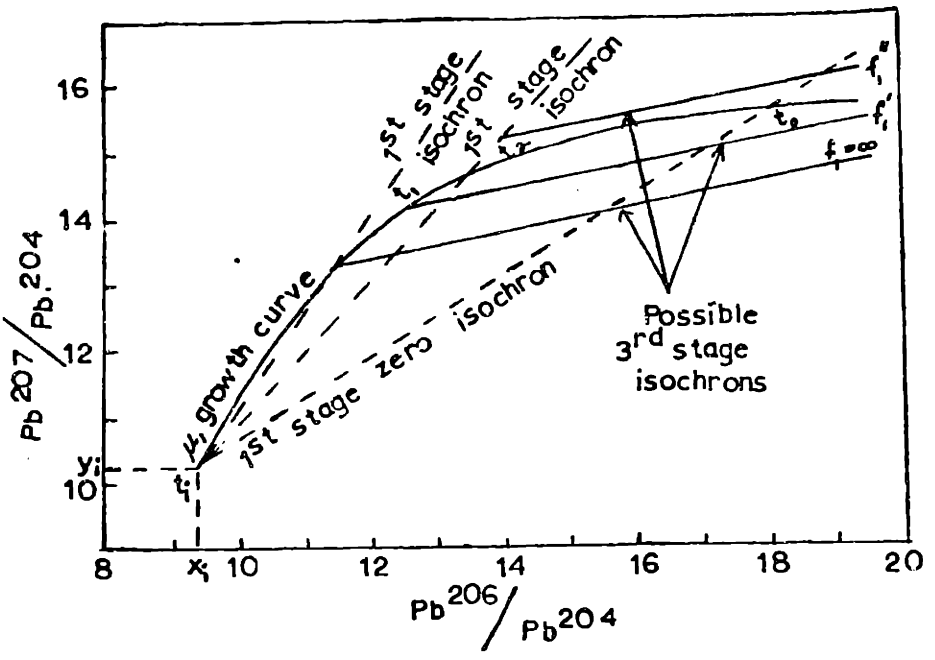
16
14
12
10
8
Pb^{207}/Pb^{204}
Pb^{206}/Pb^{204}
y_i
x_i 10
12
14
16
18
20
μ_i growth curve
1st stage isochron
1st stage isochron
1st stage isochron
1st stage zero isochron
Possible 3rd stage isochrons
t_1
t_2
t_1'
t_1''
f_1''
f_1'
$f_1=\infty$

(c)

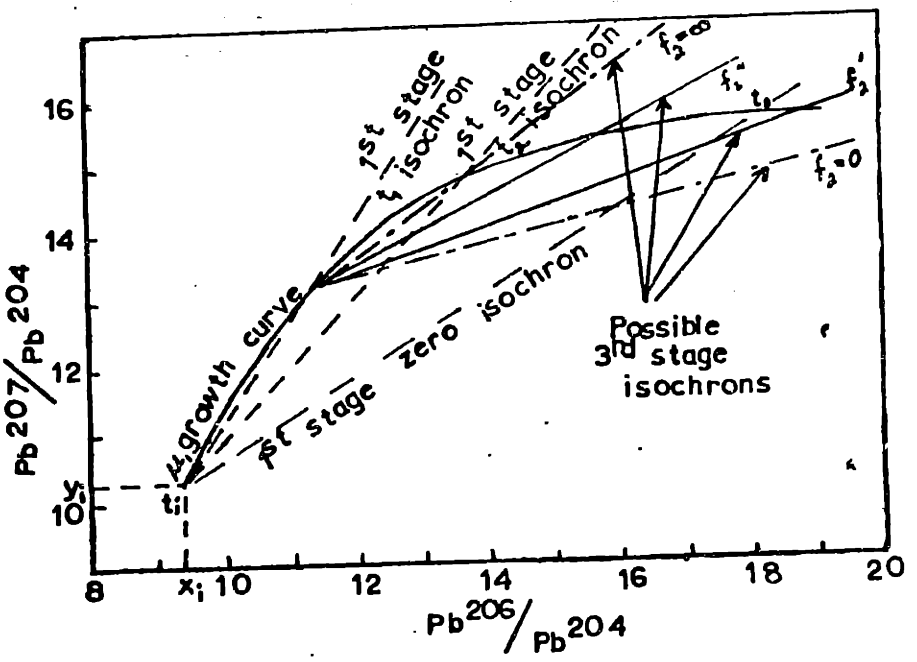
16
14
12
10
8
Pb^{207}/Pb^{204}
Pb^{206}/Pb^{204}
y_i
x_i 10
12
14
16
18
20
μ_i growth curve
1st stage isochron
1st stage isochron
1st stage isochron
1st stage zero isochron
Possible 3rd stage isochrons
t_1
t_2
t_2'
t_2''
$f_2=\infty$
$f_2=0$

(d)

$$m = \frac{1}{137.88}\left(\frac{e^{\lambda' t_1} - 1}{e^{\lambda t_1} - 1}\right)$$

Moreover, if the growth curve corresponding to $\mu = \mu_1$ is constructed on the same diagram, this secondary isochron intersects the growth curve at two points corresponding to $t=t_1$ and $t=0$ (present). (For mathematical analyses of this and subsequent cases, see any of the review papers cited at the beginning of this Appendix.)

Geologic systems frequently involve three-stage or higher-order models. Only certain special cases of three-stage model result in straight-line plots on a lead-lead diagram; general higher-order models never yield straight lines unless simplifying assumptions can be made to reduce them to a two-stage or special three-stage case. Consider a three-stage system where the first stage (t_i to t_1) is characterized by $\mu = \mu_1$, the second stage (t_1 to t_2) has $\mu = \mu_{2i}$, and the third stage (t_2 to the present) has $\mu = \mu_{3j}$ (the subscripts i and j denoting subdivision of the original system into subsystems). If we define a parameter f such that $f_{1i} = \mu_1/\mu_{2i}$ and $f_{2j} = \mu_{2i}/\mu_{3j}$, then the only cases of three-stage evolution which produce rectilinear plots are f_1 = constant or f_2 = constant (Gale and Mussett, 1973). These two cases are illustrated in Figures B-2(c) and (d). If f_{1i} = constant for all i (c), the family of isochrons share a common slope defined by

$$m = \frac{1}{137.88}\left(\frac{e^{\lambda' t_2} - 1}{e^{\lambda t_2} - 1}\right)$$

(analogous to the two-stage case). Only in cases $f_1=1$ (the two-stage model) or $f_1 = \infty$ will the tertiary isochron have meaningful intercepts with the μ, growth curve; in the latter case the single meaningful intercept will be at $t=t_1$. By contrast, if f_2 = constant (d), the family of tertiary isochrons have variable slopes, but all intercept the μ, growth curve at $t = t_1$. For extreme values of f_2, these conditions hold:

$$\lim_{f_2 \to 0} (m) = \frac{1}{137.88}\left(\frac{e^{\lambda' t_2} - 1}{e^{\lambda t_2} - 1}\right) \quad \text{and}$$

$$\lim_{f_2 \to \infty} (m) = \frac{1}{137.88}\left(\frac{e^{\lambda' t_1} - e^{\lambda' t_2}}{e^{\lambda t_1} - e^{\lambda t_2}}\right) .$$

IV. Concordia diagram (Wetherill, 1956). The Concordia diagram is a plot of Pb^{206}/U^{238} (vertical axis) against Pb^{207}/U^{235} (horizontal axis). It was originally used for phases such as zircon, which when formed incorporate virtually no common lead, so essentially all the lead present is radiogenic lead produced by the decay of the uranium in the mineral. (When used for whole rocks, the diagram is generally termed a "modified" Concordia plot: the lead content of the rock is customarily corrected for primordial lead present at t_i, so that one is con-

sidering only radiogenic lead produced since then.) Information is obtained from such a plot by reference to the Concordia curve, defined by the parametric equations

$$\frac{Pb^{206}}{U^{238}} = e^{\lambda t} - 1 \qquad \text{and} \qquad \frac{Pb^{207}}{U^{235}} = e^{\lambda' t} - 1$$

Note that the curve itself is μ-independent, so all single-stage systems simply move along the curve with time. See Figure B-3(a).

In the two-stage case, suppose that the system develops undisturbed from t_i to t_1, at which time episodic loss or gain of uranium or lead takes place in varying degrees in different subsystems (generally the process involved is loss of one of the components relative to the other). The locus of points defined by current measured values of (radiogenic) Pb^{206}/U^{238} and Pb^{207}/U^{235} is a straight line (discordia) which intercepts the Concordia curve at $t=t_i$ and $t=t_1$ (Figure B-3(b)).

Once again only special cases of three-stage model give rectilinear plots: those for f_1 = constant or f_2 = constant (Gale and Mussett, 1973). For f_1 = constant, the family of possible straight lines all intercept Concordia at $t=t_2$ (Figure B-3(c)); if $f_1 = \infty$, the other intercept with Concordia will correspond to $t=t_1$, but otherwise the older intercept is meaningless (unless

Figure B-3. Illustrations of Concordia diagrams. In all cases, t_i = age of the earth. Ratios designated with asterisks denote radiogenic lead only. After Gale and Mussett, 1973.

(a) Single-stage evolution.

(b) Two-stage model with episodic disturbance at t= t_1.

(c) Three-stage model, f_1 = constant, with events at t_1 and t_2.

(d) Three-stage model, f_2 = constant, with events at t_1 and t_2.

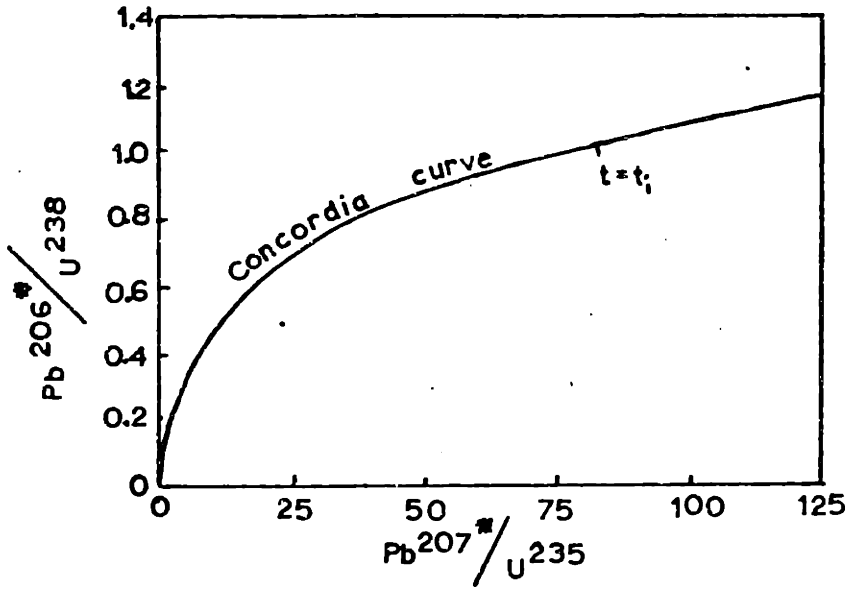
1.4
1.2
1.0
0.8
0.6
0.4
0.2
0
0
25
50
75
100
125
Concordia curve
t=t_i
Pb^206*/U^238
Pb^207*/U^235

(a)

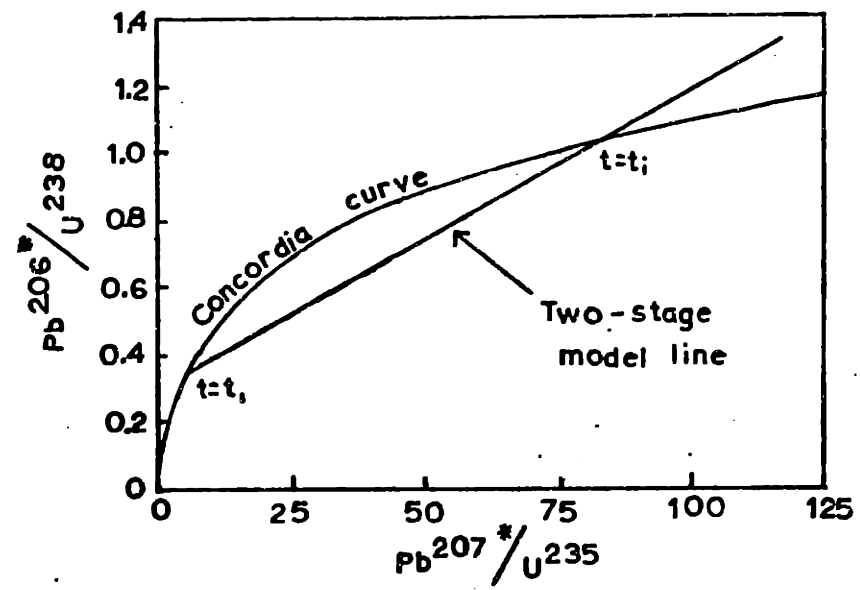
1.4
1.2
1.0
0.8
0.6
0.4
0.2
0
0
25
50
75
100
125
Concordia curve
t=t_i
t=t_1
Two-stage
model line
Pb^206*/U^238
Pb^207*/U^235

(b)

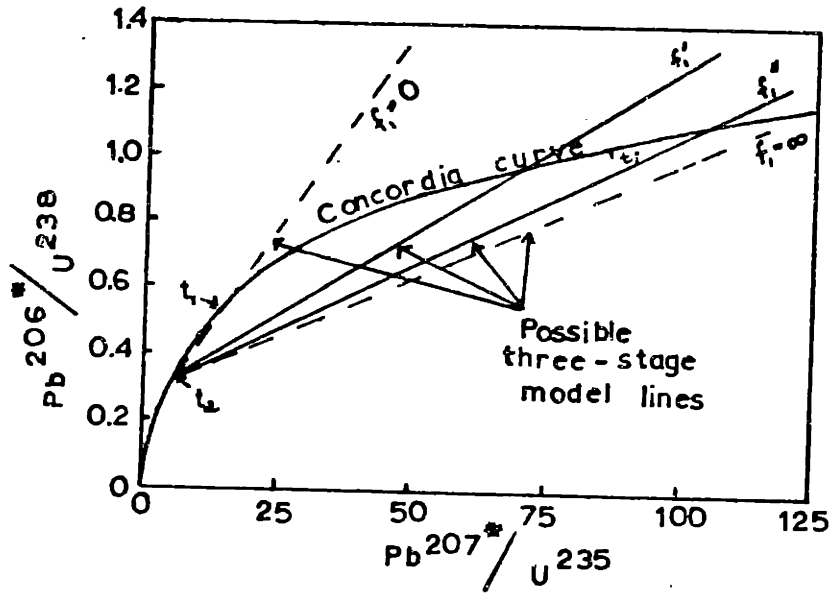
1.4
1.2
1.0
0.8
0.6
0.4
0.2
0
0
25
50
75
100
125
Pb206*/U238
Pb207*/U235
Concordia curve
Possible
three-stage
model lines

(c)

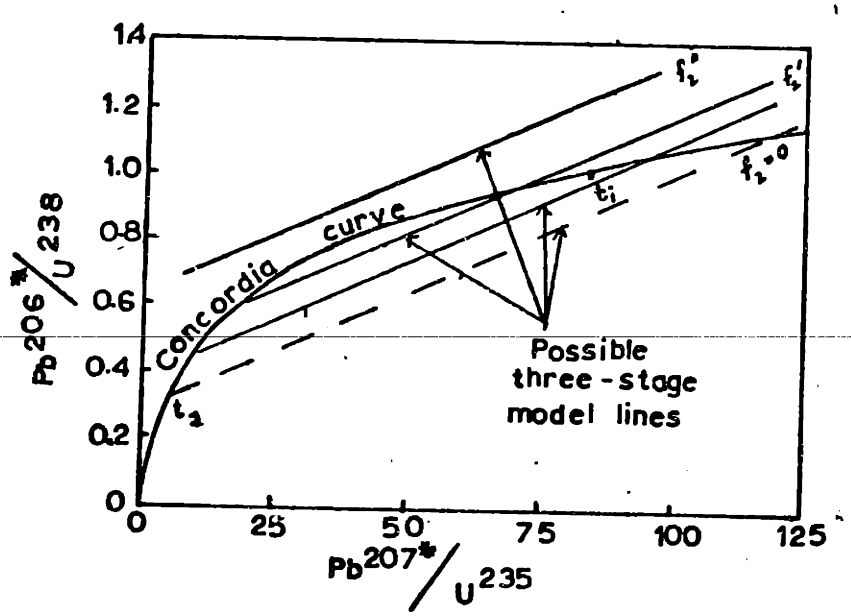
1.4
1.2
1.0
0.8
0.6
0.4
0.2
0
0
25
50
75
100
125
Pb206*/U238
Pb207*/U235
Concordia curve
Possible
three-stage
model lines

(d)

$f_1 = 1$, in which case we are back to the two-stage model). The family of lines for the f_2 = constant case (Figure B-3 (d)) are parallel. Only if $f_2 = 0$ is any meaningful intercept produced: in this instance the younger intercept corresponds to $t=t_2$. The slope of lines in the f_2 = constant case is, however, given by

$$m = \frac{e^{\lambda t_i} - e^{\lambda t_j}}{e^{\lambda t_i} - e^{\lambda t_1}}$$

so that if t_i can be assumed with reasonable certainty, t_1 can be calculated also.

In general, then, alternative interpretations of rectilinear arrays of points on these various diagrams may be advanced. Consideration of other geologic or geochronologic information is necessary if the interpretation is to be made with confidence.

References Cited

Adams, J.A.S., Osmond, J.K., and Rogers, J.J.W., 1959. The geochemistry of thorium and uranium: in Ahrens, L.H., Press, F., Rankama, K., and Runcorn, S.K. (eds.), Physics and Chemistry of the Earth, Pergamon Press, N.Y., v. 3, pp. 298-348.

Ahrens, L.H., 1965. The comparative geochemistry of K, Rb, Ca, Ar, Sr, U, Th, and Pb: in Hamilton, E.I. (ed.), Applied Geochronology, Academic Press, N.Y., pp. vii-xiv.

Albee, A.L., and Ray, L., 1970. Correction factors for electron probe microanalysis of silicates, oxides, carbonates, phosphates, and sulfates: Anal. Chem., v. 42, pp. 1408-1414.

Annheuser, C.R., Mason, R., Viljoen, M.J., and Viljoen, R.P., 1969. A reappraisal of some aspects of Precambrian shield geology: Geol. Soc. Amer. Bull., v. 80, pp. 2175-2200.

Armstrong, R.L., 1968. A model for the evolution of strontium and lead isotopes in a dynamic earth: Rev. Geophys., v. 6, pp. 175-199.

Bellizzia, C.M., 1972. Paleotectonica del Escudo de Guayana: Proc. Ninth Inter-Guayanas Geol. Conf., Spec. Publ. 6, Ministerio de Minas e Hidrocarburos, Venezuela, pp. 251-305.

Benavides, V., 1968. Saline deposits of South America: Geol. Soc. Amer. Spec. Paper 88, pp. 249-290.

Black, L.P., Moorbath, S., Pankhurst, R.J., and Windley, B.F., 1973. $^{207}Pb/^{206}Pb$ whole rock age of the Archean granulite facies metamorphic event in West Greenland: Nature Phys. Sci., v. 244, pp. 50-53.

Black, L.P., Gale, N.H., Moorbath, S., Pankhurst, R.J., and McGregor, V.R., 1971. Isotopic dating of very early Precambrian amphibolite facies gneisses from the Godthaab district, West Greenland: Earth and Plan. Sci. Lett., v. 12, pp. 245-259.

Blackburn, W.H., 1968. The spatial extent of chemical equilibrium in some highgrade metamorphic rocks from the Grenville of southeastern Ontario: Contrib. Mineral. and Petrol., v. 19, pp. 72-92.

Boulos, N.S., and Manuel, O.K., 1971. The xenon record of extinct radioactivities in the earth: Science, v. 174, pp. 1334-1336.

Boyd, F.R., and England, J.L., 1964. The system enstatite-pyrope: Carnegie Inst. Wash. Yearbook, v. 63, pp. 157-161.

Brooks, C., Hart, S.R., and Wendt, I., 1972. Realistic use of two-error regression treatments as applied to rubidium - strontium data: Rev. Geophys. and Space Phys., v. 10, pp. 551-577.

Brown, G.C., and Fyfe, W.S., 1970. The production of granitic melts during ultrametamorphism: Contrib. Mineral. and Petrol., v. 28, pp.310-318.

Buddington, A.F., and Lindsley, D.H., 1964. Iron-titanium oxide minerals and synthetic equivalents: Jour. Petrol., v. 5, pp. 310-357.

Cameron, A.E., Smith, D.H., and Walker, R.L., 1969. Mass spectrometry of nanogram-size samples of lead: Anal. Chem., v. 41, pp. 525-526.

Catanzaro, E.J., and Gast, P.W., 1960. Isotopic composition of lead in pegmatite feldspars: Geochim. et Cosmochim. Acta, v. 19, pp. 113-126.

Chase, R.L., 1965. El Complejo de Imataca, la Anfibolita de Panamo, y la Tronjemita de Guri, rocas precámbricas del Cuadrilatero de Adjuntas-Panamo, Estado Bólivar, Venezuela: Bol. Geol., Caracas, v. 7, #13.

Cloud, P., 1972. A working model of the primitive earth: Amer. Jour. Sci., v. 272, pp. 537-548.

Cloud, P., 1973. Paleoecological significance of banded iron formation: Econ. Geol., v. 68, pp. 1135-1143.

Cooray, P.G., 1962. Charnockites and their associated gneisses in the Precambrian of Ceylon: Quart. Jour. Geol. Soc. Lond., v. 118, pp. 239-273.

Cooray, P.G., 1969. Charnockites as metamorphic rocks: Amer. Jour. Sci., v. 267, pp. 969-982.

Cumming, G.L., Tsong, F., and Gudjurgis, P.J., 1970. Fractional removal of lead from rocks by volatilization: Earth and Plan. Sci. Lett., v. 9, pp. 49-54.

Dahlberg, E.H., 1972. Granulites of sedimentary origin associated with rocks of the charnockite suite in the Bakhuys Mountains, N. W. Suriname: Proc. Ninth Inter-Guayanas Geol. Conf., Spec. Publ. 6, Ministerio de Minas e Hidrocarburos, Venezuela, pp. 414-423.

Davies, F.B., and Windley, B.F., 1976. Significance of major Proterozoic highgrade linear belts in continental evolution: Nature, v. 263, pp. 383-385.

deRaaumiroff, G., 1965. Origen y metamorfismo del paragneiss principal del Complejo Precambrico de Imataca, Cuadrilatero de Upata, Estado Bolivar, Venezuela: Bol. Geol., Caracas, v. 7, #13.

DeWaard, D., 1965. The occurrence of garnet in the granulite-facies terrane of the Adirondack Highlands: Jour. Petrol., v. 6, pp.165-191.

Diamond, R.M., Street, K, and Seaborg, G.T., 1954. Ion-exchange study of possible hybridized 5f bonding in the actinides: Jour. Amer. Chem. Soc., v. 76, pp. 1461-1469.

Dimroth, E., and Kimberley, M.M., 1976. Precambrian atmospheric oxygen: evidence in the sedimentary distributions of carbon, sulfur, uranium, and iron: Can. Jour. Earth Sci., v. 13, pp. 1161-1185.

Doe, B.R., 1970. Lead Isotopes: Springer-Verlag, N.Y., 137 pp.

Doe, B.R., and Hart, S.R., 1963. The effect of contact metamorphism on lead in potassium feldspars near the Eldora stock, Colorado: Jour. Geophys. Res., v. 68, pp. 3521-3530.

Doe, B.R., and Zartman, R.E., 1977. Plumbotectonics I, The Phanerozoic: in press, in Barnes, H. (ed.), Geochemistry of Hydrothermal Ore Deposits, 2nd.ed.

Doe, B.R., Tilton, G.R., and Hopson, C.A., 1965. Lead isotopes in feldspars from selected granitic rocks associated with regional metamorphism: Jour. Geophys. Res., v. 70, pp. 1947-1968.

Dorr, J.van N. II, 1973. Iron-formation in South America: Econ. Geol., v. 68, pp. 1005-1022.

Dougan, T.W., 1974. Cordierite gneisses and associated lithologies of the Guri Area, Northwest Guayana Shield, Venezuela: Contrib. Mineral. and Petrol., v. 46, pp. 169-188.

Dougan, T.W., 1976. A protolith model for the Archean Imataca Complex in an area near Cerro Bolivar, Venezuelan Guayana Shield: Precamb. Res., v. 3, pp. 317-342.

Eckelmann, F.D., and Kulp, J.L., 1956. The sedimentary origin and stratigraphic equivalence of the so-called Cranberry and Henderson Granites in western North Carolina: Amer. Jour. Sci., v. 254, pp. 288-315.

Espejo, A. and Santamaria, F., 1972. Significado de nuevas determinaciones de edades potasio-argon en la Guayana Venezolana: Proc. Ninth Inter-Guayanas Geol. Conf., Spec. Publ. 6, Ministerio de Minas e Hidrocarburos, Venezuela, pp. 424-430.

Fahrig, W.F., Eade, K.E., and Adams, J.A.S., 1967. Abundance of radioactive elements in crystalline shield rocks: Nature, v. 214, pp. 1002-1003.

Finger, L.W., and Hadidiacos, L., 1972. Electron microprobe automation: Carnegie Inst. Wash. Yearbook, v. 71, pp. 598-600.

Friedlander, G., Kennedy, J.W., and Miller, J.M., 1964. Nuclear and Radiochemistry: John Wiley and Sons, N.Y., 585 pp.

Gale, N.H., and Mussett, A.E., 1973. Episodic uranium-lead models and the interpretation of variations in the isotopic composition of lead in rocks: Rev. Geophys. and Space Phys., v. 11, pp. 37-86.

Gastil, R.G., DeLisle, M., and Morgan, J.R., 1967. Some effects of progressive metamorphism on zircons: Geol. Soc. Amer. Bull., v. 78, pp. 879-906.

Gaudette, H.E., Hurley, P.M., and Fairbairn, H.W., 1973. Uranium-lead zircon ages from the northern Guayana Shield: Proc. 2nd Latin-American Geol. Conf., pp. 54-55.

Gaudette, H.E., Hurley, P.M., Fairbairn, H.W., and Espejo, A., 1974. A 2600 m.y. zircon age for the Supamo basement, Venezuelan Guayana Shield (abs.): Geol. Soc. Amer. Abs., v. 6, pp. 749-750.

Glikson, A.Y., 1970. Geosynclinal evolution and geochemical affinities for early Precambrian systems: Teconophys., v. 9, pp. 397-433.

Glikson, A.Y., and Sheraton, J.W., 1972. Early Precambrian trondhjemitic suite in Western Australia and Northwest Scotland, and the geochemical evolution of shields: Earth and Plan. Sci. Lett., v. 17, pp. 227-242.

Goodwin, A.M., 1968. Archean protocontinental growth and early crustal history of the Canadian Shield: Proc. 23rd Int. Geol. Cong., Prague, v. 1, pp. 69-89.

Goodwin, A.M., 1973. Plate tectonics and evolution of Precambrian crust: in Tarling, D.H., and Runcorn, S.K. (eds.), Implications of Continental Drift to the Earth Sciences, Academic Press, N.Y., pp. 1047-1069.

Grauert, B., and Hall, L., 1973. Age and origin of zircons from metamorphic rocks in the Manhattan Prong, White Plains Area, southeast New York: Carnegie Inst. Wash. Yearbook, v. 72, pp. 293-297.

Gray, C.M., and Oversby, V.M., 1972. The behavior of lead isotopes during granulite facies metamorphism: Geochim. et Cosmochim. Acta, v. 36, pp. 939-952.

Groves, A.W., 1935. The charnockite series of Uganda, British East Africa: Quart. Jour. Geol. Soc. Lond., v. 91, pp. 150-207.

Hall, H.T., and Murthy, R.V., 1971. The early chemical history of the earth: some critical elemental fractionation: Earth and Plan. Sci. Lett., v. 11, pp. 239-244.

Hanks, T.C., and Anderson, D.L., 1969. The early thermal history of the earth: Phys. Earth and Planet. Interiors, v. 2, pp. 19-29.

Heier, K.S., and Adams, J.A.S., 1965. Concentrations of radioactive elements in deep crustal material: Geochim. et Cosmochim. Acta, v. 29, pp. 53-61.

Heier, K.S., and Thoresen, K., 1971. Geochemistry of high-grade metamorphic rocks, Lofoten-Vesterålen, North Norway: Geochim. et Cosmochim. Acta, v. 35, pp. 89-99.

Holland, T.H., 1893. The petrology of Job Charnock's tombstone: Jour. Asiatic Soc. Bengal, v. 62, pp. 162-164.

Holland, T.H., 1900. The charnockite series, a group of Archean hypersthenic rocks in Peninsular India: Mem. Geol. Surv. India, v. 28, pp. 119-249.

Houtermans, F.G., 1953. Determination of the age of the earth from the isotopic composition of meteoritic lead: Nuovo Cimento, v. 10, pp. 1622-1633.

Howie, R.A., 1964. Charnockites: Sci. Progress, v. 52, pp. 628-644.

Hurley, P.M., 1972. Can the subduction process of mountain building be extended to Pan-African and similar orogenic belts?: Earth and Plan. Sci. Lett., v. 15, pp. 305-314.

Hurley, P.M., and Rand, J.R., 1969. Pre-drift continental nuclei: Science, v. 164, pp. 1229-1242.

Hurley, P.M., Fairbairn, H.W., and Gaudette, H.E., 1976a. Progress report on early Archean rocks in Liberia, Sierra Leone, and Guayana, and their general stratigraphic setting: in Windley, B.F. (ed.), The Early History of the Earth, Proc. NATO Adv. Study Inst., John Wiley and Sons, N.Y., pp. 511-521.

Hurley, P.M., Fairbairn, H.W., and Montgomery, C.W., 1976b. Domains of chemical and isotopic equilibrium in granulites: application to radiometric dating (abs.): Trans. Amer. Geophys. Union, v. 57, p. 348.

Hurley, P.M., Kalliokoski, J., Fairbairn, H.W., and Pinson, W.H., 1972. Progress report on the age of granulite facies rocks in the Imataca Complex, Venezuela: Proc. Ninth Inter-Guayanas Geol. Conf., Spec. Publ. 6, Ministerio de Minas e Hidrocarburos, Venezuela, pp. 431-433.

Hurley, P.M., Fairbairn, H.W., Gaudette, H.E., Mendoza, V., Martin, C.B., and Espejo, A., 1973. Progress report on age dating in the northern Guayana Shield (abs.): Proc. 2nd Latin-American Geol. Conf., p. 1.

Jaffey, A.H., Flynn, K.F., Glendenin, L.E., Bentley, W.C., and Essling, A.M., 1971. Precision measurement of half-lives and specific activities of ^{235}U and ^{238}U: Phys. Rev., v. 4, pp. 1889-1906.

Jenks, W.F. (ed.), 1956. Handbook of South American Geology: Geol. Soc. Amer. Memoir 65, 378 pp.

Kalliokoski, J., 1965a. Geology of north-central Guayana Shield, Venezuela: Geol. Soc. Amer. Bull., v. 76, pp. 1027-1049.

Kalliokoski, J., 1965b. The metamorphosed iron ore of El Pao, Venezuela: Econ. Geol., v. 60, pp. 100-116.

Kanasewich, E.R., 1968. The interpretation of lead isotopes and their geological significance: in Hamilton, E.I. and Farquhar, R.M., (eds.), Radiometric Dating for Geologists, Interscience Publishers, N.Y., pp. 147-223.

Krogh, T.E., 1973. A low-contamination method for hydrothermal decomposition of zircon and extraction of U and Pb for isotopic age determinations: Geochim. et Cosmochim. Acta, v. 37, pp. 485-494.

Krogh, T.E., and Davis, G.L., 1968. Geological history of the Grenville Province: Carnegie Inst. Wash. Yearbook, v. 66, pp. 44-52.

Krogh, T.E., and Davis, G.L., 1969. Old isotopic ages in the northwestern Grenville Province, Ontario: Geol. Assn. Can. Spec. Paper 5, pp. 189-192.

Liddle, R.A., 1946. The Geology of Venezuela and Trinidad (2nd ed.): Paleontological Res. Inst., Ithaca, N.Y., 890 pp.

López, V.M., Hedberg, H.D., and Kehrer, L., 1956. Venezuela: Geol. Soc. Amer. Memoir 65, pp. 327-349.

MacGregor, I.D., 1974. The system $MgO-Al_2O_3-SiO_2$: solubility of Al_2O_3 in enstatite for spinel and garnet peridotite compositions: Amer. Mineral., v. 59, pp. 110-119.

Mattinson, J.M., 1971. Preparation of ultrapure HF, HCl, and HNO_3. Carnegie Inst. Wash. Yearbook, v. 70, pp. 266-268.

Mendoza, V., 1972. Geologia del area del Rio Suapure, parte noroccidental del escudo de Guayana, Estado Bólivar, Venezuela: Proc. Ninth Inter-Guayanas Geol. Conf., Spec. Publ. 6, Ministerio de Minas e Hidrocarburos, Venezuela, pp. 306-338.

Menéndez, A., 1968. Revisión de la estratigrafía de la Provincia de Pastora según el estudio de la región de Guasipati, Guayana venezolana: Bol. Geol., Caracas, v. 10, pp. 310-338.

Menéndez, A., 1972. Guia de la excursion geologica Guasipati el Callao - Canaima: Proc. Ninth Inter-Guayanas Geol. Conf., Spec. Publ. 6, Ministerio de Minas e Hidrocarburos, Venezuela, pp. 49-62.

Menéndez, A., Benaim, N., and Espejo, A., 1972. Estratigrafica precámbrica de la provincia geologica de Pastora al este del Rio Caroni y su correlacion tentativa interguayana: Proc. Ninth Inter-Guayanas Geol. Conf., Spec. Publ. 6, Ministerio de Minas e Hidrocarburos, Venezuela, pp. 339-342.

Miyashiro, A., 1973. Metamorphism and Metamorphic Belts: John Wiley and Sons, N.Y., 492 pp.

Montgomery, C.W., Hurley, P.M., Fairbairn, H.W., and Gaudette, H.E., 1977. Equilibrated domains and combined Rb-Sr and U-Pb systematics in the history of a granulite: in Variations in Isotopic Abundances of Strontium, Lead, and Argon and Related Topics, 21st Prog. Rep., M.I.T. Geochronology Lab., pp. 1-25.

Moorbath, S., 1976. Age and isotope constraints for the evolution of Archean crust: in Windley, B.F. (ed.), The Early History of the Earth: Proc. NATO Adv. Study Inst., John Wiley and Sons, N.Y., pp. 351-360.

Moorbath, S., O'Nions, R.K., and Pankhurst, R.J., 1973. Early Archean age for the Isua Iron Formation, West Greenland: Nature, v. 245, pp. 138-139.

Moorbath, S., Wēlke, H., and Gale, N.H., 1969. The significance of lead isotope studies in ancient high-grade metamorphic basement complexes, as exemplified by the Lewisian rocks of northwest Scotland: Earth and Plan. Sci. Lett., v. 6, pp. 245-256.

Nelson, F., Murase, T., and Kraus, K.A., 1964. Ion exchange procedures - I. Cation exchange in concentrated HCl and $HClO_4$ solutions: Jour. Chromatog., v. 13, pp. 503-535.

Nier, A.O., 1947. A mass spectrometer for isotope and gas analysis: Rev. Sci. Inst., v. 18, pp. 398-411.

Oversby, V.M., 1975. Lead isotopic systematics and ages of Archean acid intrusives in the Kalgoorlie-Norseman area, Western Australia: Geochim. et Cosmochim. Acta, v. 39, pp. 1107-1125.

Oversby, V.M., 1976. Isotopic ages and geochemistry of Archean acid igneous rocks from the Pilbara, Western Australia: Geochim. et Cosmochim. Acta, v. 40, pp. 817-829.

Oversby, V.M., and Ringwood, A.E., 1971. Time of formation of earth's core: Nature, v. 234, pp. 463-465.

Patterson, C., 1956. Age of meteorites and the earth: Geochim. et Cosmochim. Acta, v. 10, pp. 230-237.

Posadas, V.G., and Kalliokoski, J., 1967. Rb-Sr ages of the Encrucijada Granite intrusive in the Imataca Complex, Venezuela: Earth and Plan. Sci. Lett., v. 2, pp. 210-214.

Quesada, A., Blackburn, W.H., Dennen, W.H., and Lopez, V.W., 1968. Composicion quimica y origen probable de las rocas del area de Guri, Geos. Central Univ., Caracas, #18, pp. 7-23.

Richardson, K.A., and Adams, J.A.S., 1964. Effect of weathering on radioactive elements in the Conway Granite (abs.): Geol. Soc. Amer. Spec. Paper 76, p. 137.

Richardson, S.W., Gilbert, M.C., and Bell, P.M., 1969. Experimental determination of kyanite-andalusite and andalusite-sillimanite equilibria: the aluminum silicate triple point: Amer. Jour. Sci., v. 267, pp. 259-272.

Ríos, J.H.F., 1972. Geologia de la región Upata - El Palmar - Villa Lola: Proc. Ninth Inter-Guayanas Geol. Conf., Spec. Publ. 6, Ministerio de Minas e Hidrocarburos, Venezuela, pp. 354-371.

Rosholt, J.N., Zartman, R.E., and Nkomo, I.T., 1973. Lead isotope systematics and uranium depletion in the Granite Mountains, Wyoming: Geol. Soc. Amer. Bull., v. 84, pp. 989-1002.

Ruckmick, J.C., 1963. The iron ores of Cerro Bolivar, Venezuela: Econ. Geol., v. 58, pp. 218-236.

Russell, R.D., Slawson, W.F., Ulrych, T.J., and Reynolds, P.H., 1968. Further applications of concordia plots to rock lead abundances: Earth and Plan. Sci. Lett., v. 3, pp. 284-288.

Sighinolfi, G.P., 1971. Investigations into deep crustal levels: fractionating effects and geochemical trends related to high grade metamorphism: Geochim. et Cosmochim. Acta, v. 35, pp. 1005-1021.

Singh, S., 1966. Orthopyroxene-bearing rocks of charnockitic affinities in the South Savanna-Kanuku Complex of British Guiana: Jour. Petrol., v. 7, pp. 171-192.

Stacey, J.S., and Kramers, J.D., 1975. Approximation of terrestrial lead isotope evolution by a two-stage model: Earth and Plan. Sci. Lett., v. 26, pp. 207-221.

Stacey, J.S., and Stern, T.W., 1973. Revised tables for the calculation of lead isotope ages: U. S. Geol. Surv. Rep. GD-73-016, 37 pp.

Steiger, R.H., and Hart, S.R., 1967. The microcline-orthoclase transition within a contact aureole: Amer. Mineral., v. 52, pp. 87-116.

Stern, T.W., Newell, M.F., Kistler, R.W., and Shawe, D.R., 1965. Zircon U-Pb and Th-Pb ages and mineral K-Ar ages of La Sal Mountains rocks, Utah: Jour. Geophys. Res., v. 70, pp. 1503-1507.

Subramanian, A.P., 1959. Charnockites of the type area near Madras - a reinterpretation: Amer. Jour. Sci., v. 257, pp. 321-353.

Subramanian, A.P., 1962. Pyroxenes and garnets from charnockites and associated granulites: in Engel, A.E.J., James, H.L., and Leonard, B.F. (eds.), Petrologic Studies: A Volume in Honor of A.F. Buddington, Geol. Soc. Amer., pp. 21-36.

Sutton, J., 1963. Long-term cycles in the evolution of continents: Nature, v. 198, pp. 731-735.

Tatsumoto, M., Knight, R.J., and Allegre, C.J., 1973. Time differences in the formation of meteorites as determined from the ratio of lead-207 to lead-206: Science, v. 180, pp. 1279-1283.

Taylor, S.R., 1967. The origin and growth of continents: Tectonophys., v. 4, pp. 17-34.

Tilley, C.E., 1936. Enderbite, a new member of the charnockite series: Geol. Mag., v. 73, pp. 312-316.

Turner, F.J., 1968. Metamorphic Petrology - Mineralogical and Field Aspects: McGraw - Hill Book Co., N.Y., 403 pp.

Tuttle, O.F., and Bowen, N.L., 1958. Origin of granite in the light of experimental studies in the system $NaAlSi_3O_8$ - $KAlSi_3O_8$ - SiO_2 - H_2O: Geol. Soc. Amer. Memoir 74, 153 pp.

Ulrych, T.J., 1967. Oceanic basalt leads: a new interpretation and an independent age for the earth: Science, v. 158, pp. 252-256.

Wasserburg, G.J., 1963. Diffusion processes in lead-uranium systems: Jour. Geophys. Res., v. 68, pp. 4823-4846.

Wetherill, G.W., 1956. Discordant uranium-lead ages: Trans. Amer. Geophys. Union, v. 37, pp. 320-326.

Wilson, A.F., 1959. The charnockitic rocks of Australia: Geol. Rundsch., v. 47, pp. 491-509.

Windley, B.F., 1973. Crustal development in the Precambrian: Phil. Trans. Roy. Soc. Lond. A, v. 273, pp. 321-341.

Windley, B.F. (ed.), 1976. The Early History of the Earth: Proc. NATO Adv. Study Inst., John Wiley and Sons, N.Y., 619 pp.

Winkler, H.G.F., 1967. Petrogenesis of Metamorphic Rocks: Springer-Verlag, N.Y., 237 pp.

Wones, D.R., 1972. Stability of biotite: a reply: Amer. Mineral., v. 57, pp. 316-317.

Wones, D.R., and Eugster, H.P., 1965. Stability of biotite: experiment, theory, and application: Amer. Mineral., v. 50, pp. 1228-1272.

Wood, B.J., 1974. The solubility of alumina in orthopyroxene coexisting with garnet: Contrib. Mineral. and Petrol., v. 46, pp. 1-15.

Wood, B.J., and Banno, S., 1973. Garnet - orthopyroxene and orthopyroxene - clinopyroxene relationships in simple and complex systems: Contrib. Mineral. and Petrol., v. 42, pp. 109-124.

Wynne-Edwards, H.R., and Hay, P.W., 1963. Coexisting cordierite and garnet in regionally metamorphosed rocks from the Westport area, Ontario: Can. Mineral., v. 7, pp. 453-478.

Yoder, H.S., and Tilley, C.E., 1962. Origin of basalt magmas: an experimental study of natural and synthetic rock systems: Jour. Petrol., v. 3, pp. 342-532.

York, D., 1969. Least-squares fitting of a straight line with correlated errors: Earth and Plan. Sci. Lett., v. 5, pp. 320-324.

Zartman, R.F., 1965. The isotopic composition of lead in microclines from the Llano Uplift, Texas: Jour. Geophys. Res., v. 70, pp. 965-975.

Zweig, G., and Sherma, J. (eds.), 1972. CRC Handbook of Chromatography: CRC Press, Cleveland, Ohio, pp. 280-281.

Biographic Sketch

The author was born in Providence, R.I. on September 26, 1951. She was educated in the Cranston, R.I. public schools, and graduated from Cranston High School West as valedictorian of the class of 1969.

Her undergraduate education was obtained at Wellesley College and Dartmouth College. She completed a double major in mathematics and geology, receiving her A.B. degree with highest honors from Wellesley College in 1972. In the same year she was elected to membership in Phi Beta Kappa and associate membership in Sigma Xi.

Having developed a great fondness for Dartmouth, she began her graduate studies there, and received her A.M. degreee in geology in 1974. Her master's thesis research, carried out under Dr. John B. Lyons, was a study of contact metamorphism at Mont Rougemont, Quebec. While at Dartmouth, she was also married, in 1973, to Warren Alan Montgomery (Dartmouth '73).

Since September, 1973 the author has been a graduate student in geochemistry at M.I.T. After graduation, she plans to stay on as a postdoctoral research associate in geochemistry.

Publications include:

Westlund, C.P., 1971. Pyritization in fossils from the Silica Formation, Medusa Quarry, Ohio: N.Y. State Geol. Assn., Guidebook to 43rd Ann. Mtg., p. G-3 (abs.).

Westlund, C.P., 1972. Etruscan Archaic art with special reference to the style of Veii: Dartmouth Classical Journal.

Montgomery, C.W., and Brace, W.F., 1975. Micropores in plagioclase: Contrib. Mineral. and Petrol., v. 52, pp. 17-28.

Schutts, L., Brecher, A., Hurley, P.M., Montgomery, C.W., and Krueger, L., 1976. A case study of the time and nature of paleomagnetic resetting in a mafic complex in New England: Can. Jour. Earth Sci., v. 13, pp. 898-907.

Hurley, P.M., Fairbairn, H.W., and Montgomery, C.W., 1976. Domains of chemical and isotopic equilibrium in granulites: application to radiometric dating: Trans. Amer. Geophys. Union, v. 57, p. 348 (abs.).

Montgomery, C.W., Hurley, P.M., Fairbairn, H.W., and Gaudette, H.E., 1977. Equilibrated domains and combined Rb-Sr and U-Pb systematics in the history of a granulite: in Variations in isotopic abundances of strontium, lead, and argon, and related topics, Twenty-first Progress Report, M.I.T. Geochronology Laboratory, pp. 1-25.

Montgomery, C.W., Hurley, P.M., Fairbairn, H.W., and Gaudette, H.E., 1977. Combined Rb-Sr and U-Pb systematics in the history of a granulite: submitted to the Spring, 1977 meeting of the American Geophysical Union (abs.).